Synthesis and characterization of aliphatic hyperbranched polyesters

Dissertation

zur Erlangung des Grades eines Doktors

der Naturwissenschaften

- Dr. rer. nat. -

von

Jasna Vuković

aus Jagodina (Serbien)

September 2006

Die vorliegende Arbeit wurde im Zeitraum von November 2003 bis September 2006 in der Arbeitsgruppe „Physikalische Chemie“ am Institut für Chemie der Universität Osnabrück angefertigt

1. Gutachter: Prof. Dr. M. D. Lechner (Universität Osnabrück)

2. Gutachter: Prof. Dr. S. Jovanović (Universität Belgrad, Serbien)

Acknowledgements

I would like to express my deep gratitude to Prof. Dr. M. D. Lechner and Prof. Dr. S. Jovanović for providing continuous support and tutorial to this work. Their expertise, guidance and understanding were a significant help throughout my work.

A very special thanks goes to Dr. D. Steinmeier for numerous discussions, suggestions and valuable advices which were important contribution to this research.

I also owe my sincere appreciation to Prof. Dr. L. Walder who gave important comments considering NMR spectra and accepted to be a member of my committee.

To Dr. H. Rosemeyer and M. Gather I would like to thank for their help with NMR measurements.

To E. Michalek, E. Stürenberg and Dr. K. Shaikh I owe my thanks for MALDI-TOF measurements.

I want to thank to Dipl.-Ing. Chem. D. Jacobi (Institute for Technical Chemistry, University Duisburg-Essen) for his patience and help with VPO measurements.

To K. Vilsmeier (BASF) I want to thank for UC measurements.

I also owe my thanks to Prof. Dr. M. Haase and Prof. Dr. C. Kummerlöwe for allowing me to use instruments in their laboratories.

Special appreciation goes to my friends and colleagues Dipl.-Biol. C. Schröper, Dr. W. Nierling, E. Möller, Dipl.-Chem. B. Hartmann-Azanza, L. Schlösser and H. Tobergte for their support, suggestions, helpful discussions at various times and particularly for pleasant working atmosphere.

I gratefully acknowledge my family and Enis for being a continuous source of encouragements. For that I doubt I will ever be able to convey my appreciation fully. I dedicate this work to them.

Abstract

Two series of hydroxy-functional hyperbranched polymers based on aliphatic polyesters have been prepared from the 2,2-bis(hydroxymethyl)propionic acid (AB_2 monomer) and the di-trimethylolpropane (B_4 functional core). A pseudo-one-step procedure was used for the synthesis of seven different pseudo generation hyperbranched polyesters of the first series (second, third, fourth, fifth, sixth, eight and tenth pseudo generation), while samples of the second series (fourth, sixth and eight pseudo generation) were prepared by an one-step procedure. The term "pseudo generation" refers to the presence of certain amount of the linear repeating units in the structure of hyperbranched polymers. The structure and properties of the self-synthesized hyperbranched polyesters investigated with different characterization techniques were compared between each other, as well as with commercially available hyperbranched polyesters of the similar structure and samples obtained by modification of the end –OH groups with β-alanine and stearic acid. Beside that, several investigated hyperbranched polyesters were fractionated and a characterization of the obtained fractions was performed in order to get more information about the structure of these polymers.

The experimental results obtained from NMR spectroscopy indicate that during the synthesis of these hyperbranched polymers –OH groups belonging to the terminal units had bigger reactivity than linear ones. As a consequence of that, the degree of branching for all investigated samples is lower than 0.50. The existence of side reaction products has been proved qualitatively and quantitatively by NMR, acid number titration, MALDI-TOF and ESI MS measurements. The side reaction which occurred to a highest amount during the synthesis is the formation of the poly(bis-MPA) and the deactivation of its focal –COOH group. The degree of conversion of –COOH groups decreases with increasing theoretical number of pseudo generation. The formation of cyclic structures through intramolecular etherification and/or esterification is another side reaction which occurred during the synthesis of polymers investigated in this work. The extent of cyclization through the ester and ether bonds increased with increasing degree of polymerization. The experimental results have also shown that up to the fifth theoretical pseudo generation (or sixth in the case of the samples of series II) cyclization occurred through ester and ether bonds, while for the higher generation samples cycles are formed as a consequence of the intramolecular esterification. The results obtained in this work as well as by other authors have shown that for the commercial samples the extent of the side reactions occurred to a higher degree than for the samples synthesized in this dissertation. NMR, VPO, GPC and DLS measurements indicate that the main consequences of the side reactions are: a) molar mass increases only up to the sixth pseudo generation, b) determined values of the number average molar mass are significantly lower than theoretical ones and c) distribution of the molar masses and sizes of all samples are broad.

The best solvents for the polymers synthesized in this work and commercial hyperbranched polyesters are 0.7 mass % solution of LiCl in DMAc and NMP. The limiting viscosity number and the hydrodynamic radius of these samples increase up to the sixth pseudo generation in these two solvents. The exponents obtained from the scaling relations of the limiting viscosity number and hydrodynamic radii with molar mass for the samples of the first series and commercial polymers all had values less than 0.50.

According to the data obtained by SLS, DLS and rheological techniques these polymers have a high ability for the aggregation in the solution and in melt due to the presence of numerous –OH groups. In solution, this ability decreased with increasing theoretical number of pseudo generation, with decreasing concentration and with increasing temperature of the solution. Therefore, at temperatures lower than 50 ^{0}C solutions which

concentration is higher than 45 mass % show shear-thinning behaviour in NMP. On the other side, lower concentration solutions of all investigated hyperbranched polymers act as non-entangled *Newtonian* liquids. *Newtonian* behaviour is also observed at higher temperatures ($T > 70\ ^0C$) in melt for the polyesters from fourth till sixth pseudo generation.

The thermal stability of investigated hyperbranched polyesters, determined by thermogravimetry, increases with increasing theoretical number of the pseudo generation. Using the *Ozawa-Flynn-Wall* method the activation energy of thermal degradation of these samples was determined.

A comparison between the hyperbranched polyesters synthesized by pseudo-one-step and one-step procedure reveals that their properties are different from each other. It was generally concluded that polymers of the second series have lower values of degree of branching, i.e. higher portion of the linear units, higher extent of side reactions, broader molar mass distribution, higher values of the limiting viscosity number, higher values of complex viscosity in melt and poorer thermal stability than samples synthesized by pseudo-one-step procedure, which indicates significant influence of the type of the synthesis on the properties of the final products.

The marked influence of the nature of the terminal groups on the rheological and thermal properties has been detected. By modification of the end –OH groups with stearic acid thermal stability has been improved. On the other side, the presence of the long alkyl chain ends, instead of the polar –OH groups, has reduced the possibility for the H-bonding and value of the glass transition temperature.

1. INTRODUCTION 3

2. THEORETICAL PART 5

2.1. Types of branched polymers 5
2.1.1. Regularly branched polymers 5
2.1.2. Statistically branched polymers 6

2.2. Synthesis of dendritic polymers 7
2.2.1. Synthesis of dendrimers 7
2.2.2. Synthesis of hyperbranched polymers 9

2.3. Structure of dendritic polymers 14

2.4. Properties of dendritic polymers 17
2.4.1. Molar mass and molar mass distribution 17
2.4.1.1. Vapour pressure osmometry 19
2.4.1.2. Mass spectrometry 20
2.4.1.3. Gel permeation chromatography 21
2.4.1.4. Static light scattering 22
2.4.2. Viscosimetry of dendritic polymers 24
2.4.3. Dimensions of dendritic polymers 27
2.4.3.1. Dynamic light scattering 28
2.4.3.2. Ultracentrifugation 29
2.4.4. Rheology of dendritic polymers 34
2.4.5. Thermal analysis of dendritic polymers 39

2.5. Applications of dendritic polymers 42

3. EXPERIMENTAL PART 43

3.1. Materials 43

3.2. Sample preparation 44
3.2.1. Synthesis of hyperbranched polyesters 44
3.2.2. Fractionation of hyperbranched polyesters 44
3.2.3. Modification of hyperbranched polyesters with β-alanine 45
3.2.4. Modification of hyperbranched polyesters with stearic acid 45

3.3. Characterization methods 45
3.3.1. IR spectroscopy 45
3.3.2. NMR spectroscopy 45
3.3.3. Determination of acid and hydroxyl number by titration 46
3.3.4. Determination of the moisture content 46
3.3.5. Vapour pressure osmometry 46
3.3.6. MALDI-TOF mass spectrometry 47
3.3.7. Electrospray Ionization mass spectrometry 47
3.3.8. Gel permeation chromatography 47
3.3.9. Determination of the refractive index increment by differential refractometer 48
3.3.10. Static light scattering 48
3.3.11. Dynamic light scattering 48
3.3.12. Ultracentrifugation 49
3.3.13. Viscosimetry of the diluted solutions 49
3.3.14. Rheology of the concentrated solutions and melt 49

3.3.15. Thermogravimetry 50

4. RESULTS AND DISCUSSION 51

4.1. Synthesis of the hyperbranched polyesters 51

4.2. Determination of the molar mass 66
4.2.1. Results from the ^{1}H NMR spectroscopy 66
4.2.2. Results from the vapour pressure osmometry 78
4.2.3. Results from the MALDI-TOF and ESI mass spectrometry 80
4.2.4. Results from the gel permeation chromatography 89
4.2.5. Results from the static light scattering 96

4.3. Dimensions of the hyperbranched polyesters 98
4.3.1. Results from the dynamic light scattering 98
4.3.2. Results from the ultracentrifugation measurements 104

4.4. Viscosimetry of the diluted solutions 105

4.5. Rheological properties of the hyperbranched polyesters 113
4.5.1. Concentrated solutions 113
4.5.2. Melt rheology 121

4.6. Thermal stability of the hyperbranched polyesters 129

5. CONCLUSIONS 133

6. REFERENCES 136

7. APPENDIX 141

7.1. IR spectra of selected hyperbranched polyesters 141

7.2. NMR spectra of selected hyperbranched polyesters 142
7.2.1. ^{13}C NMR spectra 142
7.2.2. ^{1}H NMR spectra 143

7.3. Mass spectra of selected hyperbranched polyesters 148
7.3.1. MALDI-TOF mass spectra 148
7.3.2. ESI mass spectra 149

7.4. GPC chromatograms of selected hyperbranched polyesters 150

7.5. Rheological measurements of selected hyperbranched polyesters 151
7.5.1. Concentrated solutions 151
7.5.2. Melt rheology 155

8. LIST OF ABBREVIATIONS 156

DECLARATION 157

VITA 158

1. Introduction

The unique, nonlinear structure and specific physical and chemical properties of dendritic polymers, i.e. dendrimers and hyperbranched polymers, have been intensively studied over the last twenty years. According to the increasing number of publications, the interest in these complex, three-dimensional macromolecules is growing rapidly. Their compact structure and presence of a large number of functional end groups enable a spectrum of unusual properties in comparison with analogue linear polymers, and consequently, numerous possible applications.

The synthesis of the perfect dendrimers was first introduced by *Vogtle*[1] in 1978 and in 1985 developed by *Tomalia*[2] and *Newkome*[3]. Dendrimers represent regularly branched, monodisperse polymers with precise functionality and end group multiplicity. They have perfect symmetrical globular shape which can be constructed only in a step-by-step synthesis. These multi-step synthesis procedures consist of numerous protection, deprotection and purification steps, which have to be applied to ensure good definition of the molecular structure. Therefore, synthesis of dendrimers is often very expensive and time consuming, and consequently, restrictive for the use in large scale applications. On the other hand, hyperbranched polymers can be synthesized in one-step polycondensation of AB_x-monomers ($x \geq 2$)[4] at a reasonable cost. Although, this simple procedure yields randomly branched polymers with broad molar mass distribution and less perfect globular shape, hyperbranched polymers resemble dendrimers in many physical and chemical properties. Therefore, hyperbranched polymers are usually considered as irregular analogues of dendrimers and can be used in applications where the perfect structure of dendrimers is less important. The imperfection of their structure originates from the fact that beside fully reacted (dendritic) units, hyperbranched polymers also have some linear units in their structure. As a consequence of that the inner layers of these polymers are usually called pseudo generations.

The most intriguing and at the moment well known properties of hyperbranched polymers are high solubility and reactivity (due to the large number of end groups), low viscosity in solution and melt (as a result of packed structure), absence of entanglement and good compatibility with other materials. These polymers have been used in several applications such as additives[5], coatings[6], blends[7], nonlinear optics[8], in molecular imprinting[9], in catalysis[10], etc. Additionally, some of hyperbranched polymers are already commercially available on the market.

Although, there has been great progress in synthesis and characterization of hyperbranched polymers so far, their full application potentials will not be achieved before complete understanding of the relation between their molecular structure and properties. Therefore, the detailed investigation of the structure and properties in solution, melt and solid state of the self-synthesized and commercial hyperbranched polyesters was the aim of this work, since some of their properties are till now only briefly reported in the literature. Samples of hyperbranched polyesters of the second, third, fourth, fifth, sixth, eighth and tenth pseudo generation were synthesized via pseudo-one-step polycondensation starting from 2,2-bis(hydroxymethyl)propionic acid and di-trimethylolpropane (samples of the series I). The same components were also used for the synthesis of the fourth, sixth and eighth generation samples which was performed via one-step polycondensation (samples of the series II). Beside them, second, third and fourth pseudo generation of the commercial available Boltorn® hyperbranched polyesters with similar structure were also investigated. Seven samples of the hyperbranched polyesters were fractionated. The characterization of these fractions is performed in order to obtain more information about the structure of these polymers. The structure is also investigated with IR and NMR spectroscopy. Side reactions which occurred

during the synthesis of these hyperbranched polymers were qualitatively and quantitatively investigated with NMR spectroscopy, acid number titration, MALDI-TOF and electrospray ionization mass spectrometry. Using several different characterization methods such as NMR spectroscopy, vapour pressure osmometry, MALDI-TOF mass spectrometry, gel permeation chromatography and static light scattering molar mass averages and molar mass distribution of the investigated polyesters were determined. Dimensions of these polymers were measured with techniques like dynamic light scattering and ultracentrifuge and they were also calculated from the results obtained by viscosimetry of the diluted solutions. Rheological properties of all previously mentioned samples were investigated in concentrated solutions and in melt. And finally, the thermal stability of these hyperbranched polymers was determined with thermogravimetry. The obtained results were compared between different pseudo generations of hyperbranched polyesters, between samples synthesized using two different procedures, with commercial hyperbranched polymers, as well as, with modified samples obtained by reacting the end –OH groups with β-alanine or stearic acid.

2. Theoretical Part

2.1. Types of branched polymers

Polymers are traditionally classified according to their macromolecular chain architecture into three categories: linear, cross-linked and branched polymers. Further classification of branched macromolecules is very complex, because modern synthesis methods have enabled numerous different branching structures. Additionally, any unit on a linear chain is a potential branching point for another chain, which can also branch further more or less regularly. Therefore, it is possible to make difference between regularly and statistically branched polymers[11].

2.1.1. Regularly branched polymers

There are three types of regularly branched polymers:
1. regular star polymers,
2. regular comb polymers and
3. dendrimers.

Regular star polymers contain three or more linear chain (arms) emanating from a single branch point (Figure 2.1a). Arms of one star polymer can have identical constitution and degree of polymerization (uniform star polymers) or they can be composed of different monomeric units and have different lengths (nonuniform star polymers). Because of their specific structure, properties of star polymers deviate considerably from those of linear polymers.

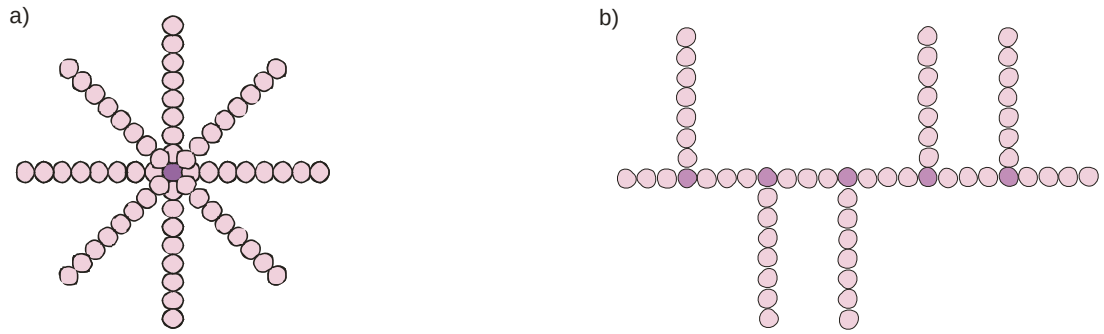

Figure 2.1. a) Regular star polymer, b) regular comb polymer

Regular comb polymers consist of a linear flexible chain of known length (backbone) with multiple trifunctional branch points from each of which (uniformly or randomly) a linear side chain emanates (Figure 2.1b). If the side chains are much shorter than the backbone, structure of comb polymer resembles a linear chain. On the other hand, if the backbone is shorter than the grafted long side chains, structure will approach the behaviour of star molecules.

Dendrimers (*dendron*, Greek = tree) are well-defined, regularly branched macromolecules comprised of AB_x type ($x \geq 2$) monomers attached in concentric layers around a central B_y core (Figure 2.2). Each layer is called a generation, where all B functional groups have reacted with A functional groups from the next layer. Unreacted B functional groups can be found at the surface of the molecule (last generation). Dendrimers possess highly branched, three-dimensional architecture, with a perfect symmetrical globular shape, and therefore, different properties from those of linear polymers of the same molar mass.

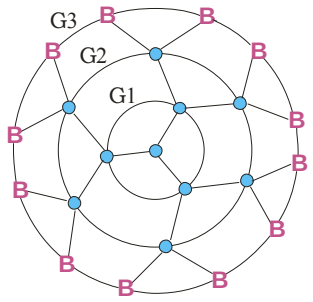

Figure 2.2. Dendrimer

2.1.2. Statistically branched polymers

When regularity of branching is not the aim of the synthesis, statistically branched polymers can be obtained by simple mixing of multifunctional monomers in adequate reaction without any constraints. These kinds of polymers are in fact randomly branched systems, among whose it is supposed that reactivity of all functional groups is the same, and that the reaction between functional groups belonging to the same macromolecule is neglected (ring formation). Randomly branched systems can be studied by theories of random statistics, i.e. by the mean field theory, which is based on the extent of reaction, α_A, as defined by *Flory*[12]:

$$\alpha_A = \frac{[A_t]}{[A_0]} \tag{2.1}$$

where $[A_t]$ is the number of reacted functional groups and $[A_0]$ is the number of all functional groups, while subscripts *t* and *0* denote the time of reaction and the starting time of reaction, respectively. Thus the extent of reaction is actually a probability of reaction. Further, *Stockmayer*[13] has shown that random branched processes will have extremely broad molar mass distribution, which is quite different from all other molar distributions known from the polymerization kinetics of linear chains. Consequently, the treatment of random branching is often called the *Flory-Stockmayer* theory.

However, randomly branched polymers represent an idealized model, since no real system is fully random. Particularly important influence in this case has the presence of excluded volume, because individual monomer units can approach each other only up to their diameter. Excluded volume can cause swelling of the branched structures and provoke the change in expected architectures. Therefore, this kind of system can not be described by the theory of random statistics.

On the other side, hyperbranched (HB) polymers represent a special group of branched structures, for which the mean filed theory can be used (Figure 2.3). They are

formed from AB_x monomers (like dendrimers), where only groups A can react with one of the B groups from another monomer unit to give bond AB. In principle, HB polymers have narrower molar mass distributions compared to randomly branched products. In contrast to dendrimers, HB polymers can have a certain number of unreacted B groups in their inner layers of molecules, which are therefore usually called pseudo generations. The reason for this is, that the extent of reaction α_A of the A groups can have values from 0 to 1, while the extent of reaction α_B, of the equally reactive B groups, cannot become larger than $\alpha_B = \alpha_A /(x\text{-}1)$. As a consequence of this, gelation can never occur, while a much higher branching density than by random polycondensation can be achieved. Although HB polymers are polydisperse and have less perfect globular shape than dendrimers, their properties are quite similar to dendrimers.

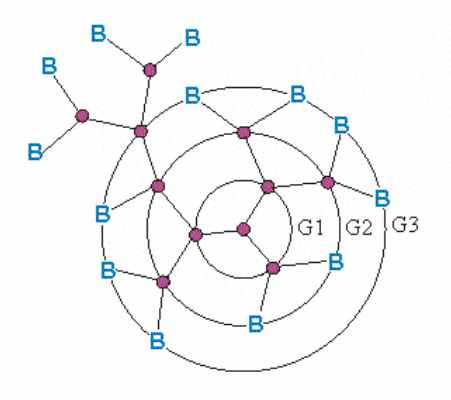

Figure 2.3. Hyperbranched polymer

2.2. Synthesis of dendritic polymers

Flory[14] was the first who had, in the early 1950s, theoretically described the synthesis of highly branched polymers by polycondensation of multifunctional AB_x monomers ($x \geq 2$), where A and B stands for independent functional groups, which can react only with each other and not among themselves. However, because it was presumed that these highly branched, nonentangled polymers would have broad molar mass distribution and poor mechanical properties, further investigation of these polymers was not done. The first paper concerning the synthesis of dendritic polymers was published 30 years later. It turned out, that dendritic polymers have unique and specific properties compared to linear analogues.

2.2.1. Synthesis of dendrimers

In 1978, *Vogtle*[1] introduced a first attempt of dendrimers synthesis, and in the middle of 1980s *Tomalia*[2] and *Newkome*[3] developed further synthesis methods for dendrimers and studied their properties. Since then, a wide variety of different monomers were used to prepare these perfectly branched structures. Some of the compositionally different families of dendrimers published in the literature are based on poly(amidoamines) (PAMAM)[2], poly(arylethers)[15], aliphatic-aromatic and fully aromatic amides[16,17], aliphatic polyethers[18] and polyesters[19], etc. A certain number of dendrimers are also commercially available like PAMAM dendrimers (Dow Chemical Co.) or poly(propyleneimine) (PPI) dendrimers (DSM).

There are two generic, conceptually different methods for the synthesis of dendrimers: the divergent[2] and the convergent[20] approach. Both methods involve multistep polymerization of AB_x - type monomers in a repetitive protection – deprotection manner, often requiring purification between each step. This time consuming, tedious and expensive nature of synthesis is necessary to produce dendrimers possessing concentric layers of repeating units (generations) and branch junctures, without unreacted B groups in the inner generations. Both approaches consist of the stepwise growth of the macromolecule, starting from the branched repeating units, connected in a way to provide a series of regularly, radially concentric generations around the core molecule. In the divergent method, dendrimers growth starts from a polyfunctional central core and proceeds radially outward by addition of monomers (Figure 2.4a). For production of every following generation, the number of needful reactions increases exponentially. The biggest problem in this approach is the possibility of incomplete reactions at dendrimers end groups, which is the primary reason for structural defects in inner generations. The convergent approach starts from the chain ends (periphery of the final macromolecule) and progresses inward by coupling with an AB_x building block to form larger dendrons. Finally, a dendritic macromolecule is formed by attachment of the dendrons to a polyfunctional core (Figure 2.4b). The advantages of the convergent method are that each generation requires limited (usually two) reactions per molecule. Additionally, unreacted material is easily separable, because it is substantially different in molar mass from the product, which significantly decrease number of protection – deprotection and purification reactions, compared with divergent approach.

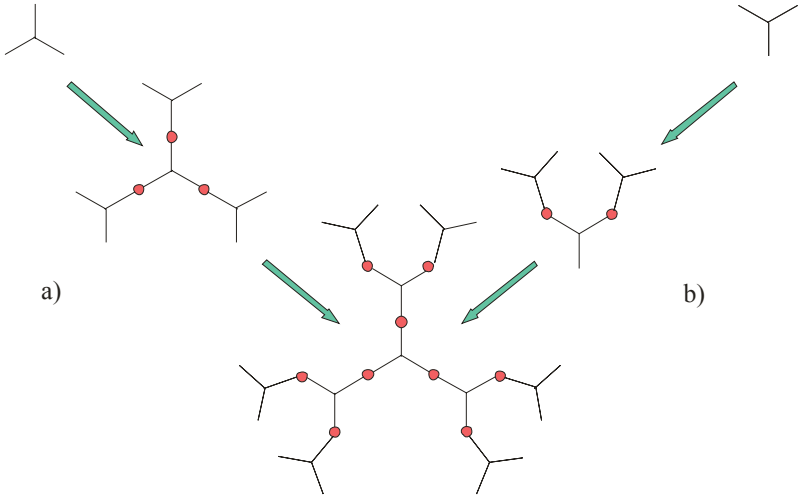

Figure 2.4. Synthesis of dendrimers: a) divergent and b) convergent approach

Dendrimers can also be synthesized by the double – stage convergent approach[21], which is in fact a combination of the divergent and convergent methodologies. In this approach dendrimers of lower generations (or dendrons), synthesized by divergent or convergent method, can be used as a core for a reaction (in a divergent manner) with certain number of convergent dendrons each containing a reactive focal group. In this way, double – stage convergent approach reduce the total number of synthesis and purification steps. To simplify preparation of dendrimers by reducing the number of deprotection steps, an orthogonal approach can be used[22]. In this case, synthesis can be done by the successive use of two different building blocks in two coupling reactions. However, the resulting dendrimers will not be homogeneous in chemical constituents, because two different coupling reactions

give different linkages. Orthogonal approach can be used to obtain homogeneous dendrimers only if these two different reactions are selected to form the same linkage.

Irrespective of which method is used for the dendrimers synthesis many protection – deprotection steps in combination with intermediate purification reactions are needed to ensure the synthesis of perfect globular structure of dendrimers. Consequently, they are quite expensive so their applications are limited to the fields where high costs can be tolerated, like in medicine or specialized electronics.

2.2.2. Synthesis of hyperbranched polymers

To avoid complicated and expensive preparation of dendrimers and still keep some important properties of these regularly branched polymers, *Kim* and *Webster*[5] developed a simpler method for the synthesis of highly branched polymers which they named hyperbranched (HB) polymers. These polymers are polydisperse and their structure is not as perfect as the structure of dendrimers, but they still have some properties that resembles to dendrimers. Since than, they became of interest for many researchers, who had further developed new, interesting routes for their synthesis, using wide spectra of different monomers. Today, the list of HB polymers with different chemical composition is quite long, including also commercially available products, but fully understanding of their properties is still not accomplished. Some of well known HB polymers synthesized and described till now are HB polyphenylenes[5], aromatic[23,24] and aliphatic polyesters[25], polyamides[26], polyethers[27], polyacrylates[28], polycarbonates[29] and polyurethanes[30].

There is a large number of possible ways to synthesize HB polymers. In the early days of research, these polymers were mostly synthesized by one-step polycondensation of multifunctional monomers (AB_x) with functionality two or greater than two. In *Flory*'s theoretical description of synthesis of highly branched polymers starting from AB_x monomers[14], he assumed that only functional group A can react with functional groups B, that intramolecular condensation reaction doesn't occur and that all functional groups have equal reactivity at any stage of the polymerization. With these assumptions gelation is prevented, because all other reactions are excluded except the reaction between A and B functional groups. Using this method for synthesis it is possible to obtain HB macromolecules containing a single A functionality at the focal point. In other words, polycondensation of n AB_x monomers will lead to highly branched structures with one A functional group and (n+1) differently connected B functional groups in every molecule (Figure 2.5). Despite the presence of stoichiometric imbalance in AB_x monomers, a high molar mass polymer can be achieved, because both functionalities are placed on the same molecule. For this reason, it is very important to remove the condensate by using either low pressures or a dry nitrogen purge at high temperatures, since molar mass increases with conversion. Compared to linear polymers, these HB polymers possess numerous branching and end groups. However, loss of the unique A functionality can occur if intramolecular cyclization reaction between functional groups A and B from the same growing chain take place during the synthesis. Another possible side reaction can happen between two B groups of one molecule resulting in ring formation. On the other side, if intermolecular reaction occurs between B groups of different molecules than this reaction can lead to molecules with two or more A groups and can result in the formation of cross-linked structures and subsequently to gelation. The occurrence of this side reaction can often be excluded, because it depends on the type of monomer and the reaction conditions.

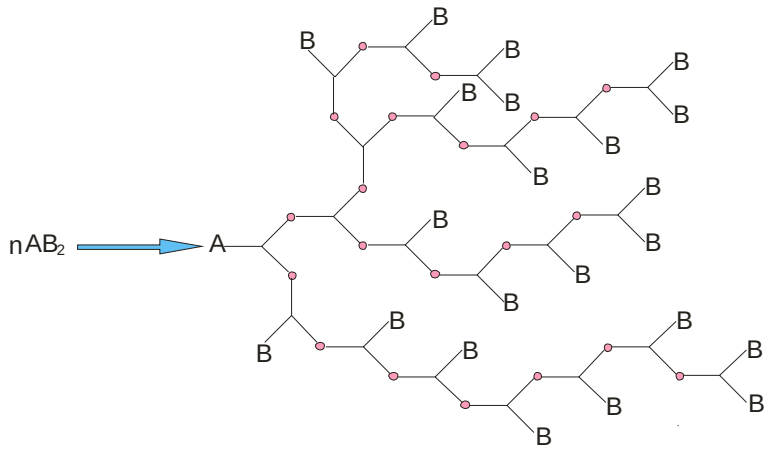

Figure 2.5. Polymerization of AB_2 monomers

The major drawback of homopolymerization of AB_x monomers is that the final product will have highly irregular structure and extremely broad molar mass distribution. *Müller* and co-workers used a kinetic approach to show that the polydispersity index of AB_2 HB polymers is approximately $P_n/2$ at high conversions, where P_n is the number average degree of polymerization[31]. Broad molar mass distributions can have a significant influence on properties of HB polymers, especially on solution properties. However, by copolymerization of AB_x monomers with B_y core molecules, polydispersity can be lowered considerably. In this method, growing HB molecules are coupling with multifunctional molecules B_y, which is actually analogue to the core in dendrimers (Figure 2.6). The polydispersity initially increases, reaches a maximum, but when the polycondensation is near to the end, the presence of a small amount of core moiety will cause a considerable narrowing of the molar mass distribution. Also, the greater the number of the functional groups of the core, the narrower the molar mass distribution will be[32]. The decrease in polydispersity can be quantitatively expressed as $(1+1/y)$, where y is the core functionality[33]. By varying the core/monomer ratio it is possible to systematically obtain HB polymers of different molar masses.

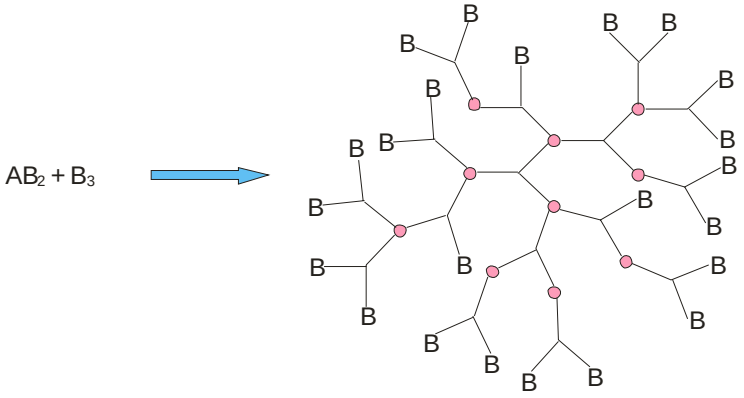

Figure 2.6. Copolymerization of AB_2 monomers with B_3 core molecule

Using this method, *Hult* and co-workers[34] have synthesized aliphatic HB polyesters in the molten state, starting from 2,2-bis(hydroxymethyl)propionic acid (bis-MPA), as AB_2 monomer, and 2-ethyl-2-(hydroxymethyl)-1,3-propanediol (TMP) as a core moiety. The synthesis was done as a common acid catalyzed esterification reaction, with continuous water

removing in order to achieve high molar mass of the final product (Figure 2.7). The reaction was also controlled by successive adding of bis-MPA portions corresponding to the stoichometric amount for the next theoretical pseudo generation, to favour the reaction between unreacted acid groups with the hydroxyl-functional HB skeleton and not with another free monomer. Therefore, the synthesis was done as pseudo-one-step procedure. In order to prevent unwanted side reactions (etherification and trans-esterification), a low reaction temperature (140 ^{0}C) was chosen. The obtained HB polyester had high solubility in common solvents and relatively low polydispersity. This work resulted in the commercially available HB polyesters (Perstorp, Boltorn®), which are based on bis-MPA, as an AB_2 monomer, and tetrafunctional ethoxylated pentaerythritol (PP50) core.

Using the same reaction conditions, polymerisation of bis-MPA will result in a gel only few hours after being heated[35]. The final product is insoluble and rubberlike, probably due to the high molar mass or cross-linking. This shows the importance of the core moiety. Furthermore, it was shown that the presence of a core molecule during the synthesis will provide HB polymers which have properties more resembling to that of dendrimers, which is less probable for the HB polymers obtained by polymerization without core[36]. By using this method for synthesis of HB polymers, it is easier to control geometrical shape and to achieve higher degree of branching.

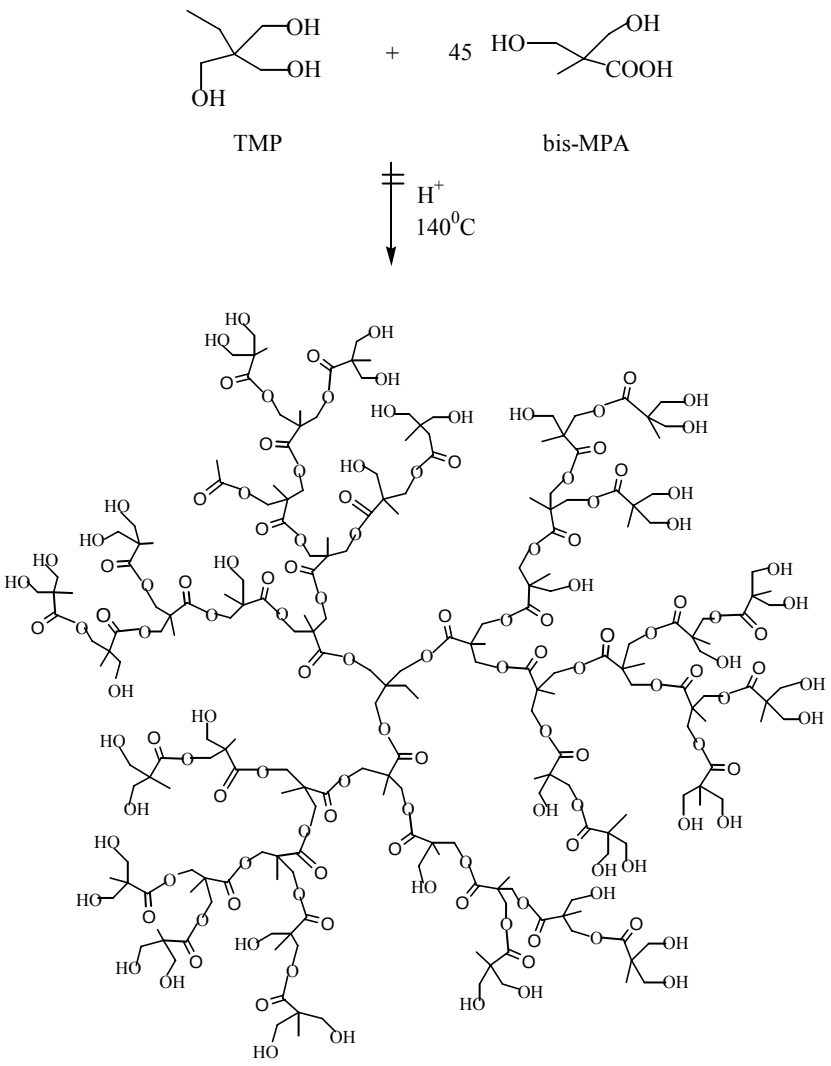

Figure 2.7. Schematic representation of the synthesis of hydroxyfunctional HB polyester, as described by *Hult* and co-workers[34]

However, during the polycondensation of multifunctional monomers (AB_x or AB_x/B_y case), a reaction between A and B functional groups may occur intermolecularly to give polymer growth or it may occur intramolecularly which will lead to ring formation. In many theoretical treatments, including *Flory*'s discussion of AB_x polycondensation[14], the presence of cycles is neglected, even if it is known that cyclization can have big influence on structure and properties of HB polymers, especially on reaction kinetics and molar mass. In contrast to linear polycondensation, where cyclization will lead to termination of growth, because two reactive chain ends are removed, cycles formed in HB polymers can react further due to the presence of a large number of B reactive functional groups, so that the degree of polymerization of the entire molecule will still increase. Usually, the extent of cyclization depends on used method for the synthesis and on the monomer structure. Mostly, cyclization was observed when highly flexible monomers are used for the polymerization. As mentioned before in AB_x polycondensation, due to the intramolecular cyclization reaction between B functional groups and single A functionality (focal point) present in the same HB macromolecule, loss of this unique A functionality will occur. Polymerization will still proceed but only through B groups. According to the *Monte-Carlo* simulation of distributions composed of acyclic and cyclic molecules formed during the AB_2 polymerization, number and weight average molar masses do not change but reach some limiting values[37]. It was also found that the final values of molar masses depend on the extent of cyclization and distribution of cycles among molecules of different size. During the synthesis of HB polyesters (starting from AB_x monomers) it is possible that transesterification reactions are involved, so the formation of cycles is often explained as "backbiting degradation"[38]. *Kricheldorf* and co-workers have shown that the extent of cyclization increases with conversion (i.e. with increasing molar mass), that cyclization limits the chain growth and that at 100% conversion all reaction products are cyclic[39]. According to them, large HB molecules have a bigger ability to cyclization due to the larger number of B functional groups. In other words, cycles are present at each degree of polymerization.

On the other side, appearance of cyclization during the copolymerization of AB_x monomers with core molecules is studied very seldom. However, during the synthesis growing HB species are capable to form poly – B – functional macrocycles by intramolecular cyclization, which competes with the desired intermolecular reaction (Figure 2.8). In this way, additional polyfunctional B_n core is formed. Because of that, the influence of this side reaction has to be taken into account.

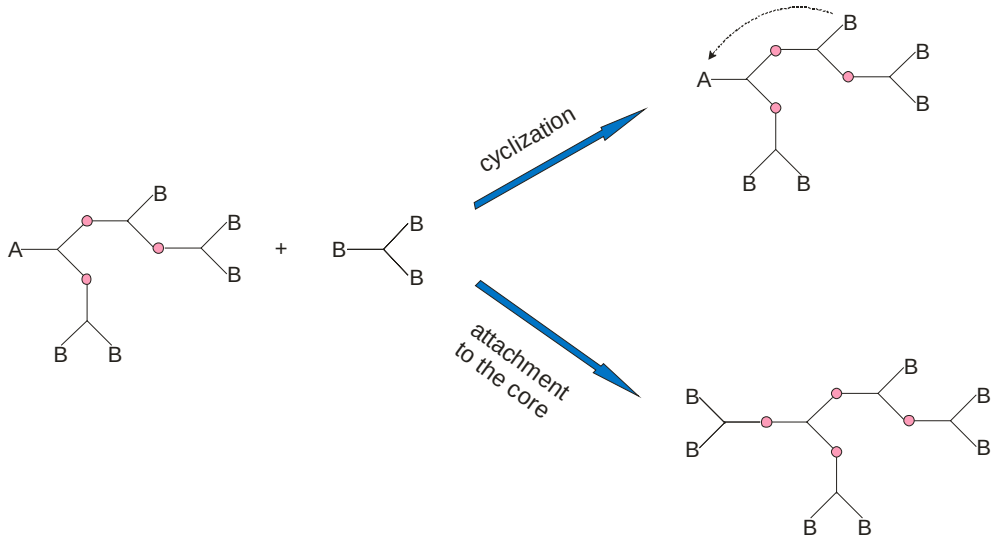

Figure 2.8. Possible reactions during the copolymerization of AB_2 monomer with B_3 core molecule[40]

To derive the expression for the extent of cyclization in AB_x or AB_x/B_y polycondensation, it is necessary to start from the basic equation which is related to the polycondensation kinetics. The growth of the macromolecular chain can be described by the number average degree of polymerization, P_n, which is connected to the conversion p of the individual functional groups by the so-called *Carother's* equation[12]:

$$P_n = \frac{1}{1-p} \tag{2.2}$$

The conversion is defined as the number of molecules present in the reaction mixture at a certain time over the number of molecules present before any reaction has occurred. When ^{1}H NMR is used to analyze HB polymers synthesized by AB_x or AB_x/B_y polycondensation, P_n can be calculated from the integrals of the signals corresponding to the groups present in the investigated HB structure. Degree of polymerization $(P_n)_{NMR}$ calculated using the informations from ^{1}H NMR spectra is usually called "apparent degree of polymerization"[40]. The actual P_n can be determined using some absolute molar mass method (e.g. vapour pressure osmometry – VPO). If during the polycondensation reaction (AB_2 or AB_2/B_y case) no cyclization occurs, $(P_n)_{NMR}$ and P_n will have the same value. However, the probability of cyclization for this kind of reactions is very high. Using $(P_n)_{NMR}$ and P_n it is possible to calculate the extent of cyclization, ξ, i.e. the number of cyclic molecules, N_{cycles}, compared to the total number of molecules in the mixture, N[40]:

$$\xi = \frac{N_{cycles}}{N} = \frac{N - N_{NMR}}{N} = 1 - \frac{P_n}{(P_n)_{NMR}} = 1 - \frac{M_n}{(M_n)_{NMR}} \tag{2.3}$$

In the last equation, N_{cycles} is the difference between the measured number of molecules N (VPO) and the apparent number of molecules N_{NMR} (^{1}H NMR), while M_n and $(M_n)_{NMR}$ are number average molar masses determined using some absolute method and NMR spectroscopy, respectively.

It was shown that at a given conversion, the fraction of cyclic structures in HB polymers without the core molecule increases with increasing molar mass[37], while in HB polymers with the core molecule it decreases[40]. Presence of the cycles in HB polymers can be also detected by Electrospray Ionization Mass Spectrometry (ESI MS) or by Matrix Assisted Laser Desorption/Ionization Time of Flight Mass Spectrometry (MALDI-TOF MS).

Beside the two already described methods for the synthesis of HB polymers (AB_x and AB_x/B_y polymerization) there is a large number of other reactions that can be used to prepare this type of polymers, such as controlled copolymerization of A_2 and B_3 monomers which has to be stopped prior the gel point[41] or ring opening polymerization of cyclic AB_2 monomers[42]. *Fréchet* and co-workers[43] developed a self – condensing vinyl polymerization (SCVP) method for synthesis HB polymers starting from vinyl monomers. After the activation of B groups in monomers an initiator – monomer ("inimer") is formed (Figure 2.9). Group B* is capable of initiating the propagation of vinyl group in monomer, forming a dimer with a vinyl group, a growth site and an initiating site. Further polymerization steps will lead to the HB polymer.

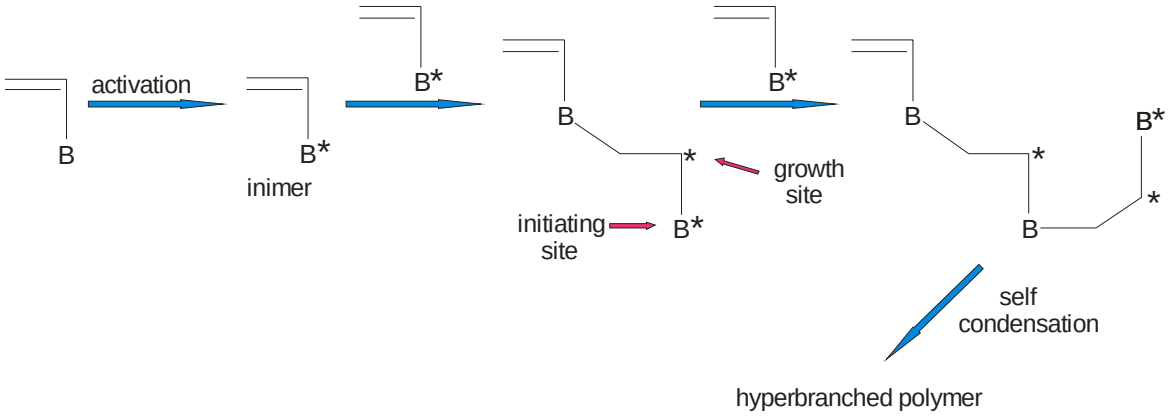

Figure 2.9. Schematic representation of the SCVP[43]

The disadvantages of SCVP are side reactions which can lead to gelation. Also, molar mass distribution is very broad and it is complicated to determine the degree of branching. Since the functional group B* can be transformed to an active centre (such as cationic or radical) living cationic[43] and atom transfer radical polymerization (ATRP)[28] have been applied to synthesize HB polymers by SCVP, to avoid cross-linking.

2.3. Structure of dendritic polymers

As mentioned before, dendrimers are regularly branched polymers which consist of a core molecule, layers of branched repeating units (i.e. dendritic units) and terminal groups (peripheral of the molecule). According to this, successive generations radiate outwardly from the core, which makes the core a centre of symmetry for the entire molecule. As the number of generation increases, sphericity of the dendrimers is also increasing. However, a large number of bonds in the interior of the dendrimers provide a certain range of conformations, and subsequently the core is not necessarily the physical centre of the dendrimers nor are all end groups located at the periphery. Because of the highly branched structure of dendrimers, the mass of the molecule increases exponentially and more rapidly with the number of generation than the available volume. This is known as a concept of the "starburst limit" from which it is obvious that there is a point beyond which the dendrimers cannot grow because of a lack of space. This mostly depends on core functionality, the branching multiplicity, the branch length and the volumes of the core and branches. The effect of such behaviour is that dendrimers of lower generation have a structure similar to those of star polymers and a large number of possible conformations, while the high generation dendrimers have a densely packed radial structure and exhibit much less internal degree of freedom. Several theoretical studies have investigated the structure of flexible dendrimers in solution, because of their application as nanocapsules.

De Gennes and *Hervet*[44] suggested the first model for the conformation of dendrimers with large linear segments between successive branch points in a good solvent. According to this model, segment density is low in the centre and increasing parabolically with generation to unity ("dense shell" model), with all end groups placed on the periphery of the molecule. However, by simulation of random growth in dendrimers with flexible spacers it is concluded that the segment density has its maximum in the core ("dense core" model)[45]. It is also observed, that higher generations of dendrimers show considering flexibility, so that the end

groups can be found in the entire volume of the dendrimers as a consequence of back-folding of the chains toward to the core. End groups will be mostly located in the periphery of the dendrimer, but there is a finite probability to find certain number of end groups in the interior of the dendrimer, near to the core. With a help of small-angle X-ray scattering (SAXS) experiments performed on PAMAM dendrimers, it was demonstrated that they act as a homogeneous sphere with a relatively uniform density profile[46]. In a good solvent the internal configuration of dendrimers is quite open, while in a poor solvent they possess more globular shape, which makes them ideal for the guest-host chemistry[47]. On the other side, recent study of *Petkov* and co-workers[48] of PAMAM dendrimers of higher generation have shown that they have a globular shape and a relatively open structure, when they are not affected by any solvent. Another property that was found in this study was that branches inside dendrimers are not arranged in exactly concentric shells, but in a semi-regular pattern. Beside PAMAM dendrimers, this group of researchers has also studied HB PAMAM macromolecules with the same characterization methods. They found out that HB macromolecules have irregular atomic arrangement and no globular shape, with relatively open structure. Because of that, their interior is less accessible than that of dendrimers, but they still may be used in controlled delivery applications.

The imperfection of the structure of HB polymers originates from the fact that beside fully reacted (dendritic) and unreacted (terminal) units, HB polymers have also some linear units in their molecular structure. As can be seen from the Figure 2.10, in dendritic units all B groups have reacted, linear units have one unreacted B group, while terminal units possess two unreacted B groups. Linear segments in the structure of HB polymers are usually described as defects and their presence has big influence on physical properties of these macromolecules, such as glass temperature, melting point, crystallinity, etc. To define and better understand structure of HB polymers, *Fréchet* and co-workers[23] introduced the average degree of branching, *DB*, for the HB polymers formed in the polycondensation of AB_2 monomers, which can be calculated with the following equation:

$$DB_{\text{Frechet}} = \frac{n_{\text{D}} + n_{\text{T}}}{n_{\text{D}} + n_{\text{L}} + n_{\text{T}}} \tag{2.4}$$

where n_{D}, n_{T} and n_{L} represent the numbers of dendritic, terminal and linear units, respectively. The core of the molecule is not counted as a unit and that is the reason why it is not taken into account. *Fréchet*'s definition of *DB* has one disadvantage, since he didn't consider the fact that the presence of unreacted monomer can bring to overestimating of the *DB*. In other words, monomer units have terminal groups, which can contribute to the *DB*. Furthermore, *DB* for the perfect dendrimers should be 1, for the linear structures 0 and consequently, *DB* for the HB polymers is between 0 and 1. However, according to the *Fréchet* definition, linear polymers based on AB_2 monomers have $DB > 0$, because of the presence of terminal groups. Therefore, *Frey*[49] proposed another definition for *DB*, where the active number of growth directions of the polymer chain is compared to the maximum number of growth directions:

$$DB_{\text{Frey}} = \frac{2n_{\text{D}}}{2n_{\text{D}} + n_{\text{L}}} \tag{2.5}$$

Most HB polymers, formed by the polymerization of AB_2 monomers or by copolymerization of the core molecule B_y with AB_2 monomers, have a *DB* close to the 0.5, or in ideal case 0.5, when the reactivity of all functional groups is the same.

Experimentally *DB* can be calculated from ^{13}C NMR spectra by comparing the integrals of the different units (D, T and L) in the HB polymer. If the position of peaks

corresponding to different units is not known, model compounds resembling to repeat units in HB polymer should be synthesized and characterized with ^{13}C NMR. Another method that can be used to calculate *DB* is the modification of end groups and thence fully degradation of HB skeleton by hydrolysis[50]. Using capillary chromatography, degradation products can be identified. Theoretically and experimentally it was shown that the *DB* of HB polymers can be enhanced by three different methods: (i) slow addition of AB_x monomers to the core molecule B_y in solution (core dilution/slow monomer addition technique)[51], (ii) activation of the second B groups of the AB_2 units, after reaction of the first B group[49] and (iii) polymerization of prefabricated perfect dendrons[52].

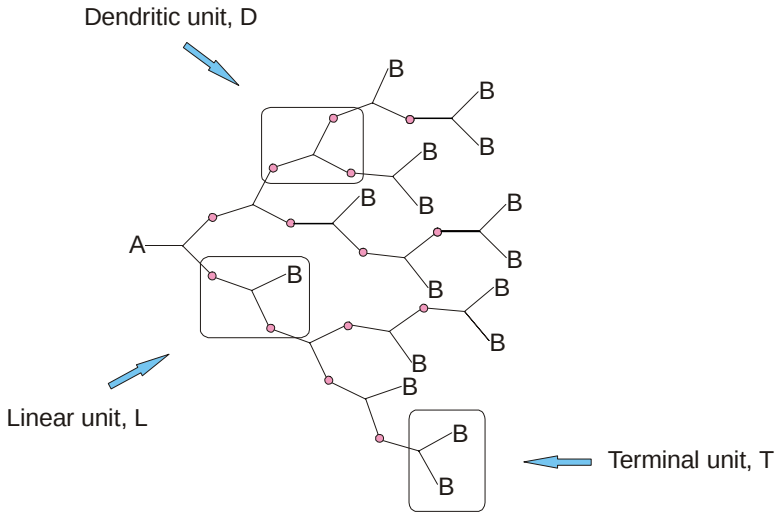

Figure 2.10. Different types of units present in the structure of HB polymer

However, *DB* cannot give the full picture about the topology of HB polymers. One of the reasons for this is the possibility of forming isomeric structures due to the random adding of monomers during the polymerization. Another alternative parameter that can be used to describe the molecular architecture of HB polymers is the branching ratio or "shrinking" factor (*g*) which can be calculated in the following manners[53]:

$$g = \frac{\left\langle R_g^2 \right\rangle_{branched}}{\left\langle R_g^2 \right\rangle_{linear}} \quad \text{or} \quad g' = \frac{[\eta]_{branched}}{[\eta]_{linear}} \tag{2.6}$$

$\left\langle R_g^2 \right\rangle_{branched}$ and $\left\langle R_g^2 \right\rangle_{linear}$ represent the mean-square radius of gyration and $[\eta]_{branched}$ and $[\eta]_{linear}$ the limiting viscosity number of the given HB polymer and its linear analogue, respectively. Because of their amorphous nature, HB polymers are less densely packed in solid state than linear analogues of the same molar mass. Nevertheless, in a good solvent HB molecules are less solvated than linear polymers due to their branched structure and hence their dimensions are smaller. In these conditions, completely dissolved linear polymers become larger, because the entangled chains and the crystalline regions are free of restricting forces. Beside this, the dimensions and molar mass of HB polymers decreases with increasing *DB*. Therefore, the branching ratio can be used to get more information about relative *DB* of HB polymers.

However, the structure of HB polymers in solution is still not completely understood. It can be only concluded that they have more globular shape than analogue linear polymers.

There are so many different parameters that have big influence on the structure of HB polymers, like the effect of monomer size on the molecule density or the influence of the nature of solvent. All these have to be taken into account when the discussion of HB structure is made.

2.4. Properties of dendritic polymers

The reasons for increasing interest in dendritic polymers are their unique and specific properties that mostly distinguish them form those of linear analogues (i.e. linear polymers of the same nature and molar mass). As discussed in previous chapters, in contrast to the tedious and expensive synthesis of dendrimers, HB polymers are produced more rapidly and economically on a large scale trough a one-step polycondensation reaction. Despite the fact that this way of synthesis will cause irregular branching and broad molar mass distribution, and consequently, will make experimental characterization more difficult, HB polymers still resemble dendrimers in several unusual properties, specific for this type of polymers. Because of their highly branched architecture and presence of a large number of end groups, HB polymers exhibit (like dendrimers) lower viscosity in solution and in the molten state[54,55], better solubility in common organic solvents[56], lower degree of entanglement[57], a different relationship between hydrodynamic volume and molar mass[44] than linear polymers. The presence of the large number of terminal functional groups in these polymers has a big influence on polymer miscibility and solubility[58], as well as on the molecular relaxation processes[59], thermal behaviour and viscosity[55]. Furthermore, by modification of end groups chemical and physical properties can be tailored and controlled, especially glass transition temperature[60] and properties in solution[56]. Therefore, although HB polymers can be structurally considered as intermediates between linear polymers and perfect dendrimers, they still mimic most of the interesting properties of dendrimers and can be used to replace dendrimers in most cases. Additionally, modern chemistry has provided the possibility to synthesize a large variation of different HB polymers, which are already reported in the literature. Each of this new HB structures has some specific properties which can be used to increase their field of applications. As a consequence of that, detailed description and explanation of properties of HB polymers has to be done stepwise, with a periodical retrospective view on properties of dendrimers and linear polymers.

2.4.1. Molar mass and molar mass distribution

It is important to know the average molar mass and the molar mass distribution of polymers, because these parameters have a big influence on physical properties, processing behaviour of polymers and consequently, on their application areas. By controlling both, molar mass and molar mass distribution, properties like melt viscosity, solubility, mechanical and thermal behaviour can be regulated[61]. Depending on which method is used for measurements, the number average molar mass, M_n, or the weight average molar mass, M_w, can be obtained. The ratio between these two molar mass averages (M_w/M_n) is called polydispersity index and can give more information about the breadth of the molar mass range in a polymer sample.

Theoretically and experimentally was shown that HB polymers have a very wide molar mass distribution. One of the reasons for such broad molar mass distribution of these polymers is the fact that in their structure branched and linear repeating units can be found.

Another reason is that the rate of a given HB species added to other ones during the synthesis is proportional to the number of its functional groups, while at the same time, the number of functional groups is proportional to its degree of polymerization. This means that large molecules grow faster than smaller ones, broadening the molar mass distribution of the final products. Therefore, the width of distribution for the branched polymers increases asymptotically with the weight average degree of polymerization[11]. In the case when HB polymers are synthesized from AB_x monomers, molar mass averages (M_n and M_w) depend on conversion p, and functionality x of the monomer. When reaction approaches completion (high values of p), the molar mass distribution is very broad and polydispersity index is assumed to achieve infinity. By adding a small amount of multifunctional core molecule, B_y, to the polycondensation reaction of AB_x monomers, the molar mass average can be controlled and molar mass distribution can be reduced. This can also prevent in certain extent the coupling of the polymeric species itself. Molar mass of the final HB polymer will depend on core/monomer ratio, while polydispersity depends on the core functionality[32]. *Feast* and *Stainton*[62] have shown that if the core content is increased during the synthesis of HB polymer, the molar mass decrease rapidly. This was observed for the HB polyester after 5 hours of polymerization. However, *Parker* and *Feast*[63] have observed that if longer polymerization times are applied, the molar mass of the final HB polyester can be remarkably increased. A possible reason for this behaviour is, that 5 hours of polymerization is not enough for the complete consumption of the A groups in monomers or further polymerization proceeds via an alternative mechanism, e.g. ester-ester interchange. *Parker* and *Feast* have also tried to explain the influence of the core functionality on the molar mass and molar mass distribution, by comparing B_2 and B_3 core systems. They have synthesized a series of HB polyesters, starting from AB_2 monomer dimethyl 5-(2-hydroxy-ethoxy) isophthalate and core molecules of different functionality (B_2 and B_3). Theoretically, if it is assumed that all B core groups are used and that the core molecule is completely terminated, then for a certain core/monomer ratio, the average molar mass will not depend on the core functionality. In other words, a structure with a B_3 core will have, on average, the same number of incorporated monomer units as in the case of B_2 core, but distributed among three arms rather than two. However, the HB polyester used by *Parker* and *Feast* shows some deviations from the previous theoretical description, which can be observed on Figure 2.11. If the molar mass is plotted versus the core/monomer ratio, it can be seen that the presence of more B core groups will cause a great lowering of the molar mass. This can be explained by the fact that the investigated HB polyesters were not fully core-terminated and that they are actually mixtures of macromolecules derived from either a simple AB_2 polycondensation, ultimately terminated by cyclization, or core-terminated species. B_2 core system have lower amounts of core-terminated species and more macromolecules arising from AB_2 polycondensation, which is the reason for the higher average molar mass in contrast to the B_3 core system, since the simple AB_2 polycondensation tend to give higher molar masses than AB_2/B_y system. Therefore, according to *Parker* and *Feast*, the lowering of the polydispersity by copolymerization of AB_x monomers with a core molecule is maybe just a consequence of the lower molar masses present in the core-terminated systems.

Another problem that has to be taken into account, when a discussion about molar mass averages and molar mass distribution of HB polymers is made, is a big influence of the side reactions. Deviations from the expected molar mass are usually caused by cyclization or intra- or inter-molecular reaction of two B groups, which compete with the desired intermolecular reaction between A and B groups. The occurrence of the intramolecular reactions increases the number of molecules, and that is the reason why M_n does not continue to rise but reaches a maximum value after relatively short times of polymerization, which has a big influence on polydispersity. The presence of the side reaction, especially cyclization, is an important deviation from the growth behaviour predicted by *Flory*[14].

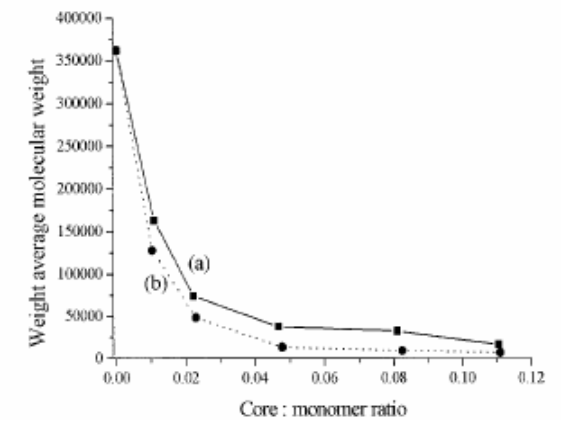

Figure 2.11. The influence of the core functionality upon the molar mass of HB polyesters obtained by *Parker* and *Feast*[63]. a) B_2 core, b) B_3 core system

2.4.1.1. Vapour pressure osmometry

Vapour pressure osmometry (VPO) is a well known method for the determination of molar mass, and it is more suitable than membrane osmometry for analysis of dendritic polymers, because of their small dimensions and (in some cases) relatively law values of molar mass. VPO is based on the fact that the vapour pressure of a solution is lower than that of the pure solvent at the same temperature and pressure. If different concentrations of the dilute solutions of polymers are used for the measurements, decrease of the vapour pressure is directly proportional to the molar concentration of the dissolved polymer, which can be used to obtain molar mass. Since the depression of the vapour pressure of a solution is one of the colligative properties (properties that depend only on the number of particles in the solution and not on their nature), by VPO it is possible to determine the number average molar mass, M_n, of a polymer with a help of the following equation[64]:

$$\frac{\Delta T}{c} = K_e^{th}\left(\frac{1}{M_n} + A_{2,v}\,\rho_0\,c\right) \tag{2.7}$$

where ΔT is the temperature change, measured by the change in resistance of the thermistor, c is the concentration of the solution in g/kg, $A_{2,v}$ is the second virial coefficient of vapour pressure osmosis, ρ_0 is the density of the solvent and K_e^{th} is a theoretical calibration constant, which can be obtained from the enthalpy of vaporization, ΔH_v, gas constant, R, and absolute temperature, T:

$$K_e^{th} = \frac{RT^2}{\Delta H_v} \tag{2.8}$$

However, it was experimentally shown that the deviations of the measured values can be corrected by using an experimental rather than the theoretical calibration constant. The experimental calibration constant, K_e^{exp}, can be obtained by measuring the voltage change

(quantity usually measured in the vapour pressure osmometry instruments) and c for a series of known molar mass species. A voltage change is proportional to the temperature difference ΔT. By plotting ratio between voltage change and concentration versus c, experimental calibration constant can be graphically calculated. K_e^{exp} can then be used in the reverse manner to determine the molar mass of the measured polymer sample.

VPO has been used in several cases to determine number average molar mass of dendritic polymers[65,66,40], since this method is independent from the structure of the samples. Therefore, VPO can be considered as a reliable method for analysis of HB polymers, and furthermore, it can be used in combination with ^{1}H NMR to calculate the extent of cyclization according to the equation (2.3).

2.4.1.2. Mass spectrometry

Methods of mass spectrometry have been often employed as a useful tool for analyzing dendritic polymers, since they can achieve a better understanding of the effects of polymer structure upon the physical properties. One of the frequently used methods is MALDI-TOF mass spectrometry, which can provide information about molar mass averages, molar mass distribution and end group compositions. MALDI-TOF MS is mostly used in the analysis of biopolymers such as proteins, but also for the characterization of synthetic polymers as well as for dendritic polymers. In MALDI-TOF mass spectrometry, ionization of the sample is achieved by bombardment of sample molecules with laser light. Preparation of the sample, taking place before the measurement, has to include a highly absorbing matrix compound, which is pre-mixed with the sample. The presence of the matrix compound will lead to the transformation of the laser energy into excitation energy for the sample. In this way, most of the laser energy is absorbed by the matrix, which prevents unwanted decomposition of the investigated sample. Therefore, a low concentration of the sample to matrix works the best. The ionized molecules travel through a flight tube, where the time-of-flight analyser separates different ions according to their mass to charge ratio (m/z) and reach the detector at different times (the lighter ions are faster than the heavier ones). By using MALDI-TOF mass spectrometry for characterization of polymers, a distribution of oligomers can be detected, from which one can obtain the mass of each oligomer, the average molar mass and the polydispersity. Usually, in the mass spectra of polymers, peaks which correspondent to every oligomer are located at the equal distances that reflect the mass of the polymer repeating unit.

However, when the molar mass of the polymer or its polydispersity is relatively high (which is the case for HB polymers), the reliability of MALDI-TOF is decreasing, because in that case it is very difficult to determine if the entire molar mass distribution travels equally through the spectrometer tube. Furthermore, higher laser power, that is necessary to apply for the high molar mass species to have desired desorption/ionization process, can cause, that high mass component have smaller peak areas and therefore narrower polydispersity. These greater levels of laser power can also lead to a fragmentation of components of the lower degree of polymerization, which can bring an error in the determination of the molar mass averages of polydisperse polymers by MALDI-TOF mass spectrometry[67,68]. However, by using this method it is possible to obtain the masses of individual oligomers in the low molar mass region for these types of polymers.

In the case of HB polymers (with or without a core molecule), this method is mostly used as a powerful technique to verify the presence of the cyclic structures by comparing the m/z values with the possible products[36,40,63,69]. When HB aliphatic polyesters (synthesized from TMP-core and bis-MPA as a monomer) were studied with the help of MALDI-TOF MS, it was possible to distinguish the cyclization and attachment of the monomers to the core

molecule. This research was done by *Frey* and co-workers[40]. According to the mass peaks obtained in the MALDI-TOF mass spectra of HB polyesters, molar masses for the several possible reactions were calculated, by a consideration of the polymerization process. From the obtained results *Frey* and co-workers have concluded, that the molar mass was increasing from the second to the fifth pseudo generation of HB polyester, however the peak maximum was shifted only slightly. Besides the main peaks, series of other peaks of lower intensity were also detected, which were ascribed to the cyclized species. The intensity of the secondary peaks was much stronger for the higher pseudo generations. This indicates that when a larger amount of the monomer is copolymerized with the core molecule, the probability for the cyclization is increasing. Similar conclusions were derived for the HB poly(amidoamine)[36], HB polyesters based on dimethyl 5-(2-hydroxyethoxy)isophthalate[63] and HB poly(arylene ether)s[69].

Another mass spectrometric method that can be used for characterization of dendritic polymers is ESI mass spectrometry. To apply this method, the sample has to be dissolved in a polar, volatile solvent and then this solution is pumped through a capillary with a known flow rate. Due to the high voltage applied to the tip of the capillary and existence of the strong electric field, the sample emerging from the tip is dispersed into an aerosol of highly charged droplets. With a help of a drying gas, the solvent evaporates from the charged droplets, and consequently charged sample ions (free from the solvent) are released from the droplets and travel further into the analyser of the mass spectrometer[70]. With this very sensitive analytical method cyclic species in the structure of HB polymers can be detected[37,71].

2.4.1.3. Gel permeation chromatography

The measurements on GPC are based on a separation phenomenon which is accomplished on a column packed with a highly porous material that separates the polymer molecules according to size (sometimes the general technique is called size exclusion chromatography - SEC). Therefore, separation is based on the hydrodynamic volume. Since small molecules can diffuse into the pores of the column packing, they are eluted last, in contrast to high molar mass fractions. Detection of polymer fractions is usually done by refractive index or spectroscopic (ultraviolet and infrared) detectors. Because GPC is a relative method for molar mass determination, it is necessary to calibrate particular GPC column with polymer standards of known molar mass and narrow molar mass distribution. Therefore, unknown molar mass at a given retention volume can be determined by comparing the obtained chromatogram with a reference chromatogram of standard polymers of different molar mass fractions in the same solvent and at the same temperature[61].

When GPC is used to determine molar mass distribution of dendritic polymers, several problems have to be taken into account. In this method calibration is usually done by linear polymer standards, which can cause big error in measurements, since dendritic polymers have different relationship between hydrodynamic radius, R_h, and molar mass than those for their linear counterparts of the same molar mass[44]. The hydrodynamic chain size of dendritic polymers does not increase with molar mass as much as in the case of linear polymers. Also, R_h of HB polymers depends on the degree of polymerization, degree of branching and possible solvent-polymer interactions. Because of their branched structure, R_h of dendritic polymers is smaller than for the linear analogues. Therefore, molar masses determined with GPC can be lower than real values if linear polymer standards are used for calibration. A second problem can arise from the fact that dendritic polymers possess a large number of (in most cases polar) end groups. This can cause interaction and adsorption of dendritic polymers in the stationary phase of the GPC column[36]. Beside this, depending on how dendritic

molecules interact with the solvent, they can occupy different volumes, i.e. aggregation can occur[72], which will further lead to erroneous molar mass characterization. However, in some cases it is possible to use GPC for characterization of HB polymers if the interaction with the column is prevented. This can be done by end capping HB polymer with some relatively non-polar groups[73]. Additionally, if the sample solutions are prepared without aggregation, fractions of HB polymer can be characterized by GPC[71].

2.4.1.4. Static light scattering

Another widely used and highly effective method for the characterization of polymer samples is static light scattering (SLS). With this method the absolute molar mass can be obtained, because no reference is needed and no further assumption about the polymer or its behaviour has to be made. Beside molar mass, SLS can give information about the radius of gyration, R_g, and the second virial coefficient, A_2, which are the properties that can provide certain knowledge about the shape and the nature of the molecule in the solution.

When electromagnetic ray of light in its path come across one small spherical particle, then the electric field of the light wave, E, will induce a dipole in the particle, having magnitude P[74]:

$$P = \alpha_P E \tag{2.9}$$

where α_P is the polarizability of the particle. The dipole P will oscillate with the same frequency as that of the incident beam and will itself radiate energy in the form of light, which is called scattered light or secondary radiation. The scattered light has lower intensity than incident light, different direction of scattering and it is coherent, i.e. capable to interference. This type of light scattering is called static light scattering. If a ray of light passes through the pure liquid, scattering will be very small and it arises from finite inhomogeneities in the distribution of molecules within adjacent areas that give rise to differences in density. However, when a dilute solution of large polymer molecules in a pure liquid of low molar mass is made, each large particle will have its own separate contribution to the scattering of light. The intensity of the light scattered from a polymer solution depends on the intensity, I_0, and the wavelength, λ_0, of the incident light, refractive index of the solution, n, and solvent, n_0, weight average molar mass, M_w, radius of gyration, R_g, the shape of the macromolecules in solution, interaction between macromolecules and solvent described by the virial coefficients A_2 and A_3, and angle θ at which the scattered light is measured relative to the direction of the incident light. To calculate molar mass and dimensions of the polymer in dilute solution the following equation can be used[74,75]:

$$\frac{Kc}{R_\theta} = \frac{1}{M_w P_\theta} + 2A_2 c + 3A_3 c^2 + \ldots \tag{2.10}$$

where c is the concentration of the polymer in solution, R_θ is the *Rayleigh* ratio (s.b.), P_θ is the particle scattering function and K is the constant given by:

$$K = \frac{4\pi^2 n_0^2}{\lambda_0^4 N_A}\left(\frac{dn}{dc}\right)^2 f_K \frac{1+\cos^2\theta}{2} \tag{2.11}$$

where d*n*/d*c*, N_A and f_K are the refractive index increment, *Avogadro*'s number and *Kabannes* factor, respectively. With the *Kabannes* factor polarization phenomena of the light is taken into account (for the macromolecules with molar mass bigger than 5×10^4 g/mol value for the f_K is equal to one). If the incident light is vertically polarized, the term $(1 + \cos^2\theta)/2$ in the equation (2.11) can be excluded. For the small-angle neutron scattering (SANS) and small-angle X-ray scattering (SAXS) constant *K* is defined in a different way.

The refractive index increment, d*n*/d*c*, is a constant for a given polymer, solvent and temperature. The change of the refractive index with concentration of solute can be found by the use of a differential refractometer, an instrument which does not measure refractive index in absolute terms, but can determine very small differences in the refractive index of two liquids (solution and solvent). If the polymer sample is soluble in different solvents, it is better to choose a solvent in which the value d*n*/d*c* is the biggest. In the case when d*n*/d*c* < 0.05 cm^3/g, the intensity of the scattered light is to small for the precise measurement[75].

The *Rayleigh* ratio, R_θ, is the normalized scattering intensity at an scattering angle θ and it can be calculated from the intensity of light, I_θ, scattered in the direction at an angle θ to the incident light, scattered intensity of the solvent, $I_{\theta,\text{solvent}}$, intensity of the incident light, I_0, scattering volume, V_S, and from the distance between the scattering volume and the detector, r', by using the following equation:

$$R_\theta = \frac{\left(I_\theta - I_{\theta,\text{solvent}}\right) r'^2}{I_0 V_S} \tag{2.12}$$

By using R_θ, changes of the scattered light as a consequence of the angular dependence of degree of polarization and dependence of the scattering intensity on apparatus parameters can be excluded.

The scattering function P_θ describes the dependence of the intensity of the light, scattered by the solution, on the angle used in measurement, size and shape of the macromolecules in the solution. When dimensions of the macromolecules are smaller than $\lambda/20$ (typical for $M < 10^5$ g/mol), dissolved macromolecules have only one centre of scattering, so the value of P_θ is equal to one. In this case, the intensity of the scattered light is independent on the angle and it is found out that $A_3 = 0$[75]. Therefore, equation (2.10) can be written as:

$$\frac{Kc}{R_\theta} = \frac{1}{M_w} + 2A_2 c \tag{2.13}$$

If at least one dimension of the polymer molecule exceeds $\lambda/20$, the macromolecules no longer can be considered as a point source of radiant energy, but individual parts vibrate out of phase with one another. This will produce interference and causes the decrease of the scattered light intensity with increasing the angle used in the measurement, i.e. $P_\theta < 1$. If the polymer is in the form of a randomly-coiled chain in solution, then the reciprocal value of the scattering function can be calculated as:

$$\frac{1}{P_\theta} = 1 + \frac{16\pi^2}{3\lambda_0^2} R_g^2 \sin^2\frac{\theta}{2} \tag{2.14}$$

By combination of the equations (2.10) and (2.14), and assuming that $A_3 = 0$, the following equation can be obtained:

$$\frac{Kc}{R_\theta} = \frac{1}{M_w}\left[1 + \frac{16\pi^2}{3\lambda_0^2} R_g^2 \sin^2\frac{\theta}{2}\right] + 2A_2c \qquad (2.15)$$

The term Kc/R_θ can be calculated from the experimental results obtained by measuring the scattering intensity as a function of angle. Thence, a *Zimm* diagram can be made by plotting Kc/R_θ against $\sin^2(\theta/2) + kc$, where k is an arbitrary constant chosen to spread the plotted points out into suitable grid. From such a plot it is possible to determine M_w from the intercept, from the slope of the concentration dependence the second virial coefficient and from the slope of the angular dependence, the radius of gyration of the polymer molecule. Intensity of scattered light and hence the accuracy of the determination increases as the molar mass increases.

Branching has a big influence on the dimensions and the shape of the macromolecules, and consequently on the angular distribution of the scattered light intensity. Furthermore, polydisperse HB molecules of the same molar mass can have a different number of branching points, i.e. different structure, and therefore different intensities of the scattered light. As mentioned before, dendritic polymers have smaller dimensions than analogue linear polymers, and hence have a bigger density of segments, which can have certain effect on the thermodynamical interactions between polymer and solvent, and therefore on the second virial coefficient. Theory predicts that A_2 will decrease with increasing degree of branching[75]. Generally it is more difficult to perform SLS measurements with dendritic polymers than with linear ones, since the molar masses are mostly found to be near the lower detection limit of light scattering. It is often necessary to have a relatively high concentration of particles to obtain sufficiant scattering intensity[65]. The first SLS studies of dendrimers were done on poly (α,ε-L-lysine) dendrimers up to tenth generation[76]. The polylysine dendrimers have a radius of gyration between 0.8 nm (for third generation, M_w = 1900 g/mol) and 4.3 nm (for tenth generation, $M_w = 2.3 \times 10^5$ g/mol). These small dimensions were proof for the compactness of the dendrimers.

One of the problems that were observed in SLS measurements of HB polyesters was the formation of the high molar mass associates in solution[71]. This can happen when polymer samples are not dissolved in the used solvent on a molecular level. In that case the intensity of the scattered light will increase with decreasing scattering angle, and on the other side, molar mass will increase with increasing concentration of the solution, indicating a higher degree of aggregation. The main consequence of this behaviour is a huge overestimating of the measured molar mass in contrast to the theoretically calculated value. If it is possible to achieve complete dissolution on a molecular level, still a new problem can arise from the fact that HB polymers have quite small dimensions (mostly only several nanometres) [71]. Because of this property of HB polymers, intensity of the scattered light does not change with scattering angle, so the measurements are mostly done only at the angle of 90^0.

2.4.2. Viscosimetry of dendritic polymers

The viscosimetry of the diluted polymer solutions is one of the easiest, low priced, fast and at the same time quite significant analytical method for characterization of dendritic polymers. A well known characteristic of polymer solutions is that they have higher viscosity than the pure solvent. From the results obtained with this method, limiting ability of polymer to increase viscosity of the solvent at a given temperature can be determinate. A parameter that can be calculated in this manner, the limiting viscosity number (or intrinsic viscosity), may provide

more information about the size of the polymer molecules in solution, and in particular, about interactions between polymer and solvent.

The determination of the dilute polymer solutions viscosity with a capillary viscosimeter is based on the *Hagen-Poiseuille* law. This law describes the capillary flow for *Newtonian* fluids, which is achieved under its own weight, i.e. through gravity[77]:

$$\frac{V}{t_f} = \frac{\pi r_c^4 \Delta p}{8\eta l} \tag{2.16}$$

With the help of the capillary viscosimeter, flow time (or time for the meniscus to pass between two measurement points on the viscosimeter), t_f, which is necessary for the known sample volume, V, to flow through a capillary of the known radius, r_c, and length, l, when at the end of the capillary pressure difference, Δp, exist, can be measured. In the equation (2.16), η represents dynamic viscosity. *Hagen-Poiseuille* law is derived for the laminar flow conditions, i.e. for the infinitely long capillaries, and for the case when the Δp is used to cope with resistance of the liquid flow. However, on entering the capillary, the liquid is accelerated and loses potential energy which is converted into frictional heat. Beside that, the increased friction in the inlet length of the capillary can lead to an increase pressure drop. Therefore, *Hagenbach-Couette* correction is usually used as a correction for the measured flow time and comes in a table together with commercially available capillaries. Since $\Delta p = \rho g h$, equation (2.16) can be written:

$$\eta = K_C \rho t' \tag{2.17}$$

where ρ is density and K_C is the capillary constant defined as:

$$K_C = \frac{\pi r_c^4 g h}{8 l V} \tag{2.18}$$

while t' is measured flow time corrected with the *Hagenbach-Couette* correction term, t_h:

$$t' = t_f - t_h \tag{2.19}$$

In equation (2.18), g and h represent the gravity constant and the average height of the liquid column in a capillary viscosimeter, respectively.

From the results obtained with viscosimetry, the relative increase of the polymer solution viscosity in relation to viscosity of the solvent can be calculated. In the literature this parameter is called specific viscosity, η_{sp}, and it represents the ratio between the difference of the solution viscosity, η, and solvent viscosity, η_s, and the solvent viscosity[77]:

$$\eta_{sp} = \frac{\eta - \eta_s}{\eta_s} \tag{2.20}$$

The viscosity of the solvent can be obtained using the equations (2.17) and (2.19). At constant temperature, the specific viscosity is a function of the mass concentration of the polymer in solution, c, the gradient of speed (at which viscosity is measured), G, the molar mass of the polymer, M, and the hydrodynamic volume of the dissolved macromolecules, V_h. If the ratio between specific viscosity and the mass concentration, η_{sp}/c, is extrapolated to $c \rightarrow 0$ and $G \rightarrow 0$, the limiting viscosity number, $[\eta]$, can be obtained:

$$[\eta] = \lim_{\substack{c\to 0 \\ G\to 0}} \frac{\eta_{sp}}{c} \tag{2.21}$$

In this way concentration effects are eliminated. When the measurement is obtained at constant G it is necessary to determinate the viscosity of the several polymer solutions of the different mass concentrations and then by extrapolation to infinitely dissolution, $[\eta]$ can be calculated. The extrapolation to $c = 0$ is usually carried out graphically with the help of the *Huggins* empirical equation[78]:

$$\frac{\eta_{sp}}{c} = [\eta] + k_H [\eta]^2 c \tag{2.22}$$

where k_H is *Huggins* constant.

Staudinger realized that for macromolecules $[\eta]$ depends on the molar mass, which can be expressed by the *Kuhn-Mark-Houwink-Sakurada* (KMHS) equation:

$$[\eta] = K_\eta M_\eta^a \tag{2.23}$$

where K_η and a are constants that vary with the nature of the polymer and the quality of the solvent, i.e. they are dependent on the hydrodynamic volume of the dissolved macromolecules and on their interactions with the solvent. Beside that, these constants also depend on the polydispersity of the polymer sample, the molar mass range and temperature. M_η is the viscosity average molar mass, whose values are between those of the corresponding M_w and M_n[61]. Since molar mass is related to the size of the polymer in the solution, equation (2.23) also describes relationship between $[\eta]$ and hydrodynamic radius, R_h.

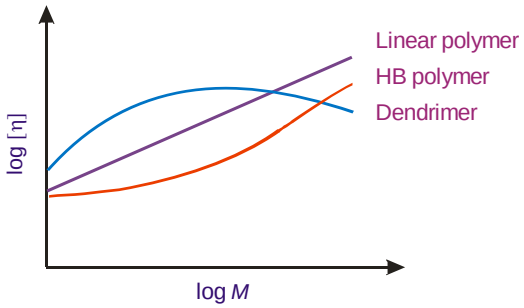

Figure 2.12. Generalized dependence of the limiting viscosity number on the molar mass for linear polymers, HB polymers and dendrimers as described by *Fréchet*[57]

Because of the specific, densely packed structure, dendritic polymers have lower values of the $[\eta]$ than linear polymers of the same molar mass and chemical composition. *Fréchet* compared the dependence of the $[\eta]$ on the molar mass for the linear polymers, HB polymers and dendrimers (Figure 2.12)[57]. From the Figure 2.12 it can be seen that $[\eta]$ of linear polymers increases linearly with the molar mass, while for dendrimers a maximum occurs and it is usually situated between the third and the fifth generation. In theta solvent this specific property of dendrimers is in contrast to the behaviour of linear (*Gaussian*) chains whose $[\eta]$ is proportional to the square root of the molar mass. Apparently these differences arise from the various structures of these polymers and can be observed already at low molar masses, which have big impact on the $[\eta]$.

The existence of a maximum in [η] as a function of the molar mass of dendrimers has been confirmed in several publications[58,65,79]. Beside experimental work, there are also different simulation methods that predict the same behaviour. *Lescanec* and *Methukumar*[47] have proposed one model based on the simulation of the kinetic growth of the dendrimers, from which they have determined that for the lower generations [η] ~ $M^{0.5}$ and for the higher generations [η] ~ $M^{-0.4}$. This specific behaviour can be explained by the fact that hydrodynamic radius linearly increases with the number of generation, n, while the molar mass grows as 2^n (the factor "2" comes from the assumed dendrimer functionality). For the low generation number the volume increases faster with n until the point where the growth of the molar mass is the determining factor. This does not mean that there is a sudden collapse of the molecule rather that the molar mass increases faster than the volume. Therefore, for dendrimers the dependence between [η] and molar mass can not be presented in a simple manner as in the case for linear polymers. However, poly (α,ε-L-lysine) dendrimers in N, N-dimethylformamide as a solvent show a constant value of the [η], i.e. [η] is independent of the molar mass, indicating a constant density of the dendrimer in the solution[76]. For this dendrimer the exponent a is equal to zero over the whole accessible molar mass range. This special behaviour is ascribed to the asymmetric nature of the branching pattern in these dendrimers and the existence of a different density profile than in the case of other dendrimers. A similar behaviour was observed for the poly(benzyl ether) dendrimers in chloroform[80], however for this type of dendrimers this phenomenon was explained by the bad quality of the solvent, which was the reason for the collapsed architecture with constant molecular density and radius that scales with $M^{1/3}$.

As concerning HB polymers, *Fréchet* and co-workers have suggested that [η] always increases with the molar mass, but slower than for the linear polymers[81]. However, the [η] of poly(amidoamine) HB polymers has the same trend as for the dendrimers, i.e. [η] passes through a maximum and then decreases with increasing molar mass[82]. One of the first simulations of the [η] of HB polymers was done by *Widmann* and *Davies*[83] with the help of the *Monte Carlo* method, while *Aerts*[84] has done a simulation with a model used by *Lescanec* and *Methukumar*. Both methods predict the presence of the maximum in the dependence of the [η] on molar mass, but this maximum is placed on the higher value than for the equivalent dendrimers and it disappears when the degree of branching is lower than 0.3. On the other side, for several HB polymers this maximum was not observed, since in these cases [η] increases linearly with molar mass[38,85,86]. Therefore, HB polymers may not necessary follow the same trend as in the case of dendrimers, but they still have significantly lower values of the [η] than for the analogue linear polymers. Beside that, the exponent a from the KMHS equation is for HB polymers in a good solvent smaller than 0.5, while for the linear polymers a is generally in the range of 0.5-0.8, indicating that HB polymers are more compact than linear polymers[77,87].

2.4.3. Dimensions of dendritic polymers

By knowing the dimensions of dendritic polymers, more information can be gathered about the shape of these polymers. In the literature different radii are used to describe this property, such as radius of gyration, R_g, hydrodynamic radius, R_h, viscosity radius, R_η, etc. Beside this, the influence of the solvent quality on the dimensions, as well as the relationship between different radii and molar mass are also important information that has to be taken into account. The size of dendritic polymers can be determinated with various experimental methods and some of them will be described in the following text.

2.4.3.1. Dynamic light scattering

The precise definition of a laser source frequency has enabled the use of light scattering for studying movement of the particles. In the solution, particles are randomly moving due to *Brownian* motion and diffusion. *Brownian* motion represents the random movement of the particles suspended in a fluid due to the collisions with the particles from its surrounding. This specific movement causes the frequency spectrum of the scattered light to change, a phenomenon called *Doppler* shift. In this case, scattering of the light is quasi-elastic, therefore dynamic light scattering (DLS) is also called quasi-elastic light scattering. The *Doppler* shift is associated with the speed and direction of the particles movement in the solution, and therefore with their diffusion coefficient, which further depends on the dimension and the shape of the particles. In order to calculate the diffusion coefficient of a dissolved polymer, it is necessary to determinate the autocorrelation function, which represents the averaging over the product of the scattered intensities at different times[64]. Correlation functions are used to express the degree to which two dynamical properties are correlated over a period of time. Due to the *Brownian* motion of the particles, the intensity of the scattered light will fluctuate in time. Important structural and dynamic information of the molecules can be obtained from the fluctuations of the scattered light at the detector. These fluctuations can be analyzed by comparison of the scattered light intensities for two successive, short time intervals or for two time intervals that are divided by longer delay in time. Comparison can be done by multiplication of the number of photons (or intensity of the light) which are arriving at the detector in these two intervals of time. In the same manner, the autocorrelation function can be formed by multiple repetitions of the calculations and taking into account the average value. In DLS experiments the autocorrelator calculates the time-correlation function, $g_2(q, t)$, of the scattering intensity, which is often written as[88]:

$$g_2(q,t) = \frac{\langle I(q,t) I(q,0) \rangle}{\langle I(q,\infty) \rangle^2} \tag{2.24}$$

where $I(q,0)$ is the scattering intensity at the time zero, $I(q,t)$ is the scattering intensity at a short delay time t later and consequently $I(q,\infty)$ is the scattering intensity at delay time $t \rightarrow \infty$. The scattering vector, q, is defined by equation (2.25):

$$q = \frac{4\pi n_0}{\lambda_0} \sin\frac{\theta}{2} \tag{2.25}$$

The intensity of $g_2(q, t)$ is related to the normalized, field time-correlated function $g_1(q, t)$ through the *Siegert* relationship[88]:

$$g_2(q,t) = 1 + \beta' [g_1(q,t)]^2 \tag{2.26}$$

In equation (2.26) β' is the constant of the instrument, which shows the degree of deviation from the ideal correlation. The field time-correlation function $g_1(q, t)$ can be defined for small monodisperse particles and homogeneous spheres in the following manner:

$$g_1(q,t) = e^{-\Gamma(q)t} \tag{2.27}$$

The initial time dependence of the $g_1(q, t)$ is described by a single exponential decay time, which is related to the translational diffusion coefficient, D, as:

$$\Gamma(q) = q^2 D \tag{2.28}$$

For the polydisperse polymers it is necessary to determine the integral of the equation (2.27) for all possible quantities, i.e. for all appropriate Γ.

The translational diffusion coefficient depends on the concentration in the following manner[11]:

$$D = D_z(1 + k_D c)(1 + CR_g^2 q^2 - ...) \tag{2.29}$$

Coefficient k_D depends on the second virial coefficient and on the concentration dependence of the hydrodynamic friction, while coefficient C is determined by the longest internal mode of motion with respect to the centre of mass[89]. For the hard spheres coefficient C is equal to zero and it is increasing with increasing flexibility of the chains[90]. On the other side, branching reduces the value of the C[89]. D_z is the z-average diffusion coefficient of the particle's centre of mass. For the small particles equation (2.29) can be written as a linear dependence:

$$D = D_z(1 + k_D c) \tag{2.30}$$

Finally, the hydrodynamic radius, R_h, which represents the radius of the equivalent sphere with the constant density, can be obtained from the translational diffusion coefficient by using the well known *Stokes-Einstein* equation[11]:

$$R_h = \frac{k_B T}{6\pi\eta_s D} \tag{2.31}$$

where k_B is the *Boltzmann's* constant and η_s is the viscosity of the solvent.

2.4.3.2. Ultracentrifugation

Ultracentrifugation (UC) is one of the characterization methods for polymers where the motion of dissolved particles in a gravitational field is observed. With this method it is possible to determinate the weight average molar mass, but also the size distribution of particles, due to the fractionation of the particles during sedimentation. In UC experiments, sedimentation in the polymer solution occurs under the influence of the strong centrifugal force, which is enormously greater than gravitational force. As long as the density of the polymer is bigger than that of the solvent, sedimentation will occur, i.e. particles will sediment in the direction of the gravitational field. Heavy particles will sediment first, followed by the smaller ones. Sedimentation can be described with the modified equation of the *Fick's* first law[91]:

$$J = cS\omega^2 r - D\frac{\partial c}{\partial r} \tag{2.32}$$

J represents the flow of the solute, the first term on the right side of this equation describes the sedimentation, while the second term describes the diffusion. In equation (2.32) c is the concentration of the polymer solution, S is the sedimentation coefficient, ω is the angular frequency of the rotor, r is the distance from the axis of rotation and D is the diffusion coefficient. According to this equation there are two methods in UC: equilibrium measurements and rate measurements. In the equilibrium measurements it is allowed to the gravitational field of the ultracentrifuge to act long enough until the polymer solution reaches sedimentation equilibrium. With this method the change in the concentration of polymer from top (meniscus) to bottom of the cell is determined. However, sedimentation equilibrium can be established only after relatively long measuring times. As soon as the equilibrium is reached, the force of diffusion and the force of sedimentation become equal, so the equation (2.32) can be written as follows:

$$0 = cS\omega^2 r - D\frac{\partial c}{\partial r} \tag{2.33}$$

On the other side, the sedimentation coefficient can be determinate from the *Svedberg* equation:

$$S = \frac{M\left(1-\bar{v}\rho\right)}{f_{\mathrm{F}}} \tag{2.34}$$

where M is the molar mass, $\bar{v}$ is the partial specific volume of the polymer, ρ is the density of the solution and f_{F} is the coefficient of friction which can be calculated from measurements of the diffusion coefficient:

$$f_{\mathrm{F}} = \frac{k_{\mathrm{B}}T}{D} \tag{2.35}$$

The combination of the last three equations can be used to determinate molar mass of the polymer:

$$M = \frac{2k_{\mathrm{B}}T}{\left(1-\bar{v}\rho\right)\omega^2}\frac{\mathrm{d}\ln c}{\mathrm{d}r^2} \tag{2.36}$$

The second method in UC is based on the measurements of the sedimentation rate, and it is usually used to determinate the size and the shape of the particles, as well as the size distribution. If on dilute polymer solutions a high centrifugal force is applied, a boundary between the pure solvent placed at the top of the measuring cell and the concentrated polymer solution beneath will be formed. In the rate measurements, the rate at which this boundary moves is measured. The numbers of the boundaries which can appear in this case depend on the polydispersity of the polymer, while in the case of the monodisperse polymers only one quite sharp boundary will be formed. Beside that, if the particles are larger than ≈ 50 nm, diffusion will have no influence on the sedimentation, but if the dimensions of the particles are smaller than ≈ 50 nm, the diffusion broadening of the sedimenting particles boundary will occur, which has to be taken into account[92]. If it is assumed that the boundary is sharp, which means that diffusion did not occur, equation (2.32) can be then written:

$$J = cS\omega^2 r \tag{2.37}$$

However, at r, the flow of the solute can be expressed in another manner:

$$J = c\frac{\mathrm{d}r}{\mathrm{d}t} \tag{2.38}$$

where t is the running time. By introducing equation (2.38) in equation (2.37), the sedimentation coefficient can be obtained:

$$S = \frac{1}{\omega^2 r}\frac{\mathrm{d}r}{\mathrm{d}t} = \frac{1}{\omega^2}\frac{\mathrm{d}\ln r}{\mathrm{d}t} \tag{2.39}$$

With the help of the *Stokes* law, the distribution of the particle diameter can be determined from the distribution of the sedimentation coefficient[93]:

$$d = \left(\frac{18\eta_s S}{\rho - \rho_0}\right)^{1/2} \tag{2.40}$$

where d is the diameter of the particle, η_s is the viscosity of the solvent, ρ is the density of the particle and ρ_0 is the density of the solvent. Differential $w(d)$ and integral $W(d)$ distribution functions of the diameter can be determined from the measured distribution of the sedimentation coefficient and its distribution functions:

$$W(d) = G(S) \qquad \text{and} \qquad w(d)\mathrm{d}d = g(S)\mathrm{d}S \tag{2.41}$$

where $G(S)$ and $g(S)$ represent the integral and the differential distribution functions of the sedimentation coefficient, respectively.

However, if the diameter of the particles is smaller than ≈ 50 nm, diffusion has to be also taken into account, since it has additional effect on the boundary broadening beside the effect of the broad particle size distribution. For smaller particles, the influence of the diffusion becomes much stronger. This additional effect of the diffusion can be considered separately or equations which represent the combination between diffusion and sedimentation can be used. To accomplish that, two different ways can be used in the case of polydisperse particles. The first method is based on the extrapolation procedures of the running time[94], because it is known that the sedimentation of the particles is proportional to the running time, while diffusion is proportional to $t^{1/2}$. The second procedure is developed by *Lechner* and *Mächtle*, and it is based on the correction of the distribution of the apparent sedimentation coefficient with respect to an average diffusion coefficient[92].

Beside previously described methods (SLS, DLS and UC), the diameter of dendritic polymers can be also obtained from viscosity measurements. While studying suspensions of hard spheres, *Einstein* has found that the radius of the sphere R can be calculated from measurements of the $[\eta]$[95]:

$$[\eta] = 2.5N_\mathrm{A}\left(\frac{V_M}{M}\right)_{\text{sphere}} = \frac{10\pi}{3}N_\mathrm{A}\left(\frac{R^3}{M}\right)_{\text{sphere}} \tag{2.42}$$

If the molecular volume V_M is expressed as a cube of the radius of gyration, equation (2.42) becomes:

$$[\eta] = \Phi\left(\frac{R_g^3}{M}\right) \tag{2.43}$$

Equation (2.43) is known as the *Fox-Flory* relationship[96]. It was found that the factor Φ depends on the hydrodynamic interactions, which further depend on segmental concentration[97]. Therefore, it can be expected that the factor Φ will increase with branching, since dendritic polymers have larger segment density. If the radius of an equivalent sphere, R_η (or viscosity radius), is introduced in equation (2.42), then:

$$[\eta] = \frac{10\pi}{3} N_A \frac{R_\eta^3}{M} \tag{2.44}$$

or:

$$R_\eta = \left(\frac{3[\eta]M}{10\pi N_A}\right)^{1/3} \tag{2.45}$$

Now factor Φ can be written as:

$$\Phi = \frac{10\pi}{3} N_A \frac{R_\eta^3}{R_g^3} \tag{2.46}$$

Factor Φ gives more information how deep particles are drained by the solvent. If the draining is relatively deep, the hydrodynamic effective sphere radius decreases and factor Φ becomes small. However, when the solvent only slightly drains in the particles, R_η is much larger than R_g[11].

R_h (or R_η) differs from R_g as a consequence of the intermolecular interactions between the segments of the polymer. These interactions increase with increasing segment density. Beside that, if chains with same R_g are compared, it can be noticed that R_h increases with increasing branching density. Therefore, the ratio between R_h and R_g can be used to valorise the degree of branching in dendritic polymers[98]. This ratio varies from 0.73-0.80 for linear unperturbed polymers to ~ 1.0 for regular star polymers, and for hard spheres of uniform density this ratio should be 1.29[99]. If dendrimers are considered to behave as homogenous spheres, then experimentally obtained values of R_η and R_g may be compared. In that case it can be written:

$$R_\eta \cong \sqrt{\frac{5}{3}} R_g \tag{2.47}$$

The relationship presented with the previous equation was confirmed for the poly(propylene imine) dendrimers in different solvents and it corresponds to the behaviour of the non-draining, equal density spheres[65,100]. However, *Mansfield* and *Klushin* have found that for low generation dendrimers R_η is smaller than R_g, but the opposite occurs for high generation dendrimers[101]. *Burchard* has obtained that the limiting value of relation between R_h and R_g for the high generation dendritic polymers does not exceed 1.023, which is closer to the value for the hollow spheres ($R_h/R_g \sim 1$) than to the value presented with equation (2.47)[102]. On the other side, for the PAMAM dendrimers it was calculated that the ratio R_h/R_g is approximately 1.4 for all except the tenth generation[103]. In the case of the second pseudo generation HB

polymers, the values of the R_h/R_g are in the range of 0.85-1.04, which is similar to the behaviour of the soft spheres[99]. Furthermore, computer simulations of HB polymers have shown that R_h/R_g tends to unity with increasing degree of branching and molar mass[104].

It can be often found in the literature that different radii of dendritic polymers are expressed as a function of the molar mass to the power of the exponent v[44,45,47]:

$$R \sim M^{v} \tag{2.48}$$

The exponent v in the relationship between R_g and molar mass can vary from 0.33 for hard spheres to ~ 0.5 for unperturbed coils of linear chains up to 1.0 for rigid rods[11]. It was observed that for small generation dendrimers the exponent v is ~ 0.50, while for the higher generations 0.22-0.24, if R_g is observed as a function of molar mass[45,47]. Similar to that, PAMAM dendrimers[103] up to the fourth generation shows $R_\eta \sim M^{0.4}$, while poly(propylene imine) dendrimers[100] have $R_h \sim M^{0.37}$. Generally, from the different studies of R_g, R_h and R_η of dendrimers it can be written that exponent v is changing from $v = 0.45 \pm 0.05$ to $v = 0.25 \pm 0.05$ with generation. From this it can be concluded that sphericity of dendrimers increases with the number of generation. These results correspond with the specific dependence of $[\eta]$ on the molar mass of dendrimers, which is mentioned in the section 2.4.2. The power law relationship (equation 2.48) between the different radii and the molar mass for the HB polymers was found to be similar with those for the dendrimers. Small differences that can appear are the consequence of the less densely packed structure of HB polymers compared with those of dendrimers[105,106].

The thermodynamic quality of the solvent can have a great influence on the dimensions of dendritic polymers. For low generations, the interactions of the excluded volume between residues of the monomers have only a small contribution. However, for high generation dendritic polymers, the quality of the solvent may have great influence on the hydrodynamic dimensions of the molecule. With increasing generation number, a significant part of the inner area and volume of the dendritic molecules is accessible to the solvent. Therefore, it can be expected that dendritic polymers have the ability to swell (i.e. that their dimensions depend on the solvent quality), which can be used for the certain applications. Dimension of dendritic polymers increase with increasing interactions with solvent. In other words, in a good solvent these polymers will expand, while in the poor solvents the dimensions of dendritic polymers appear to be shrunk, since in that case intramolecular interactions of the polymer segments are increasing. This behaviour is typical for polymers and shows the level of solvent influence on long-range interactions, i.e. on interactions between the macromolecular chains and the molecules of the solvent. The quality of the solvent has a similar effect on the values of $[\eta]$ of dendritic polymers in different solvents. In a poorer solvent $[\eta]$ will be lower than in the case when the measurements are done in a good solvent.

With the help of molecular dynamic simulations, *Murat* and *Grest* have found out that R_g of dendrimers is significantly changing with solvent quality[107]. They have concluded that the density of the dendrons depends on the used solvent, and it is bigger in the poorer solvent. These results are in a good agreement with the assumption that the segments of the higher generations are back-folding and can occupy the central region of the molecule. The same effect was observed by *Welch* and co-workers[108]. *Matos* and co-workers have also shown that dendrimers can collapse as a consequence of the solvent change[109]. The effect of the solvent quality on the dimension of HB polymers is similar for dendrimers[110]. In some cases, the volume of the HB polymers can be changed by a factor 2[111].

2.4.4. Rheology of dendritic polymers

The rheological behaviour of dendritic polymers is one of the most important property of these unique polymers, which can determinate their industrial processing and application fields. It depends on the structure, dimensions, density, and above all, on the specific nature of the intermolecular interactions. Furthermore, with the help of this type of characterization it is possible to find more about the effects of the molecular variables, such as degree of branching, nature of the end groups and number of generation and on the melt or solution properties of these polymers. Most experiments concerning rheology are done in the area of the linear viscoelasticity (LVE), where the intensity of the applied stress is relatively low. In the LVE region of polymers a linear superposition principle is valid between stress and deformation (or strain), and therefore, characterization of polymers is much easier in this region[112]. On the other side, from the adequate empirical relations it is possible to predict the nonlinear behaviour of polymers from their properties gathered in the LVE region.

If the shear stress is applied gradually on the polymer in the molten state or in the concentrated solution, the molecules will begin to flow one past another. The ability of molecules to flow depends on the molecular structure of the polymer (i.e. on the intensity of the intermolecular forces), on the molar mass (i.e. on the entanglements of the molecules) and on the temperature (how much kinetic energy they possess). In the case of linear polymers above the critical molar mass, the presence of chain entanglements and frictional effects will make the polymer very viscous. When the shear stress increases proportionally to the shear rate, the *Newton's* law of viscosity can be applied[61]:

$$\sigma = \eta \dot{\gamma} \tag{2.49}$$

In equation (2.49) σ represents the shear stress, $\dot{\gamma}$ is shear rate and the proportionality constant, η, is the viscosity. Fluids which obey this law are called *Newtonian* fluids, because in this case viscosity remains constant, since it is independent of the shear rate (Figure 2.13A). Therefore, this viscosity is usually named zero shear viscosity (η_0). However, for some polymers (especially linear polymers) an increase of the shear rate above a critical value leads to a deviation of the viscosity from its zero shear value so that η_0 becomes a decreasing function of the shear rate. The critical value of the shear rate increases with increasing molar mass or with increasing concentration. This non-*Newtonian* behaviour is called shear thinning (Figure 2.13B). Polymers that exhibit this type of behaviour are called pseudoplastics. On the other side, fluids which show an increase in viscosity as the shear rate increases have thickening (or dilatant) behaviour (Figure 2.13C). The third possibility of non-*Newtonian* behaviour can be observed in the case of so-called *Bingham* fluids (Figure 2.13D). These type of fluids can not begin to flow before a critical stress (or yield stress) has been exceeded, after which they can exhibit shear thinning, shear thickening or *Newtonian* behaviour.

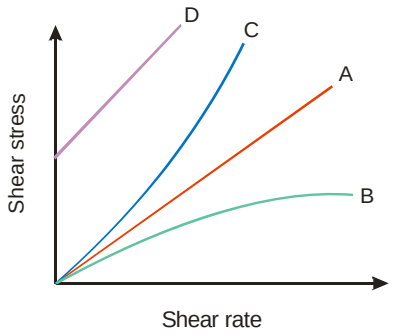

Figure 2.13. Types of shear flow: A) *Newtonian*, B) shear thinning, C) shear thickening, D) *Bingham Newtonian*

The rheological behaviour of the concentrated solutions of polymers is more complicated than in the dilute solutions. It depends not only on the interaction with the solvent molecules and intramolecular interactions between polymer segments, but also on the intermolecular interactions between different macromolecules. For the concentrated solutions, the zero shear viscosity represents the viscous part of the flow behaviour of the polymer solution and depends on the molar mass and concentration. It is well known that for the linear polymer melts below a critical molar mass, η_0 is directly proportional to the molar mass. However, above a critical molar mass the so called 3.4-power low is found to be valid ($\eta_0 \propto M^{3.4}$)[113]. Such behaviour of the linear polymer melts above a critical molar mass is thought to be due to the existence of entanglements between the macromolecules. However, in the case of concentrated polymer solutions it has been shown that η_0 depends on different powers on concentration and molar mass. Therefore, the usual plot of log η_0 versus log (cM) does not lead to a satisfactory η_0-M-c correlation for every polymer-solvent system. Because of that, another method is developed which correlates the viscometric behaviour with the dimensionless product of $c[\eta]$[114].

In the case of concentrated solutions, specific viscosity, η_{sp}, can be defined in the similar manner as for the dilute solutions (equation 2.20) [114]:

$$\eta_{sp} = \frac{\eta_0 - \eta_s}{\eta_s} \tag{2.50}$$

where η_0 is zero shear viscosity of the samples and η_s is viscosity of the solvent. Beside that, η_{sp} can be written as a general virial equation:

$$\eta_{sp} = \sum_{k=1}^{s} \left(B_k \left(c \cdot [\eta] \right)^k \right) \tag{2.51}$$

If all parameters with exponent higher than two are collected in one term, then equation (2.51) becomes:

$$\eta_{sp} = B_1 \cdot c \cdot [\eta] + B_2 \left(c \cdot [\eta] \right)^2 + B_s \left(c \cdot [\eta] \right)^s \tag{2.52}$$

Since, the first three terms in the equation (2.52) represent *Huggins* equation (2.22) can be written:

$$\eta_{sp} = c \cdot [\eta] + k_H (c \cdot [\eta])^2 + B_s (c \cdot [\eta])^s \tag{2.53}$$

When the investigated concentration range is relatively wide it can be observed that by plotting log η_{sp} versus log ($c[\eta]$) a linear dependence is obtained for the high values of the $c[\eta]$ (Figure 4.57a). From this linear relationship between log η_{sp} and log ($c[\eta]$) at high $c[\eta]$, it is possible to obtain unknown quantities, B_s and s. By combination of the KMHS (equation 2.23) and (2.53) equations it is possible to obtain the following relationship[114]:

$$\eta_0 = \eta_s \left(cK_\eta M^a + k_H c^2 K_\eta^2 M^{2a} + B_s c^s K_\eta^s M^{as} + 1 \right) \tag{2.54}$$

From the last equation it can be seen that for the η_0-M-c correlation it is necessary to know the *Huggins* constant (k_H), the values of the quantities, B_s and s, and the $[\eta]$-M relationship for the given polymer-solvent system.

Beside shear flow, polymer fluids can also be characterized in dynamic measurements by:

$$|\eta^*| = f(\omega) \tag{2.55}$$

where $|\eta^*|$ represents the absolute value of the complex dynamic viscosity at angular frequency ω. When the oscillation technique is used for the characterization of viscoelastic liquids, i.e. polymer melts and concentrated solutions the behaviour is intermediate between the solids and fluids:

$$\sigma(t) = \gamma_0 [G'(\omega)\cos(\omega t) - G''(\omega)\sin(\omega t)] \tag{2.56}$$

where γ_0 is strain and $G'(\omega)$ and $G''(\omega)$ are storage and loss modulus, respectively. The combination of $G'(\omega)$ and $G''(\omega)$ will give complex modulus, $G^*(\omega)$:

$$G^*(\omega) = G'(\omega) + G''(\omega) \tag{2.57}$$

The real part of the complex modulus, $G'(\omega)$, is a measure of the elastic stored energy, while the imaginary part, $G''(\omega)$, is a measure of viscous losses. For the linear polymers at the lowest frequencies (terminal or flow region) a double logarithmic plot of G' and G'' will have limiting slopes of 2 and 1 respectively. At this region the behaviour of the polymers is mainly liquid ($G' < G''$). However, with increasing frequency the loss of the energy through the viscous flow becomes smaller, i.e. at the end of the terminal region $G' = G''$. With the help of the previous equation, the dynamic complex viscosity, $\eta^*(\omega)$, can also be defined:

$$\eta^*(\omega) = \frac{G^*(\omega)}{i\omega} = \eta'(\omega) + i\eta''(\omega) \tag{2.58}$$

Another parameter that is important in oscillatory measurements is tan δ, which represents the ratio between loss and storage modulus:

$$\tan\delta = \frac{G''(\omega)}{G'(\omega)} \tag{2.59}$$

For the most polymer melts it can be observed that the steady shear viscosity, $\eta(\dot{\gamma})$, and the complex viscosity, $\eta^*(\omega)$, have the same value at the same deformation rate.

$$\eta\left(\dot{\gamma}\right) = \left|\eta^*(\omega)\right|_{\omega=\dot{\gamma}} \tag{2.60}$$

Equation (2.60) is the so-called *Cox-Merz* rule and it shows that there is a relation between linear and non-linear viscoelastic properties. Therefore, it is possible to obtain shear viscosity information when only linear viscoelastic data are available and the reverse[112].

From the maximum of the G'' and tan δ temperature dependences in the polymer melts it is possible to determine the value of the glass transition temperature (T_g). The glass transition temperature can also be determined from the inflection point of the G' temperature dependence. Furthermore, the relation between zero shear viscosity and the temperature can be modelled with an *Arrhenius*-type equation:

$$\eta_0 = Ae^{\frac{E_a^s}{RT}} \tag{2.61}$$

where A is a constant, R is the gas constant, T is the temperature and E_a^s is the activation energy of flow. E_a^s is determined by localized segmental motion of the polymer chains and it depends on the chain structure and branching. The temperature dependence of the rheological parameters can also be described by the time-temperature superposition rule, i.e. by the *Williams-Landel-Ferry* (WLF) equation, which states that above the glass transition temperature, T_g, changing the temperature is approximately equivalent to changing the time scale. The WLF equation can be presented as follows:

$$\log a_T = \frac{-C_1\left(T - T_0\right)}{C_2 + \left(T - T_0\right)} \tag{2.62}$$

In equation (2.62) a_T is the shift factor, T_0 is the reference temperature and C_1 and C_2 are constants. The shift factor can be determined by the horizontal shift necessary to obtain superposition on the corresponding rheological curve of the reference temperature. When the values of the a_T at different temperatures are known then the constants C_1 and C_2 can be graphically determined from the linear form of the WLF equation. Finally, the activation energy of flow can be calculated in the following manner[115]:

$$E_a^m = \frac{2.303RC_1C_2T^2}{\left(C_2 + T - T_0\right)^2} \tag{2.63}$$

The WLF equation can also be presented in terms of the free volume theory if it is assumed that the fractional free volume, f, increases linearly with temperature and that the chain mobility at any temperature depends on the free volume[115]:

$$f = f_g + \alpha_f\left(T - T_g\right) \tag{2.64}$$

where f_g and α_f are the fractional free volume at T_g and the thermal expansion coefficient, respectively. They can be calculated in the following way:

$$f_g = \frac{B}{2.303 C_1^g} \tag{2.65}$$

$$\alpha_f = \frac{B}{2.303 C_1^g C_2^g} \tag{2.66}$$

B is the empirical constant usually arbitrarily set to unity, while constants C_1^g and C_2^g are the constants from WLF equation obtained when T_g is set as reference temperature[115]. These constants can be calculated from C_1 and C_2 in the following manner:

$$C_1^g = \frac{C_1 C_2}{C_2 + T_g - T_0} \tag{2.67}$$

$$C_2^g = C_2 + T_g - T_0 \tag{2.68}$$

Rheological properties of dendritic polymers are relatively often examined in the literature, since these polymers exhibit interesting rheological behaviour, which is in some cases quite different than those observed for the analogue linear polymers. Both, dendrimers and HB polymers, are mostly characterized by a *Newtonian* behaviour in the melt and at medium and high concentrated solutions over a wide range of shear rates[73,105,116,117]. From this it can be concluded that in dendritic polymers entanglements are absent, which is also proved by the fact that melt and solution viscosities of these polymers are much lower than those of linear ones. The lack of the entanglements can be explained by the presence of the relatively short spacer length between branch points. This specific property of dendritic polymers is the reason why they do not show characteristic relationship between zero shear viscosity and molar mass, often observed for linear polymers. The sharp slope change in the dependence between viscosity and molar mass is not observed for most dendritic polymers[116,117]. For the poly(propylene imine) dendrimers and HB polyesters the zero shear rate viscosity exhibit a gradual decrease in slope with increasing molar mass, which is believed to reflect a transition from more open structure at lower generations, to closed globular structures at higher generations[118]. However, in concentrated solutions (above 30 wt %) of high molar mass HB poly(ether-imide)s the shear thinning occurred, which was explained by the significant degree of coil overlap at intermediate concentrations and entanglement coupling at higher solution concentrations[118]. Similar behaviour was observed for the second and the third generation of the Boltorn® HB polyesters in melt[119]. However, when the same samples are heated to 150 ^{0}C prior to measurements at lower temperatures, they behaved as *Newtonian* fluids[73,106]. The formation of the hydrogen bonding is associated with the presence of the large number of hydroxyl end groups in Boltorn® polymers. It was also observed that the physical aging of these HB polymers is thermally reversible[106].

Another commonly reported rheological property of dendritic polymers is the applicability of the *Cox-Merz* rule[73,117,120]. Again, this rule was not valid for the Boltorn® samples of the second and third generation characterized without previous heating treatment[119]. The temperature effects on the rheological properties of dendritic polymers were also widely investigated with the help of *Arrhenius* and WLF equation[106,118,119,121]. It was found out that the activation energy of flow for some dendritic polymers increases up to a certain generation, where it reaches a steady value. On the other side the free volume of dendritic polymers decreases with increasing molar mass, which verifies the assumption that the molecular structure becomes more and more compact as molar mass increases.

The glass transition temperature is an important characteristic of dendritic polymers, which can be determined with rheological measurements. The reason for this is that dendritic polymers are mostly considered to be amorphous polymers, because it is expected that the presence of the branching in the backbone reduce the ability to crystallize in the same manner as linear polymers. The glass transition temperature mostly depends on the chemical structure of the polymer and the molar mass. Generally it can be said that T_g of linear polymers will increase with branching, molar mass, presence of larger number of polar groups and hydrogen bonding. However, for dendritic polymers this classical definition of T_g brings some important questions, such as: what produces the T_g in this kind of polymers, what type of molecular motions determine it, does the different parts of molecule have different values of T_g, etc. It is obvious that in dendritic polymers segmental motions are restricted because of the large number of branching points. Another interesting fact concerning T_g in dendritic polymers is that there is no significant dependence of T_g on the molar mass, as in the case of linear polymers[122]. The reason for this behaviour is that the effect that can increase T_g (number of branches) and the effect that brings the decrease in T_g (number of end groups) grow in parallel. This was experimentally confirmed by *Wooley* and co-workers that have reported a slightly increase in T_g of dendritic polymers with the generation number to a certain value, above which it remains practically constant[123]. The influence of end groups on T_g of linear polymers can only be noticeable at low molar mass, while in dendritic polymers the intensity of this influence is increasing with the generation.

Generally, T_g of dendritic polymers depends strongly on the degree of branching, steric interactions due to crowding, backbone rigidity and on the nature of the end functional groups and the backbone[124]. The latter two factors are especially important since it is possible that there are large differences in the polarity of the connecting groups and the terminal ones. The influence of the type of end functional groups on the T_g can be quite strong, which was confirmed for the large number of HB polymers[54,56,59,123,125]. When polar groups are introduced in the HB polymer, an increase of T_g was observed and an decrease when the polymer was modified hydrophobically. It is also observed that HB polymers have smaller values of T_g than the analogue linear polymers[36]. The lack of crystallinity has been reported for many dendritic polymers[36]. However, the small portion of crystallinity is observed for HB polyols, probably due to the presence of the linear arm segments[126]. Crystallization can also be induced in the dendritic polymers by attachment of the long alkyl chains to their end groups[125].

2.4.5. Thermal analysis of dendritic polymers

Thermal properties of dendritic polymers, especially thermal stability, have been subject of discussion of many studies. One of the widely used thermoanalytical methods for determination of polymers thermal stability is the thermogravimetric (TG) analysis. This method is based on continuous measurement of weight loss as the sample temperature is increased with a constant rate, usually in an inert atmosphere. With such nonisothermal technique it is possible to determinate thermal stability, kinetics of thermal degradation, content of moisture or low molar mass compounds (volatilities), activation energy of thermal degradation and other thermal properties of polymers. Results obtained with this method are presented in a thermogram, where the weight loss is plotted versus temperature. If the heating rate is increased, the temperature of degradation will also increase. Consequently, when the heating rate is too high it can happen that a two-step process is presented as one-step, since the equilibrium conditions are not achieved. The shape of the thermogram depends on

degradation kinetic, order of the degradation reaction, activation energy of degradation and on the pre-exponential factor from the *Arrhenius* equation. For some polymers temperatures at which certain process occurs are quite close to each other, so they can not be determinate easily. In such case differential thermograms gathered at different heating rates can be used. Beside that, in this way the complexity of the degradation process can be analyzed and independent reactions with different activation energies can be divided.

If the nonisothermal TG experiments are done at different heating rates, the activation energy of thermal degradation can be calculated. During the thermal degradation of polymers, their physical properties are changing, which further leads to the change of activation energy. Therefore, by the analysis of several thermograms obtained at different heating rates it is possible to distinguish between few separated regions of temperature and weight loss where activation energy is constant. If the activation energy of degradation is constant during the heating process, then the kinetic of degradation can be presented by a single mechanism.

A mathematical model that can be used to describe the degradation kinetic, followed by certain chemical change, is often expressed in the following way[127]:

$$\frac{\mathrm{d}\alpha}{\mathrm{d}t} = f(\alpha)k(T) \tag{2.69}$$

The rate of change of degree of reaction, $\mathrm{d}\alpha/\mathrm{d}t$ is equate with the conversion function $f(\alpha)$ and the rate constant $k(T)$. The equation (2.69) can be used to describe the degradation process in polymers only if all physical and chemical factors that can have any influence on the rate of chemical reaction (physical properties of the sample, presence of the labile groups or impurities in the sample, gas flow rate, etc.) are controlled. The relationship between the rate constant and the temperature can be expressed by the *Arrhenius* equation:

$$k(T) = A\exp\left(-\frac{E_\mathrm{a}^\mathrm{d}}{RT}\right) \tag{2.70}$$

where A is the pre-exponential factor and E_a^d is the activation energy of degradation, which can be determined by combination of equations (2.69) and (2.70) if it is supposed that function $f(\alpha)$ can be written as follows:

$$f(\alpha) = (1-\alpha)^n \tag{2.71}$$

Therefore equation (2.69) becomes:

$$\frac{\mathrm{d}\alpha}{\mathrm{d}t} = (1-\alpha)^n A\exp\left(-\frac{E_\mathrm{a}^\mathrm{d}}{RT}\right) \tag{2.72}$$

If the sample is continuously heated with the heating rate $\beta = \mathrm{d}T/\mathrm{d}t$, then:

$$\frac{\mathrm{d}\alpha}{\mathrm{d}t} = \frac{\beta\mathrm{d}\alpha}{\mathrm{d}T} = (1-\alpha)^n A\exp\left(-\frac{E_\mathrm{a}^\mathrm{d}}{RT}\right) \tag{2.73}$$

or:

$$\ln\left(\frac{\mathrm{d}\alpha}{\mathrm{d}t}\right) = n\ln(1-\alpha) + \ln A - \frac{E_\mathrm{a}^\mathrm{d}}{RT} \tag{2.74}$$

The activation energy of degradation can be calculated from the previous equation by using differential or integration method, however in that way it is not possible to obtain adequate information, because of the complexity of polymers degradation kinetics[127]. Therefore, the following method is commonly used to determine E_a^d. By combining equations (2.69) and (2.70) it can be written:

$$\ln\left(\frac{\mathrm{d}\alpha}{\mathrm{d}t}\right) = \ln f(\alpha) + \ln A - \frac{E_\mathrm{a}^\mathrm{d}}{RT} \tag{2.75}$$

From the integral of the equation (2.75) calculated for two isothermal experiments at temperatures T_1 and T_2, equation (2.76) may be written:

$$\frac{E_\mathrm{a}^\mathrm{d}}{R} = \frac{\ln t_2 - \ln t_1}{\frac{1}{T_1} - \frac{1}{T_2}} \qquad (\alpha = \text{const.}) \tag{2.76}$$

where t_1 and t_2 are the times and T_1 and T_2 are the temperatures when the degree of reaction α is reached. If the equation (2.75) is integrated at constant heating rates β_1 and β_2 for two separated experiments, then:

$$\frac{E_\mathrm{a}^\mathrm{d}}{R} \cong \frac{1.05(\ln \beta_2 - \ln \beta_1)}{\frac{1}{T_1} - \frac{1}{T_2}} \qquad (\alpha = \text{const.}) \tag{2.77}$$

Equation (2.77) is known as *Ozawa-Flynn-Wall* method for determination of the activation energy of degradation and can be written in the following way:

$$E_\mathrm{a}^\mathrm{d} \cong -18.23\frac{\mathrm{d}\log\beta}{\mathrm{d}\left(\frac{1}{T}\right)} \tag{2.78}$$

Activation energy of polymer degradation can be finally calculated from the slope of the dependence log β versus $1/T$. Equations (2.76) and (2.78) can be used in a wide range of temperatures or heating rates.

The thermal stability of dendritic polymers depends on the chemical structure in the same manner as in the case of linear polymers (e.g. presence of aromatic groups will increase thermal stability). Beside that, the nature of the functional end groups can also have significant influence. TG analysis of most HB polymers has shown that this type of polymers has a relatively good thermal stability[34,126]. A detailed study of the thermal stability and E_a^d of aliphatic HB polyesters of different generations and with different end functional groups has been done by *Vuković* and co-workers[128].

2.5. Applications of dendritic polymers

The field of applications for dendritic polymers has been significantly increased in the past years. Their specific structure gives the possibility to use them in a large variety of industrial and medical areas. Dendritic polymers blended with different linear polymers are used to improve the thermal stability and to reduce the melt viscosity of linear polymers (i.e. as a rheology modifiers for processing)[7,56], to reduce the melt flow instabilities in film blowing[129] and as a dye carriers[130]. They can also be used to coat and functionalize carbon nanotubes[131]. Furthermore, dendrimers can be used in gene therapy and sensors[132]. The most interesting and at the same time important application of dendrimers is as a controlled drug delivery system, because they can act as molecular encapsulants[133]. Since dendrimers possess controlled multivalency, several drug molecules, targeting groups and solubilizing groups can be attached to the periphery of the dendrimer in a well-defined manner. It is already proved that dendrimers can be used as anticancer drug carriers[134]. This property of dendrimers to encapsulate molecules is also used for protection against quenching[135]. Another important application of these polymers is that dendrimer-based polyanions can be used as inhibitors of HIV and other enveloped viruses[136].

Applications of HB polymers are mostly based on their nature and the presence of the large number of end functional groups within a molecule. HB polymers are mostly used in high solid or powder coatings, because of their low viscosity and high functionality and solubility[6], which enables them to be used also as multifunctional crosslinkers[25,55]. Beside that, HB polymers are used as additives[5], as components in nonlinear optics[8], in molecular imprinting[9], in catalysis[10], as thermoset resins[25], as modifiers of metal surfaces[137], as adhesive agents[138], as compatilizers[139], as dispersers[140], for gas separation[141], etc. HB polyesters have also been suggested as materials that can be used to control the drug concentration and delivery rate in the body[142,143].

3. Experimental Part

3.1. Materials

Aliphatic HB polyesters of the second (HBP-2I), third (HBP-3I), fourth (HBP-4I and HBP-4II), fifth (HBP-5I), sixth (HBP-6I and HBP-6II), eighth (HBP-8I and HBP-8II) and tenth (HBP-10I) pseudo generation used in this dissertation, were synthesized starting from 2,2-bis(hydroxymethyl)propionic acid (Aldrich), as an AB_2 monomer, and di-trimethylolpropane (Fluka Chemika), as the tetrafunctional core molecule. In this work three commercially available HB polyesters (Boltorn®) of the second (BH-2), third (BH-3) and fourth (BH-4) pseudo generation were also used, which were supplied by Perstorp (Specialty Chemicals AB, Sweden). End -OH groups of several HB and Boltorn® polyesters were modified with β-alanine (Fluka BioChemika). In this manner, four modified samples were obtained (HBP-$3I_{AL}$, HBP-$4I_{AL}$, BH-2_{AL} and BH-3_{AL}). Beside them, a sample of the third pseudo generation modified with stearic acid (HBP-$3I_{SA}$) was supplied by "DUGANOVA" (Belgrade).

The following solvents and chemicals were also used:

- 2,5-Dihydroxybenzoic acid (Aldrich)
- Acetic anhydride (Aldrich)
- Acetone (Fluka)
- Deuterium oxide (Fluka)
- Diethyl ether (Fluka)
- Dimethylsulfoxide (Merck)
- Ethanol (Aldrich)
- Lithium bromide (Fluka Chemika)
- Lithium chloride (Aldrich)
- Methanesulphonic acid (Aldrich)
- N,N-dimethylacetamide (Aldrich)
- N,N-dimethylformamide (Fluka)
- N-hexane (Roth)
- N-methyl-2-pyrrolidinon (Aldrich)
- Phenolphthalein (Merck)
- Potassium bromide (Fluka Chemika)
- Potassium hydroxide (Aldrich)
- Potassium hydroxide, 0.5 M solution in water (Aldrich)
- Potassium iodide (Fluka Chemika)
- Pyridine (Fluka Chemika)
- Sodium hydroxide (Aldrich)
- Sodium iodide (Aldrich)
- Sodium nitrate (Fluka)
- Tetrahydrofuran (Aldrich)
- Zinc chloride (Fluka Chemika)

All chemicals and solvents were used as received, without further purification.

3.2. Sample preparation

3.2.1. Synthesis of hyperbranched polyesters

HB polyesters of different pseudo generations were synthesized in an acid-catalyzed polyesterification reaction. The procedure for the synthesis will be described for the HB polyester of the second (HBP-2I) and third (HBP-3I) pseudo generations. 35.00 g (0.14 mol) of di-trimethylolpropane (DiTMP), 225.12 g (1.68 mol) of 2,2-bis(hydroxymethyl)propionic acid (bis-MPA), and 1.86 g of methanesulphonic acid (MSA) were mixed in a four necked flask equipped with N_2 inlet, a drying tube, a mechanical stirrer and a contact thermometer. The flask was placed in an oil bath and heated to 140 ^{0}C. The mixture was then left to react for two hours under a stream of N_2, which was used to remove the formed water. After that, a reduced pressure was applied to the flask, at the same temperature, until the reaction reached the completion. The course of the reaction was controlled by the acid number titration (see chapter 3.3.3).

For the synthesis of the third (HBP-3I) pseudo generation, 95.00 g of HBP-2I was placed in a four necked flask and heated to ~ 110 ^{0}C for one hour with an oil bath. After that, 124.05 g (0.93 mol, calculated from the theoretical molar mass) of bis-MPA and 0.89 g of MSA were added into the flask. N_2 inlet, a drying tube and a mechanical stirrer were then connected to the flask and the temperature increased to 140 ^{0}C. The polymerization reaction was completed in the same way as it was previously described for the sample HBP-2I. The synthesis of other HB polyesters of the higher pseudo generations (HBP-4I, HBP-5I, HBP-6I, HBP-8I and HBP-10I) was done in the same manner, starting from the previous generation and adding the stoichometric amount of bis-MPA and an adequate amount of MSA necessary to obtain the wanted number of generation, i.e. or molar mass.

On the other hand, samples HBP-4II, HBP-6II and HBP-8II were synthesized in the same way as sample HBP-2I, by adding an adequate stoichometric amount of DiTMP and bis-MPA at once to obtain HB polyesters of the fourth, sixth and eighth pseudo generation. Further reaction was done as it was previously described.

All samples were obtained as transparent light yellow solids. After the synthesis, the samples were dried in a vacuum oven until constant mass was achieved. For the purpose of some experimental methods, self-synthesized HB polyesters and commercial samples were purified by precipitating from acetone into the n-hexane to give samples as white solids.

3.2.2. Fractionation of hyperbranched polyesters

Seven samples of self-synthesized and Boltorn® HB polyesters (HBP-3I, HBP-4I, HBP-6I, HBP-8I, HBP-10I, BH-3 and BH-4) were fractionated using the precipitation fractionation method from a solvent/non-solvent mixture to obtain three fractions of each sample. In a continuously stirred 5 wt % solution of the parent HB polyester in acetone, an adequate amount of n-hexane (determinated from the previously obtained titration curve for the sample HBP-6I) was added in a drop-wise manner. After that, the solution was heated until homogeneity was reached and then left over night to cool back slowly at room temperature. The first fraction, precipitated on the bottom of the vessel as a white solid, was removed and the same procedure was repeated on the remaining solution to obtain other two fractions. All fractions were dried in the vacuum oven to remove the volatile materials.

3.2.3. Modification of hyperbranched polyesters with β-alanine

HB polyesters of the third and fourth pseudo generation (HBP-3I and HBP-4I) as well as two commercial samples (BH-2 and BH-3) were modified with β-alanine. Reactions of the modification will be described for the synthesis of the modified HB polyester of the third pseudo generation (HBP-3I_{AL}). In a three-necked flask 10.00 g of HBP-3 and 73 cm^3 of N,N-dimethylformamide were placed. The mixture was stirred for 24 h at room temperature. Then the flask was connected with N_2 inlet, a drying tube and a contact thermometer, and 8.15 g (0.09 mol) of β-alanine and 0.13 g MSA was slowly added into the flask. After that the flask was placed in an oil bath and heated to 160 ^{0}C under a stream of N_2, which was used to remove the formed water. After 7 h of reaction at 160 ^{0}C, the content of the flask was cooled down and precipitated with diethyl ether to give HBP-3I_{AL} as a light yellow viscous liquid. All modified samples were placed in the vacuum oven to remove the volatile materials.

3.2.4. Modification of hyperbranched polyesters with stearic acid

The sample modified with stearic acid was synthesized by melting 48.62 g of HBP-3I, mixed with small portion of xylol (3 mass% of reaction mass), in a four-necked flask equipped with an N_2 inlet, a drying tube, Dean-Stark unit (filled with xylol) and a stirrer. The flask was placed in an electrical heater. In a molten HBP-3I, 126.62 g (0.45 mol) of stearic acid was added and this mixture was then heated up to the 230 ^{0}C. After 7.5 h the mixture was cooled until the temperature of 130 ^{0}C was reached. The N_2 stream was turned off and the flask was connected to a vacuum line. Mixture was then heated 45 min at 200 ^{0}C. The modified sample HBP-3I_{SA} was obtained as pink waxy solid.

3.3. Characterization methods

3.3.1. IR spectroscopy

IR measurements were carried out on a Bruker Vector 22 (Opus 2.2 Software) spectrometer in 50 scans, as KBr pellets.

3.3.2. NMR spectroscopy

^{1}H and ^{13}C NMR spectra of samples were recorded on two different spectrometers: AMX-500 (500 MHz, Bruker, Germany) and Bruker (250 MHz) NMR spectrometer. ^{13}C NMR spectra were obtained using deuterated dimethylsulfoxide (DMSO-d_6) as solvent, while for recording ^{1}H NMR spectra, samples were dissolved in DMSO-d_6 and in the mixture deuterium oxide (D_2O)/ DMSO-d_6 (1:4 by volume). Signal of the DMSO-d_6 resonate at around 2.5 ppm in the ^{1}H NMR spectra and at around 39.6 ppm in the ^{13}C NMR spectra, while D_2O resonate at around 4.0 ppm in ^{1}H NMR spectra.

3.3.3. Determination of acid and hydroxyl number by titration

The acid number (N_{AN}) of the HB samples was determined as follows. Samples of 0.2-0.3 g were taken out from the reaction mixture at different times during the synthesis. The samples were dissolved in 50 cm^3 of acetone/ethanol (1:1 by volume) and titrated with 0.50 M KOH using phenolphthalein as an indicator. Blank tests were done on the pure solvent mixture. Acid number was then calculated according to the following equation:

$$N_{AN} = \frac{56.1 \times c_{KOH} \times (V_{KOH} - V_{BT})}{m_{sample}} \quad (3.1)$$

Where c_{KOH} is the concentration of the KOH solution, V_{KOH} is the volume of KOH used for the sample titration, V_{BT} is the volume of the KOH used for the blank test and m_{sample} is the mass of the sample. However, since the V_{BT} was not possible to measure (less than one drop of KOH), it was taken that $V_{BT} = 0$. The acid number of the fractions and linear polyester were also determined.

The hydroxyl number (N_{HN}) was determined after the synthesis, by dissolving ~ 1 g of the sample in 15 cm^3 of a mixture acetic anhydride/pyridine (1:9 by volume) in a 250 cm^3 erlenmeyer flask. The solution was then heated for 1h with reflux. After cooling, ~ 50 cm^3 of distilled water was slowly added through the drying tube, and the other 50 cm^3 of distilled water were added into the solution when the erlenmeyer flask was disconnected from the drying tube. The solution was then titrated with 0.50 M KOH using phenolphthalein as an indicator. Blank tests were done on the pure solvent mixture. Finally N_{HN} was calculated as follows:

$$N_{HN} = \frac{56.1 \times c_{KOH} \times (V_{BT} - V_{KOH})}{m_{sample}} \quad (3.2)$$

For the purpose of this measurement pyridine was dried above solid KOH for several days. N_{HN} was also determined for the fractions of HB polyesters and commercial samples, as well as for the modified samples.

3.3.4. Determination of the moisture content

Moisture content of the samples was determined in a Moisture Analyser Sartorius MA 40. Measurements were repeated three times and then the middle value was used.

3.3.5. Vapour pressure osmometry

Vapour pressure osmometry was carried out using a Knauer vapour pressure osmometer. Measurements were done with four different concentrations of polymer solutions in N,N-dimethylformamide at 90 ^{0}C. For the calibration benzyl was used and the obtained calibration constant was K_e^{exp} = 1242.10 Ωkg/mol.

3.3.6. MALDI-TOF mass spectrometry

MALDI-TOF mass spectra were run on a BIFLEX III instrument (Bruker Saxonia Analytik GmbH, Leipzig, Germany) in the reflection mode. The average power of the nitrogen laser (337.1 nm) at 20 Hz was 3-4 mW (150-200 μJ/pulse) with a delay time of 200 ns. All measurements were performed using the positive detection mode with the following parameters: dwell time – 0.50 ns, delay – 19000 ns, Uis1 – 19.00 kV, Uis2 – 16.80 kV, Ulens – 9.35 kV. The spectra were obtained by overlaying 200-350 single pulses. The sample preparation was performed on Scout MTP MALDI targets (Bruker). An aliquot (1 μL) of polymer solution in tetrahydrofuran (15 g/dm^3) and an equal volume of the saturated solution of matrix (2,5-dihydroxybenzoic acid) in tetrahydrofuran (or in water) were spotted on a target and allowed to air-dry before inserting into the vacuum chamber of the MALDI instrument.

3.3.7. Electrospray Ionization mass spectrometry

ESI mass spectra of HB polyesters were recorded using a HP 1100 Series (MS Mod. 1946 A) mass spectrometer with Flow-Injection-Analysis (FIA) (bypassing HPLC-column) scan mode and Atmospheric Pressure Ionization-Electrospray (API-ES) ionization mode. The samples were introduced through the electrospray interface by infusion a N,N-dimethylformamide solution containing small amount of sodium or potassium iodide. The flow rate of the solvent was 0.4 cm^3/min. Nitrogen was used as a drying gas (flow: 10 dm^3/min and temperature: 350^{0}C) with nebulizer pressure 50 psig. The capillary voltage was 3500 V and the fragmentor voltage 100 V. A positive scan was obtained at *m*/*z* values from 50.0-2000.0. The mass spectral data were processed with the HP Chemstation Software.

3.3.8. Gel permeation chromatography

GPC measurements of unmodified HBP samples were performed with a Spectra-Physics chromatograph equipped with Rheodyne universal injector and Spectra-Physics differential refractive index detector. The separation was achieved across a set of two gel columns (MZGPC columns) with porosities of (1000 Å, 5 μm). Tetrahydrofuran was used as eluent at a nominal flow rate of 1 cm^3/min. Polymer solutions in tetrahydrofuran were filtered through a 0.2 μm RC filter (Schleicher and Schuell) before injected into the column. The quantity of injected polymer was 100 μL and the measurements were carried out at room temperature (25 ^{0}C). The molar mass characteristics of the polymers were calculated by a polystyrene calibration curve constructed with narrow molar mass polystyrene standards (Polymer Standards Service) using the Chrom Gate 3.1.4. software (Knauer).

Molar masses averages and the molar mass distribution of modified HBP samples were determined with GPC apparatus equipped with TSP P100 Isocratic HPLC pump (Thermo Separation Products), Rheodyne 7725i injector, Shodex RI-71 differential refractive index detector (Showa Denko), and a set of three gel columns (one with gel porosity of 40 Å and two with gel porosities of 1000 Å). Measurements were performed at 25 ^{0}C in aqueous sodium nitrate solution (0.1 mol/dm^3) as mobile phase, eluting at a nominal flow rate of 1 cm^3/min. Polymers were dissolved in water or in 0.10 mol/dm^3 solution of NaOH in water, filtered through a 0.45 μm CA filter (Schleicher and Schuell) and injected into the column

(200 μL). The molar mass characteristics of the polymers were calculated on the basis of poly(ethylene glycol) (Serva) calibration.

3.3.9. Determination of the refractive index increment by differential refractometer

The refractive index increment (dn/dc) of HB polyesters was determined with the differential refractometer Brice-Phoenix, model BP-2000-V (Phoenix Precision Instruments). Measurements were done at 25 ^{0}C for the five different concentrations of polymer in N,N-dimethylformamide or in N,N-dimethylacetamide. The calibration constant of the instrument for the used wavelength (436 nm) was determined as $K_\lambda = 2.42 \times 10^{-4}$. d$n$/d$c$ was calculated from the slope of the dependence between refractive index of the solution (n) and the concentration (c) of the solution. The refractive index of the solution was calculated from the following equation:

$$n = K_\lambda d_1 \tag{3.3}$$

where d_1 is the corrected difference of the refractive index, calculated as the difference between measured refractive index difference (between solvent and solution) and blank test.

3.3.10. Static light scattering

Static light scattering was performed on a FICA 50 photometer. Measurements were carried out at a temperature of 25 ^{0}C and at the wavelength of 436 nm. The scattering angles were in the range 30-150 ^{0} (except in some cases when measurements were done only at 90^0) and benzene was used as standard. Five different concentrations of polymer solutions in N,N-dimethylformamide or in N,N-dimethylacetamide were filtered through RC filters with a nominal pore of 0.20 μm (Schleicher and Schuell) just before the measurements, to ensure that solutions were dust free. From the obtained results and using the adequate computer program based on the equation 2.15, *Zimm* diagrams were made and values for M_w, R_g and A_2 of polymers were determined.

3.3.11. Dynamic light scattering

Dynamic light scattering was carried out on a Zetasizer Nano S series (Malvern Instruments). The DLS experiments were performed at a temperature of 25 ^{0}C and at the wavelength of 633 nm. The scattering angle was 173 ^{0}. Polymer solutions (10-20 g/dm^3) were prepared in several different solvents and filtered through RC filters with a nominal pore of 0.2 μm (Schleicher and Schuell) just before measurements to ensure that solutions were dust free. Intensity, volume and number size distributions were determined by Zetasizer Software from the obtained correlation function.

3.3.12. Ultracentrifugation

The sedimentation rate of the HB polyesters was determined on an Optima XL-AI (BASF) analytical ultracentrifuge equipped with 8-cells-rotor. All measurements were carried out at 25 ^{0}C and at the wavelength of 675 nm. The aqueous dispersions of HB polymers (4.0-5.0 g/L) were prepared by adding a diluent containing ~ 0.5 g/dm^3 of emulsifier K30 (sodium salt of a C_{14}-alkyl sulfonate, Bayer, Leverkusen, FRG). The length of the cell was 1.2 cm, the rotor speed was 50000 min^{-1} and the run time was 2-3 h.

As a requirement for these measurements it was necessary to determine values of the density and refractive index of the HB polyesters. The density of the samples was obtained using the immersion technique at 25 ^{0}C by sinking a small amount of the solid sample into the 72 mass% solution of zinc chloride ($ZnCl_2$) in water. The density of this solution was 1.95 g/cm^3. Since the density of the HB polyesters was smaller than that of the solution, samples were floating. However, by dilution of the initial solution $ZnCl_2/H_2O$ with water, the HB sample started to immerge into the solution. Dilution was continued until equilibrium between the densities of the sample and solution was achieved. After that, the density of the diluted solution was determined with a pycnometer, and that was taken as a density of the HB samples.

The refractive index (n) of HB polyesters was determined by using the *Gladstone-Dale* equation[144]**:**

$$n = \frac{\mathrm{d}n}{\mathrm{d}c}\rho_0 + n_0 \tag{3.4}$$

where dn/dc is refractive index increment of the HB samples determined in N,N-dimethylformamide as a solvent, ρ_0 is the density of the solvent and n_0 is the refractive index of the solvent.

3.3.13. Viscosimetry of the diluted solutions

The viscosity measurements of HB polyesters were performed in an Ubbelohde capillary viscometer (Schott, size 0_a and I) using an automatic timer (Schott AVS 300), at 25 ± 0.1 ^{0}C in different solvents. The flow time measurements of the solvent and polymer solutions were conducted in triplicate for each concentration (measured to ~ 0.1% accuracy depending on flow time). The limiting viscosity number, [η], of the samples was determined graphically by extrapolation of the η_{sp}/c, determined at five different concentrations, to infinite dilution, using *Huggins* equation (2.22). Densities of the solutions were measured with a 25 cm^3 capacity pycnometer. The hydrodynamic radius R_η of HB polyesters was calculated from the limiting viscosity number by using the equation (2.45).

3.3.14. Rheology of the concentrated solutions and melt

The rheological measurements of HB polymers in concentrated solutions and in melt were performed on a Carri-Med CSL-100 (TA Instruments) stress controlled cone and plate rheometer. All experiments were conducted with a 2 cm diameter cone (cone angle - 2^0). Six

solutions of HB polyesters were prepared in N-methyl-2-pyrrolidinon, with concentrations ranging from 30 to 55 mass % (or from 10 to 55 mass % for commercial samples). Flow experiments were done with each solution at nine different temperatures (10-50 ^{0}C). Viscosity and shear stress were measured as a function of shear rate. The shear rate was varied from 0.3 to 1000 s^{-1} at a strain of 2 %.

Oscillatory experiments of the HB polyesters in the molten state were performed in the linear viscoelastic region using a temperature and frequency ramp. The temperature ramp was performed at a frequency of 1 Hz and strain of 2 % in the temperature region between 20 and 80 ^{0}C (i.e. between 15 and 60 ^{0}C for the samples HBP-3_{SA}). The frequency ramp was done at thirteen different temperatures (30-80 ^{0}C) for the investigated HB polyesters and at ten different temperatures (15-60 ^{0}C) for the samples HBP-3_{SA}, in the frequency region between 0.1 and 40 Hz and at the strain of 2 %. The dependence of G', G'', η^* and tan δ versus temperature and frequency were measured.

In all experiments the temperature control was achieved with a Peltier plate (0-80 ^{0}C) to a precision of 0.1 ^{0}C. Activation energy of flow for the HB polyesters was calculated using the equations 2.61 and 2.63.

3.3.15. Thermogravimetry

The thermal stability of HB polyesters were determined by nonisothermic thermogravimetric analysis using a NETZSCH TG 209 instrument in nitrogen atmosphere at heating rates of 5, 10, 15 and 20 ^{0}C/min (flow rate of N_2 was 25 cm^3/min). The activation energy of degradation for the polymers was determined using the equation (2.77) and software from the company NETZSCH – Netzsch Thermokinetic Analysis (Model free Estimation of Activation Energy – *Ozawa-Flynn-Wall* plot).

4. Results and Discussion

4.1. Synthesis of the hyperbranched polyesters

The hydroxy-functional HB polyesters used in this dissertation were synthesized via an acid-catalyzed esterification procedure in melt (Figure 4.1) from the aliphatic AB_2 monomer, bis-MPA, and the B_4 functional core, DiTMP. Samples of different pseudo generations were obtained by changing the molar core/monomer ratio. In order to compare two different ways of synthesis, two series of HB polyesters were synthesized (series I and II). The higher generations (from third till tenth) of the HB polyesters (series I) were synthesized from the previous pseudo generation by adding a stoichiometric amount of bis-MPA to obtain the next pseudo generation, i.e. a pseudo-one-step procedure was used. On the other side, the samples HBP-4II, HBP-6II and HBP-8II (series II) were synthesized by an one-step procedure, i.e. by adding an adequate amount of monomer to the core at once.

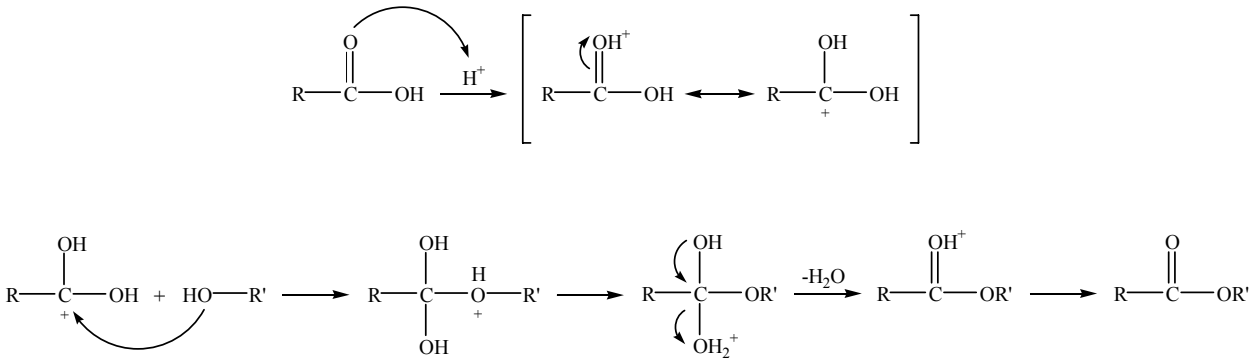

Figure 4.1. Acid-catalyzed esterification reaction

A schematic representation of the synthesis of HB polyesters is presented in Figure 4.2. Due to the possibility that monomers react with each other instead with the hydroxyl (-OH) groups from the DiTMP or with -OH groups from the linear or terminal repeating units of the hyperbranched polymer, in both ways of synthesis only a stoichiometric amount of bis-MPA was added to obtain the wanted pseudo generation. Therefore, the ratio between free bis-MPA and -OH groups of the DiTMP or from the HB skeleton was kept as low as possible. Beside that, both ways of synthesis were done at a relatively low reaction temperature (140 ^{0}C), i.e. at lower temperature than the melting point of bis-MPA (~ 190 ^{0}C). On the other side, the melting point of the core DiTMP is ~ 110 ^{0}C. Therefore, during the synthesis, bis-MPA was relatively slowly molten in the polymer melt. In addition to this, the electron-withdrawing effect of the carbonyl group of bis-MPA also contributes to the bigger reactivity of –OH groups of the DiTMP or from the polyol than those from bis-MPA. In this manner, the probability that carboxyl (-COOH) groups of bis-MPA react with –OH groups from the DiTMP or from the polyol is bigger than that they react with –OH groups of another bis-MPA to form poly(bis-MPA). In a certain degree, this can also decrease the possibility of the side reactions appearance, such as etherification and trans-esterification or formation of cyclic ethers by dehydration of bis-MPA. However, it is not completely possible to prevent the formation of poly(bis-MPA). As it was shown for the other similar HB polymers[35], in the

early stage of the reaction, oligomers of different size can be formed from bis-MPA. The probability for this reaction to occur is increasing with higher ratio between bis-MPA and core, i.e. during the synthesis of the HB polyesters of the higher generation number. In this way, hyperbranched species without core will be formed. Nevertheless, at high conversions focal –COOH group of these HB species can be coupled with the terminal –OH groups from the polyol and in this way partly disappear from the reaction system. The reaction of the focal –COOH group from poly(bis-MPA) with the –OH group from a linear repeating unit is less likely to occur, due to the large segment density. To obtain relatively high molar masses, water (side product) was permanently removed during the synthesis using either nitrogen purge or reduced pressure. At high conversions (> 90 %) the removal of the water was slowed down, due to the increased viscosity of the reaction mixture.

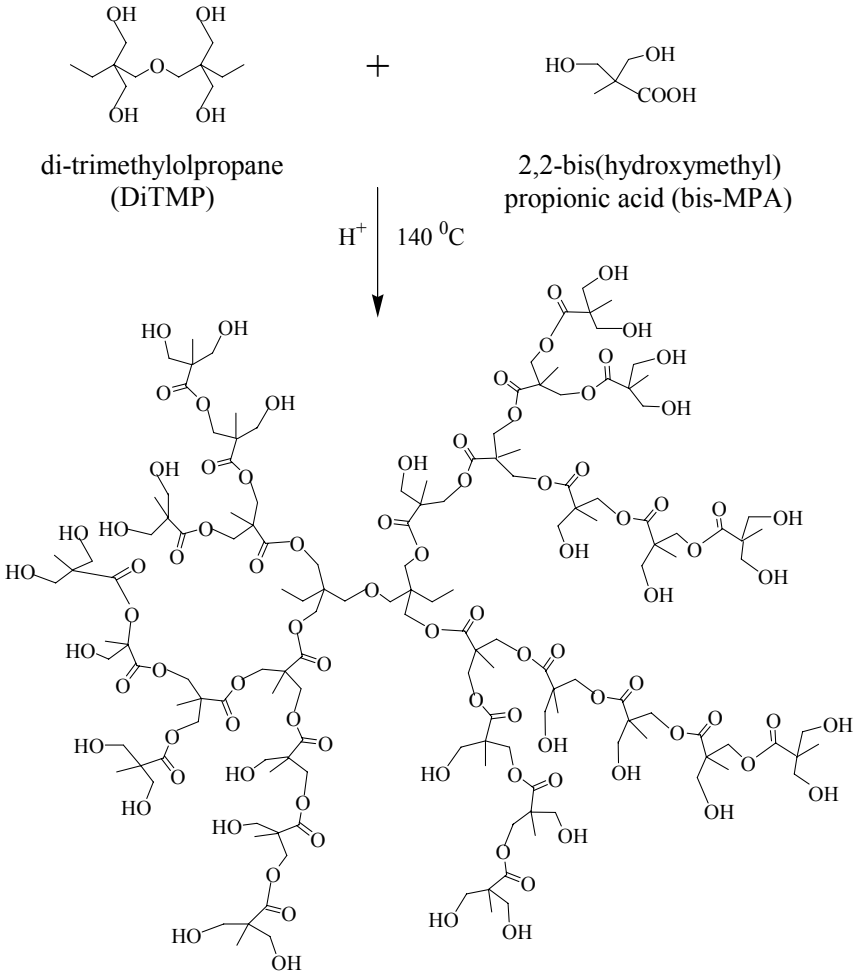

Figure 4.2. Schematic representation of the synthesis of HB polyesters

Beside the polymers synthesized in this work, three commercial hydroxyl-functional HB polyesters of different pseudo generations (BH-2, BH-3 and BH-4) were also used. The trade name of these samples is Boltorn® and they were synthesized via pseudo-one-step procedure from the bis-MPA as monomer and a tetrafunctional ethoxylated pentaerythrytol (PP50) core (Figure 4.3). In Table 4.1 selected characteristics of the self-synthesized and commercial HB polyesters are listed.

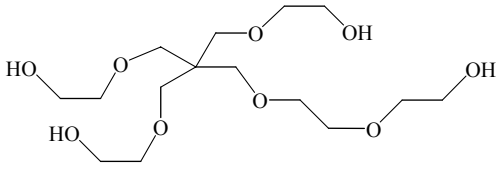

Figure 4.3. Schematic representation of the ethoxylated pentaerythrytol (PP50) core

Table 4.1. Selected characteristics of the HB polyesters and Boltorn® samples

Sample	Molar ratio core/monomer	Theor. number of generation	$(n_{OH})_{theor}$	M_{theor} [g/mol]	$(N_{BU})_{theor}$
HBP-2I	1/12	2	16	1642	12.1
HBP-3I	1/28	3	32	3498	28.2
HBP-4I and HBP-4II	1/60	4	64	7210	60.5
HBP-5I	1/124	5	128	14634	125.1
HBP-6I and HBP-6II	1/252	6	256	29482	254.2
HBP-8I and HBP-8II	1/1020	8	1024	118570	1028.9
HBP-10I	1/4092	10	4096	474922	4127.6
BH-2	1/12	2	16	1747	12.1
BH-3	1/28	3	32	3604	28.2
BH-4	1/60	4	64	7316	60.5

The theoretical molar mass, M_{theor}, and the theoretical number of end –OH groups, $(n_{OH})_{theor}$, listed in the Table 4.1 were calculated with the assumption that the reaction was carried out up to the conversion of 100 % and that no linear repeating units were formed during the synthesis. In this table is also presented the theoretical number of branching units, $(N_{BU})_{theor}$, calculated from the following equation[111]:

$$\left(N_{BU}\right)_{theor} = \frac{M_{theor} - M_{core}}{M_{BU}} \tag{4.1}$$

where M_{core} is the molar mass of the core molecule (M_{DiTMP} = 250 g/mol; M_{PP50} = 356 g/mol) and M_{BU} = 115 g/mol is the molar mass of the branching unit.

The presence of the ester groups in the HB samples can be detected with IR spectroscopy (1735 cm^{-1} and 1309-1044 cm^{-1}). Beside them, at 3431 cm^{-1} a peak, which corresponds to the –OH group, can be seen, while peaks at 2980 and 2888 cm^{-1} originate from $–CH_2$ and $–CH_3$ groups. The peak which appears at 1475 cm^{-1} is due to the $–CH_2$ scissors deformation vibration. However, the existence of the –COOH groups in the samples (1696 cm^{-1}) is not visible in the IR spectra of the HB polyesters. As an illustration, an IR spectrum of sample HBP-5I is presented in Figure 4.4, while IR spectra for the selected HB polyesters are shown in the Appendix 7.1.

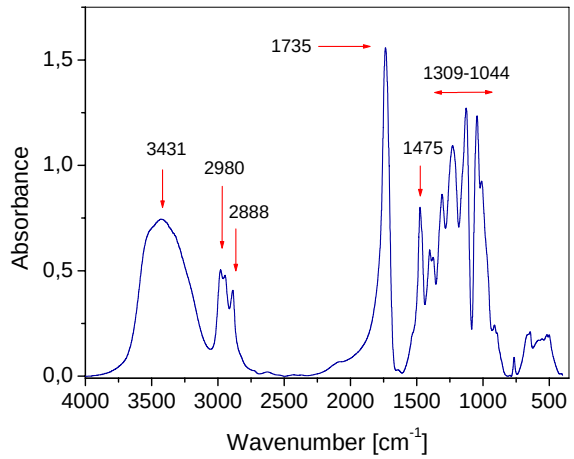

Figure 4.4. IR spectra of the sample HBP-5I

In ^{13}C NMR spectra of the HB polyesters carbonyl groups can be seen (between 172 and 175 ppm), methylene groups (between 63 and 66 ppm), quaternary carbons (between 46 and 51 ppm) and methyl groups around 17 ppm. In ^{13}C NMR spectra of some samples, a signal of small intensity around 71 ppm was also detected. This signal is assigned to the ether carbon. In Figure 4.5, a ^{13}C NMR spectrum of the sample HBP-10I is presented. Spectra of other selected HB samples can be found in Appendix 7.2.1.

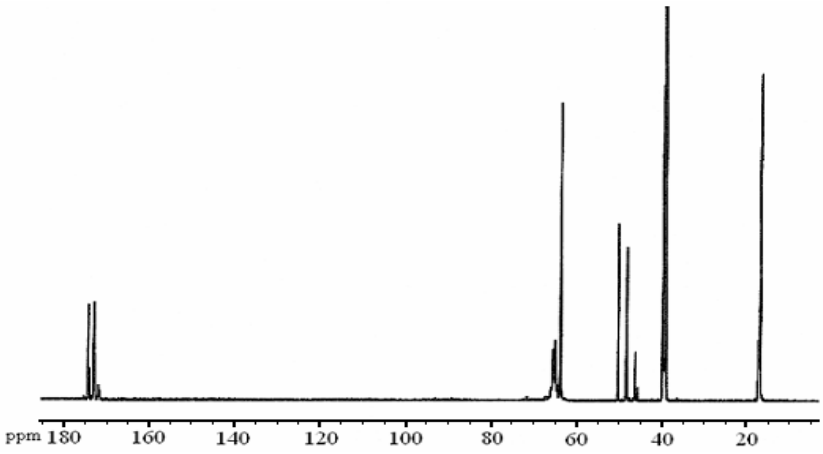

Figure 4.5. ^{13}C NMR spectrum of HBP-10I in DMSO-d_6

From the ^{13}C NMR spectra of the HB polyesters the degree of branching (*DB*) can be calculated, by comparing the integrals of the different units, i.e. of the terminal, linear and dendritic unit, to determine their relative amounts. As can be seen from Figure 4.6, terminal units (T) have two unreacted –OH groups from bis-MPA and they are located in the external layer of the HB polymer. Linear units (L) have one unreacted –OH group and therefore do not contribute to the branching. As it was already described in the chapter 2.3, linear units are usually considered as defects in these types of polymers. On the other side, in dendritic units (D) both –OH groups have reacted.

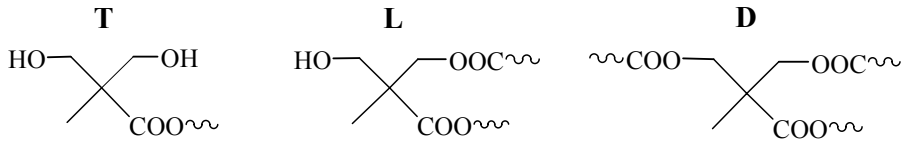

Figure 4.6. Terminal (T), linear (L) and dendritic (D) repeating units of the HB polyesters

The signal of the quaternary carbon belonging to the terminal units can be found at $\delta_T \approx 50.3$ ppm, while at $\delta_L \approx 48.3$ ppm and $\delta_D \approx 46.3$ ppm are the signals which belong to the linear and dendritic units[34], respectively (Figure 4.7). The splitting of some signals is due to the different neighbouring units. For the samples HBP-6II and HBP-8II the corresponding signals are slightly shifted ($\delta_T \approx 51.1$ ppm, $\delta_L \approx 49.1$ ppm and $\delta_D \approx 47.1$ ppm). The integrated intensities of signals which correspond to the different units are listed in Table 4.2, as well as the values of *DB* calculated according to the equations (2.4) and (2.5).

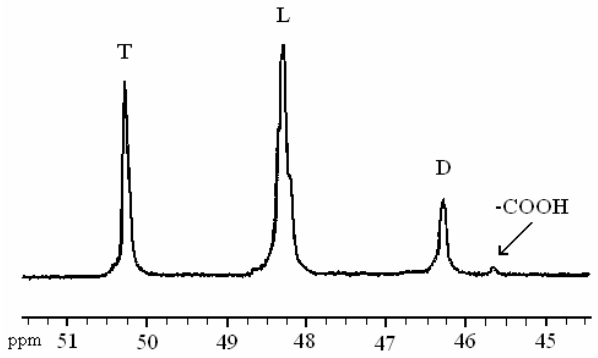

Figure 4.7. Magnification of the quaternary carbon region of the ^{13}C NMR spectrum of HBP-4I in DMSO-d_6

Table 4.2. Results obtained from the ^{13}C NMR spectra of HB polyesters

Sample	Integrated intensities of the signals				$DB_{Fréchet}$	DB_{Frey}
	I(T)	*I*(L)	*I*(D)	*I*(COOH)		
HBP-2I	1.0000	1.4077	0.2702	/	0.47	0.28
HBP-3I	1.0000	1.7144	0.3963	0.0160	0.45	0.32
HBP-4I	1.0000	1.9166	0.4951	0.0277	0.44	0.34
HBP-4II	1.0000	1.9432	0.4275	/	0.42	0.30
HBP-5I	1.0000	1.9158	0.5595	0.0458	0.45	0.37
HBP-6I	1.0000	2.0366	0.5392	0.0395	0.43	0.35
HBP-6II	1.0000	1.8406	0.3800	0.0821	0.43	0.29
HBP-8I	1.0000	2.0856	0.5651	0.0757	0.43	0.35
HBP-8II	1.0000	2.2889	0.3305	0.0739	0.37	0.22
HBP-10I	1.0000	2.1283	0.5378	0.0799	0.42	0.34
BH-2	/	/	/	/	0.43[a]	0.30[a]
BH-3	/	/	/	/	0.42[a]	0.31[a]
BH-4	/	/	/	/	0.40[a]	0.34[a]

[a]data of *Luciani* and co-workers[106]

From the Table 4.2 and Figure 4.8 it can be observed that values of $DB_{\text{Fréchet}}$ decrease and DB_{Frey} increase with the theoretical number of generation, except for the sample HBP-5I. The reason for such behaviour is the different definition of $DB_{\text{Fréchet}}$ and DB_{Frey}, which is already explained in the chapter 2.3 of this dissertation. However, *DB* of these samples did not reach the value of 0.50, probably due to the relatively high functionality (y = 4) of the core molecule, which further causes that –OH groups in linear units are less reactive because of the relatively high segment density, i.e. because of the spatial constraints. Similar conclusions can be made for the commercial HB polyesters. Beside that, it can be seen that Boltorn® samples have slightly lower values of the degree of branching than the analogue HB polyesters synthesized with DiTMP as core.

For the samples HBP-4II, HBP-6II and HBP-8II values of *DB* are lower than for the samples HBP-4I, HBP-6I and HBP-8I, which means that the procedure for the synthesis can have a big influence on the branching frequency in these polymers. This is especially uttered for the sample HBP-8II, where during the synthesis the ratio between monomer and core was the highest. It is obvious that pseudo-one-step procedure can provide bigger accessibility of carboxyl groups of bis-MPA, i.e. bis-MPA can react easier with –OH groups from the linear repeating units to create a new dendritic unit. From these results it can be concluded that sequential addition of the stoichiometric amount of a monomer to the previously synthesized pseudo generation can increase degree of branching of the HB samples. This is important since, the higher degree of branching can provide more dendrimer-like properties.

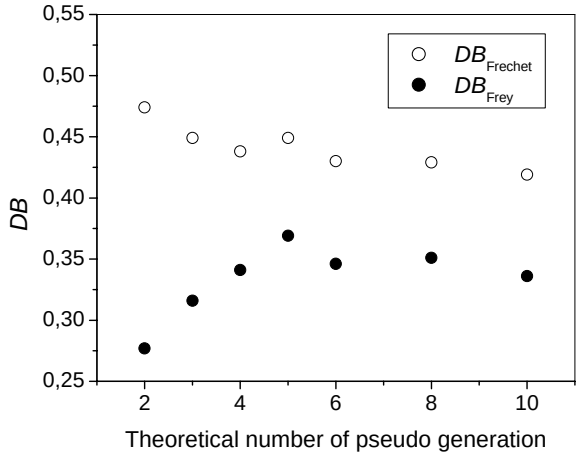

Figure 4.8. Dependence of $DB_{\text{Fréchet}}$ and DB_{Frey} versus theoretical number of pseudo generation for the HB polyesters of series I

From the degree of conversion of bis-MPA carboxyl groups, p_A, the branching coefficient, DB_p, of an AB_2 monomer can be calculated according to the equation (4.2)[14]:

$$DB_p = \frac{p_A}{2} \tag{4.2}$$

As it was mentioned before, in IR spectra of HB polyesters, a peak that corresponds to the –COOH group was not detected. However, from the results obtained with ^{13}C NMR spectroscopy (Figure 4.7), it was possible to detect a small peak ($\delta \approx 45.65$ ppm) which corresponds to the quaternary carbon attached to an unreacted –COOH group and two reacted hydroxyl groups, i.e. focal –COOH group of poly(bis-MPA)[35]. For the second pseudo generation and for the sample HBP-4II, this peak did not appear. However, for all other

samples the existence of this signal was pointed out (Figure 4.9). This shows that hyperbranched structures without the core molecule (DiTMP) were also formed during the synthesis of most HB polyesters. The degree of conversion of carboxyl groups can be calculated from the following equation:

$$p_A = 1 - \frac{N_t}{N_0} \tag{4.3}$$

where N_0 and N_t are the number of molecules present at times $t = 0$ and $t = t$ in the mixture, respectively. When ^{13}C NMR is used to calculate the degree of conversion, then N_t represents the integral of quaternary carbon attached to the carboxyl group and N_0 is the sum of the integrals of all quaternary carbons. Values of the integral necessary to calculate N_t (I(COOH)) for different HB polyesters are listed in Table 4.2 and it can be seen that they generally increase with the number of pseudo generation. This indicates that for the higher pseudo generations carboxyl groups are more protected from the further reaction during the synthesis, probably due to the intra- or intermolecular hydrogen bonding. The twice bigger value of the I(COOH) for the sample HBP-6II compared with the value for the HBP-6I again shows that the procedure for the synthesis can have significant influence on the structure of the final HB polyester, i.e. a bigger amount of the poly(bis-MPA) was formed in this case. Values of the p_A calculated from the ^{13}C NMR spectra and corresponding values of the DB_p are listed in Table 4.3. Values for the I(COOH) and integrals of the other signals for the commercial HB polyesters are not presented in the Table 4.2, because they were not available in the mentioned article[106]. Therefore, it was not possible to calculate p_A from the ^{13}C NMR spectra of these polymers. However, the presence of the signal for the quaternary carbon attached to an unreacted –COOH group in ^{13}C NMR spectra of Boltorn® samples was already pointed out in the literature[71].

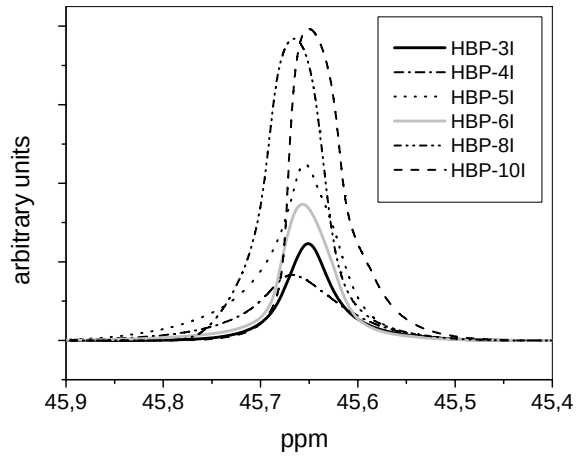

Figure 4.9. Magnification of the signal for the quaternary carbon attached to an unreacted –COOH group for the different HB polyesters of series I

In Table 4.3 the values for the degree of conversion of carboxyl acid groups of bis-MPA calculated from the acid number titration (N_{AN}) are also presented. These values were also calculated using the equation (4.3), but in this case N_t is the acid number of the sample after the reaction was finished and N_0 is the acid number of bis-MPA (418 mg KOH/g). Both N_{AN} were calculated from equation (3.1). Acid number titrations were done during the synthesis to control the course of the reaction. Therefore, the reaction was carried out up to

the lowest possible acid number, i.e. until N_{AN} became constant. Values of the p_A calculated from the acid number titration and corresponding values of the DB_p for the HB polyesters are also listed in Table 4.3.

Table 4.3. Values of the p_A and DB_p calculated from the ^{13}C NMR and acid number titration and values of the N_{AN} for the different pseudo generations of HB polyesters

Sample	p_A (^{13}C NMR)	DB_p (^{13}C NMR)	N_{AN} [mg KOH/g]	p_A (N_{AN})	DB_p (N_{AN})
HBP-2I	1.00	0.50	5.87	0.99	0.49
HBP-3I	0.99	0.49	8.88	0.98	0.49
HBP-4I	0.99	0.49	10.82	0.97	0.48
HBP-4II	1.00	0.50	9.00	0.98	0.49
HBP-5I	0.99	0.49	11.83	0.97	0.48
HBP-6I	0.99	0.49	12.21	0.97	0.48
HBP-6II	0.97	0.48	10.98	0.97	0.48
HBP-8I	0.98	0.49	14.11	0.97	0.48
HBP-8II	0.98	0.49	13.23	0.97	0.48
HBP-10I	0.98	0.49	14.57	0.96	0.48
BH-2	/	/	7.50[a]	0.98	0.49
BH-3	/	/	7.10[a]	0.98	0.49
BH-4	/	/	6.50[a]	0.98	0.49

[a]data from supplier

By comparing the values of the *DB* presented in Table 4.2 and DB_p presented in Table 4.3 it can be seen that the values of DB_p are much higher. The degree of conversion of the acid groups calculated from the ^{13}C NMR spectra is slightly higher than values obtained from the acid number titration (Table 4.3). This can be due to the relatively small signal of the peak which corresponds to the quaternary carbon attached to the unreacted –COOH group. Consequently, the integration of such a small peak brings errors in the further calculations. On the other side, values for the degree of conversion determined from the acid number titration are probably slightly underestimated, since at higher conversion, the number of the acid groups is quite small. Therefore, it is possible that samples are over titrated during the acid number titration to a certain amount, because only very small volumes of the base were required to neutralize the sample. Slightly higher values of the p_A and DB_p calculated from the N_{AN} for the second series of the samples and for the commercial samples show that these samples were synthesized up to the somewhat bigger degree of conversion.

From the Table 4.3 and Figure 4.10 it can be seen that values of the N_{AN} increase with the theoretical number of pseudo generation. This also indicates that the availability of the carboxyl groups from the bis-MPA becomes smaller with increasing number of pseudo generation.

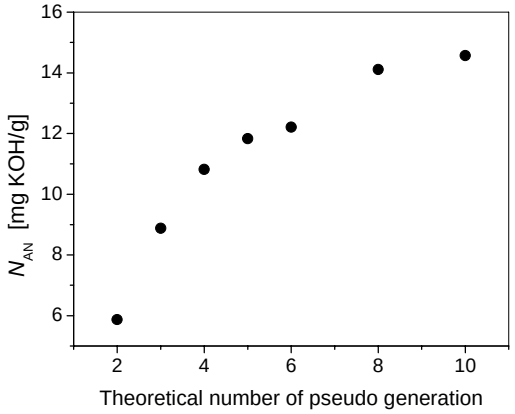

Figure 4.10. Dependence of the N_{AN} versus theoretical number of pseudo generation for the HB polyesters of the series I

From the integrated values of adequate signals, determined with ^{13}C NMR spectroscopy (Table 4.2), the portion of every monomer unit (terminal, linear or dendritic) in HB polyesters can be calculated (Table 4.4). These experimentally determined values are compared with portions of different repeating units which were calculated using the following equations developed by *Frey* and co-workers[51]:

$$(n_T)_{theor} = \left(1 - \frac{1}{2} p_A\right)^2 A_0 \tag{4.4}$$

$$(n_L)_{theor} = \left(p_A - \frac{1}{2} p_A^2\right) A_0 \tag{4.5}$$

$$(n_D)_{theor} = \frac{1}{4} p_A^2 A_0 \tag{4.6}$$

where $(n_T)_{theor}$, $(n_L)_{theor}$ and $(n_D)_{theor}$ are theoretical number of terminal, linear and dendritic repeating units, respectively, proportional to their concentrations. A_0 is the initial number of carboxyl groups at the beginning of the reaction. These equations are made for the ideal case assuming the equal reactivity of –OH groups belonging to the terminal and linear repeating units and absence of the undesired side reactions. By using the values of the p_A, determined from the ^{13}C NMR spectra of the samples (Table 4.3), portions of different repeating units were calculated according to the model described with equations (4.4) to (4.6) and these values are also listed in Table 4.4. For all samples the experimentally determined portions of linear units are higher than for the model, which means that reactivity of different –OH groups is not the same, i.e. that terminal –OH groups have bigger reactivity than linear ones. The reason for this is probably the relatively high density of the segments, which makes it difficult for the free bis-MPA to react with –OH groups from linear units and/or due to the changes in reactivity when one of the –OH groups has reacted. As a consequence of that, for all samples, experimentally determined portions of terminal units are higher, while the portions of dendritic units are lower, than in the ideal case. Beside that, for the samples of the series I, the portion of dendritic units increases up to the fifth pseudo generation, after which $(x_D)_{exp}$ slightly decreases. This fact shows again the big influence of the segment density on the synthesis of HB polyesters. As it was expected, samples of the series II (synthesized by

one-step procedure) have lower perfection of the structure compared with the adequate samples synthesized by pseudo-one-step procedure ($(x_D)_{exp}$ (II series samples) < $(x_D)_{exp}$ (I series samples)).

Table 4.4. Values of the experimentally determined ($(x_T)_{exp}$, $(x_L)_{exp}$ and $(x_D)_{exp}$) and calculated ($(x_T)_{theor}$, $(x_L)_{theor}$ and $(x_D)_{theor}$) portions of different repeating units in the HB samples

Sample	$(x_T)_{exp}$ [%]	$(x_L)_{exp}$ [%]	$(x_D)_{exp}$ [%]	$(x_T)_{theor}$ [%]	$(x_L)_{theor}$ [%]	$(x_D)_{theor}$ [%]
HBP-2I	37.3	52.6	10.1	25.0	50.0	25.0
HBP-3I	32.2	55.1	12.7	25.2	50.0	24.8
HBP-4I	29.3	56.2	14.5	25.4	50.0	24.6
HBP-4II	29.7	57.6	12.7	25.0	50.0	25.0
HBP-5I	28.8	55.1	16.1	25.6	50.0	24.4
HBP-6I	28.0	56.9	15.1	25.6	50.0	24.4
HBP-6II	31.0	57.2	11.8	26.2	50.0	23.8
HBP-8I	27.4	57.1	15.5	26.0	50.0	24.0
HBP-8II	27.6	63.3	9.1	25.0	50.0	25.0
HBP-10I	27.3	58.0	14.7	26.1	50.0	23.9

In order to calculate the hydroxyl number (N_{HN}) of the investigated HB polyesters, a hydroxyl number titration was performed. The experimentally determined hydroxyl number of the samples, $(N_{HN})_{exp}$, was calculated according to the equation (3.2). On the other side, the theoretical hydroxyl number, $(N_{HN})_{theor}$, was calculated with assumption that all acid groups have reacted ($N_{AN} = 0$) using the following equation:

$$(N_{HN})_{theor} = \frac{56100 \times (n_{OH})_{theor}}{M_{theor}} \tag{4.7}$$

In equation (4.7) $(n_{OH})_{theor}$ is the theoretical number of end –OH groups (Table 4.1) and 56100 is the molar mass of KOH (in mg/mol). From the values of $(N_{HN})_{exp}$, $(N_{HN})_{theor}$ and $(n_{OH})_{theor}$, the mass fraction of the end –OH groups (w_{OH}^{tot}) and the total number of end –OH groups per molecule ($(n_{OH}^{tot})_{exp}$) were calculated. Furthermore, the ratio between the –OH groups belonging to the linear and terminal repeating units in every sample can be calculated from the corresponding integrals from ^{13}C NMR spectra (Table 4.2), since it is known that terminal units have two unreacted –OH groups and linear units have only one. Finally, using all these values it was possible to calculate the percentage of terminal –OH groups, i.e. the percentage of –OH groups that belong to the terminal repeating units, the number of terminal –OH groups per molecule ($(n_{OH}^{T})_{exp}$) and the mass fraction of terminal –OH groups in each sample (w_{OH}^{T}). All these values are listed in the Table 4.5.

By comparing the theoretical number of end –OH groups, $(n_{OH})_{theor}$, (Table 4.1) with the obtained value $(n_{OH}^{T})_{exp}$ (Table 4.5) it can be seen that only ~ 50 % of all –OH groups which are present in the molecule of HB polyesters belong to the terminal groups, while the rest is situated on the linear repeating units. This property is typical for the HB polymers and

the main reason why they do not have such a perfect structure as dendrimers. Furthermore, the percentage of end, and at the same time, terminal –OH groups decreases for the samples of higher pseudo generation, i.e. low generation HB polymers have a higher concentration of terminal hydroxyl groups (Figure 4.11), which means that the ratio between linear and terminal repeating units increases with the number of generation. This behaviour is due to the higher density of the segments in these samples, which further complicates the access of the monomer to the –OH groups in the linear units during the synthesis. Beside that, from the results listed in the Table 4.5 it can be seen that the samples which were synthesized using the one-step procedure (HBP-4II, HBP-6II and HBP-8II) have lower values of the $(N_{HN})_{exp}$ than analogue HB samples synthesized by pseudo-one-step procedure. When all components required for the synthesis were added at once (one-step procedure), conversion of the –COOH groups from the bis-MPA was somewhat higher, which can be seen from the obtained acid number titration (Table 4.3) and the absence of the signal corresponding to the quaternary carbon attached to an unreacted –COOH group in ^{13}C NMR (sample HBP-4II, Table 4.2). However, that did not provide higher hydroxyl number and higher *DB*, which can be explained by the greater possibility of side reactions during the one-pot synthesis. A slightly higher value of the $(n_{OH}^{T})_{exp}$ for the sample HBP-6II than for the sample HBP-6I is due to the lower ratio between linear and terminal repeating units in HBP-6II. This can be explained by the fact that during the synthesis of HBP-6II a bigger amount of poly(bis-MPA) was formed (Table 4.2). For the free bis-MPA it is much easier to react with the –OH groups from the linear repeating units from poly(bis-MPA) than from the HB polyol due to the lower density of the segments. Therefore, the average ratio between linear and terminal repeating units in the sample HBP-6II is lower than in the sample HBP-6I. This also explains why there is such a small difference between the $DB_{Fréchet}$ for these two samples (Table 4.2).

Table 4.5. Values of the $(N_{HN})_{theor}$, $(N_{HN})_{exp}$, w_{OH}^{tot}, $(n_{OH}^{tot})_{exp}$, percentage of terminal –OH groups (in the total number of –OH groups), $(n_{OH}^{T})_{exp}$) and (w_{OH}^{T}) for the HB polyesters

Sample	$(N_{HN})_{theor}$ [mg KOH/g]	$(N_{HN})_{exp}$ [mg KOH/g]	w_{OH}^{tot} [mass %]	$(n_{OH}^{tot})_{exp}$	% of terminal –OH groups	$(n_{OH}^{T})_{exp}$	w_{OH}^{T} [mass %]
HBP-2I	546.6	541.1	16.4	16	58.7	9	9.6
HBP-3I	513.2	507.2	15.4	32	53.8	17	8.3
HBP-4I	498.0	492.5	14.9	63	51.1	32	7.6
HBP-4II	498.0	488.5	14.8	63	50.1	31	7.4
HBP-5I	490.7	487.4	14.8	127	51.1	65	7.6
HBP-6I	487.1	480.2	14.5	252	49.5	125	7.2
HBP-6II	487.1	467.6	14.2	246	52.1	128	7.4
HBP-8I	484.5	476.9	14.4	1008	48.9	493	7.0
HBP-8II	484.5	464.7	14.1	982	46.6	458	6.6
HBP-10I	483.8	473.7	14.3	4010	48.4	1943	6.9
BH-2	513.8	501.1	15.2	16	/	/	/
BH-3	498.1	474.1	14.4	30	/	/	/
BH-4	490.8	470.5	14.3	61	/	/	/

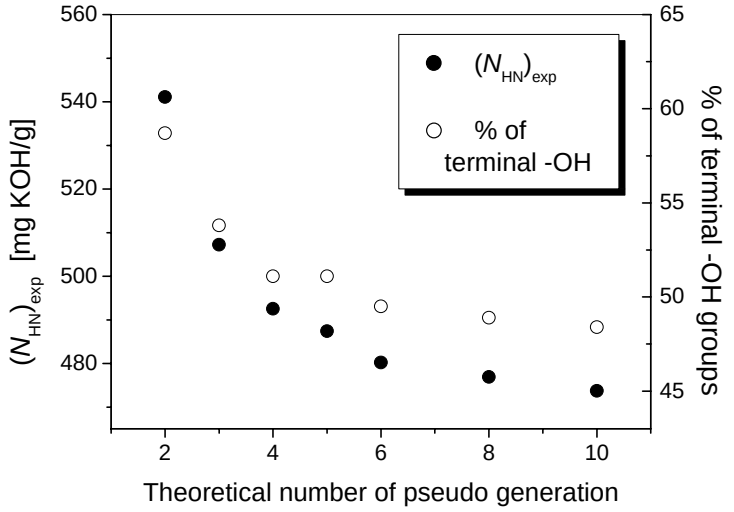

Figure 4.11. Dependence of the N_{HN} and mass percentage of terminal –OH groups versus theoretical number of pseudo generation for the HB polyesters of the series I

In order to get more information about the structure of the HB polymers synthesized in this work and commercial HB polyesters, seven samples were fractionated from a solvent/non-solvent mixture to obtain three fractions (F1, F2 and F3) of each sample. Five HB polyesters (HBP-3I, HBP-4I, HBP-6I, HBP-8I and HBP-10I) and two Boltorn® samples (BH-3 and BH-4) were fractionated using this procedure. The efficiency of the fractionation procedure was proved with the so called *Philippoff* rule[145] (see chapter 4.4, Table 4.29):

$$[\eta] = \sum_{i=1}^{\infty} w_i [\eta_i] \tag{4.8}$$

where w_i is the mass fraction of the *i*-th fraction and $[\eta]$ and $[\eta_i]$ are the limiting viscosity numbers of the parent sample and fractions, respectively.

As it was described in the chapter 3.2.2, the fractionation was performed according to the previously determined titration curve (for the sample HBP-6I) in order to obtain approximately the same amount of each fraction. However, that was not accomplished for most of the fractionated samples (especially for the lower generation samples), which can be seen from the value of the mass portion of fractions (w_F) presented in the Table 4.6. The reason for this is probably that HB polyesters of different pseudo generations have different indices of polydispersity. For each fraction, the acid and hydroxyl number was determined and these values are also listed in Table 4.6. Beside that, values of the p_A and DB_p (calculated from the obtained N_{AN}), mass fraction of end –OH groups (w_{OH}^{tot}) and total number of end –OH groups per molecule $(n_{OH}^{tot})_{exp}$ were calculated. For an easier comparison, adequate values of the corresponding parent samples are also listed.

Table 4.6. Values of the mass portion (w_F), N_{AN}, $p_A(N_{AN})$, DB_p (N_{AN}), $(N_{HN})_{exp}$, mass fraction of end –OH groups (w_{OH}^{tot}) and total number of end –OH groups per molecule $(n_{OH}^{tot})_{exp}$ for each fraction of the investigated HB polyesters

Sample	w_F [mass %]	N_{AN} [mg KOH/g]	p_A (N_{AN})	DB_p (N_{AN})	$(N_{HN})_{exp}$ [mg KOH/g]	w_{OH}^{tot} [mass %]	$(n_{OH}^{tot})_{exp}$
HBP-3I	/	8.88	0.98	0.49	507.2	15.4	32
F1	16.4	8.77	0.98	0.49	441.1	13.4	27
F2	16.4	9.65	0.98	0.49	470.8	14.3	29
F3	67.2	11.23	0.97	0.48	409.4	12.4	25
HBP-4I	/	10.82	0.97	0.48	492.5	14.9	63
F1	21.1	8.53	0.98	0.49	426.0	12.9	55
F2	25.3	11.01	0.97	0.48	410.1	12.4	53
F3	53.6	12.86	0.97	0.48	373.9	11.3	48
HBP-6I	/	12.21	0.97	0.48	480.2	14.5	252
F1	25.4	9.11	0.98	0.49	414.5	12.6	218
F2	37.4	9.70	0.98	0.49	405.8	12.3	213
F3	37.2	19.56	0.95	0.47	451.2	13.7	237
HBP-8I	/	14.11	0.97	0.48	476.9	14.4	1008
F1	28.1	9.09	0.98	0.49	425.6	12.9	899
F2	32.7	10.11	0.98	0.49	411.1	12.5	869
F3	39.2	20.68	0.95	0.47	445.6	13.5	942
HBP-10I	/	14.57	0.96	0.48	473.7	14.3	4010
F1	35.1	9.90	0.98	0.49	412.3	12.5	3491
F2	24.2	10.63	0.97	0.48	393.2	11.9	3329
F3	40.7	15.50	0.96	0.48	361.4	10.9	3060
BH-3	/	7.10	0.98	0.49	474.1	14.4	30
F1	25.7	6.90	0.98	0.49	382.2	11.6	24
F2	19.0	8.72	0.98	0.49	386.9	11.7	25
F3	55.3	9.48	0.98	0.49	370.6	11.2	24
BH-4	/	6.50	0.98	0.49	470.5	14.3	61
F1	27.9	5.95	0.99	0.49	379.5	11.5	49
F2	23.4	8.08	0.98	0.49	378.8	11.5	49
F3	48.7	9.54	0.98	0.49	355.9	10.8	46

Values obtained from the acid number titration show that for all fractionated samples N_{AN} increases in the following manner: $(N_{AN})_{F1} < (N_{AN})_{F2} < (N_{AN})_{F3}$ (Figure 4.12), i.e. the third fraction has the biggest amount of the unreacted –COOH groups, as it was expected. The value of the N_{AN}, and consequently values of the p_A and DB_p (calculated from N_{AN}), for the first fraction were bigger in most cases than for the parent sample. From this it can be concluded that the fraction of dendritic units decreases from F1 to F3. On the other side, values of the $(N_{HN})_{exp}$ and w_{OH}^{tot} do not show the same tendency and they are for all fractions lower than the corresponding values for the parent samples.

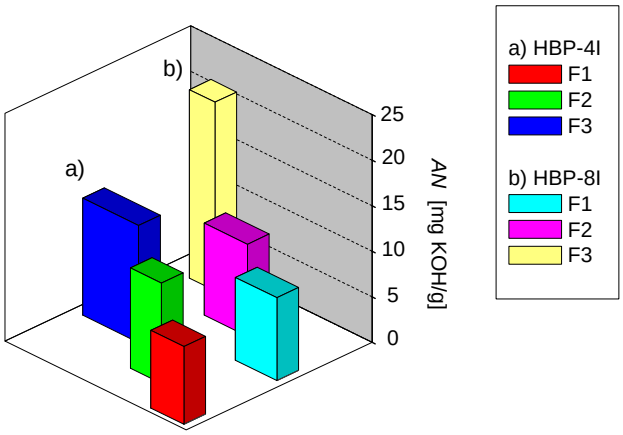

Figure 4.12. N_{AN} values for the fractions of samples a) HBP-4I and b) HBP-8I (volume of the bars is proportional to the mass fraction)

From the results obtained by ^{13}C NMR spectroscopy (Figure 4.13, Table 4.7), values of the *DB* for the fractions of the samples HBP-4I and HBP-6I were calculated according to the equations (2.4) and (2.5) and these values are listed in Table 4.7. From these values it can be seen that DB_{Frey} is decreasing in the order F1 > F2 > F3, due to the decreasing of the dendritic units portion (Table 4.8). On the other side, values of the $DB_{Fréchet}$ do not change very much for different fractions of the samples HBP-4I and HBP-6I. This is due to the different definitions of DB_{Frey} and $DB_{Fréchet}$. The degree of branching calculated according to the equation (2.4) decreases from 1 (degree of conversion of acid groups, $p_A = 0$) to 0.5 at complete conversion. On the other side, DB_{Frey} increases from zero ($p_A = 0$) to 0.5[49]. In other words, $DB_{Fréchet}$ is overestimated at low molar masses. For the fractions of the sample HBP-4I the number of terminal –OH groups per molecule is changing in the order $((n_{OH}^{T})_{exp})_{F1} > ((n_{OH}^{T})_{exp})_{F2} > ((n_{OH}^{T})_{exp})_{F3}$. On the other side, the value of the $(n_{OH}^{T})_{exp}$ is the highest for the third fraction of the sample HBP-6I, because of the lower ratio between the integral of linear and terminal units to the other fractions and the parent sample. Furthermore, the signal of the quaternary carbon attached to an unreacted –COOH group was detected only in the ^{13}C NMR spectrum of the third fraction of this sample (Figure 4.13) and the integral of this signal is much higher than the integral of the equivalent signal for the parent sample. As a consequence, the degree of conversion of carboxyl groups, calculated form the integrated values of the T, L, D and –COOH signals for the third fraction of sample HBP-6I ($p_A = 0.92$), is quite lower than the corresponding value for the parent sample (Table 4.3). This result is in accordance with the surprisingly higher value of the N_{AN} for the fraction F3, comparing with the N_{AN} values for the HBP-6I and other fractions (Table 4.6). The presence of unreacted carboxyl groups confirms the assumption that during the synthesis poly(bis-MPA), i.e. HB structures without the DiTMP core molecule were also formed and that the reaction probably proceeds not only by addition of monomer to the growing HB molecule, but also between the oligomers. A signal of the unreacted –COOH groups was not detected in the ^{13}C NMR spectra of the HBP-4I fractions.

Table 4.7. Results obtained from the ^{13}C NMR spectra (integrated intensities of the signals, DB_p, $DB_{\text{Fréchet}}$, DB_{Frey}), percentage of terminal –OH groups and values of the $(n_{\text{OH}}^{\text{T}})_{\text{exp}}$ for the samples HBP-4I and HBP-6I and their fractions

Sample	Integrated intensities of the signals				DB_p	$DB_{\text{Fréchet}}$	DB_{Frey}	% of ter. –OH groups	$(n_{\text{OH}}^{\text{T}})_{\text{exp}}$
	I(T)	I(L)	I(D)	I(COOH)					
HBP-4I	1.0000	1.9166	0.4951	0.0277	0.49	0.44	0.34	51.1	32
F1	1.0000	1.7880	0.5579	/	0.50	0.47	0.38	52.8	29
F2	1.0000	1.9157	0.5304	/	0.50	0.44	0.36	51.1	27
F3	1.0000	1.8399	0.4793	/	0.50	0.45	0.34	52.1	25
HBP-6I	1.0000	2.0366	0.5392	0.0395	0.49	0.43	0.35	49.5	125
F1	1.0000	2.0616	0.6301	/	0.50	0.44	0.38	49.2	107
F2	1.0000	2.0733	0.5951	/	0.50	0.43	0.36	49.1	105
F3	1.0000	1.7283	0.3446	0.2292	0.46	0.44	0.28	53.6	127

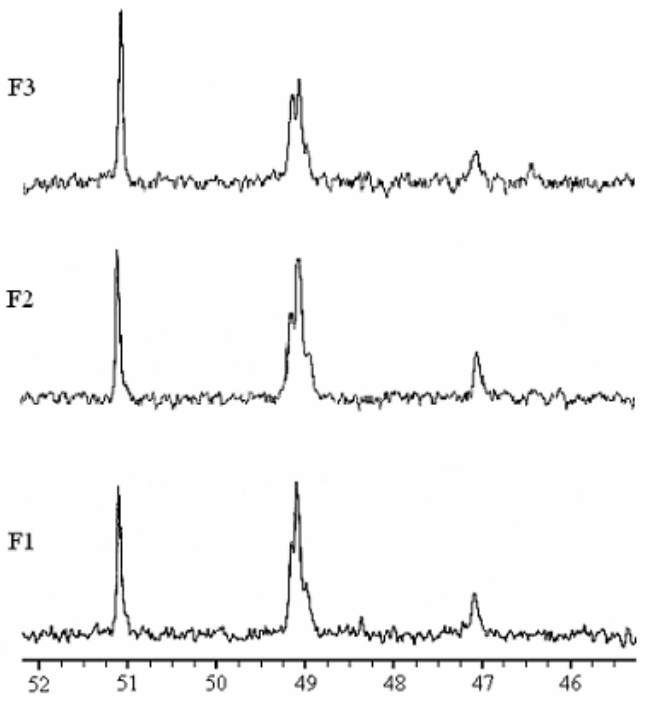

Figure 4.13. Magnification of the quaternary carbon region ^{13}C NMR spectra of HBP-6I fractions

By comparing the experimentally determined values ($(x_T)_{exp}$, $(x_L)_{exp}$ and $(x_D)_{exp}$) for the HBP-4I and HBP-6I fractions with values calculated according to the model developed by *Frey* and co-workers ($(x_T)_{theor}$, $(x_L)_{theor}$ and $(x_D)_{theor}$)[51], again a big influence of the high segmental density and different reactivity of the end –OH groups belonging to the linear and terminal repeating units can be noticed (Table 4.8). According to these results it can be seen that the portion of the dendritic units is decreasing from the first up to the third fraction. In other words, the portion of dendritic units is decreasing with decreasing degree of conversion

of the bis-MPA carboxyl groups. At the same time the portion of terminal units is increasing from the first up to the third fraction.

Table 4.8. Values of the experimentally determined ($(x_T)_{exp}$, $(x_L)_{exp}$ and $(x_D)_{exp}$) and calculated ($(x_T)_{theor}$, $(x_L)_{theor}$ and $(x_D)_{theor}$) portions of different repeating units in the fractions of the samples HBP-4I and HBP-6I

Sample	$(x_T)_{exp}$ [%]	$(x_L)_{exp}$ [%]	$(x_D)_{exp}$ [%]	$(x_T)_{theor}$ [%]	$(x_L)_{theor}$ [%]	$(x_D)_{theor}$ [%]
HBP-4I	29.3	56.1	14.5	25.4	50.0	24.6
F1	29.9	53.4	16.7	25.0	50.0	25.0
F2	29.0	55.6	15.4	25.0	50.0	25.0
F3	30.1	55.4	14.5	25.0	50.0	25.0
HBP-6I	28.0	56.9	15.1	25.6	50.0	24.4
F1	27.1	55.8	17.1	25.0	50.0	25.0
F2	27.3	56.5	16.2	25.0	50.0	25.0
F3	32.5	56.3	11.2	28.6	49.7	21.7

4.2. Determination of the molar mass

4.2.1. Results from the ^{1}H NMR spectroscopy

From the ^{1}H NMR spectra of the HB polyesters the structure of these polymers can be proved. Beside that, using the integrated intensities of the adequate signals it is possible to calculate the degree of polymerization, and consequently, the number average molar mass of the HB polyesters. ^{1}H NMR spectra of the samples synthesized in this work were obtained using two different solvents, i.e. DMSO-d_6 and a mixture D_2O/DMSO-d_6 (1:4 by volume). In ^{1}H NMR spectra obtained in DMSO-d_6 as solvent (Figure 4.14 and 4.15) the methyl protons belonging to the terminal (T), linear (L) and dendritic (D) units resonate at around 1.01, 1.07 and 1.16 ppm, respectively. When the mixture D_2O/DMSO-d_6 was used to dissolve samples (Figure 4.16), these signals were slightly shifted ($\Delta\delta$ = –0.04 ppm). However, signals of the terminal, linear and dendritic units are poorly resolved in both types of solvents and therefore they were not used to quantify T, L and D units in the HB structure and to calculate *DB* from ^{1}H NMR spectra. Additional signals of the methyl groups from the linear repeating units can be found at around 1.12 ppm in DMSO-d_6 and 1.09 ppm in the mixture D_2O/DMSO-d_6. By comparing the ^{1}H NMR spectrum of the core DiTMP with spectra of the HB polyesters (Appendix 7.2.2) it was concluded that methyl protons from the DiTMP resonate at around 0.80 ppm in DMSO-d_6 and 0.75 ppm in the mixture D_2O/DMSO-d_6. This signal is very well detectable in the spectra of the lower generation HB polyesters, i.e. up to the fourth theoretical pseudo generation (Figure 4.14). However, the intensity of this signal decreases for the higher pseudo generations, due to the higher ratio between monomer and core molecule (Figure 4.15). The same conclusions are valid for methylene protons signals of the core, which resonate at around 1.3 and 3.2 ppm.

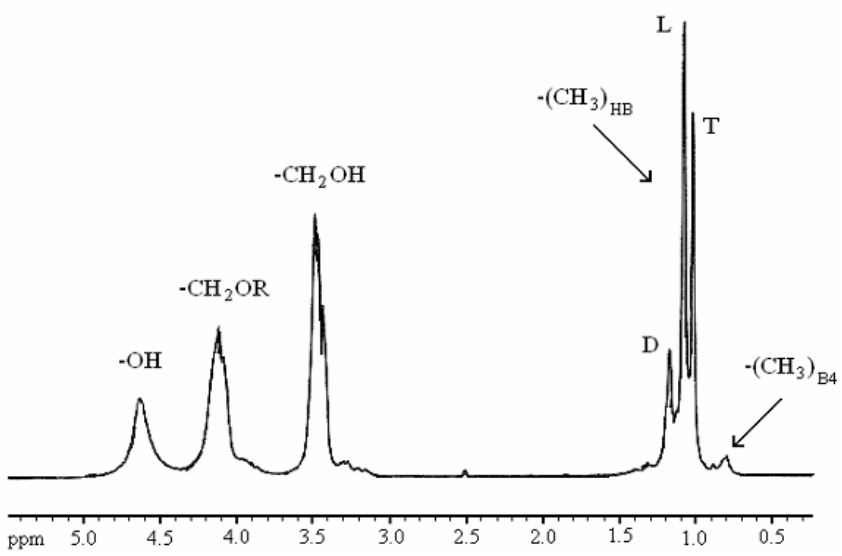

Figure 4.14. ^{1}H NMR spectrum of the sample HBP-4I in DMSO-d_6 (14 wt. %)

When the concentration of the HB polyester in DMSO-d_6 was relatively high (~ 14 wt. %), the signal which corresponds to the protons of the hydroxyl groups appears at around 4.60 ppm (Figure 4.14). However, when the measurements were done with lower concentrated solutions (~ 3 wt. %), two signals which correspond to the hydroxyl group protons were detected (Figure 4.15). The first signal appears at around 4.64 ppm (protons of the –OH groups from the terminal units) and another at around 4.95 ppm (protons of the –OH groups from the linear units)[71]. The absence of the second signal when the higher concentrated solution is used is due to the lower accessibility of the solvent to the linear units in the inner layers because of the high segment density. Therefore, to have a better resolution of the –OH protons signals, ^{1}H NMR spectra were done with lower concentrated solutions.

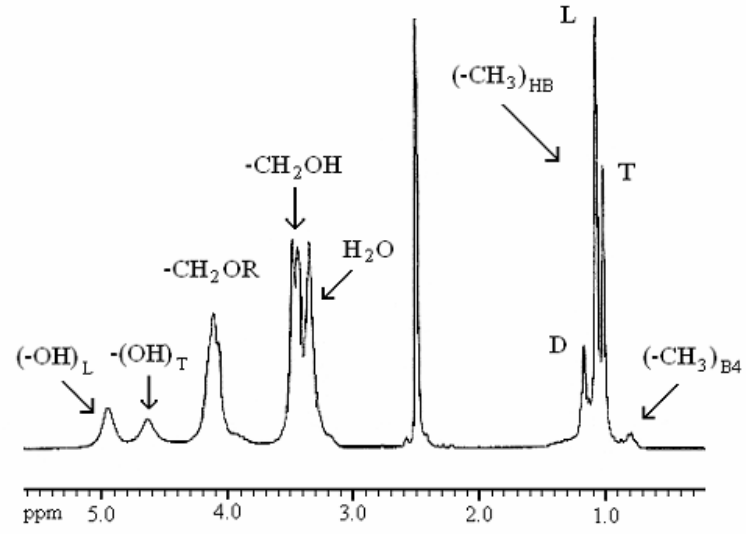

Figure 4.15. ^{1}H NMR spectrum of the sample HBP-4I in DMSO-d_6 (3 wt. %)

When DMSO-d_6 was used to prepare solutions for the ^{1}H NMR spectroscopy, the methylene groups in vicinity of reacted hydroxyl groups (-CH_2OR) resonate at around 4.10 ppm, while methylene groups attached to unreacted hydroxyl groups (-CH_2OH) resonate at around 3.40 ppm[40]. However, since the measurements with 3 wt. % solutions were done at room temperature, H_2O protons coincide with those of the –CH_2OH (Figure 4.15)[71]. This makes it difficult to obtain the real integral of the –CH_2OH signal, which is necessary to have for the calculation of the number average degree of polymerization for higher generation samples. On the other side, when a small portion of D_2O was added into the solution of the samples in DMSO-d_6, the signal of the water protons was shifted to around 4.0 ppm (Figure 4.16). Therefore, the real integral of the –CH_2OH protons signal can be calculated by comparing the integrals of the signals for –CH_2OH and –CH_3 groups (belonging to the monomer units) obtained in DMSO-d_6 and in the mixture D_2O/DMSO-d_6 in the following way:

$$I(\mathrm{CH_2OH})_{\mathrm{DMSO}} = \frac{I(\mathrm{CH_3})_{\mathrm{HB,\,DMSO}}\, I(\mathrm{CH_2OH})_{\mathrm{mix}}}{I(\mathrm{CH_3})_{\mathrm{HB,\,mix}}} \tag{4.9}$$

In equation (4.9) $I(\mathrm{CH_2OH})_{\mathrm{DMSO}}$ and $I(\mathrm{CH_2OH})_{\mathrm{mix}}$ are the integrals of the –CH_2OH group and $I(\mathrm{CH_3})_{\mathrm{HB,DMSO}}$ and $I(\mathrm{CH_3})_{\mathrm{HB,mix}}$ are the integrals of the –CH_3 groups in DMSO-d_6 and mixture D_2O/DMSO-d_6, respectively. When a small portion of D_2O is added into the solution, it is no longer possible to detect signals of the –OH and –CH_2OR groups. Therefore, integrals of these signals were calculated from the spectra obtained in DMSO-d_6.

In Figures 4.14, 4.15 and 4.16 ^{1}H NMR spectra of the sample HBP-4I determined with different concentrated solutions and in both types of solvent are presented, while spectra of other selected HB polyesters can be found in Appendix 7.2.2. The integrated intensities of the signals from ^{1}H NMR spectra of HB polyesters are listed in Table 4.9.

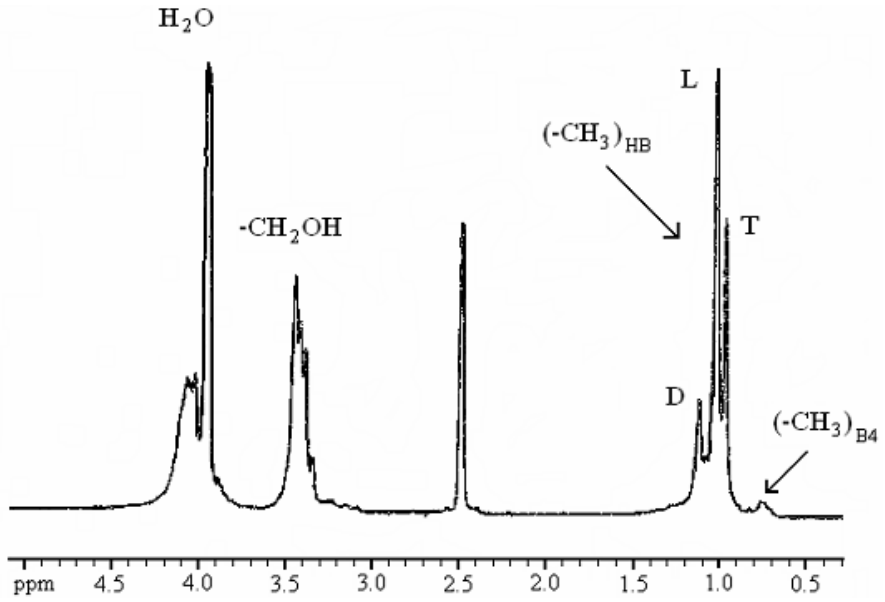

Figure 4.16. ^{1}H NMR spectrum of the sample HBP-4I determined in mixture D_2O/DMSO-d_6 (3 wt. %)

Table 4.9. Integrated intensities of different signals from the ^{1}H NMR spectra of HB polyesters (I(OH) = I(OH)$_L$ + I(OH)$_T$)

Sample	Integrated intensities of the signals				
	$I(CH_3)_{HB}$	$I(CH_3)_{B4}$	$I(CH_2OH)$	$I(CH_2OR)$	I(OH)
HBP-2I	5.9312	1.0875	4.8565	3.6422	2.3457
HBP-3I	5.4638	0.4183	4.1923	3.4897	2.0437
HBP-4I	5.7715	0.2116	4.0976	3.6773	2.0345
F1	5.4352	0.1715	3.5396	3.2374	1.7173
F2	5.7277	0.2815	3.6313	3.2454	1.7849
F3	6.1015	0.4450	3.8742	3.3145	1.9326
HBP-4II	5.3122	0.2841	3.7630	3.2401	1.7873
HBP-5I	5.1003	/	3.7357	3.2966	1.8370
HBP-6I	5.1987	/	3.6220	3.4276	1.7965
HBP-6II	5.8764	/	4.0766	3.9272	1.9548
HBP-8I	5.1370	/	3.5538	3.3284	1.7805
HBP-8II	5.0038	/	3.4286	3.2877	1.8050
HBP-10I	4.9620	/	3.4437	3.1801	1.7231

Although the synthesis conditions were chosen to avoid side reactions, it is not possible to prevent them completely. Beside the desirable reaction between –COOH group from bis-MPA (or from the growing HB structures) with –OH groups from the core molecule and/or from the linear or terminal repeating units from the already formed polyol, several possible side reactions can occur during the synthesis of these HB polyesters. The most important side reactions which can happen in this type of synthesis are:

1) **The deactivation of the –COOH group from the monomer or from the growing HB species.** This leads to formation of a HB macromolecule (poly(bis-MPA)) with bis-MPA as a new core with functionality 2 (B_2 core). If this polymer consists of z bis-MPA monomer units, it will have one unreacted –COOH group and (z+1) –OH groups. The deactivation of –COOH groups occurs probably due to their entrapment by hydrogen bonding (inter- or intramolecularly) and/or because they are shielded from the surrounding media by the rest of the molecule. In that manner, carboxyl groups become less accessible to further reaction and this is probably the main reason why the degree of conversion never reaches 100 %. The presence of unreacted carboxyl groups is already pointed out in ^{13}C NMR spectra of HB polyesters (signal of the quaternary carbon attached to an unreacted –COOH group and two reacted –OH groups). Therefore, it is necessary to include the presence of this new core in the calculation of the number average molar mass from the results obtained by ^{1}H NMR spectroscopy.

2) **Intramolecular esterification (cyclization) in growing HB species between focal –COOH group and –OH group from the same molecule.** In this way, poly-B-functional macrocycles with new B_2 core will be formed in the course of the reaction (Figure 2.8). The cyclic formation due to the intramolecular esterification can also occur through the hydroxy-ester interchange. This type of side reaction will result in

chain scission and formation of the HB molecules with one cyclic ester branch and without core unit (Figure 4.17).

3) **Intramolecular etherification between two –OH groups from the same molecule.** This can happen either in the HB polyol or in HB species with unreacted –COOH groups, i.e. with B_2 core. This reaction will also lead to cylices formation. The presence of cyclic structures, formed by intramolecular esterification or etherification, can be detected by comparing the number average molar mass, M_n, determined with some absolute method with $(M_n)_{NMR}$ calculated from the ^{1}H NMR spectra of the polymers. In this manner the extent of cyclization can be calculated and this calculation will be presented in the further text. Beside that, these structures can also be detected by MALDI-TOF or ESI mass spectrometry, which will be discussed later.

4) **Intermolecular etherification between two –OH groups from different molecules.** This reaction will increase the degree of polymerization of the final product, since in this way a new monomer unit is also built up in the polymer structure. The amount of the ether bonds in these HB polyesters, formed by intra- or intermolecular etherification, can be calculated from the ^{1}H NMR spectra.

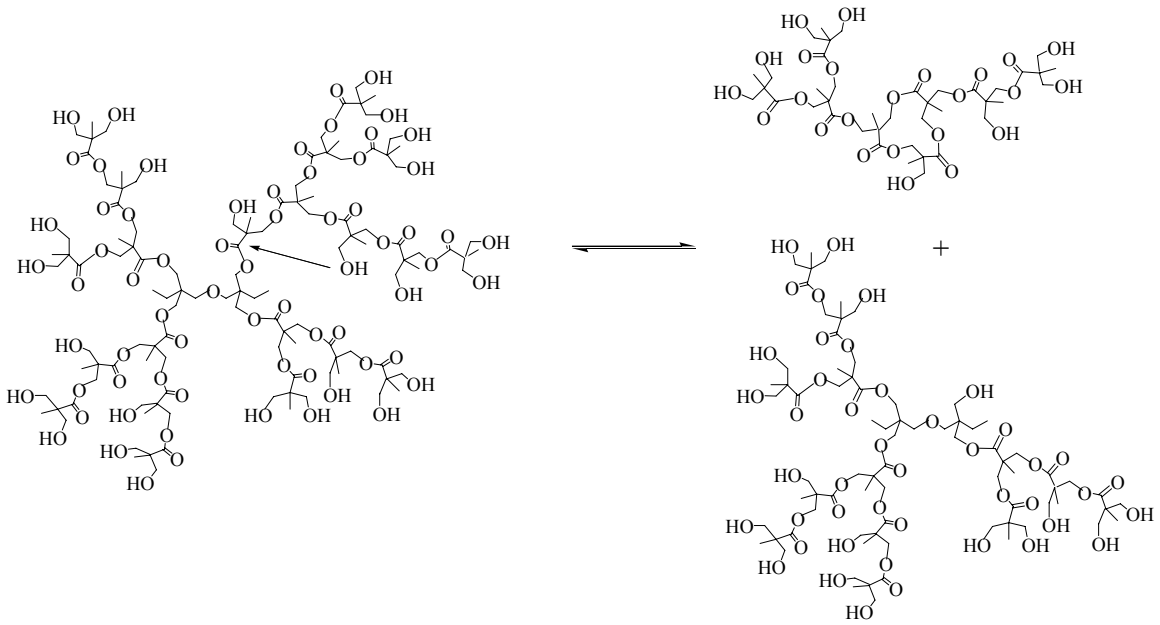

Figure 4.17. Schematic representation of the hydroxy-ester interchange

As it was mentioned before, for the calculation of the $(M_n)_{NMR}$ it is necessary to include also the presence of the newly formed B_2 core. This can be done by using the results obtained with ^{13}C and ^{1}H NMR spectroscopy. Beside that, the calculation will be carried out with assumption that other side reactions (cyclization through ether or ester bonds or intermolecular etherification) did not occur during the synthesis. These side reactions will be discussed later.

For the lower generation HB polyesters (up to the fourth theoretical pseudo generation) the calculation of the number average degree of polymerization, $(P_n)_{NMR}$, is relatively simple, since the portion of the DiTMP core molecule, N_{B4}, can be calculated from the integral of its methyl protons signal, $I(CH_3)_{B4}$, in the following way:

$$N_{B4} = \frac{I(CH_3)_{B4}}{6} \tag{4.10}$$

On the other side, for the higher generation HB polyesters (from fifth till tenth theoretical pseudo generation) N_{B4} can not be calculated according to the equation (4.10), since the signal of the DiTMP core is too small, which can introduce a big error in the further calculation. Therefore, N_{B4} has to be determined in another way. Since the B_2 core is formed from the monomer, his methyl protons will resonate at the same location as methyl protons from the monomer units which are built up in the HB structure of the polymer, i.e. from the bis-MPA. Using this integral, $I(CH_3)_{HB}$, the integral of the methylene protons from the HB structure and B_2 core, $I(CH_2)_{HB+B2}$, can be calculated using equation (4.11):

$$I(CH_2)_{HB+B2} = \frac{4}{3} I(CH_3)_{HB} \tag{4.11}$$

Furthermore, the integral of the methylene protons which belong to the entire molecule with both types of core, $I(CH_2)$, can be determined from the integrals of the signals corresponding to $-CH_2OH$ and $-CH_2OR$ groups:

$$I(CH_2) = I(CH_2OH) + I(CH_2OR) \tag{4.12}$$

Finally, the integral of the methylene protons in the B_4 core, $I(CH_2)_{B4}$ is:

$$I(CH_2)_{B4} = I(CH_2) - I(CH_2)_{HB+B2} \tag{4.13}$$

Since the DiTMP core has 16 methylene protons, the portion of the B_4 core for the higher generation samples can be calculated according to equation (4.14):

$$N_{B4} = \frac{I(CH_2)_{B4}}{16} \tag{4.14}$$

Because $I(CH_3)_{HB}$ represents the integral of the methyl protons signal which belongs to the HB structure and B_2 core, i.e. bis-MPA, the portion of the monomer units plus the newly formed B_2 core, N_{M+B2}, can be determined from the integral of the signal belonging to the methyl protons bis-MPA, $I(CH_3)_{HB}$, using the equation (4.15):

$$N_{M+B2} = \frac{I(CH_3)_{HB}}{3} \tag{4.15}$$

Consequently, the ratio N_{M+B2}/N_{B4} represents the average number of monomer units plus B_2 core per B_4 core molecule:

$$\frac{N_{M+B2}}{N_{B4}} = n_T + n_L + n_D + n_{B2} \tag{4.16}$$

where n_T, n_L, n_D and n_{B2} are the average numbers of terminal, linear, dendritic units and B_2 core molecule, respectively. Values of the n_T, n_L, n_D and n_{B2} can be calculated from the ratio N_{M+B2}/N_{B4} (resulting from the ^{1}H NMR spectra, Table 4.10) and from the corresponding integrals of terminal, linear, dendritic units and the integral of the quaternary carbon attached

to the unreacted –COOH group (resulting from the ^{13}C NMR spectra, Table 4.2). Therefore, n_L, n_D and n_{B2} can be expressed in the following manner:

$$n_L = \frac{I(L)}{I(T)} n_T \tag{4.17}$$

$$n_D = \frac{I(D)}{I(T)} n_T \tag{4.18}$$

$$n_{B2} = \frac{I(COOH)}{I(T)} n_T \tag{4.19}$$

From the combination of equations (4.16) till (4.19), values of the n_T, n_L, n_D and n_{B2} can be calculated and these values are listed in Table 4.10, together with calculated values of N_{M+B2}, N_{B4} and N_{M+B2}/N_{B4}.

Table 4.10. Values calculated from the results obtained by ^{13}C and ^{1}H NMR spectroscopy

Sample	N_{M+B2}	N_{B4}	N_{B2}	$\frac{N_{M+B2}}{N_{B4}}$	n_T	n_L	n_D	n_{B2}
HBP-2I	1.9771	0.1812	0	10.9	4.1	5.7	1.1	0
HBP-3I	1.8213	0.0697	0.0070	26.1	8.4	14.3	3.3	0.1
HBP-4I	1.9238	0.0353	0.0141	54.5	15.9	30.4	7.8	0.4
F1	1.8117	0.0286	0	63.4	18.9	33.9	10.6	0
F2	1.9092	0.0469	0	40.7	11.8	22.6	6.3	0
F3	2.0338	0.0742	0	27.5	8.3	15.2	4.0	0
HBP-4II	1.7707	0.0473	0	37.4	11.1	21.6	4.7	0
HBP-5I	1.7001	0.0145	0.0218	117.2	33.3	63.8	18.6	1.5
HBP-6I	1.7329	0.0074	0.0192	234.2	64.8	131.9	34.9	2.6
HBP-6II	1.9588	0.0105	0.0483	186.5	56.5	103.9	21.5	4.6
HBP-8I	1.7123	0.0021	0.0349	815.4	218.8	456.4	123.6	16.6
HBP-8II	1.6679	0.0028	0.0333	595.7	161.3	369.2	53.3	11.9
HBP-10I	1.6540	0.0005	0.0353	3308.0	883.1	1879.4	474.9	70.6

When the $n_{B2} = 0$ (B_2 core was not formed during the synthesis), then $N_{M+B2} = N_M$, which further means that the number average degree of polymerization, $(P_n)_{NMR}$, can be calculated as follows:

$$(P_n)_{NMR} = \frac{N_M}{N_{B4}} \tag{4.20}$$

For the samples which have $n_{B2} > 0$, it is necessary to determine the portion of the newly formed B_2 core, N_{B2}, using the equation (4.21):

$$N_{B2} = \frac{n_{B2}}{n_T + n_L + n_D + n_{B2}} N_{M+B2} \tag{4.21}$$

Values of the N_{B2} are also listed in Table 4.10. The portion of the monomer units can now be calculated as a difference between N_{M+B2} and N_{B2}:

$$N_M = N_{M+B2} - N_{B2} \tag{4.22}$$

By knowing the values of the N_M, N_{B4} and N_{B2}, the degree of polymerization can be calculated as follows:

$$(P_n)_{NMR} = \frac{N_M}{N_{B2} + N_{B4}} \tag{4.23}$$

Finally, the number average molar mass $(M_n)_{NMR}$ of the HB polyesters was calculated using equation (4.24)

$$(M_n)_{NMR} = (P_n)_{NMR}\left[M_{bis-MPA} - M_{water}\right] + x_{B4}M_{B4} + x_{B2}M_{B2} \tag{4.24}$$

where $M_{bis\text{-}MPA}$, M_{water}, M_{B4} and M_{B2} are the molar masses of the monomer, water, DiTMP (B_4 core) and B_2 core (134 g/mol), respectively, while x_{B4} and x_{B2} are the fractions of the B_4 and B_2 core, which can be expressed by equations (4.25) and (4.26)

$$x_{B4} = \frac{N_{B4}}{N_{B4} + N_{B2}} \tag{4.25}$$

$$x_{B2} = 1 - x_{B4} \tag{4.26}$$

The calculated values of the $(P_n)_{NMR}$ and $(M_n)_{NMR}$ determined from the results obtained by ^{13}C and ^{1}H NMR spectroscopy with the previously described equations are listed in Table 4.11. For the samples HBP-2I and HBP-4II the signal of the unreacted –COOH groups was not detected in the ^{13}C NMR spectra ($n_{B2} = 0$; $x_{B4} = 1$) and therefore it was concluded that a new B_2 core was not formed during the synthesis of these polymers.

Table 4.11. Values of the $(P_n)_{NMR}$, fractions of the B_4 (x_{B4}) and B_2 core (x_{B2}), $(M_n)_{NMR}$, percentage of the formed ether groups (x_{ether}) and degree of conversion (p_A)

Sample	$(P_n)_{NMR}$	x_{B4}	x_{B2}	$(M_n)_{NMR}$ [g/mol]	x_{ether} [%]	p_A
HBP-2I	11	1.00	0	1514	3.4	1.00
HBP-3I	24	0.91	0.09	2977	2.5	0.99
HBP-4I	39	0.72	0.28	4707	0.7	0.99
F1	63	1.00	0	7604	3.0	1.00
F2	41	1.00	0	4971	1.7	1.00
F3	27	1.00	0	3440	0.2	1.00
HBP-4II	37	1.00	0	4588	5.0	1.00
HBP-5I	46	0.40	0.60	5540	0.1	0.99
HBP-6I	64	0.28	0.72	7637	0	0.99
HBP-6II	32	0.18	0.82	3925	3.1	0.97
HBP-8I	45	0.06	0.94	5396	0	0.98
HBP-8II	45	0.08	0.92	5398	0	0.98
HBP-10I	45	0.01	0.99	5378	0	0.98

Since the sample HBP-2I has approximately 11 monomer units in its structure, and the average number of terminal, linear and dendritic units per molecule is known (Table 4.10) it is possible to draw the most probable structure of this sample (Figure 4.18). Because this sample has four terminal units and one dendritic, the only possible structure is when one of the –OH groups from the DiTMP core did not react. On the other side, six linear units can be differently incorporated in the structure of the HBP-2I sample.

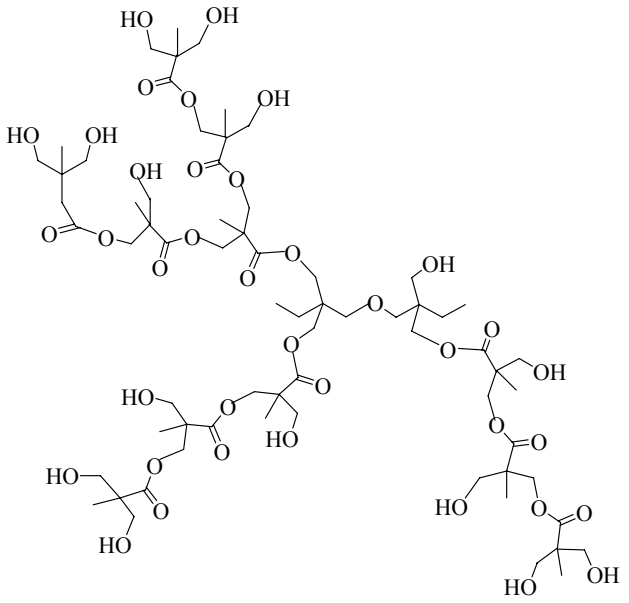

Figure 4.18. The most probable structure of the sample HBP-2I

In the same manner, the most probable structure of the sample HBP-3I is drawn (Figure 4.19). The presence of the newly formed B_2 core was not taken into account, because of the relatively small amount. For the other samples there are too many possible combinations in arrangements between different monomer units plus the influence of the other side reactions on the final structure. Consequently, the drawing of the most probable structure for the higher generation samples is much complicated.

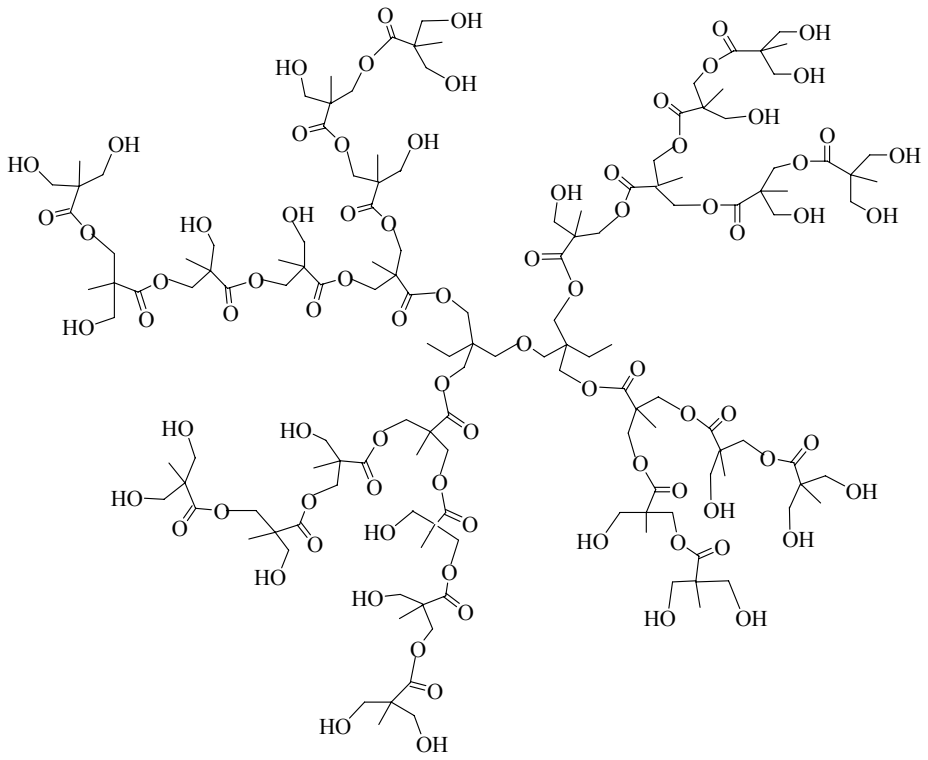

Figure 4.19. The most probable structure of the sample HBP-3I

The values of the N_{M+B2}/N_{B4} listed in Table 4.10 are in good agreement with the values of the core/monomer ratio which is used for the synthesis of the different theoretical pseudo generation HB polyesters (Table 4.1). However, only one part of the used monomers has been incorporated into the HB structure in expected manner. This is especially noticeable for the higher generation samples. The formation of the HB macromolecules with B_2 core is increasing with the theoretical number of generation (Table 4.11). At the same time, the fraction of the HB species with DiTMP core molecule, x_{B4}, is decreasing due to the self-condensation of the bis-MPA. When larger amounts of monomer are present in the reaction mixture (during the synthesis of the higher generation samples), the probability for this side reaction is strongly increased.

As it was mentioned before, intra- and intermolecular etherification can also occur during the synthesis of HB polyesters. The presence of the ether groups in the structure of these HB polymers was already detected in ^{13}C NMR spectra of some samples (Apendix 7.2.1) On the other side, the amount of the formed ether groups can be calculated from ^{1}H NMR spectra by comparing the integrals of the –OH and $–CH_2OH$ groups. Since methylene protons of the ether group ($–CH_2–O–CH_2–$) resonate at the same frequency as the protons of the $–CH_2OH$ group, ½ $I(CH_2OH)$ is for some samples not proportional to the real amount of the –OH groups in the structure, i.e. it is bigger than I(OH). This implies, that etherification as

a side reaction occurred during the synthesis of these polymers. However, when the calculation of the ether group amount is made, it is also necessary to take into account the presence of the ether groups which belongs to the DiTMP core. Protons of the methylene groups near the ether group in DiTMP resonate at around 3.2 ppm. This signal is relatively good separated from the signal of the $–CH_2OH$ groups (3.4 ppm) for the samples of the lower theoretical pseudo generation. Therefore it was not included when the calculation of the $I(CH_2OH)$ was done. Finally, the amount of the formed ether groups in the samples from second till forth theoretical pseudo generation can be calculated using the equation (4.27):

$$x_{\text{ether}} = \left[1 - \frac{I(\text{OH})}{\frac{1}{2} I(\text{CH}_2\text{OH})}\right] \times 100 \tag{4.27}$$

On the other side, in the ^1H NMR spectra of the higher generation HB polyesters the signal of the methylene protons near the ether group in the DiTMP core was not possible to distinguish anymore from the signal of the $–CH_2OH$ groups. Because of that, for the higher generation HB polyesters the percentage of the ether groups has to be calculated in the following manner:

$$x_{\text{ether}} = \left[1 - \frac{I(\text{OH})}{\frac{1}{2}\left(I(\text{CH}_2\text{OH} - \frac{1}{4} I(\text{CH}_2)_{\text{B4}}\right)}\right] \times 100 \tag{4.28}$$

¼ $I(CH_2)_{B4}$ has been used because DiTMP has eight methylene groups in its structure, from which two are located near ether group. The results obtained with equations (4.27) and (4.28) are presented in Table 4.11. Since the lower generation HB polyesters have the highest percentage of the –OH groups per molecule (Table 4.5), the possibility for the ether formation is higher. This is also verified with results listed in Table 4.11. Percentage of ether groups is decreasing from 3.4 % for the second till 0.1 % for the fifth theoretical pseudo generation. On the other side, for the samples HBP-4II and HBP-6II, synthesized by one-step procedure, the amount of the formed ether groups is higher compared with adequate samples obtained with pseudo-one-step procedure. This fact again shows the noticeable difference between these two types of reaction. When the necessary amount of the monomer is added at once into the reaction mixture, the probability for this side reaction is increased. However, the calculated amount of the ether groups in all samples is still relatively small (1-5 %) and they are probably formed during intramolecular etherification (cyclization).

In Table 4.11 values of the degree of conversion (p_A) for the HB polyesters are also listed. These values were calculated using the equation (4.29):

$$p_{\text{A}} = \frac{\frac{N_{\text{M}}}{N_{\text{B4}} + N_{\text{B2}}} - x_{\text{B2}}}{\frac{N_{\text{M}}}{N_{\text{B4}} + N_{\text{B2}}}} \tag{4.29}$$

The degree of conversion calculated with this equation is in good agreement with results listed in Table 4.3 (p_A, ^{13}C NMR). As can be seen, p_A is decreasing with increasing number of pseudo generation, i.e. with decreasing core/monomer ratio. At the same time, the fraction of

the newly formed B_2 core, x_{B2}, is increasing. During the synthesis of higher pseudo generation HB polyesters, a higher amount of monomer was added into the reaction mixture, which further increases the probability of the bis-MPA self-condensation. Because of that, the total number of macromolecules in the reaction mixture increases, as well as the number of branches with lower molar mass, which finally leads to the decreasing of the number average molar mass of the higher pseudo generation samples. When the obtained values of the $(M_n)_{NMR}$ (Table 4.11) are compared with the theoretical ones (Table 4.1), a great difference (especially for the higher generation samples) can be observed. The synthesis of high molar mass aliphatic HB polyesters (from fifth till tenth theoretical pseudo generation) is strongly influenced and hindered by a competition between side reactions and polymerization. The presence of the unreacted carboxyl groups leads to a great lowering of the number average molar mass of the final HB polyesters.

In Tables 4.9, 4.10 and 4.11 the results obtained for the fractions of the sample HBP-4I are also listed. Since the presence of unreacted carboxyl groups was not detected in any ^{13}C NMR spectra of these fractions ($n_{B2} = 0$), the degree of polymerization was calculated according to the equation (4.20). The results listed in Table 4.11 show that $(P_n)_{NMR}$ decreases from first to third fraction. In the same manner the amount of the formed ether groups is changing, which means, that cyclization through intramolecular etherification is increasing with increasing degree of polymerization. The calculated value of the number average molar mass for the first fraction of the sample HBP-4I is relatively close to the M_{theor} for the parent sample (Table 4.1). On the other side, $(M_n)_{NMR}$ of the second fraction is in a good agreement with obtained value for the HBP-4I.

^1H NMR spectroscopy was not done for the commercial Boltorn® samples, since these results are already presented in the literature by *Žagar* and co-workers[71,146]. These authors have calculated parameters previously discussed from the ^1H NMR spectra in a somewhat different manner and results which they have obtained are listed in Table 4.12.

Table 4.12. Results obtained from ^1H NMR spectra of commercial Boltorn® samples (data of *Žagar* and co-workers[71,146])

Sample	$(P_n)_{NMR}$	x_{B4}	x_{B2}	$(M_n)_{NMR}$ [g/mol]	x_{ether} [%]	p_A
BH-2	6.7	0.58	0.42	930	6.0	0.93
BH-3	10.4	0.48	0.52	1323	4.0	0.95
BH-4	21.4	0.37	0.63	2579	0.4	0.97

By comparing results listed in Table 4.12 with results obtained for the self-synthesized HB polyesters (Table 4.11) it can be observed that during the synthesis of commercial samples a higher amount of the bis-MPA self-condensation reaction has occurred. The relatively large amount of the unreacted carboxyl groups in Boltorn® samples is the main reason for noticeable lowering of the number average molar mass compared with theoretical values (Table 4.1). Beside that, the second and third pseudo generation of the Boltorn® samples have higher amounts of the ether groups in their structure than samples HBP-2I and HBP-3I, and this was also ascribed to the intramolecular etherification (cyclization). On the other side, the degree of conversion for commercial samples is increasing with the theoretical number of generation.

4.2.2. Results from the vapour pressure osmometry

The number average molar mass of the investigated HB polyesters was also determined from the results obtained with vapour pressure osmometry (VPO). Since this method does not depend on the structure of the used samples, it is more suitable than ^{1}H NMR spectroscopy for the molar mass determination. In Figures 4.20 and 4.21 VPO measurements of the HB samples are presented.

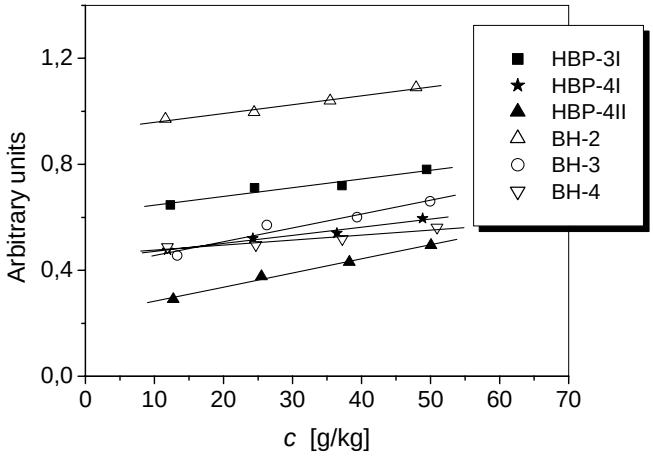

Figure 4.20. VPO measurements of the HB polyesters

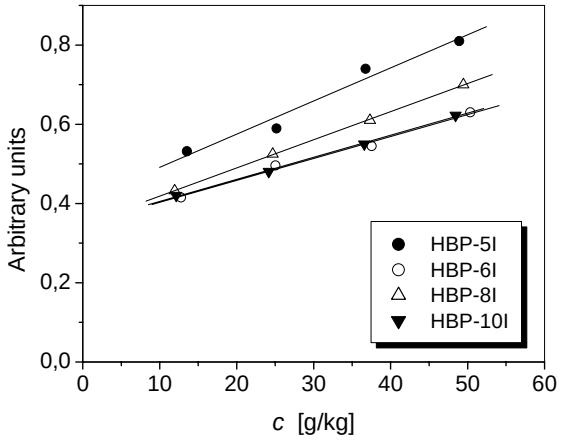

Figure 4.21. VPO measurements of the HB polyesters of the series I

Since these polymers have a large number of polar end –OH groups, in contrast to analogue linear polymers, aggregation due to the hydrogen bonding can happen in the used solvent for the VPO measurements (N,N-dimethylformamide). However, a relatively good linear correlation between VPO response and concentration of the solutions was obtained for all measured samples, i.e. a decrease of the slope with increasing concentration did not occur (Figures 4.20 and 4.21). Therefore, the presence of concentration dependent aggregates can be excluded. For the samples HBP-2I and HBP-6II a negative slope was obtained in VPO measurements, which is the reason why the results for these two samples are not presented. From the determined values of the number average molar mass, $(M_n)_{VPO}$, listed in Table 4.13

it can be seen that $(M_n)_{VPO}$ is increasing up to the sixth theoretical pseudo generation, which is in good agreement with the results obtained from ^{1}H NMR spectroscopy. However, $(M_n)_{VPO}$ is lower compared to the values calculated from ^{1}H NMR spectra of the HB polyesters (Table 4.12), as well as the increase of the number average molar mass. The reason for such differences is the formation of cyclic structures[40], which can not be taken into account in the evaluation of the ^{1}H NMR data.

Table 4.13. Values of the number average molar mass obtained from VPO measurements, $(M_n)_{VPO}$, calculated values of the extent of cyclization, ξ and $(M_n)_{VPO}^{purif}$ obtained for the purified HB polyesters

Sample	$(M_n)_{VPO}$ [g/mol]	ξ [%]	$(M_n)_{VPO}^{purif}$ [g/mol]
HBP-3I	2027	31.9	4254
HBP-4I	2819	40.1	3499
HBP-4II	5415	/	/
HBP-5I	3044	45.0	4216
HBP-6I	3575	53.2	3663
HBP-8I	3571	33.8	3869
HBP-8II	3284	39.2	/
HBP-10I	3552	33.9	3730
BH-2	1343	/	/
BH-3	3081	/	/
BH-4	2716	/	/

By comparing values of the number average molar mass determined from the VPO and ^{1}H NMR measurements, the extent of cyclization, ξ, in the HB polyesters can be calculated (equation 2.3). These values are also listed in Table 4.13. Up to the sixth theoretical pseudo generation the extent of cyclization is increasing. On the other side, for the sample HBP-8I and HBP-10I lower values of the ξ were obtained than for the sample HBP-6I, due to the smaller difference between $(M_n)_{VPO}$ and $(M_n)_{NMR}$. For these two samples the lowering of the number average molar mass is probably mostly dependent on the presence of the unreacted –COOH groups. From the ^{1}H NMR measurements (Table 4.11) it was obtained that intramolecular etherification has taken place during the synthesis of the HB polyesters from second till fifth theoretical pseudo generation. Therefore, it can be concluded that for samples HBP-3I, HBP-4I and HBP-5I the cyclization occurred through ester and ether bonds, which is quantified in the value of ξ. On the other side, for the samples HBP-6I, HBP-8I and HBP-10I the presence of the cycles, formed as a consequence of the intramolecular etherification, in the structure of these HB polyesters was not detected with ^{1}H NMR measurements. Therefore, in these polymers the cyclization probably occurred because of intramolecular esterification.

As can be seen from the results listed in Table 4.13, the extent of cyclization of the sample HBP-8II is higher than for the sample HBP-8I. However, since $(M_n)_{VPO}$ of the sample HBP-4II was higher than $(M_n)_{NMR}$, the extent of cyclization was not possible to calculate for this sample. Beside that, as it was already mentioned, a negative slope was obtained for the sample HBP-6II. Therefore, a general conclusion about the influence of the type of the

synthesis on the extent of cyclization can not be made for these HB polyesters from results obtained with VPO measurements.

For the commercial HB polyesters the extent of cyclization was not possible to calculate since for all three samples $(M_n)_{VPO} > (M_n)_{NMR}$. Similar results were obtained by Frey and co-workers[40].

VPO measurements were also done for several purified HB polyesters. Purification was accomplished by precipitation using a solvent/non-solvent system, as it was already explained in the chapter 3.2.1. Determined values of the number average molar mass for the purified samples, $(M_n)_{VPO}^{purif}$, are listed in Table 4.13. In all cases $(M_n)_{VPO}^{purif}$ was higher than $(M_n)_{VPO}$, which can be explained by the presence of the small molar mass compounds in the samples synthesized in this work. This is especially noticeable for the samples up to the fifth theoretical pseudo generation. However, for the calculation of the extent of cyclization $(M_n)_{VPO}^{purif}$ was not used, since ^{1}H NMR spectroscopy was done with the non-purified samples. If the purified HB polyesters are used for the ^{1}H NMR measurements, the ratio N_{M+B2}/N_{B4} would be smaller than in the case of the non-purified samples, since small molecules as well as unreacted monomers would be removed from the polymers. Because of that, $(DP_n)_{NMR}$ and consequently $(M_n)_{NMR}$ would decrease. On the other side, $(M_n)_{VPO}$ increases when purified samples are used. Finally, the values of the real extent of cyclization will decrease, compared to the values obtained for the non-purified samples. In which degree purification of the HB polyesters can diminish calculated value of the extent of cyclization can not be determined by simple comparing the results obtained for the $(M_n)_{NMR}$, $(M_n)_{VPO}$ and $(M_n)_{VPO}^{purif}$. There are too many different parameters that can have different influence on the number average molar mass, such as the real number of incorporated monomer units into the HB structure, amount of the HB species without B_4 core, degree of polymerization, presence and amount of the other side reaction etc. At this point it can be only concluded that purification of the HB polyesters can have significant influence on the calculated values of the extent of cyclization. This is especially noticeable for the lower generation samples, due to the bigger difference between $(M_n)_{VPO}$ and $(M_n)_{VPO}^{purif}$. For the HB polyesters of the higher theoretical pseudo generation, difference between these two number average molar masses is lower, which further means that purification should not have such large influence on the values of ξ.

4.2.3. Results from the MALDI-TOF and ESI mass spectrometry

Characterization of HB polymers by use of MALDI-TOF mass spectrometry has proven to be a valuable method, because it can provide significant information about these polymers. However, it is not possible to take complete advantages of this method in this particular case, since HB polyesters used in this work are polydisperse. It is already explained in the chapter 2.4.1.2 that reliable MALDI-TOF data are difficult to obtain for the samples with broad molar mass distribution. Due to the low molar amount of higher mass molecules, the high mass tail of the molar mass distribution is underrepresented in MALDI-TOF spectra. Beside that, oligomers of different molar mass require different intensities of the laser power. For the polydisperse samples (polydispersity higher than 1.2) the optimum laser power required for ionization/desorption process is greater for high molar mass species than for the low molar mass oligomers. When the greater levels of the laser power are used for the analysis of the high molar mass species, fragmentation of the lower molar mass oligomers can occur, which can bring a significant error in the molar mass averages calculation. Beside that, as a result of the higher laser power the quality of the baseline can be degraded, while the peak resolution becomes poor.

Typical MALDI-TOF mass spectra of the HB polyesters are given in Figures 4.22 and 4.23.

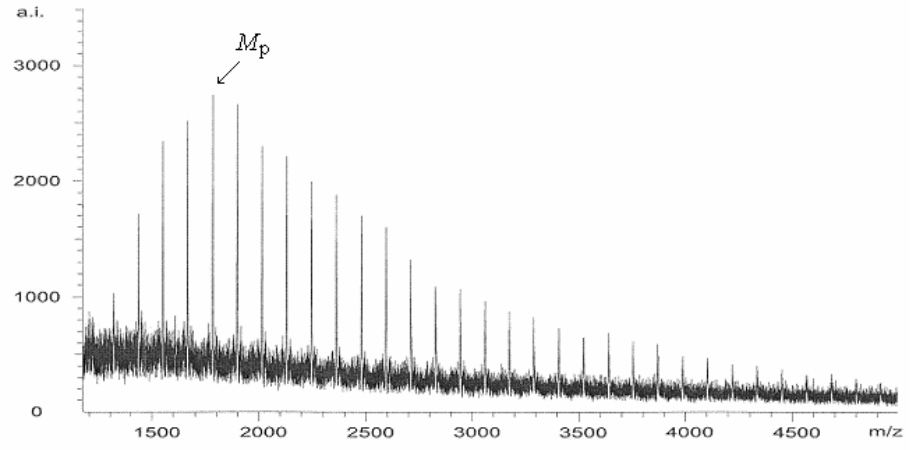

Fugure 4.22. MALDI-TOF mass spectrum of the sample HBP-2I

From the spectra presented in Figures 4.22 and 4.23 it can be seen that they consist of regularly spaced series of peaks, which are separated by 116 mass units corresponding to the molar mass of the monomer unit. Each peak in this spectrum represents an oligomer of different degree of polymerization. When MALDI-TOF mass spectra of different theoretical pseudo generation are compared, it can be noticed that the position of the highest signal (the most probable peak (M_p)), is moving toward the higher molar masses region (Figure 4.23). However, shifting of the most probable peak was relatively weak and it was observed only for the samples from second till fourth theoretical pseudo generation.

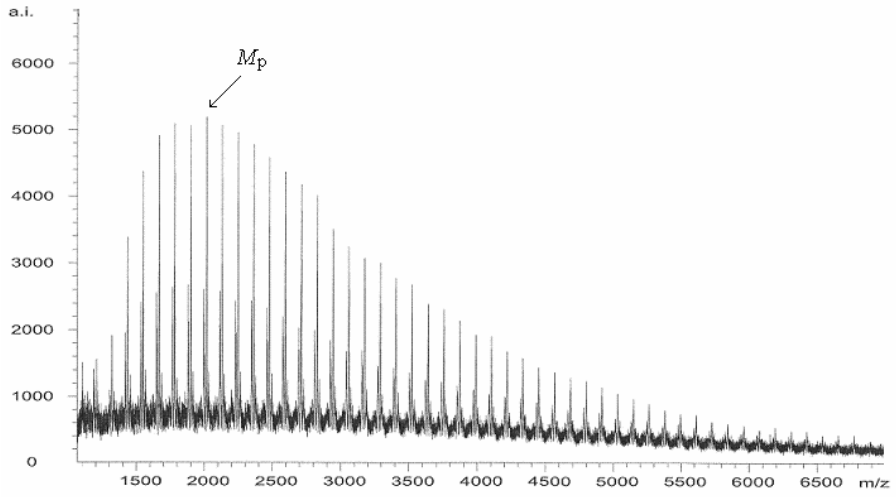

Figure 4.23. MALDI-TOF mass spectrum of the sample HBP-4I

The molar mass averages and polydispersity were calculated from MALDI-TOF mass spectra of HB polyesters using the following equations:

$$M_n = \frac{\sum_{i=1}^{k} N_i M_i}{\sum_{i=1}^{k} N_i} \tag{4.30}$$

$$M_w = \frac{\sum_{i=1}^{k} N_i M_i^2}{\sum_{i=1}^{k} N_i M_i} \tag{4.31}$$

where M_n is the number average molar mass, M_w is the weight average molar mass, N_i is the signal intensity at point i and M_i is the mass of particular oligomer at point i. Calculated values of the molar mass averages and polydispersity are listed in Table 4.14.

Table 4.14. Values of the $(M_w)_{MALDI}$, $(M_n)_{MALDI}$ and polydispersity index $(M_w/M_n)_{MALDI}$ determined from the MALDI-TOF mass spectra of the investigated HB polyesters

Sample	$(M_w)_{MALDI}$ [g/mol]	$(M_n)_{MALDI}$ [g/mol]	$(M_w/M_n)_{MALDI}$
HBP-2I	2345	2213	1.06
HBP-3I	2976	2617	1.14
F1	2940	2593	1.13
F2	3104	2677	1.16
F3	2747	2480	1.11
HBP-4I	3352	2909	1.15
F1	2181	2102	1.04
F2	2136	2027	1.05
F3	2099	1999	1.05
HBP-4II	3292	2886	1.14
HBP-5I	3276	2765	1.18
HBP-6I	3310	2824	1.17
HBP-6II	3347	2904	1.15
HBP-8I	3738	3155	1.18
HBP-8II	3078	2648	1.16
HBP-10I	2989	2565	1.16
BH-4	3258	2863	1.14

The results presented in Table 4.14 show that previously described problems with MALDI-TOF mass spectra of polydisperse polymers have strong influence on the obtained results. According to the MALDI-TOF MS measurements, polydispersity index of all samples is lower than 1.2, which is not typical for this type of HB polyesters. Increase of the polydispersity can be observed up to the fifth theoretical pseudo generation, while for the samples of the higher generation number, polydispersity fluctuate. When the calculated values

of the number average molar mass presented in Table 4.14 are compared with values obtained by VPO measurements (Table 4.13) it can be noticed that for the third and fourth theoretical generation $(M_n)_{MALDI}$ is bigger than $(M_n)_{VPO}$. On the other side, for the higher generation samples opposite observation can be noticed. The reason for such behaviour is that intensity of the signals from the high mass tail of these samples (theoretical generation higher than four) was underestimated and insufficient to distinguish it from the baseline and to use it for the analysis of the spectra. As a consequence of that, lower values of the number average molar mass were obtained. At the same time, weight average molar mass is also underestimated, which further leads to very low values of polydispersity index. Since in the MALDI-TOF mass spectrum of the sample HBP-2I (Figure 4.22) signals which correspond to molecules having a mass higher than 2000 mass units can also be observed, $(M_n)_{MALDI}$ for this sample is higher from both, theoretical values of the molar mass (Table 4.1) and $(M_n)_{NMR}$ (Table 4.11). Oligomers of higher molar mass probably appear in the sample HBP-2I as a consequence of aggregation.

From the previous discussion it is obvious that a representative picture of the molar mass averages of the whole HB samples and sensible interpretation of these data from MALDI-TOF mass spectra can not be done for all HB polyesters. However, from mass spectra of HB polyesters obtained with MALDI-TOF technique it is possible to obtain molar masses of individual oligomers in the lower molar mass region and to qualitatively determinate the extent of cyclization at each degree of polymerization. Due to this possibility, reflection mode was chosen for the measurements, since it can provide the determination of exact molar masses of each oligomer, which is necessary to have for identification of side products.

In Figure 4.24 the MALDI-TOF mass spectra of lower pseudo generation HB polyesters are presented. The same mass region was chosen for the easier comparison between results obtained for these three samples. As it was already mentioned, the main series of equally spaced signals (series 1) corresponds to oligomers with mass differences between them of 116 mass units, which represent exactly the molar mass of the repeating unit (bis-MPA). In the mass spectra of the samples HBP-3I and HBP-4I series of signals with lower intensity can be also observed (series 2). The position of the second series of signals is 18 mass units lower than the main series of peaks. Finally, in the mass spectrum of the sample HBP-4I additional series of lower intensity signals can also be found (series 3), 18 mass units after the main series. The molar mass of a particular oligomer can be calculated by consideration of the polymerization process using the equations developed by *Frey* and co-workers[40]. These equations can be used also for the HB polyesters synthesized in this dissertation, due to the similar structure with polyesters synthesized by *Frey*. Therefore, for the HB polyesters used in this study these equations can be written as follows:

Polymerization with a core molecule and without cyclization:

$$M = M_{\mathrm{DiTMP}} + P_{\mathrm{n}}(M_{\mathrm{bis-MPA}} - M_{\mathrm{water}}) \tag{4.32}$$

Cyclization without a core molecule:

$$M = P_{\mathrm{n}}(M_{\mathrm{bis-MPA}} - M_{\mathrm{water}}) \tag{4.33}$$

Polymerization without a core molecule and without cyclization:

$$M = P_{\mathrm{n}} M_{\mathrm{bis-MPA}} - (P_{\mathrm{n}} - 1) M_{\mathrm{water}} \tag{4.34}$$

M corresponds to the series of mass peaks observed in MALDI-TOF mass spectra, P_n is the number average degree of polymerization, $M_{bis\text{-}MPA}$, M_{DiTMP} and M_{water} are the molar masses of the monomer, core and water, respectively. The difference $M_{bis\text{-}MPA}$ - M_{water} indicates the molar mass of the repeating unit.

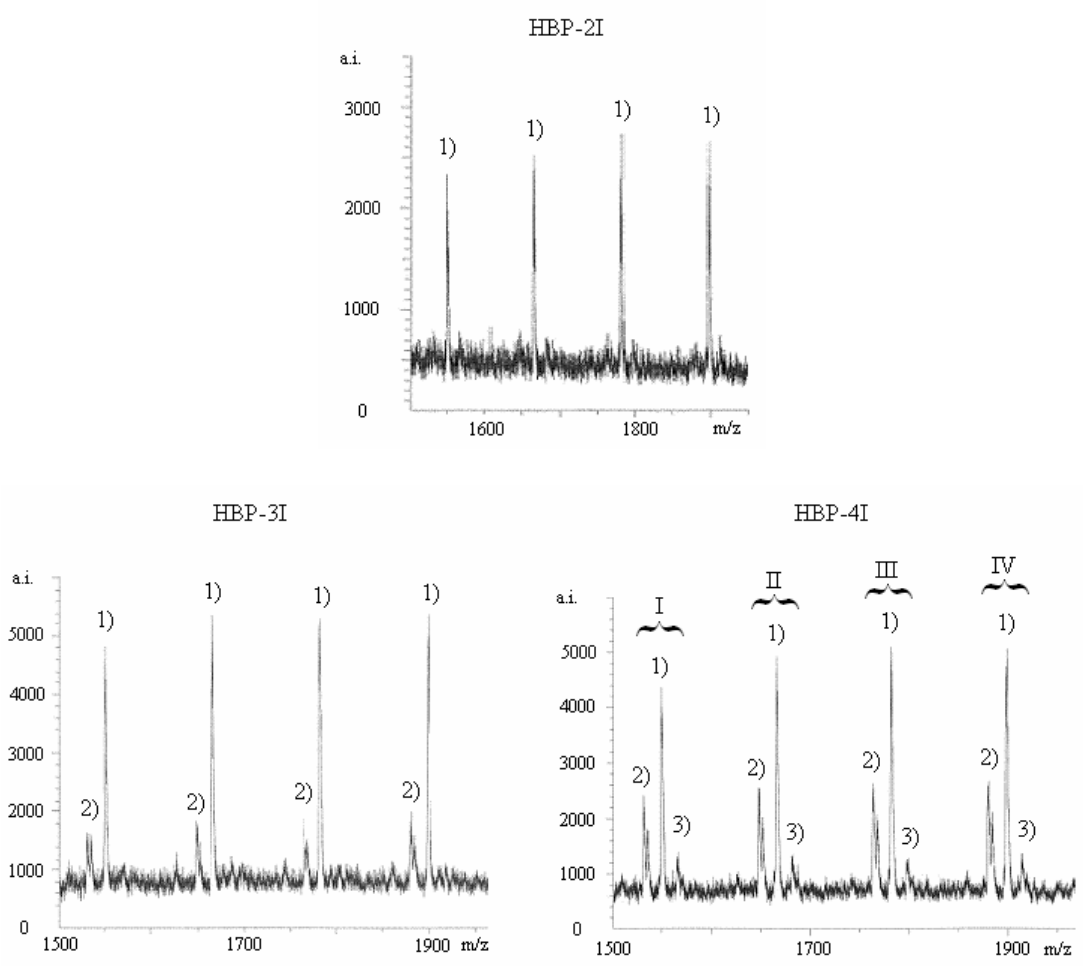

Figure 4.24. MALDI-TOF mass spectra of HBP-2I, HBP-3I and HBP-4I

In Table 4.15 *m/z* data from the MALDI-TOF mass spectra of sample HBP-4I are listed. Values of the *m/z* for the main series of signals (series 1) are the same for all three samples presented in Figure 4.24, while the second series of peaks (series 2) have the same values for the samples HBP-3I and HBP-4I.

Table 4.15. MALDI-TOF *m/z* data of the sample HBP-4I

Peaks group	*m/z* values of peaks		
	Peak 1)	Peak 2)	Peak 3)
I	1550	1532	1568
II	1666	1648	1684
III	1782	1764	1800
IV	1898	1880	1916

Using the set of equations (4.32) till (4.34), results obtained from MALDI-TOF mass spectra (Figure 4.24; Table 4.15) and values calculated from NMR spectroscopy (Table 4.11) it is possible to identify every signal from MALDI-TOF mass spectra of HB polyesters. However, the presence of ions such as sodium or potassium can not be completely excluded from the calculation, i.e. they also have to be taken into account when the calculation is made. The major series of signals (series 1) observed for the HB polyesters correspond to oligomers formed in the desired successive condensation reaction, i.e. they represent acyclic HB molecules containing a core unit, whose molar mass can be calculated with equation (4.32). The second series of signals (series 2), which occurs at 18 mass units less than the main series is attributed to the loss of the single water moiety to form cyclic structures. Oligomers presented with this series of peaks are probably formed through intramolecular esterification or by hydroxyl-ester interchange and represent macrocyclic bis-MPA macromolecules without a DiTMP core unit. In this case, the molar mass of each oligomer presented with second series of signals can be calculated using the equation (4.33), i.e. as a sum of bis-MPA repeating units. On the other hand, signals of the series 2 can also be assigned to the cycles formed by intramolecular etherification (one cyclic branch per molecule), which molar mass is simply the molar mass of the signal from the series 1 minus 18 mass units, since this cyclic species also contains a core unit. However, it is not possible to distinguish between cycles formed by intramolecular etherification and esterification using MALDI-TOF mass spectrometry. It can be excluded that the loss of the water took place during the mass spectral ionization, since the presence of the cyclic structures in the HB polyesters were already proved by ^{1}H NMR and VPO measurements. In the MALDI-TOF mass spectrum of sample HBP-2I, a second series of signals was not detected or they have very low intensity, which makes their identification difficult. This shows that the extent of cyclization in this sample is much lower than in the HB polyesters of higher generation. It is not possible to compare this observation with the extent of cyclization calculated from NMR and VPO results, due to the difficulties during the VPO measurements of the sample HBP-2I. Since the intensity of the second series of signals is increasing with the theoretical number of pseudo generations it can be concluded, that the extent of cyclization has the same trend (Figure 4.24).

In the MALDI-TOF mass spectrum of sample HBP-4I another sub-distribution of signals can be observed (series 3). Considering the results obtained with NMR spectroscopy, this series of peaks are attributed to the acyclic oligomers with unreacted –COOH groups, i.e. HB molecules without DiTMP core unit and with B_2 core. The molar mass of oligomers from the third series of signals can be calculated with equation (4.34). Unreacted –COOH groups were also detected in the sample HBP-3I (^{13}C NMR spectroscopy; Table 4.2), however a third series of signals was not observed in the MALDI-TOF mass spectrum of this sample (Figure 4.24). This is probably due to the relatively low amount of the x_{B2} for this sample in comparison to the polyester HBP-4I (Table 4.11). When the degree of polymerization is calculated using *m/z* data of series 3 and equation (4.34) and then this value is used to calculate the molar mass of cycles formed from the acyclic species without DiTMP core unit, it can be noticed that the calculated values of the molar mass are the same as *m/z* data for the main series of peaks (series 1). This practically means that signals of the cyclic structures formed from the acyclic HB species without DiTMP core are overlapping with signals from the HB species with a core unit in the MALDI-TOF mass spectra. A third series of signals was not observed in the MALDI-TOF mass spectra of sample HBP-4II (Figure 4.25), which is in good agreement with results obtained by NMR measurements ($x_{B2} = 0$).

Considering equations (4.32) till (4.34), the explanation of the MALDI-TOF mass spectra presented in the Figure 4.25 for the commercial sample of fourth theoretical generation, BH-4, is the same as for the fourth generation HB polyester (HBP-4I). These results are opposite to the results listed in Table 4.12, which shows that the fraction of the B_4 core is lower than x_{B2} for the sample BH-4[71]. Furthermore, the mass spectrum of this sample

indicates that the amount of the cyclic structures is much higher than in the samples HBP-4I and HBP-4II. The presence of the fourth (54 mass units before series 1) and fifth (36 mass units after series 1) series of signals shows that sample BH-4 has probably more than one cyclic branch per molecule.

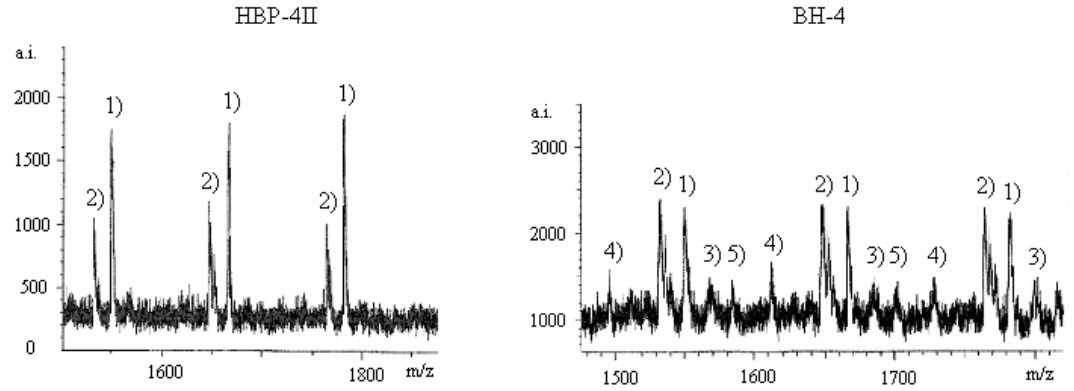

Figure 4.25. MALDI-TOF mass spectra of HBP-4II and BH-4

The identification of different oligomers in the MALDI-TOF mass spectra of higher generation HB polyesters is somewhat different than for the lower generation samples. From the NMR results it was determined that HB polyesters from fifth till tenth theoretical pseudo generation have higher fractions of the newly formed B_2 core than x_{B4} (Table 4.11). Furthermore, for the calculation of the molar mass of individual oligomers from the first and third series of signals, both equations (4.32) and (4.34) can be used. Therefore, it can be assumed that for the higher generation HB polyesters the third series of peaks corresponds to acyclic HB molecules containing a DiTMP core unit, while the first series of signals can be attributed to the acyclic oligomers with unreacted –COOH group (Figure 4.26). A second series of signals is assigned to the macrocyclic bis-MPA macromolecules with lack of the DiTMP core, while cyclic structures formed by the loss of the single water moiety from the third distribution of oligomers are overlapping with the first series of signals.

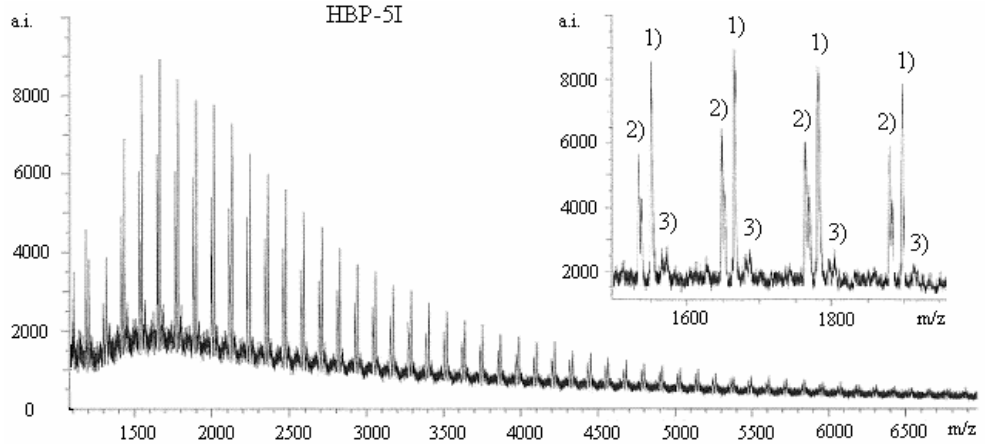

Figure 4.26. Full and enhanced MALDI-TOF mass spectra of the sample HBP-5I

By comparing MALDI-TOF mass spectra presented in Figures 4.24, 4.26 and Appendix 7.3.1 it can be confirmed again that the relative amount of the cycles is increasing with the theoretical number of pseudo generation. This increase was observed from the second up to the fifth theoretical generation. For the samples HBP-6I, HBP-8I and HBP-10I the intensities of the signals attributed to the cyclic structures do not change significantly. This is slightly different from the results obtained with VPO measurements, where it was shown that the extent of cyclization increases up to the sixth theoretical generation. The reason for these differences is probably the overlapping of the signals for the cycles with peaks which correspond to the HB structures. This also represents an additional problem when calculation of the molar mass averages is performed from the results obtained with MALDI-TOF mass spectrometry. It was also observed that the relative proportion of the signals which represent cyclic structures is increasing with the increasing size of the oligomers, i.e. with increasing degree of polymerization, especially in the mass spectra of the higher generation samples. Beside that, for these HB polyesters another series of small intensity signals was also detected, which implies that two or more cyclic branches per molecules were formed. The same conclusions can also be applied for the samples synthesized by the one-step procedure (samples HBP-6II and HBP-8II). For these two samples intensities of the signals corresponding to the cyclic structures are higher than for the analogue HB polyesters synthesized by pseudo-one-step procedure (Appendix 7.3.1). This leads to a conclusion that the amount of the formed cyclic structures can be decreased when HB polyesters are synthesized by a pseudo-one-step procedure.

MALDI-TOF mass spectrometry was also performed on the fractions of some HB polyesters. For the fractions of samples HBP-3I and HBP-4I the molar mass averages and polydispersity index were calculated (Table 4.14) and it was obtained that in both cases for all three fractions the molar mass averages were lower than for the parent sample. This is due to the low intensity of the higher molar mass peaks in the spectra of the first fraction. Furthermore, it was also determined that the polydispersity of HBP-4I fractions practically does not change, which is opposite to the trend observed with GPC measurements (Table 4.16). When enhanced parts of the MALDI-TOF mass spectra of HB polyesters fraction are observed (Figure 4.27), it can be seen that beside three already mentioned series of signals for the parent samples, another series of peaks appears (series 4). This sub-distribution of signals can not be assigned to the loss of two or more water moiety to form cyclic structures, since it does not appear on the adequate position in the mass spectra.

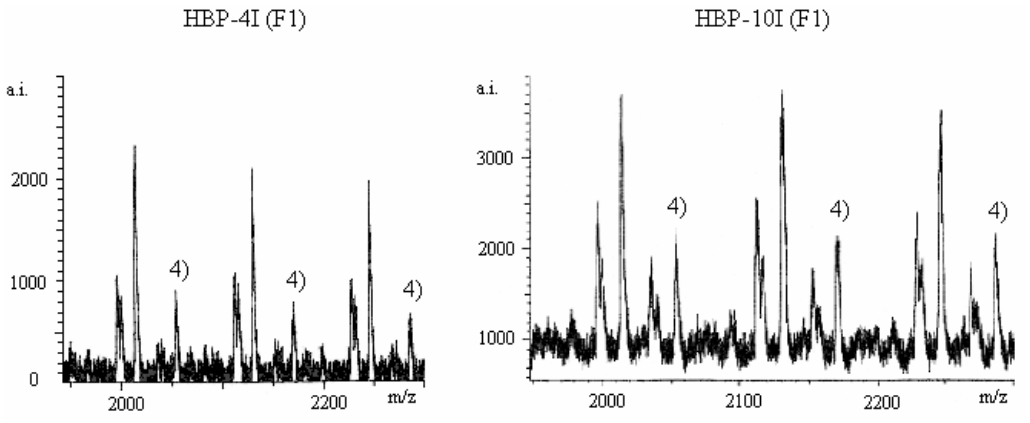

Figure 4.27. MALDI-TOF mass spectra of the first fractions of HBP-4I and HBP-10I

ESI mass spectra of the sample HBP-2I (Figure 4.28) confirmed the results obtained with MALDI-TOF mass spectrometry for this sample. In the ESI mass spectrum of HBP-2I presented in Figure 4.28a signals which corresponds to the cyclic structures were not detected, but only peaks attributed to desired acyclic oligomers with molar mass *M*+23, due to the Na ionization. These results show again that cyclization occurred in much lower extent in the second generation sample than in the HB polyesters of the higher generation. Similar results were obtained when K was used for ionization (Figure 4.28b). In both cases (Na or K ionization) regularly spaced peaks are separated by the repeat unit mass.

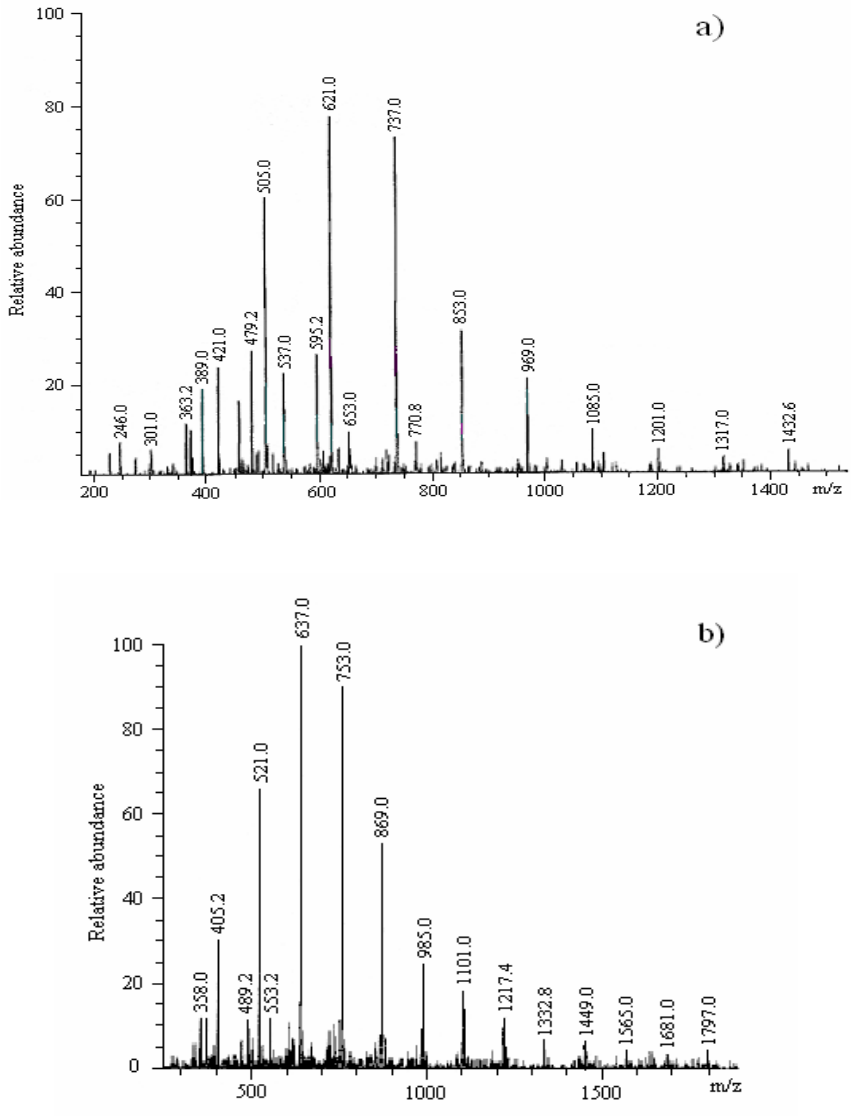

Figure 4.28. ESI mass spectra of HBP-2I: a) Na ionization (*M* + 23), b) K ionization (*M* + 39)

In the ESI mass spectra of samples HBP-3I and HBP-4I, beside the main series of signals corresponding to the acyclic oligomers with core molecule, peaks which can be attributed to the acyclic oligomers with unreacted –COOH groups are also observed, as well as signals corresponding to the cyclic structures (Figure 4.29). In contrast to MALDI-TOF MS data, ESI mass spectra of higher generation HB polyesters were very complex and difficult to interpret in detail, probably due to the significant fragmentation (Appendix 7.3.2).

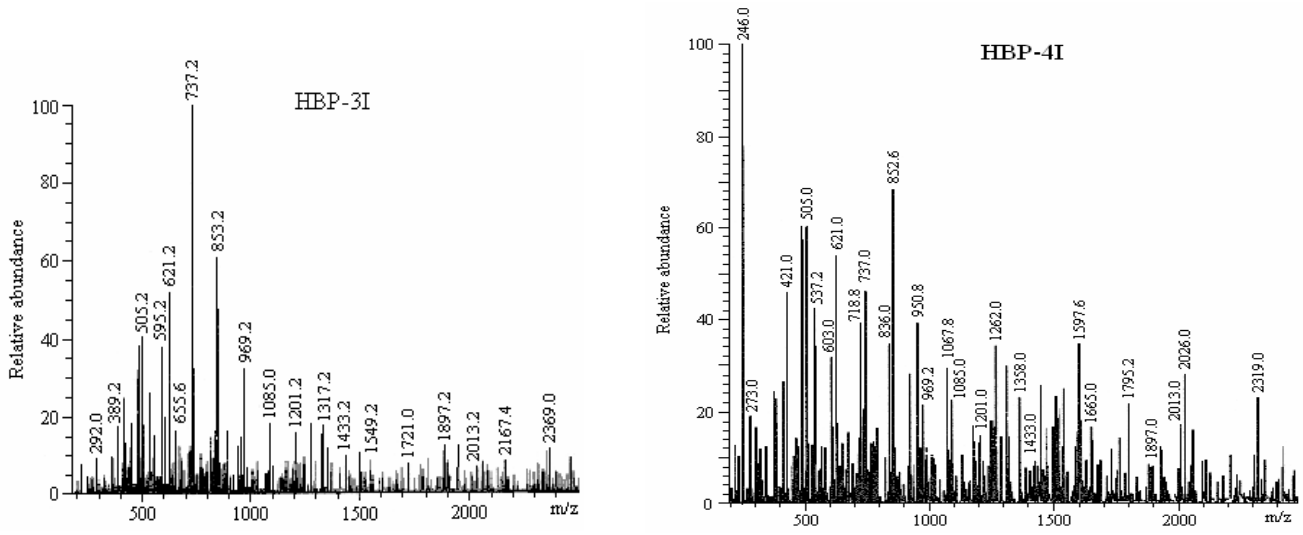

Figure 4.29. ESI mass spectra of HBP-3I and HBP-4I (Na ionization)

4.2.4. Results from the gel permeation chromatography

Gel permeation chromatography (GPC) of the investigated HB polyesters and their fractions were performed to obtain an insight into the molar mass distribution of these polymers and to compare obtained values of the polydispersity between samples of different theoretical pseudo generations or between different fractions of the HB polyesters. Values of the molar mass averages, determined using GPC measurements of HB polymers, can not be considered as absolute, since the calibration was done with linear polystyrene standards. Problems which can arise when GPC measurements of HB polymers are done using the calibration with linear polymer standards are already explained in the chapter 2.4.1.3. However, since separation in GPC is based on the sizes of molecules, the obtained values of the molar mass averages can be used for comparison between different samples. Furthermore, because it can be concluded that aggregation did not occur during the GPC measurements of the HB polyesters in THF as a solvent at chosen concentration (relatively low values of the molar mass averages were obtained for all used samples), information about the polydispersity of these polymers can be obtained.

In Figure 4.30 GPC measurements of the HB polyesters synthesized by a pseudo-one-step procedure are presented. For the sample HBP-6I, the GPC chromatogram is very similar to the chromatogram of the sample HBP-8I, and therefore is not presented in Figure 4.30. GPC traces of these HB polyesters have multimodal character as a consequence of different molar mass products present in the structure of the samples. In all GPC chromatograms of these samples a small peak appears at around 13.2 min, while for the sample HBP-8I, another extra peak was detected at around 14.0 min. Because the molar mass averages determined with GPC measurements are not absolute, it is not possible to conclude if these extra peaks appear due to the presence of the products from side reactions. However, from the results presented in Figure 4.30 it can be seen that these low molar mass distributions represent only a very minor component and therefore they were not included into the calculation of the molar mass averages and polydispersity. It is more likely that another peak which appears in the right shoulder of the larger peak comes from the self condensation of bis-MPA, since it is

observed at somewhat lower values of retention time, i.e. at higher molar masses. Beside that, this peak is not observed for the sample HBP-2I which is in good agreement with results obtained with previously described methods. When GPC traces of different generation HB polyesters are compared between each other it can be noticed that the molar mass distribution becomes broader with increasing theoretical number of generation, i.e. up to the sixth pseudo generation. This can also be observed from the calculated values of $(M_w/M_n)_{GPC}$, presented in Table 4.16. Only for the samples HBP-2I and HBP-3I symmetrical GPC profiles are obtained, while for the samples of higher generation number a broad tail on the low molar mass side of distribution can be observed. Since separations in the columns occur as a consequence of the differences in size, the broad peaks obtained in the molar mass distribution indicate that components with lower diameters are also present in the structure of the higher generation samples, probably due to the higher extent of the side reactions. This is especially noticeable in the GPC chromatograms of the samples HBP-8I and HBP-10I.

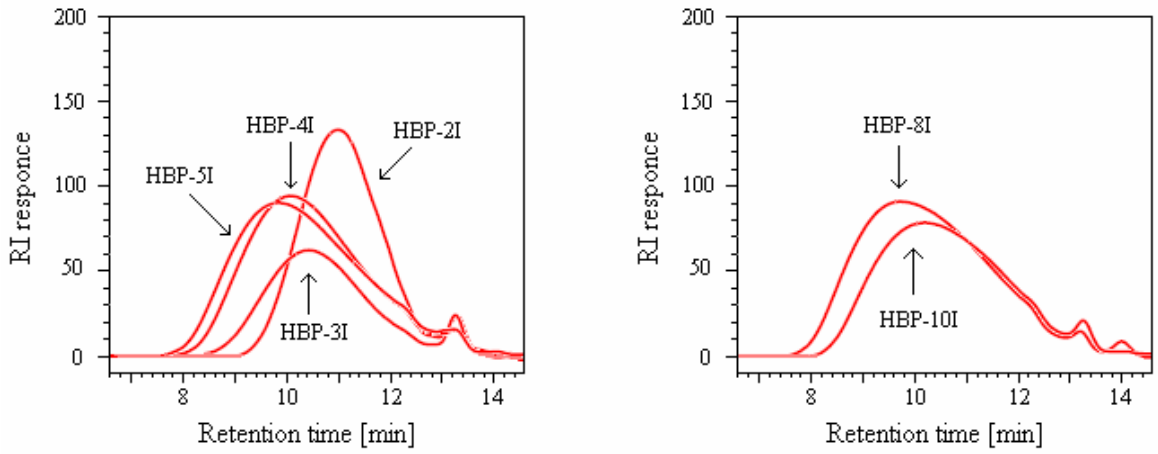

Figure 4.30. GPC profiles of HB samples synthesized by pseudo-one-step procedure

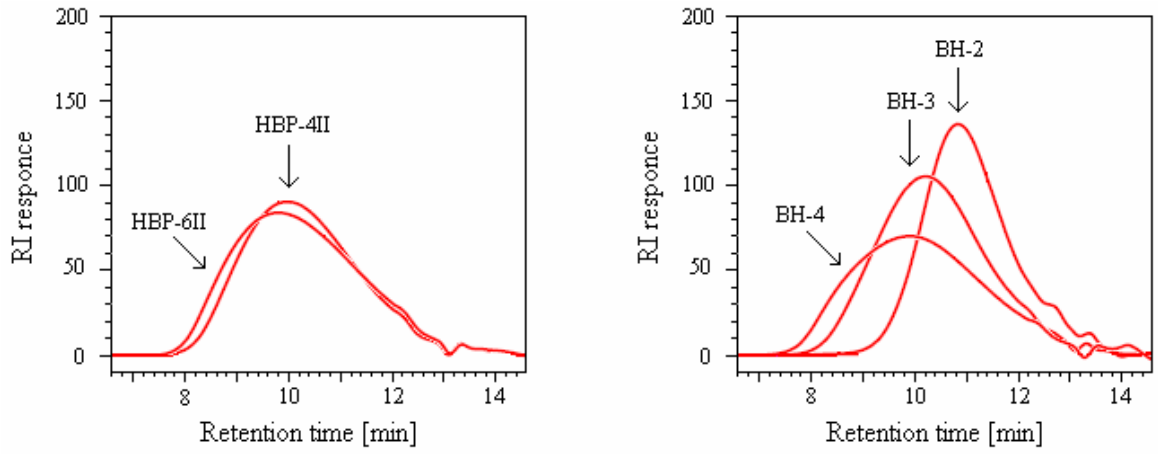

Figure 4.31. GPC profiles of HB samples synthesized by one-step procedure and commercial HB polyesters

GPC measurements of the HB polyesters synthesized by one-step procedure (Figure 4.31) have a similar profile as HB polyesters synthesized by pseudo-one-step procedure. However, these samples have a somewhat broader molar mass distribution (Table 4.16). Commercial HB polyesters also have a multimodal GPC profile (Figure 4.31) and a polydispersity which increases with the theoretical number of generation. Therefore, the same conclusions which are made for the HB polyesters synthesized in this work are also valid for the commercial ones. Determined values of the molar mass averages and polydispersity are listed in Table 4.16.

Table 4.16. Values of the average molar masses and polydispersity index $(M_w/M_n)_{GPC}$ of the investigated HB polyesters and their fractions determined from GPC measurements

Sample	$(M_w)_{GPC}$ [g/mol]	$(M_n)_{GPC}$ [g/mol]	$(M_w/M_n)_{GPC}$	Sample	$(M_w)_{GPC}$ [g/mol]	$(M_n)_{GPC}$ [g/mol]	$(M_w/M_n)_{GPC}$
HBP-2I	1041	749	1.39	HBP-8I	2994	1348	2.22
HBP-3I	1655	1008	1.64	F1	5547	2195	2.53
F1	2300	1263	1.82	F2	3931	1980	1.98
F2	2607	1551	1.68	F3	1498	1126	1.33
F3	1583	1062	1.49	HBP-10I	2111	1155	1.83
HBP-4I	2238	1172	1.91	F1	4874	2401	2.03
F1	5437	2292	2.37	F2	4404	2392	1.84
F2	4368	2274	1.92	F3	1811	1172	1.54
F3	1876	1218	1.54	BH-2	1120	782	1.43
HBP-4II	2475	1189	2.08	BH-3	2227	1147	1.94
HBP-5I	2688	1213	2.22	F1	4760	2209	2.15
HBP-6I	2993	1287	2.33	F2	3120	2017	1.55
F1	5581	2260	2.47	F3	1855	1251	1.48
F2	3832	1973	1.94	BH-4	3454	1242	2.78
F3	1080	771	1.40	F1	19707	2992	6.59
HBP-6II	2912	1179	2.47	F2	6447	3022	2.13
HBP-8II	2674	1148	2.33	F3	2244	1417	1.58

As it was expected, the molar mass averages determined using GPC measurements, calibrated with linear polystyrene standards, are too low compared with theoretical values and results obtained by other techniques (NMR, VPO, and MALDI-TOF mass spectrometry). On the other side, values of the $(M_w/M_n)_{GPC}$ were significantly higher than the same values obtained with MALDI-TOF mass spectrometry (Table 4.14), due to the already explained problems with MALDI-TOF measurements of polymers with broad molar mass distribution. There is a trend of increasing weight average molar mass with the theoretical number of pseudo generation, i.e. up to the eighth pseudo generation. On the other hand, M_n does not increase in the same levels as a consequence of the higher amount of the species with low molar mass due to the intramolecular cyclization and presence of the unreacted –COOH groups. Because of that, the polydispersity of these samples also increases with increasing

number of generation. The molar mass distribution of the HB polyesters synthesized by one-step procedure is slightly broader than for the samples synthesized by pseudo-one-step procedure, which is in a good agreement with theoretical predictions that slow monomer addition can decrease polydispersity of this type of HB polyesters[34]. It can also be observed that the $(M_w/M_n)_{GPC}$ of commercial samples is higher than values obtained for the HB polyesters synthesized in this work.

To investigate if the underestimation of the molar mass averages measured using the GPC is systematic, results of the number average molar mass obtained with GPC and VPO measurements are plotted in Figure 4.32. It can be observed that a relatively good linear correlation between $(M_n)_{GPC}$ and $(M_n)_{VPO}$ for the HB polyesters from third till eighth theoretical generation was obtained. This further indicates that $(M_n)_{GPC}$ shows a systematic deviation from the absolute values obtained by VPO technique for these samples. The only exception from this observation is the sample HBP-10I, due to the lower values of number average molar mass compared to the samples of sixth and eighth theoretical generation. The reason for this is probably the very high extent of the side reactions which occurred during the synthesis of this sample and which are already proved by the results obtained with NMR measurements (Table 4.11). The linear correlation presented in Figure 4.32 for the samples up to the eighth theoretical generation confirms that GPC columns separate HB polyesters of the series I according to hydrodynamic volume. Since it was determined that these polymers have similar density (Table 4.23), the separation also occurred according to molar mass. This practically means that GPC measurements can be used for an estimation of the polydispersity of these HB polyesters.

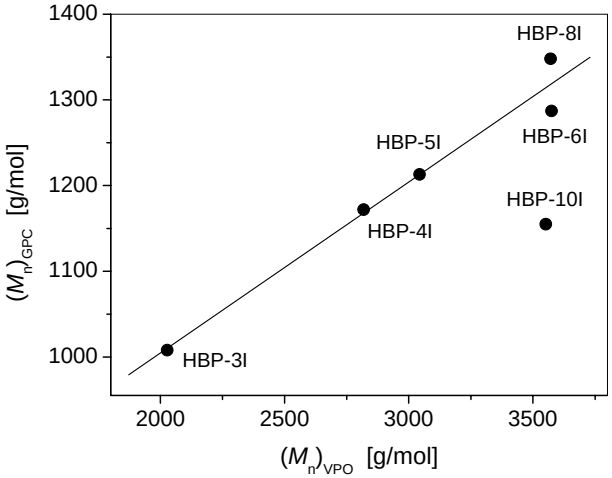

Figure 4.32. Correlation of the number average molar mass obtained from GPC and VPO measurements

GPC measurements were also performed on all fractions of the investigated HB polyesters (Table 4.16). In Figures 4.33 and 4.34 GPC traces of some of the fractionated HB polymers are presented. GPC chromatograms of other fractionated samples can be found in Appendix 7.4. From results listed in Table 4.16 it can be seen that polydispersity increases from third up to the first fraction, i.e. that the molar mass distribution becomes broader with increasing degree of polymerization. This behaviour confirms *Flory*'s predictions considering molar mass distribution of the highly branched polymers[14]. From the GPC chromatograms presented in Figures 4.33 and 4.34 the same conclusions can be made. GPC traces of the third fractions are more symmetric than traces of the second and first fractions, which have a GPC profile more similar to the profile of the parent samples. For most fractionated HB polyesters,

$(M_w)_{GPC}$ and $(M_n)_{GPC}$ decrease from first to third fraction. The decrease of the $(M_n)_{GPC}$ with decreasing degree of polymerization confirms again the previously made conclusion that GPC separates these HB polymers according to hydrodynamic volume. This behaviour was not observed for the fractions of the sample HBP-3I, where $(M_w)_{GPC}$ and $(M_n)_{GPC}$ of the second fraction are higher than values obtained for the first fraction. The same phenomenon was also detected from the results obtained using MALDI-TOF mass spectrometry of the fractions of this sample (Table 4.14). Calculation of the molar mass averages for the fractions of commercial sample BH-4 showed similar results, since for this sample $(M_n)_{GPC}$ of the second fraction is higher than for the first fraction. However, in this case the reason for such deviation is the difficulty to set the limits of integration in the GPC chromatogram of the first fraction, due to the relatively large peak which appeared at lower retention times (Figure 4.34). Therefore, the integration in this case was done over the entire chromatogram, which is the reason for such high values of the polydispersity for this sample (Table 4.16). The presence of this peak at lower retention times is due to the aggregation of some macromolecules. Similar results for the first fraction of the sample BH-4 were obtained by other authors[71]**.** The formation of the aggregates can be explained by the presence of the very stable hydrogen bond network at room temperature, which can not be completely disrupted by dissolving the sample in THF[71,146].

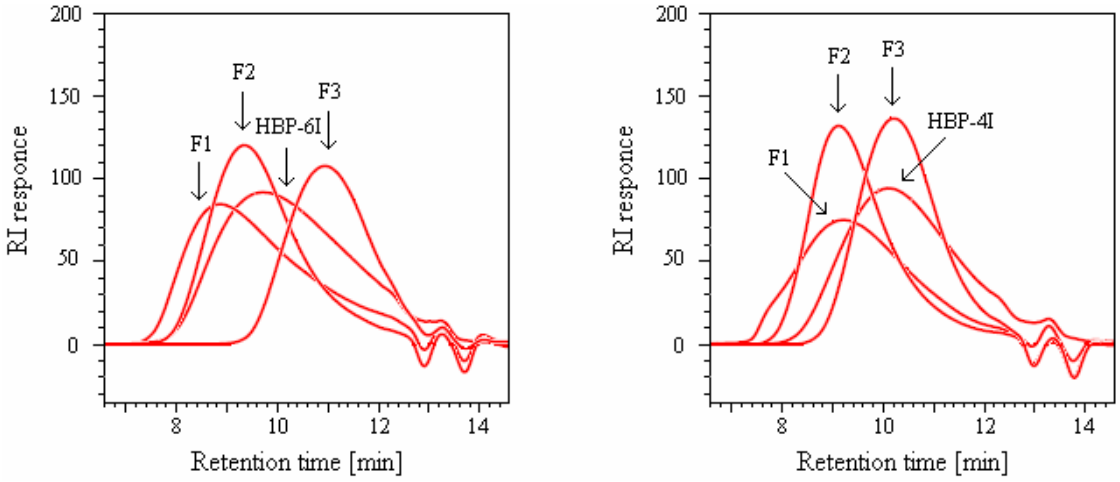

Figure 4.33. GPC profiles of HB polyesters and their fractions

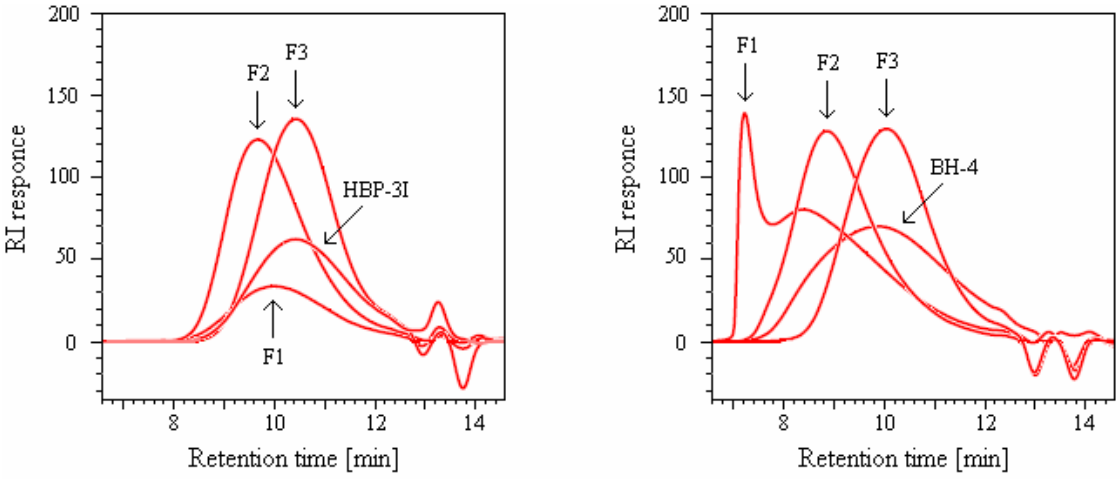

Figure 4.34. GPC profiles of HB polyesters and their fractions

Only for the samples HBP-6I and HBP-8I fractions are evenly distributed through the molar mass distribution of the parent HB polyester. On the other side, $(M_n)_{GPC}$ of the third fraction is higher for all other samples than $(M_n)_{GPC}$ of the parent polymer. The reason for this is probably that during the fractionation of these samples species with lower hydrodynamic volume are partly removed from the fractions.

Since it was confirmed that GPC columns separate HB polyesters synthesized in this work according to the hydrodynamic volume (and most probably also commercial samples due to the similar structure) it is possible to calculate values of the "shrinking" factor, *g*', for different samples (equation 2.6). This was done using the fact that the product of the limiting viscosity number and molar mass is independent of polymer type, i.e. that $[\eta]M$ is constant at a certain elution volume[61,64] or in this particular case:

$$[\eta]_{HBP} M_{HBP} = [\eta]_L M_L \tag{4.35}$$

where $[\eta]_{HBP}$ and $[\eta]_L$ are limiting viscosity numbers and M_{HBP} and M_L are molar masses of HB polyesters and linear polymer (polystyrene) used for the calibration, respectively. From the equation (4.35) it follows that *g*' can be calculated as M_L/M_{HBP}. Values of the M_L are calculated by determination of the retention time which corresponds to the position of the peak in the GPC traces of different HB samples. Then this retention times are used to determine molar masses of the corresponding polystyrene from the calibration curve. On the other side, for the M_{HBP} weight average molar mass is used, which is calculated from the ratio $(M_w/M_n)_{GPC}$ and $(M_n)_{VPO}$ (or $(M_n)_{NMP}$ in the case of the sample HBP-2I). Determined values of the factor *g*' are listed in Table 4.17.

Table 4.17. Values of the "shrinking" factor (*g*') for the investigated HB polyesters

Sample	*g*'	Sample	*g*'
HBP-2I	0.44	HBP-8II	0.30
HBP-3I	0.45	HBP-10I	0.27
HBP-4I	0.35	BH-2	0.57
HBP-5I	0.34	BH-3	0.29
HBP-6I	0.31	BH-4	0.31
HBP-8I	0.32	/	

As can be seen from the results presented in Table 4.17, values of the *g*' for all HB samples are between 0.27 and 0.57, as a consequence of the smaller hydrodynamic dimensions of the HB polyesters compared with that of linear polystyrene. Similar results are obtained for other HB polymers[99].

GPC measurements were also performed on four modified samples (two self-synthesized samples and two commercial HB polyesters). End –OH groups of these samples were modified with β-alanine using the procedure described in the chapter 3.2.3. The degree of modification was calculated by comparing values obtained from hydroxyl number titration of these samples with values determined for the corresponding unmodified HB polyesters (Table 4.5). The modification of these four samples was done with β-alanine in order to obtain samples soluble in water. That was fully accomplished only for the commercial HB polyester of the second generation ($BH\text{-}2_{AL}$). The other three samples could only partially be dissolved in water after adding a small amount of the NaOH. Therefore, GPC measurements

of these three samples were performed using the aqueous solution of NaOH as a solvent. Values of the degree of modification together with results determined from the GPC measurements are listed in Table 4.18, while GPC chromatograms of modified samples are presented in Figures 4.35 and 4.36.

Table 4.18. Values of the hydroxyl number, $(N_{HN})_{exp}$, degree of modification, molar mass averages, $(M_w)_{GPC}$ and $(M_n)_{GPC}$, and polydispersity index $(M_w/M_n)_{GPC}$ of modified HB polyesters

Sample	$(N_{HN})_{exp}$ [mg KOH/g]	Degree of modif. [%]	$(M_w)_{GPC}$ [g/mol]	$(M_n)_{GPC}$ [g/mol]	$(M_w/M_n)_{GPC}$
HBP-3I$_{AL}$	141.9	72.0	941	671	1.40
HBP-4I$_{AL}$	126.2	74.4	1013	679	1.49
BH-2$_{AL}$	136.6	72.7	1303	913	1.43
BH-3$_{AL}$	119.2	74.9	1000	709	1.41

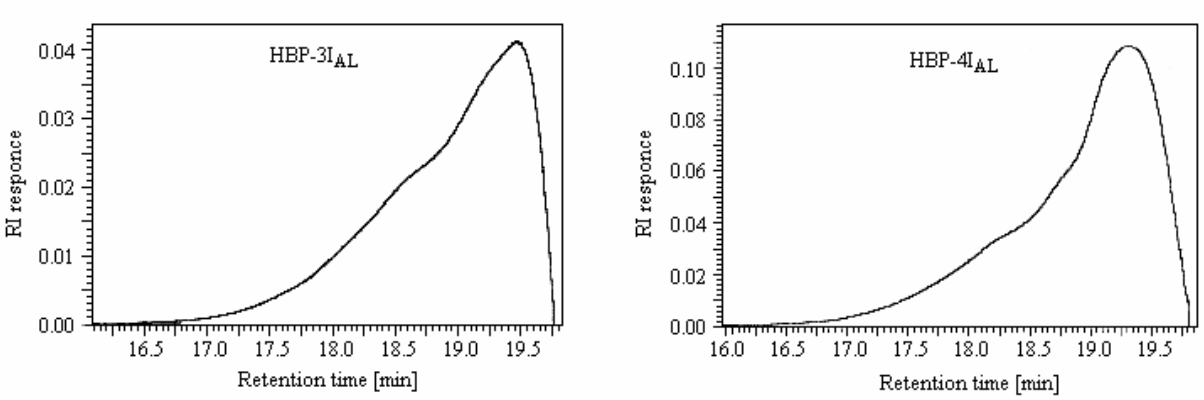

Figure 4.35. GPC profiles of the modified HB polyesters

From the results listed in Table 4.18 it can be seen that only for the modified sample BH-2$_{AL}$ the polydispersity is the same as for the unmodified sample, while for the other modified HB polyesters values are much lower than $(M_w/M_n)_{GPC}$ listed in Table 4.16. The difference between GPC measurements of modified and unmodified samples can also be observed by comparing chromatograms of these samples (Figures 4.30, 4.31, 4.35 and 4.36). GPC traces of the modified samples have a multimodal character with a broad tail on the high molar mass side of distribution, which is opposite from the results obtained for the unmodified HB polyesters. Because of that, the obtained values of the polydispersity are much lower. The reason for such a specific GPC profile of the modified samples is probably the formation of the aggregates. Therefore, the obtained values of the polydispersity can not be treated as reliable in this case.

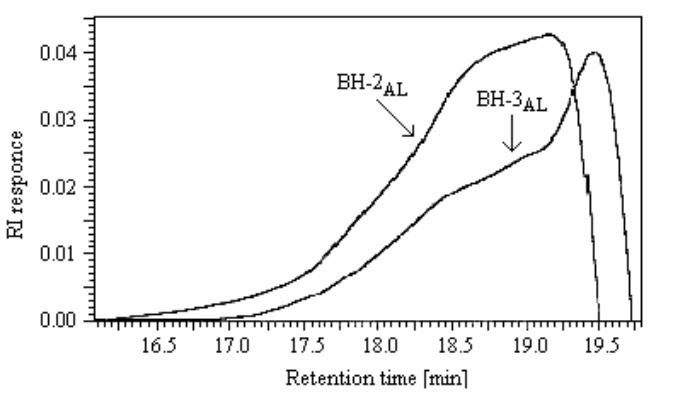

Figure 4.36. GPC profiles of the modified commercial HB polyesters

4.2.5. Results from the static light scattering

Static light scattering (SLS) of the HB polyesters of the series I and commercial samples was performed in order to get more information about the weight average molar mass of these samples. Measurements were done in two different solvents (DMF and DMAc) for comparison. *Zimm* plots for selected samples are presented in Figures 4.37 and 4.38, while the determined values of the weight average molar mass, second virial coefficient and radius of gyration are listed in Table 4.19.

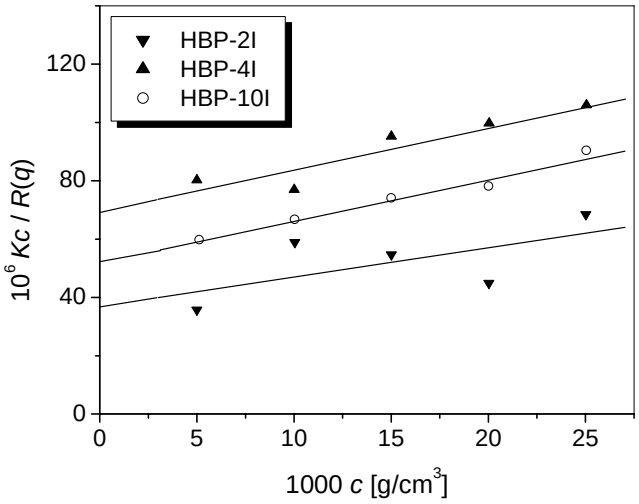

Figure 4.37. *Zimm* plots of HB polyesters (series I) determined in DMF as a solvent at scattering angle of 90^0

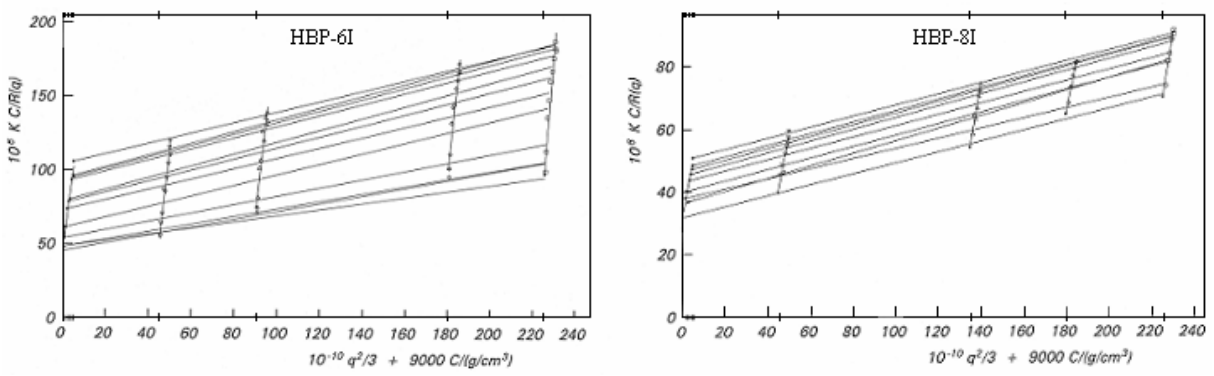

Figure 4.38. *Zimm* plots of the samples HBP-6I and HBP-8I determined in DMF as a solvent

Table 4.19. d*n*/d*c* values and results obtained from the SLS measurements for the polymers of the series I and commercial HB polyesters in DMF and DMAc as a solvent

Sample	DMF			
	d*n*/d*c*×10^2 [cm^3/g]	$(M_w)_{SLS}$ [g/mol]	A_2×10^4 [cm^{3}mol/g^2]	R_z [nm]
HBP-2I	6.16	27000	5.02	/
HBP-3I	5.62	16600	-2.43	/
HBP-4I	6.17	14400	7.15	/
HBP-5I	6.37	20700	21.76	/
HBP-6I	6.20	22000	11.96	48.7
HBP-8I	6.22	31500	7.82	32.3
HBP-10I	6.30	19200	7.09	/
BH-2	6.66	1100	-80.21	/
BH-3	6.01	6300	27.5	/
BH-4	5.96	16100	16.24	/
Sample	DMAc			
	d*n*/d*c*×10^2 [cm^3/g]	$(M_w)_{SLS}$ [g/mol]	A_2×10^4 [cm^{3}mol/g^2]	R_z [nm]
HBP-8I	6.06	7400	15.86	/
HBP-10I	6.12	15800	37.43	/

In Table 4.19 values of the refractive index increment (d*n*/d*c*) are also listed, since it was necessary to determine these values for the purpose of SLS measurements. The obtained values of d*n*/d*c* are on the lower limit for precise measurements. It was already mentioned that when d*n*/d*c* < 0.05, the intensity of the scattered light can be too low. Only for the samples HBP-6I and HBP-8I SLS measurements were possible to do at all scattering angles. For other HB polyesters the intensity of the scattered light does not change with scattering angle and therefore measurements were performed at the angle of 90^0. However, for all investigated HB polyesters, the obtained values for the weight average molar mass and radius of gyration in

both solvents are pointing out on the aggregates presence. A similar observation was made when THF was used for the SLS measurements of this type of HB polyesters[147]. DMF and DMAc were chosen for these measurements because aggregation did not occur when they were used for the solutions preparation for other characterization techniques such as VPO (Figures 4.20 and 4.21) and the limiting viscosity number measurements (Figure 4.45 and results from the reference[147]). As expected, SLS measurements are more sensible to the presence of the aggregates, which leads to a larger intensity of the scattered light and consequently to the higher values of the weight average molar mass.

From the results listed in Table 4.19 it can only be concluded that aggregation is a consequence of the polar end –OH groups. This is especially noticeable for the samples from second till fourth theoretical pseudo generation, since for them $(M_w)_{SLS}$ decreases with increasing number of generation. The reason for such behaviour is that the percentage of end, i.e. terminal –OH groups decreases with increasing number of generation (Table 4.5), which practically means that the sample of the second theoretical pseudo generation will have the highest ability for the formation of the aggregates. For the higher generation samples (from fifth till eighth) an increase in the $(M_w)_{SLS}$ can be observed, which is in a good agreement with the trend obtained from GPC measurements (Table 4.16). For the sample HBP-3I and BH-2 negative values of the second virial coefficient were determined, since for these samples negative slope was obtained. This phenomenon can not be treated as a result of the bad quality of the DMF as a solvent for these two samples, due to the relatively good results obtained from VPO (Table 4.13), dynamic light scattering (Table 4.21) and limiting viscosity number measurements[147].

4.3. Dimensions of the hyperbranched polyesters

4.3.1. Results from the dynamic light scattering

In order to determinate the hydrodynamic dimensions of the HB polyesters in solution, dynamic light scattering (DLS) measurements were performed. This technique was also used to investigate the influence of different types of solvents on the hydrodynamic radius of the samples in the solution and to study the ability of aggregates formation in different solvents. DLS measurements were also performed on the purified samples in order to establish the influence of the small size molecules on the dimensions of the HB polyesters.

There are three different distributions which can be obtained with this type of DLS measurements (Figure 4.39):

1) Number distribution from which it is possible to determinate the number of molecules of different sizes.
2) Volume distribution, where area of the peak corresponds to the volume of the specific molecule.
3) Intensity distribution, which can give more information about aggregates formation, since large particles scatter much more light than small ones (the intensity of the scattered light is proportional to the sixth power of the particle diameter according to the *Rayleigh's* approximation).

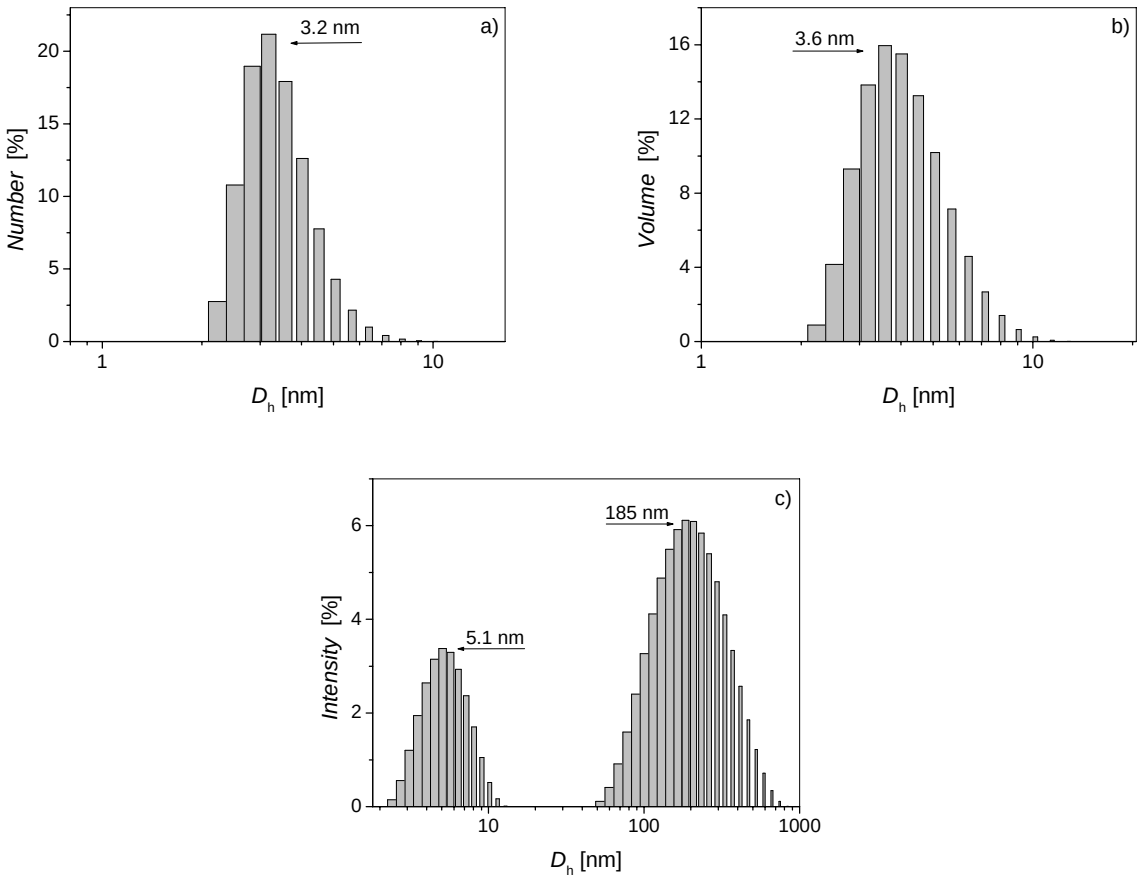

Figure 4.39. a) Number, b) volume and c) intensity distribution, determined from the DLS measurements of the sample HBP-5I in NMP as solvent

As an example, in Figure 4.39 are presented number, volume and intensity distributions of the sample HBP-5I, determined with DLS technique in N-methyl-2-pyrrolidinon (NMP) as a solvent. In the graphics which represent number and volume distributions of the different sizes, the presence of the aggregates can not be detected, while the situation is completely different in the Figure 4.39c. The absence of the peaks corresponding to the aggregates in the Figures 4.39a and 4.39b is due to their very low amount in this HB polyester. On the other side, the presence even of the small amount of the aggregates leads to the high scattering of the light which further induces the appearance of the second distribution of the peaks in the graph for the intensity distribution. A similar behaviour was observed from the results obtained for the other HB polyesters in different solvents. Associations between molecules in the aggregates probably arise from intermolecular hydrogen bonding between end –OH groups. These conclusions can be used to explain why the weight average molar mass determined with SLS technique is extremely high. For that purpose, DLS measurements of the sample HBP-4I were also performed in DMF (Table 4.21). Since the same behaviour was observed in this case, i.e. the presence of the aggregates are detected only in the graph which represents the intensity distribution, it can be concluded that they are the main reason why the intensity of the scattered light in the SLS measurements was so high.

The values of the hydrodynamic radius, i.e. hydrodynamic diameter of the investigated HB samples (purified and non-purified), determined from the DLS measurements in NMP are listed in Table 4.20.

Table 4.20. Hydrodynamic diameters of the investigated HB polyesters, determined from the number (n), volume (v) and intensity (i) distribution by DLS measurements in NMP (values in the second bracket correspond to the highest peak in the second distribution which is attributed to the formed aggregates)

Sample	D_h(non-purif.) [nm]			D_h(purif.) [nm]		
	n	v	i	n	v	i
HBP-2I	2.(2)	2.(5)	3.(2) [116]	2.(8)	3.(2)	3.(6) [116]
HBP-3I	3.(2)	4.0	4.(5) [208]	3.(2)	3.(6)	4.(5) [147]
HBP-4I	3.(6)	4.0	5.(1) [165]	3.(6)	4.0	5.(1) [116]
HBP-4II	3.(3)	4.(1)	6.(7) [449]	2.0	2.(7)	4.(5) [406]
HBP-5I	3.(2)	3.(6)	5.(1) [185]	4.0	4.(5)	5.(1) [92]
HBP-6I	3.(2)	3.(6)	5.(1) [208]	4.(5)	4.(5)	5.(1) [82]
HBP-6II	2.(7)	3.(3)	5.0 [272]	3.0	3.(7)	5.(5) [246]
HBP-8I	3.(2)	4.0	5.(7) [262]	4.0	4.(5)	5.(7) [372]
HBP-8II	3.(3)	4.(1)	5.(5) [332]	3.0	3.(7)	5.(5) [201]
HBP-10I	3.(6)	4.0	5.(7) [372]	14.(4)	14.(4) [92]	16.(2) [104]
BH-2	2.(2)	2.(5)	3.(6) [295]	/	/	/
BH-3	3.(6)	4.0	5.(7) [295]	/	/	/
BH-4	3.(6)	4.0	6.(4) [469]	/	/	/

From the results obtained by the intensity distribution it can be observed that the presence of the aggregates can be detected in all samples. Since it is not possible to see any specific trend of the aggregate sizes for samples of different generation number, the average number of molecules which are consumed for their formation can not be determinate. Another difficulty represents the broad distribution of the sizes detected for these HB polyesters, which further complicate the calculation of the formed aggregates. For the purified sample HBP-10I relatively high values of the hydrodynamic radius were obtained from all three types of distributions. Beside that, in both volume and intensity distribution a second distribution of the peaks at higher values was detected. The reason for such behaviour is probably impurities in the solution, which were not completely removed by filtration. However, the amount of this sample was insufficient to repeat the measurement. Therefore, results for this sample will not be considered in the further discussion.

Considering the previously given explanations about the different distributions which are obtained by DLS measurements, results obtained from the number distribution can be considered as the most accurate. Results listed in Table 4.20 show that the hydrodynamic radius (determined from the number distribution) of the samples synthesized by the one-step procedure are smaller than the values obtained for the HB polyesters synthesized by pseudo-one-step procedure. From this observation it is obvious that the type of the synthesis also has a significant influence on the dimensions of these HB polyesters. The only exception is the non-purified sample HBP-8II, whose dimensions are slightly bigger than for the sample HBP-8I.

The hydrodynamic radius determined from the number distribution increases up to the fourth theoretical pseudo generation when NMP is used as a solvent. On the other side, the hydrodynamic radius of the purified samples increases linearly up to the sixth theoretical generation (Figure 4.40 and 4.41). Therefore, it can be concluded that molecules with smaller

sizes were removed by the purification as it was expected, which was also observed from the results obtained by VPO measurements (Table 4.13). However, the increase of the hydrodynamic radius for both, the non-purified and the purified samples occurs in a much lower degree than it was expected from the values of theoretical molar mass (Table 4.1). Therefore, from these results it can be also confirmed that side reactions occurred in a significant degree during the synthesis of HB polyesters.

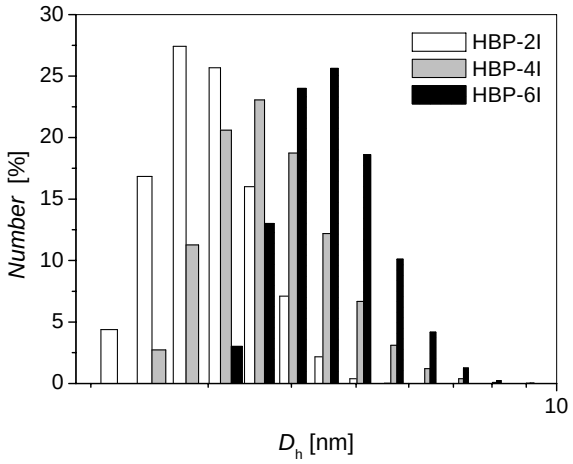

Figure 4.40. Number distributions determined from the DLS measurements in NMP of the purified samples HBP-2I, HBP-4I and HBP-6I

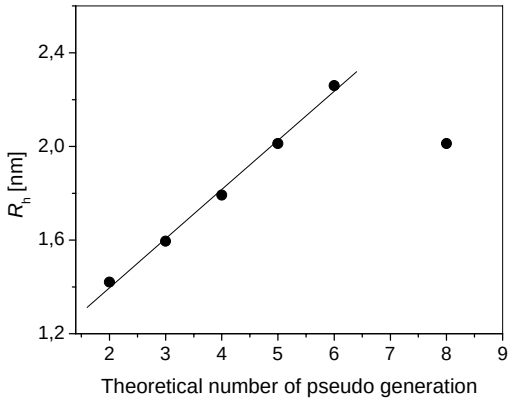

Figure 4.41. Hydrodynamic radius determined from the number distribution in NMP versus theoretical number of pseudo generation for the purified HB polyesters

A relationship between the hydrodynamic radius and molar mass can be expressed according to the equation (2.48) which can be written in this particular case as follows:

$$R_h = K_R M_w^{\upsilon} \quad \text{or} \quad \log R_h = \log K_R + \nu \log M_w \tag{2.48}$$

where K_R is the constant. For this purpose, the weight average molar mass is calculated from the values of $(M_n)_{VPO}$ and the polydispersity indices determined using GPC measurements. On the other side, for the sample HBP-2I $(M_n)_{NMR}$ is used for the calculation of M_w. The dependence of the hydrodynamic radius determined from the number distribution in NMP as a solvent versus weight average molar mass for the lower generation number HB polyesters

(non-purified samples from second till fourth theoretical generation) is presented in Figure 4.42. According to the linear relationship obtained from the Figure 4.42, it was determined that the exponent *v* has a value of 0.49 for lower generation number HB polyesters. This value of the exponent *v* is in relatively good agreement with values obtained for the dendrimers (see chapter 2.4.3), and shows that beside a significant decrease of the molar mass due to the side reaction and presence of the large amount of linear units, structure of the investigated HB polyesters is still similar to the structure of low generation number dendrimers.

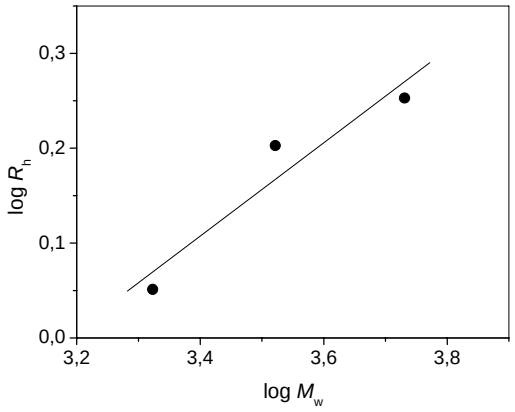

Figure 4.42. Dependence of the log R_h versus log M_w for the non-purified lower generation HB polyesters

DLS measurements are also performed to investigate the influence of different solvents on the dimensions of HB polyesters (Table 4.21). It can be observed that the hydrodynamic radius of HB polyesters decreases with decreasing polarity of the used solvents. However, when a mixture THF/CH_3OH was used as a solvent the obtained values of the diameter were around 10 times bigger than it was expected for this type of solvent.

Table 4.21. Hydrodynamic diameters of the sample HBP-4I, determined from the number (n), volume (v) and intensity (i) distribution by DLS measurements in different solvents

D_h(non-purif.) [nm]	Solvent		
	DMF	Acetone	THF/CH_3OH
n	2.(2)	2.(2)	18.(2)
v	2.(8)	2.(8) [9]	22.(9)
i	4.0 [165]	3.(2) [14] [147]	36.(5) [1495]

Dimensions of the fractions were also determined using the DLS technique. From the obtained values listed in Table 4.22 it can be seen that in most cases the hydrodynamic radius determined from the number distribution is changing in order R_h(F1) > R_h(F2) > R_h(F3) as it was expected. However, for the samples HBP-4I and HBP-8I it is obtained that R_h(F1) = R_h(F2), which is probably the consequence of the experimental error. The standard error for this type of DLS measurements is ±1 nm. For the sample BH-3, R_h(F1) is smaller than R_h(F2), which is in good agreement with results obtained by viscosimetry (Table 4.28). As an

example in Figure 4.43 are presented number distributions determined from DLS measurements for HBP-6I, HBP-10I and BH-4 fractions.

Table 4.22. Hydrodynamic diameters of the fractions, determined from the number (n), volume (v) and intensity (i) distribution by DLS measurements in NMP

Sample	D_h [nm]			Sample	D_h [nm]		
	n	v	i		n	v	i
HBP-3I F1	3.(2)	3.(6)	4.(5) [104]	HBP-8I F3	2.(5)	2.(8)	5.(7) [591]
HBP-3I F2	2.(8)	3.(2)	4.0 [234]	HBP-10I F1	4.(5)	5.(1)	7.(2) [372]
HBP-3I F3	2.0	2.(8)	7.(2) [1056]	HBP-10I F2	3.(2)	4.0	6.(4) [1679]
HBP-4I F1	3.(6)	4.0	4.(5) [165]	HBP-10I F3	2.(5)	2.(8)	3.(6) [2671]
HBP-4I F2	3.(6)	4.0	6.(4) [1886]	BH-3 F1	2.(5)	3.(2)	4.(5) [82]
HBP-4I F3	2.(5)	3.(2)	6.(4) [1332]	BH-3 F2	2.(8)	3.(2)	4.(5) [82]
HBP-6I F1	5.0	5.(5)	6.(1) [74]	BH-3 F3	1.(3)	1.(3)	6.(4) [745]
HBP-6I F2	2.(8)	3.(6)	6.(4) [1679]	BH-4 F1	4.0	4.(5)	5.(7) [104]
HBP-6I F3	1.(8)	2.(5)	7.(2)	BH-4 F2	3.(2)	3.(6)	4.(5) [104]
HBP-8I F1	3.(6)	4.(5)	7.(2) [131]	BH-4 F3	2.(2)	2.(8)	5.(7) [1332]
HBP-8I F2	3.(6)	4.0	6.(4) [1886]	/			

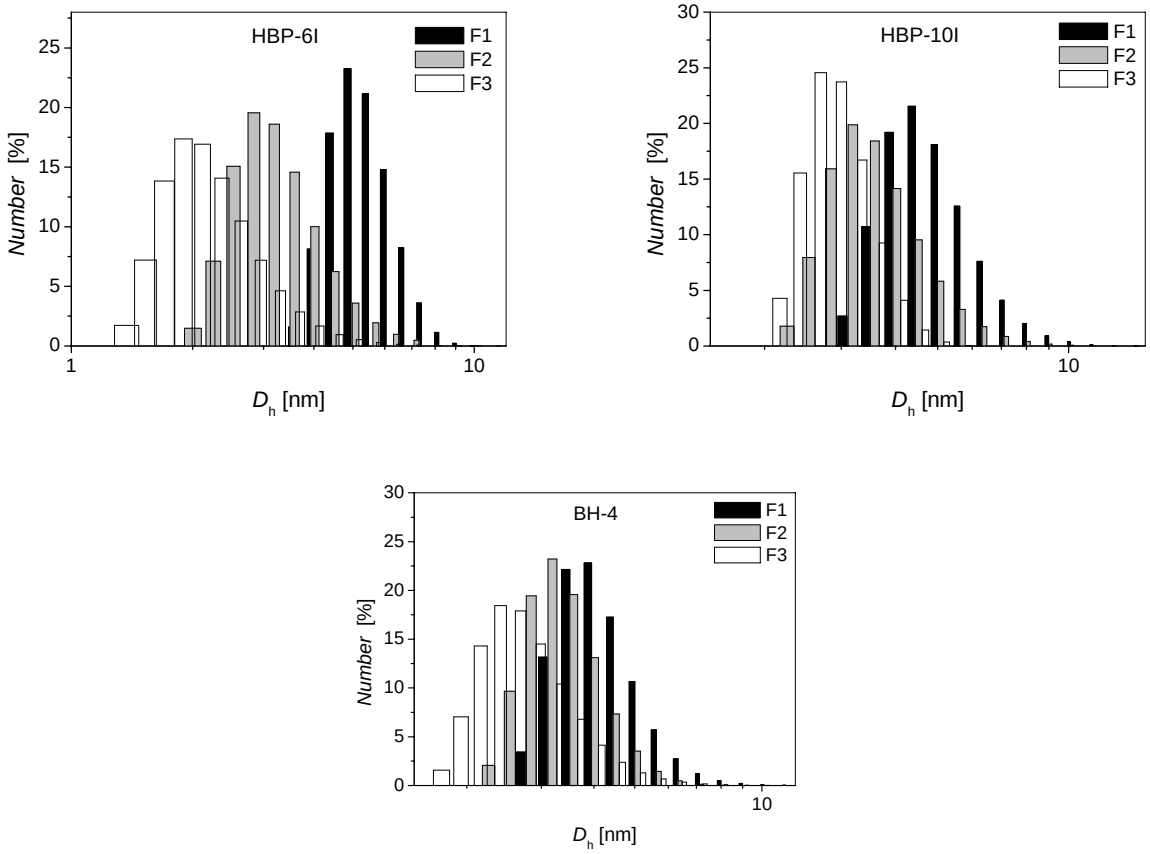

Figure 4.43. Number distributions determined from the DLS measurements in NMP of the HBP-6I, HBP-10I and BH-4 fractions

4.3.2. Results from the ultracentrifugation measurements

As it is already explained in the chapter 2.4.3.2, dimensions of the HB polyesters can also be determined from ultracentrifugation (UC) measurements. Typical UC measurement is presented in Figure 4.44, while obtained values of the diameter are listed in Table 4.23 together with values of the density determined in the manner described in the experimental part (see chapter 3.3.12) and values of the refractive index calculated according to the equation (3.4), which were necessary to have for UC measurements. As a consequence of the diffusion and relatively low sensitivity of this type of measurements on such small dimensions of the investigated samples, determined values of the diameter did not change significantly with the change of the generation number.

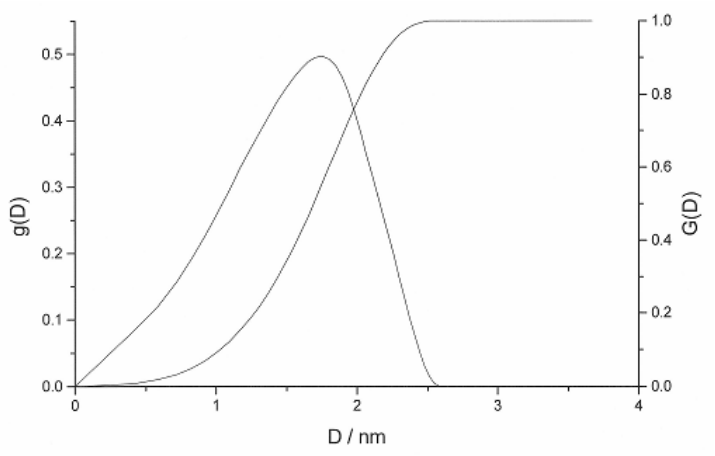

Figure 4.44. UC measurement for the sample HBP-6I

Table 4.23. Values of the diameters (*D*), determined from UC measurements, densities (*ρ*) and refractive indices (*n*) of the investigated HB polyesters

Sample	*D* [nm]	*ρ* [g/cm^3]	*n*
HBP-2I	2.1	1.28	1.49
HBP-3I	2.2	1.30	1.48
HBP-4I	2.2	1.30	1.49
HBP-4II	2.6	1.30	1.49
HBP-5I	2.3	1.30	1.49
HBP-6I	2.5	1.30	1.49
HBP-8I	2.5	1.31	1.49
HBP-8II	2.4	1.30	1.49
HBP-10	2.6	1.31	1.49
BH-4	2.4	1.29	1.49

4.4. Viscosimetry of the diluted solutions

Viscosimetry of the diluted solutions of HB polyesters were performed in order to quantitatively evaluate the limiting viscosity number, [η], in different solvents, which are further used to examine the influence of the solvent quality on [η] and at the same time on the hydrodynamic radius (R_η) of the samples. Viscosity measurements were done at 25 ^{0}C in four different solvents: in N-methyl-2-pyrrolidinon (NMP), N,N-dimethylacetamide (DMAc), 0.7 mass% solution of LiCl in DMAc (LiCl/DMAc) and in a mixture THF/CH_3OH (90:10 by volume) using the method described in chapter 3.3.13. As an example the dependences of η_{sp}/c versus c for different HB polyesters in different solvents are presented in the Figures 4.45a and 4.45b.

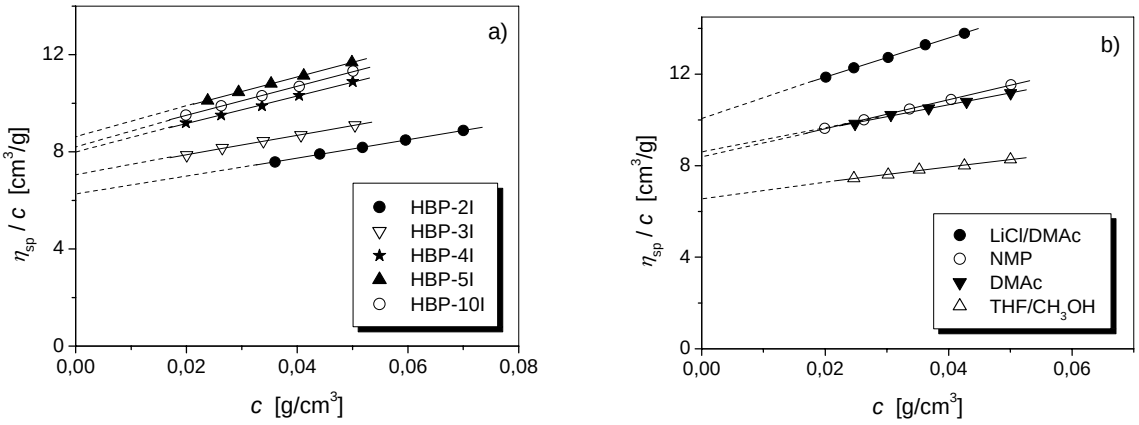

Figure 4.45. Dependence of η_{sp}/c versus c for a) different HB polyesters in NMP as a solvent and b) of the sample HBP-8I in different solvents

Since a linear relationship is obtained between η_{sp}/c and c in all used solvents, it can be concluded that no aggregation occurs in the investigated concentration range and/or that the gradient of the speed in the viscosimetry measurements is high enough to lead to the rupture of the bonds present in the formed aggregates which is not the case in SLS and DLS measurements. The same conclusion can be made from the Figure 4.46 where determined values of the limiting viscosity number in two different solvents are plotted together. Because the results are arranged around one linear plot, the presence of the aggregates can be excluded.

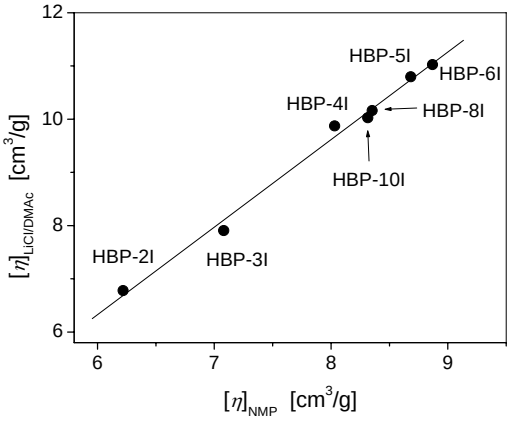

Figure 4.46. Correlation of limiting viscosity number determined in 0.7 mass% solution of LiCl in DMAc and in NMP as solvents

The difference in thermodynamic interactions between HB polyesters and different solvents can be examined from the determined values of [η], which are given in Table 4.24. The determined values of the limiting viscosity number in several different solvents can be ordered as follows:

$$[\eta]_{\text{LiCl/DMAc}} > [\eta]_{\text{NMP}} > [\eta]_{\text{DMAc}} > [\eta]_{\text{THF/CH}_3\text{OH}}$$

Only for the samples HBP-2I, BH-2 and HBP-8I, values of the [η] determined in DMAc are slightly higher than values which are obtained when NMP is used as a solvent. From the previous observation and results listed in Table 4.24 it can be seen that values of the [η] for the investigated HB polyesters are the highest when 0.7 mass % solution of LiCl in DMAc is used as a solvent. This further means that in this solvent the interactions between HB polyesters and the molecules of the solvent are most intense. In other words, from the used ones, LiCl/DMAc is thermodynamically the best solvent for this type of HB polyesters. This observation is also proved elsewhere[71,147]. Beside that, it has been shown that after a relatively long period of storage, the reduction of the limiting viscosity number of the HB polyesters solutions made in this solvent is negligible[147]. On the other side, values of the [η] determined in the mixture THF/CH_3OH are the lowest, which further indicates that this solvent is poor solvent for these HB polyesters. Samples HBP-2I, HBP-3I, BH-2 and BH-3 were only slightly soluble in THF/CH_3OH and therefore [η] is not measured for these samples since the low solubility can mismatch the real values of the limiting viscosity number.

Table 4.24. Values of the limiting viscosity number, [η], and *Huggins* constant (k_H) for the HB samples determined in different solvents

Sample	LiCl/DMAc		NMP		DMAc		THF/CH_3OH	
	[η] [cm^3/g]	k_H	[η] [cm^3/g]	k_H	[η] [cm^3/g]	k_H	[η] [cm^3/g]	k_H
HBP-2I	6.8	0.6	6.2	1.0	6.4	0.7	/	/
HBP-3I	7.9	0.8	7.1	0.8	6.5	1.1	/	/
HBP-4I	9.9	0.5	8.0	0.9	7.0	1.3	6.4	0.8
HBP-4II	/	/	8.0	1.0	/	/	/	/
HBP-5I	10.8	0.6	8.7	0.8	7.8	1.0	6.4	0.8
HBP-6I	11.0	0.5	8.9	0.6	8.3	0.8	6.5	0.7
HBP-6II	/	/	9.2	0.7	/	/	/	/
HBP-8I	10.2	0.8	8.3	0.9	8.6	0.7	6.6	0.7
HBP-8II	/	/	9.3	0.7	/	/	/	/
HBP-10I	10.0	0.7	8.3	0.9	8.2	0.9	6.4	0.7
BH-2	7.0	0.5	6.0	0.9	6.1	0.7	/	/
BH-3	9.2	0.5	7.4	0.7	/	/	5.5	1.0
BH-4	10.7	0.6	8.6	0.9	/	/	6.7	0.6

The experimental results of the *Huggins* constants (k_H) determined from the slope of the linear dependence of η_{sp}/c versus c in different solvents are also listed in Table 4.24. Since the obtained values of the k_H are different between each other, it was not possible to use them

for the calculation of [η] from *Huggins* equation (2.22) by determination of the specific viscosity (η_{sp}) for only one concentration. This phenomenon indicates that these HB polyesters do not act as a homologue row. For the linear macromolecules in a good solvent k_H has values between 0.3 and 0.4, while in theta solvents the value of the *Huggins* constant is around 0.5.

From the results presented in Table 4.24 and Figure 4.47 for the samples of series I an increase of [η] up to the certain theoretical number of generation can be observed, after which the values of the [η] decline. When viscosity measurements are performed with polymer solutions prepared in NMP and LiCl/DMAc the values of the [η] increase up to the sixth theoretical generation, while in DMAc maximum is obtained for the sample HBP-8I. Similar observation can be made for the HB polyesters of the second series, while for the commercial samples a constant increase of the [η] is detected. By comparing values of the $[\eta]_{THF/CH_3OH}$ for the samples of different theoretical number of generation it can be observed that the limiting viscosity number in this solvent practically does not change, i.e. it is independent of the molar mass. The reason for such behaviour is probably the stronger intramolecular interactions between the polymer segments in comparison to the interactions with the solvent molecules. Beside that, it can be seen from the results listed in Table 4.24 that the mixture THF/CH_3OH is a poor solvent for this type of HB polyesters, which stands in contrast with the observations made by other authors[71].

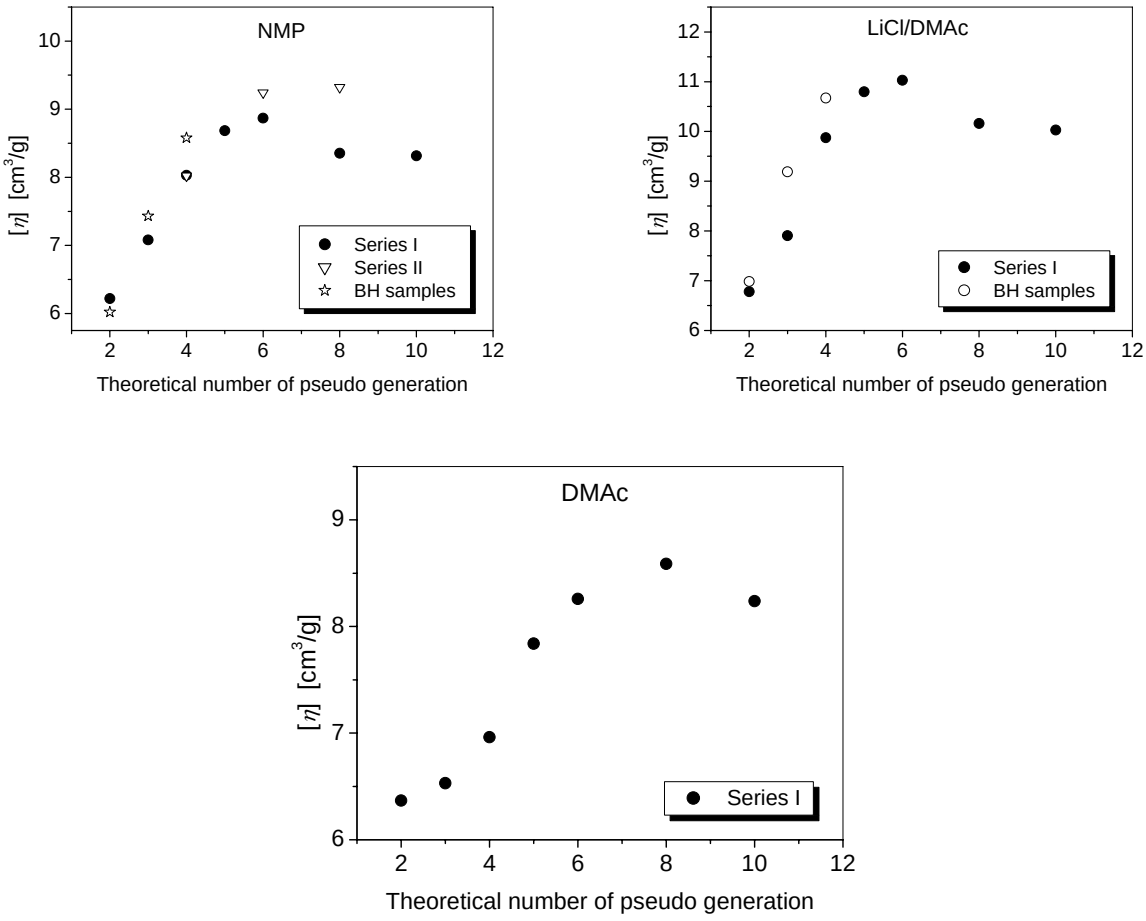

Figure 4.47. Dependence of [η] for HB polyesters determined in different solvents versus theoretical number of pseudo generation

From the logarithmic form of the *Kuhn-Mark-Houwink-Sakurada* (KMHS) equation (2.23), determined values of the [η] and values of the M_w, values of the exponent a and constant K_η for the investigated HB polyesters in different solvents are determined. Weight average molar mass is calculated from the $(M_w/M_n)_{GPC}$ (Table 4.16) and $(M_n)_{VPO}$ (Table 4.13) or in the case of the sample HBP-2I from the value $(M_n)_{NMR}$ (Table 4.11) It has been already stated elsewhere that for branched polymers the [η] – M relationship obtained from the KMHS equation is valid only for very narrow molar mass ranges[77], which is also the case for the HB polyesters used in this dissertation. In Figure 4.48 the dependence of log [η] versus log M_w is presented for the HB polyesters of series I from second till sixth theoretical pseudo generation in two different solvents. When values of the [η] determined in DMAc as solvent are used, a similar dependence is obtained. Dependences given in Figure 4.48 clearly show that there is relatively good linear relationship between log [η] and log M_w up to the fifth theoretical generation. After that, deviations from the linear correlation starts, which is in a good agreement with results reported for dendrimers[58,65,79]. However, for the samples HBP-8I and HBP-10I a large extent of side reactions (intramolecular cyclization, self-condensation of bis-MPA) lead to a significant decrease of the M_w and consequently [η] values. Therefore, results for these two samples are not included.

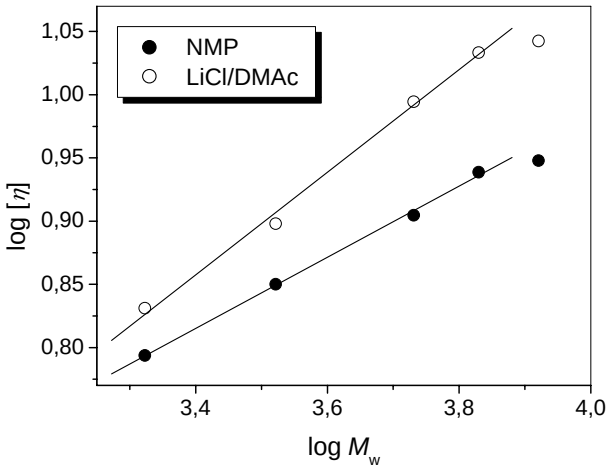

Figure 4.48. Dependence of log [η] versus log M_w for the HB polyesters of series I, using the values of [η] determined in NMP and LiCl/DMAc as solvents

The determined values of the exponent a (Table 4.25) in all presented solvents indicate that these HB polyesters are compact (for linear polymers the exponent a is usually in the range of 0.5-0.8[77]). Furthermore, it can be observed that the value of the exponent a increases with solvent quality. Values of the exponent a and constant K_η are not calculated for the second series of HB polyesters, due to the absence of the $(M_n)_{VPO}$ value for the sample HBP-6II, which is necessary for the calculation of the M_w.

Table 4.25. Values of the exponent *a* and log K_η determined from the KMHS equation in different solvents for the investigated HB polyesters

Sample group	LiCl/DMAc		NMP		DMAc	
	a	log K_η	*a*	log K_η	*a*	log K_η
Series I	0.40	-0.52	0.28	-0.14	0.25	0.16
Boltorn® samples	0.29	-0.10	0.23	0.00	/	/

Since the limiting viscosity number is a measure of the size of macromolecules in solutions and represents the ratio between hydrodynamic volume and the mass, it is possible to calculate the hydrodynamic radius of the HB polyesters in different solvents using the equation (2.45), the determined values of the [η] and the calculated values of M_w. Values of the hydrodynamic radius (R_η) in different solvents are given in Table 4.26. From the obtained results it can be observed that investigated HB polyesters have the ability to change hydrodynamic volume in variety of solvents, which is especially interesting for the HB polymers. This behaviour has already been pointed out elsewhere for the commercial Boltorn® polyesters and it is suggested that due to this phenomenon they can be used for hosting a molecule with a certain radius[111]. Since the similar behaviour is obtained for the HB polyesters synthesized in this work it can be concluded that they can also be used for the same purpose. The largest dimensions of these HB polyesters are obtained in LiCl/DMAc, which shows again that in this solvent interaction between macromolecules and the molecules of solvent are the most pronounced. By comparing values of the R_η with results obtained from DLS measurements (Table 4.20), a relatively good correlation can be observed between $(R_\eta)_{NMP}$ and values of the D_h determined for the purified samples. This can be explained by the fact that the presence of the small molecules does not have significant influence on the viscosimetry measurements.

Table 4.26. Values of the hydrodynamic radius (R_η) for the investigated HB polyesters

Sample	$(R_\eta)_{LiCl/DMAc}$ [nm]	$(R_\eta)_{NMP}$ [nm]	$(R_\eta)_{DMAc}$ [nm]	$(R_\eta)_{THF/CH_3OH}$ [nm]
HBP-2I	1.3	1.3	1.3	/
HBP-3I	1.6	1.5	1.5	/
HBP-4I	2.0	1.9	1.8	1.8
HBP-4II	/	2.4	/	/
HBP-5I	2.3	2.2	2.0	1.9
HBP-6I	2.4	2.3	2.2	2.0
HBP-8I	2.3	2.2	2.2	2.0
HBP-8II	/	2.2	/	/
HBP-10I	2.2	2.0	2.0	1.9
BH-2	1.3	1.2	1.2	/
BH-3	2.1	1.9	/	1.7
BH-4	2.3	2.2	/	2.0

The hydrodynamic radius of the samples synthesized in this work increases with the increase of the theoretical number of pseudo generation as can be seen from the results presented in Figure 4.49. In all solvents the largest dimensions are obtained for the sample HBP-6I, whereupon the value of the R_η decreases for the samples HBP-8I and HBP-10I. For the commercial HB polyesters similar dependence between R_η and number of generation is obtained.

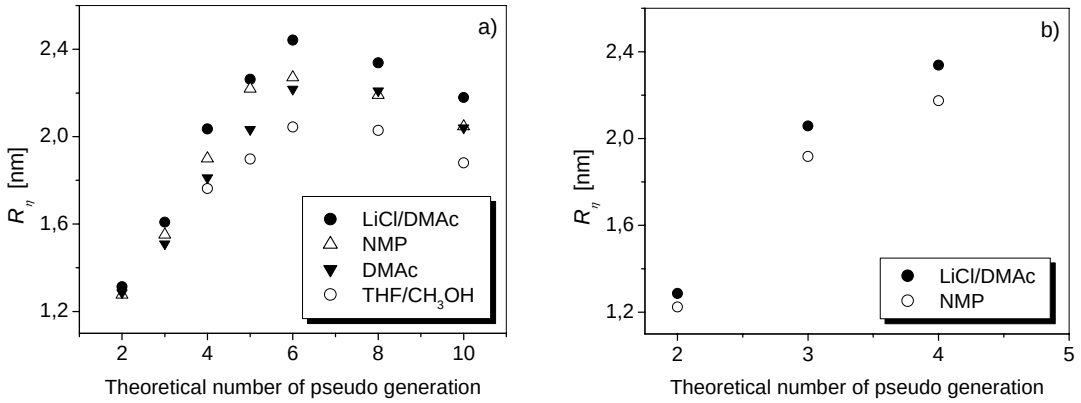

Figure 4.49. Dependence of the R_η versus theoretical number of pseudo generation for the a) samples of the series I and b) for the commercial samples in different solvents

The dependence of R_η versus the weight average molar mass (Figure 4.50a) is for the samples of the series I up to the sixth theoretical generation similar to that presented in Figure 4.49. This indicates that although side reactions occurred in a large degree during the synthesis, the increase of the hydrodynamic radius was not prevented up to the sixth theoretical number of generation. On the other side, the presence of the side reactions reduced the expected increase of the R_η values according to the values of the theoretical molar mass. The dependences given in Figure 4.50b for the commercial samples are in this case more linear than the one presented in Figure 4.49b.

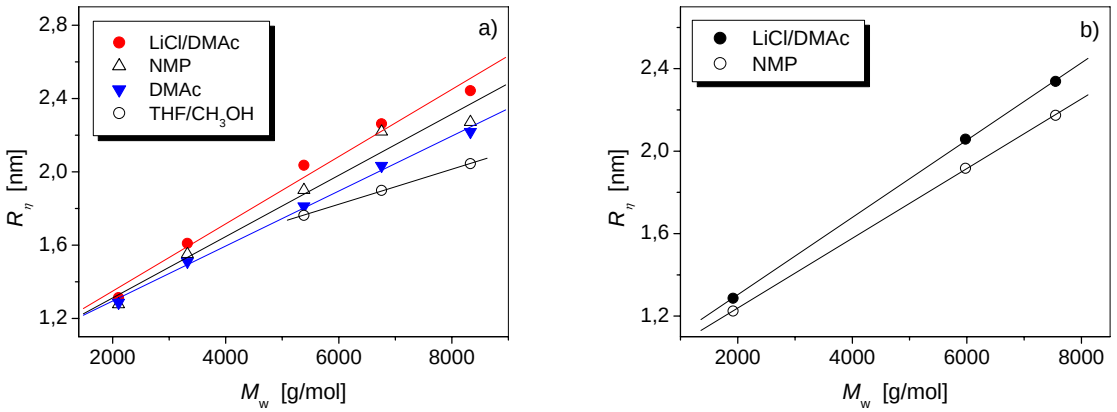

Figure 4.50. Dependence of the R_η versus M_w for the a) samples of the series I and b) for the commercial samples in different solvents

Due to the linear dependence between log R_η and log M_w the values of the exponent v and the constant K_R in different solvents were graphically determined using the logarithmic form of the equation (2.48). For all investigated HB samples values of the exponent v are lower (Table 4.27) than what is expected for the linear polymers and at the same time slightly higher than values typical for the dendrimers[11,103]. This indicates that these HB polyesters have a less densely packed structure than the dendrimers but are more compact than linear polymers. The imperfection of the HB polyesters is due to the presence of the linear units inside of their structure. The value of the exponent v changes in different solvents in the same manner as exponent a from the KMHS equation, i.e. values of the v increases with increasing solvent quality. In a poor solvent (THF/CH_3OH) HB polyesters have more compact configuration, while relatively high values of the exponent v determined in LiCl/DMAc are evidence for significant solvent interpenetration.

Table 4.27. Values of the exponent v and log K_R determined from the equation (2.48) in different solvents for the investigated HB polyesters

Sample group	LiCl/DMAc		NMP		DMAc		THF/CH_3OH	
	v	log K_R	v	log K_R	v	log K_R	v	log K_R
Series I	0.46	-1.41	0.44	-1.35	0.40	-1.21	0.34	-1.02
Boltorn® samples	0.43	-1.30	0.41	-1.27	/	/	/	/

Viscosimetry of the diluted solutions is also performed on the fractions of the HB polyesters. Due to the linear relationship obtained between η_{sp}/c and c in NMP as a solvent (Figure 4.51), it can be concluded that no aggregation occured in the investigated concentration range. Results obtained from the viscosimetry measurements of the HB polyesters fractions in NMP are listed in Table 4.28.

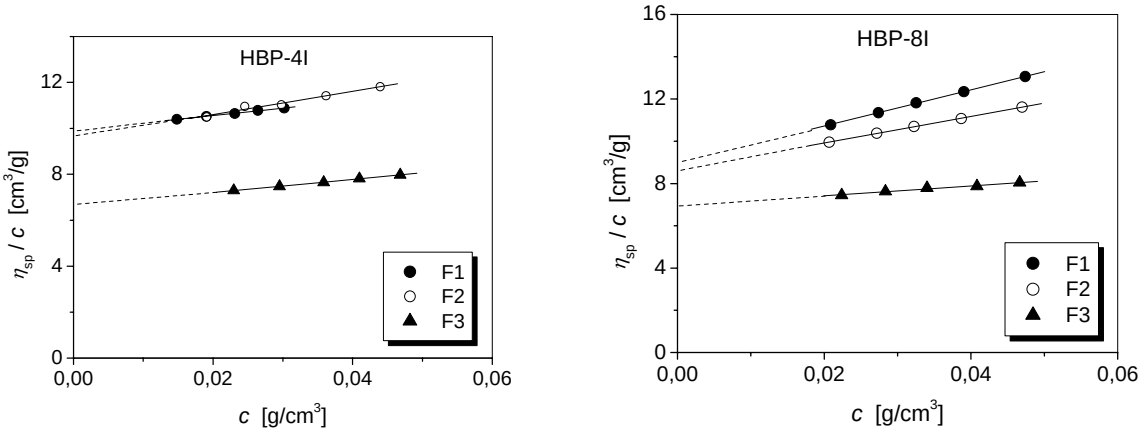

Figure 4.51. Dependence of η_{sp}/c versus c for the fractions of the samples HBP-4I and HBP-8I determined in NMP as a solvent

Table 4.28. Values of the limiting viscosity number, [η], and *Huggins* constant (k_H) for the fractions of the HB polyesters determined in NMP

Fraction	[η] [cm^3/g]	k_H	Fraction	[η] [cm^3/g]	k_H
HBP-3I F1	7.6	0.5	HBP-10I F1	9.1	0.7
HBP-3I F2	8.0	0.7	HBP-10I F2	8.8	1.1
HBP-3I F3	6.3	0.8	HBP-10I F3	6.9	0.5
HBP-4I F1	9.9	0.3	BH-3 F1	8.0	0.8
HBP-4I F2	9.6	0.5	BH-3 F2	8.1	0.8
HBP-4I F3	6.6	0.6	BH-3 F3	6.4	0.7
HBP-6I F1	10.4	0.7	BH-4 F1	10.6	0.7
HBP-6I F2	8.7	0.7	BH-4 F2	9.9	0.6
HBP-6I F3	6.5	0.5	BH-4 F3	7.1	0.6
HBP-8I F1	9.0	1.1	/		
HBP-8I F2	8.7	0.8			
HBP-8I F3	6.9	0.5			

Using the *Philippoff* rule (equation 4.8) the efficiency of the fractionation can be proved. Therefore, values of the limiting viscosity number for the parent samples are calculated from the obtained values of the [η] for the fractions and they are given in Table 4.29. For the easier comparison experimentally determined values of the [η] are also listed. It can be observed that for the most samples, differences between $[\eta]_{exp}$ and $[\eta]_{cal}$ are lower than 5.0 %, which indicates that fractionation was performed with relatively good efficiency. Only for the sample HBP-6I the obtained difference is 6.5 %, which can also be due to the experimental error made during the viscosimetry measurements as a consequence of the relatively low amount of the fractions.

Table 4.29. Experimentally determined ($[\eta]_{exp}$) and calculated values ($[\eta]_{cal}$) of the limiting viscosity number for the parent samples

/	HBP-3I	HBP-4I	HBP-6I	HBP-8I	HBP-10I	BH-3	BH-4
$[\eta]_{cal}$ [cm^3/g]	6.8	8.1	8.3	8.1	8.1	7.1	8.7
$[\eta]_{exp}$ [cm^3/g]	7.1	8.0	8.9	8.3	8.3	7.4	8.6

4.5. Rheological properties of the hyperbranched polyesters

4.5.1. Concentrated solutions

To investigate the rheological properties of the concentrated solutions of the HB polyesters, flow experiments are performed in the manner described in chapter 3.3.14. NMP is chosen as a solvent since it represents a good solvent for these polymers as it was already proven by other characterization methods (viscosimetry of the diluted solutions and DLS). Rheological measurements of the concentrated solutions are done for relatively wide spectra of concentrations and temperatures, at which two different types of the rheological behaviour are observed: *Newtonian* flow and shear thinning behaviour.

Concentrated solutions of the investigated HB polyesters exhibit *Newtonian* behaviour in NMP when the concentration of the solutions is $c \leq 45$ mass % at all measured temperatures. The same behaviour is also observed for the 50 and 55 mass % solutions at temperatures higher than the ones listed in Table 4.30. As an example of the obtained results, in Figure 4.52 are presented plots of shear stress versus shear rate for the samples HBP-6I at different concentrations and at different temperatures. From the plots presented in Figure 4.52 it can be seen that the shear stress increases proportionally to the shear rate in the previously mentioned concentration and temperature range. As a consequence of that, viscosity is independent of the shear rate and approaches a constant value (Figure 4.53), i.e. the zero shear viscosity (η_0). Similar observation is also made for the HB polyesters of the second series. Determined values of the zero shear viscosity of all examined samples solutions at different concentrations and temperatures can be found in Appendix 7.5.1.

Table 4.30. Temperature region for the 50 and 55 mass % solution of different HB polyesters, where non-*Newtonian* behaviour occurs

Sample	Temperature region [^{0}C]		Sample	Temperature region [^{0}C]	
	50 mass % solution	55 mass % solution		50 mass % solution	55 mass % solution
HBP-2I	10 - 40	10 - 45	HBP-8I	10 - 25	10 - 30
HBP-3I	10 - 35	10 - 50	HBP-8II	10 - 30	10 - 40
HBP-4I	10 - 25	10 - 30	HBP-10I	10 - 25	10 - 35
HBP-4II	10 - 30	10 - 40	BH-2	10 - 40	10 - 50
HBP-5I	10 - 25	10 - 35	BH-3	10 - 30	10 - 45
HBP-6I	10 - 25	10 - 30	BH-4	10 - 25	10 - 30
HBP-6II	10 - 30	10 - 40	/		

Newtonian behaviour was also observed for some dendrimers and other HB polymers in solution and in melt[116,119], as well as for the commercial Boltorn® HB polyesters by other authors[105]. The reason for such linearity between shear stress and shear rate of the investigated HB polyesters in the solution is the absence of the physical entanglement in these polymers. This behaviour is opposite from the one typical for linear polymers or colloidal particles, which usually show shear thinning above some critical shear rate. Furthermore, *Newtonian*

behaviour of these HB polyesters indicates that they have a globular shape. It was already proved by DLS measurements that aggregates are formed in NMP already at relatively low concentrations of the solution (Table 4.20). However, since moderate concentrated solutions (c < 50 mass %) of HB polyesters behave as *Newtonian* fluids it can be concluded that in this case the extent of aggregation is much lower than in the case of the highly concentrated solutions (50 and 55 mass % solutions). The *Newtonian* behaviour of the 50 and 55 mass % solutions at higher temperatures (Figure 4.52) indicates that increasing of the temperature has also significant contribution to the cleavage of the aggregates bonds.

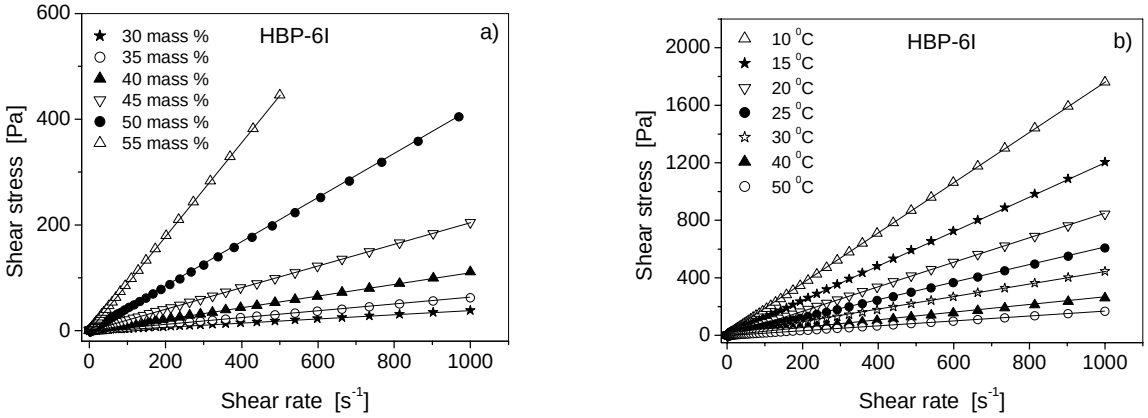

Figure 4.52. Dependence of the shear stress versus shear rate of the sample HBP-6I for a) different solution concentrations at 45 ^{0}C and for b) 45 mass % solutions at different temperatures

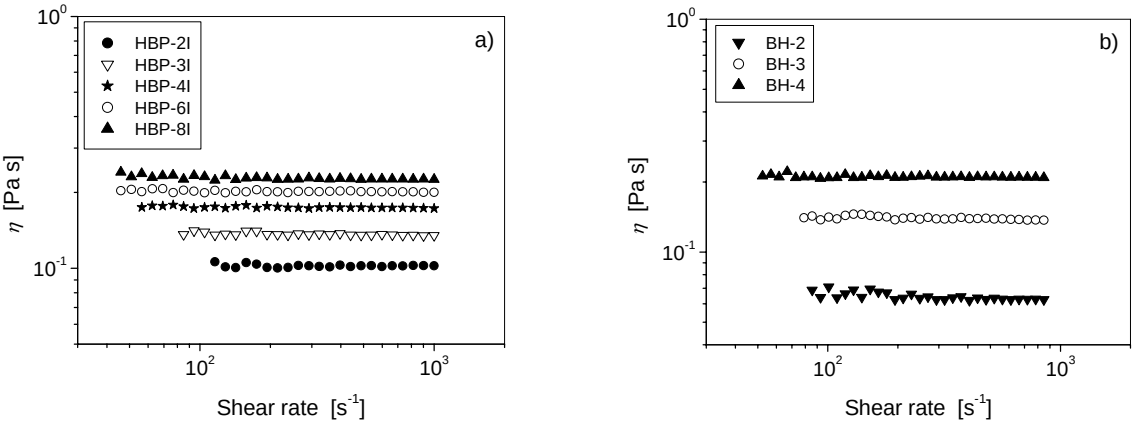

Figure 4.53. Dependence of the viscosity versus shear rate for the 40 mass % solutions at 30 ^{0}C of the samples a) of series I and of the b) commercial samples

The dependence of the flow behaviour of the HB polyesters on the concentration of the used solutions can be seen from the results presented in Figure 4.54. Such non-linear dependence of the zero shear viscosity on the concentration is typical for the concentrated solutions, while in diluted solutions the properties of the polymers usually vary linearly with concentration[114]. Furthermore, the differences between η_0 become especially noticeable at lower temperature.

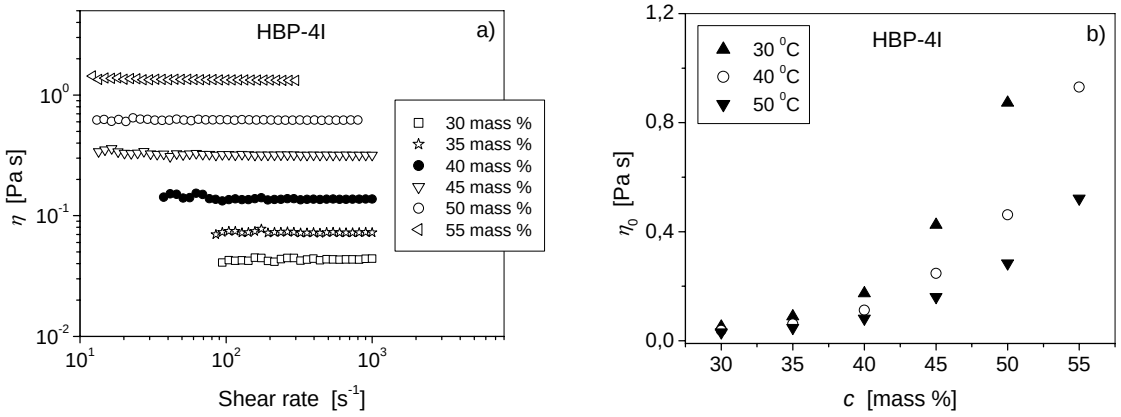

Figure 4.54. a) Dependence of the viscosity versus shear rate of the sample HBP-4I for different solution concentrations at 35 ^{0}C and b) dependences of the zero shear viscosity versus concentration of the solutions at three different temperatures

The zero shear viscosity dependence on the theoretical number of generation (Figure 4.55) has a similar trend as the dependence of the limiting viscosity number versus number of generation (Figure 4.47). The differences between η_0 values of different generations are relatively small, which is also observed for the limiting viscosity number. The general trend presented in Figure 4.55a indicates that the zero shear viscosity of the self-synthesized HB polyesters increase up to the sixth theoretical generation and than slightly decrease for the higher generation numbers in the 35 mass % solution. A similar behaviour is observed for the other solutions, with only one difference that the maximum value of the zero shear viscosity is in some cases shifted to the eighth pseudo generation (Appendix 7.5.1).

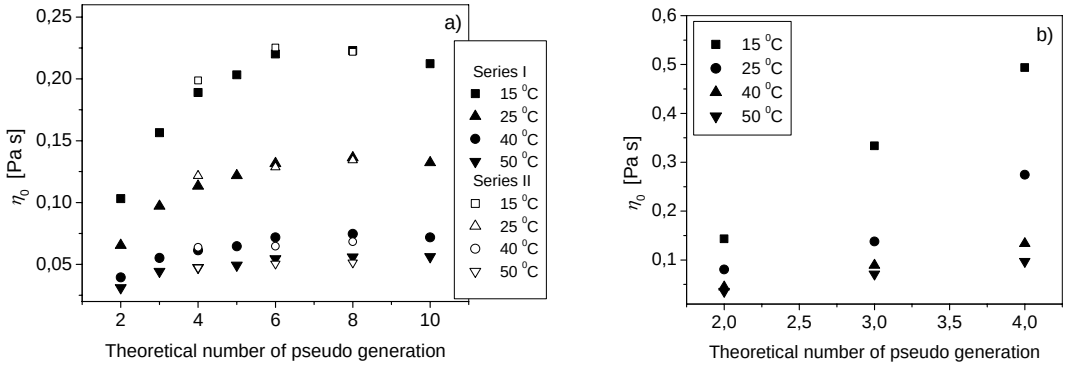

Figure 4.55. Zero shear viscosity versus theoretical number of pseudo generation for a) 35 mass % solutions of the samples of the series I and II and b) for the 40 mass % solutions of commercial samples at indicated temperatures

The dependence of the zero shear viscosity versus weight average molar mass (calculated from the $(M_w/M_n)_{GPC}$ (Table 4.16) and $(M_n)_{VPO}$ (Table 4.13) or $(M_n)_{NMR}$ (Table 4.11)) is presented in Figure 4.56. From this specific relationship it can be concluded again that in these HB polyesters there is an absence of the entanglement interactions and that they have relatively compact molecular shapes and small sizes. For the 30 mass % solutions the

slope of the dependence log η_o versus log M_w is changing from about 0.45 up to the fourth theoretical pseudo generations to about 0.22 between fifth and sixth pseudo generation. With increasing concentration of the solution values of the slope slightly increase, while the temperature has the opposite influence.

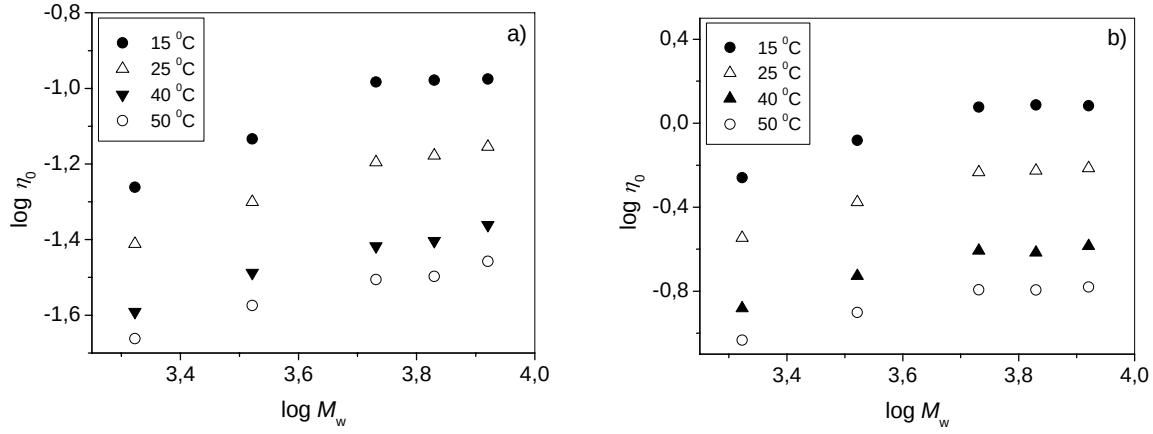

Figure 4.56. Dependence of log η_o versus log M_w for the a) 30 mass % and b) 45 mass % solutions of the HB polyesters (series I) from second till sixth theoretical generation at indicated temperatures

For the determination of the η_o–M–c relationship (equation 2.54), values of the zero shear viscosity for the $c \leq 45$ mass % determined at 25 ^{0}C are used, as well as the values of the weight average molar mass calculated from the $(M_w/M_n)_{GPC}$ (Table 4.16) and $(M_n)_{VPO}$ (Table 4.13) or $(M_n)_{NMR}$ (Table 4.11). Furthermore, values of the constant K_η and exponent a of the self-synthesized (from second till fifth pseudo generation) and commercial HB polyesters determined from the KMHS equation can be found in Table 4.25. Finally, values of the limiting viscosity number and *Huggins* constant determined in NMP are listed in Table 4.24, while viscosity of the solvent is $\eta_s = \eta_{NMP} = 1.65$ mPa s. In Figure 4.57 dependences of the log η_{sp} versus log ($c[\eta]$) for the samples of series I from second till fifth pseudo generation and commercial HB polyesters are presented. Because the investigated concentration region for the commercial samples (10-40 mass %) was somewhat wider that for the self-synthesized ones (30-45 mass %), a relatively good master curve is obtained (Figure 4.57a). From the linear regression at high values of the $c[\eta]$, values of the B_s and s are calculated and listed in Table 4.31. On the other side, due to the relatively narrow concentration range for the HB polyesters of the series I, only the last region of the dependence log η_{sp} versus log ($c[\eta]$) is obtained, from which values of the B_s and s are determined (Table 4.31).

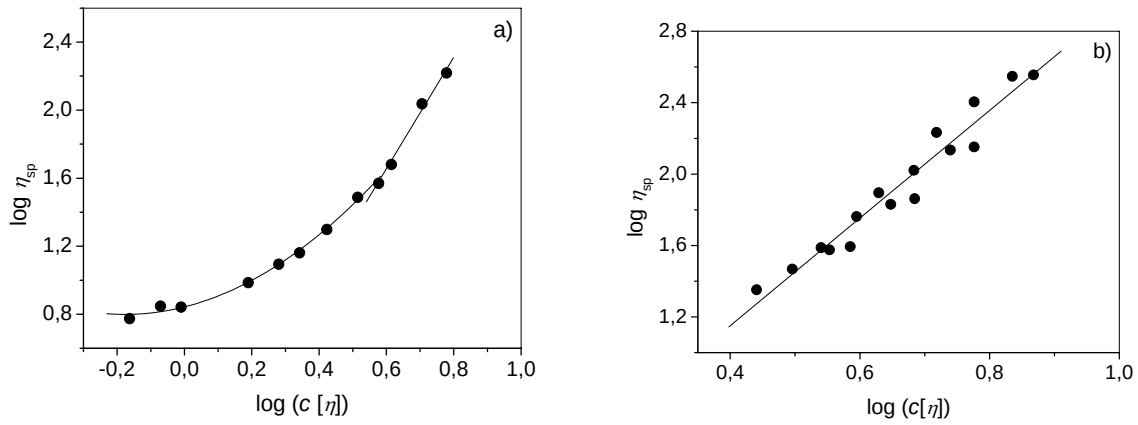

Figure 4.57. Dependence of the log η_{sp} versus log (c[η]) for the a) commercial samples and b) HB polyesters of the series I

Table 4.31. Values of the B_s and s determined from the plots presented in Figure 4.57

Sample group	B_s	s
Series I	0.88	3.01
Boltorn® samples	0.45	3.33

Using the equation (2.54) and all necessary parameters, the η_o–M–c relationship for the HB polyesters of the series I can be written as follows:

$$\eta_0 = 1.19 \cdot c \cdot M_w^{0.28} + 0.86 \cdot k_H \cdot c^2 \cdot M_w^{0.56} + 0.54 \cdot c^{3.01} \cdot M_w^{0.84} + 1.65 \quad (4.36)$$

i.e. $\eta_0 \propto c^{3.01} M_w^{0.84}$ (4.37)

While for the commercial samples it can be written:

$$\eta_0 = 1.66 \cdot c \cdot M_w^{0.23} + 1.67 \cdot k_H \cdot c^2 \cdot M_w^{0.46} + 0.75 \cdot c^{3.33} \cdot M_w^{0.77} + 1.65 \quad (4.38)$$

i.e. $\eta_0 \propto c^{3.33} M_w^{0.77}$ (4.39)

Values of the zero shear viscosities calculated from the equations (4.36) and (4.38) are listed in Table 4.32 together with experimentally determined values and percentage deviation of the calculated from the measured viscosities. Results presented in Table 4.32 show relatively high deviations of the calculated from the measured viscosities. The reason for such behaviour is probably low region of the viscosities and c[η] values. However, from the η_o–M–c relationships presented with equation (4.37) and (4.39) it can be observed that the molar mass dependence of zero shear viscosity (0.84 and 0.77) is for these HB polyesters quite smaller than value of 3.4 usually obtained for the melts and concentrated solutions of linear polymers[114], indicating considering difference in the structure between HB and linear polymers. Beside that, it can also be observed that for the investigated HB polyesters exponents which describe concentration dependence of zero shear viscosity are very similar. This indicates that for both types of samples NMP as a solvent have the same quality.

Table 4.32. Calculated, $(\eta_0)_{cal}$ and experimentally determined, $(\eta_0)_{exp}$, values of the zero shear viscosities and percentage deviation of the calculated from the measured viscosities (Δ)

c [mass %]	HBP-2I			HBP-3I			HBP-4I			HBP-5I		
	$(\eta_0)_{cal}$ [mPa s]	$(\eta_0)_{exp}$ [mPa s]	Δ [%]	$(\eta_0)_{cal}$ [mPa s]	$(\eta_0)_{exp}$ [mPa s]	Δ [%]	$(\eta_0)_{cal}$ [mPa s]	$(\eta_0)_{exp}$ [mPa s]	Δ [%]	$(\eta_0)_{cal}$ [mPa s]	$(\eta_0)_{exp}$ [mPa s]	Δ [%]
30	48.0	38.8	+24	62.9	50.1	+25	92.5	63.7	+45	106.5	66.4	+60
35	85.9	65.4	+31	113.7	97.0	+17	165.8	113.3	+46	198.1	121.8	+63
40	147.4	131.2	+12	199.2	174.9	+14	296.6	226.5	+31	356.7	235.9	+51
45	257.7	284.0	-9	362.4	420.5	-14	552.2	583.9	-5	649.6	594.8	+9

c [mass %]	BH-2			BH-3			BH-4		
	$(\eta_0)_{cal}$ [mPa s]	$(\eta_0)_{exp}$ [mPa s]	Δ [%]	$(\eta_0)_{cal}$ [mPa s]	$(\eta_0)_{exp}$ [mPa s]	Δ [%]	$(\eta_0)_{cal}$ [mPa s]	$(\eta_0)_{exp}$ [mPa s]	Δ [%]
10	3.6	11.4	-69	4.4	13.3	-67	4.8	13.1	-63
20	10.1	17.6	-43	15.6	22.1	-29	18.7	25.6	-27
30	31.5	34.4	-8	58.4	52.3	+12	71.1	62.8	+13
40	101.2	80.6	+25	206.9	181.3	+14	270.7	274.4	-1

Since for all samples the zero shear viscosity decreases with temperature it is possible to use *Arrhenius* equation (2.61) to calculate flow activation energies (E_a^s) of the investigated HB polyesters solutions. As an example in Figure 4.58 the dependences of the ln η_o versus $1/T$ for the second and eighth generation (series I) are presented, while determined values of the E_a^s are listed in Table 4.33. Dependences obtained by plotting ln η_o versus $1/T$ indicate that E_a^s has a nearly linear dependence on temperature. Therefore, determined values of E_a^s have to be considered as average. The obtained values of the flow activation energy of the commercial samples are in good agreement with results obtained by other authors[105].

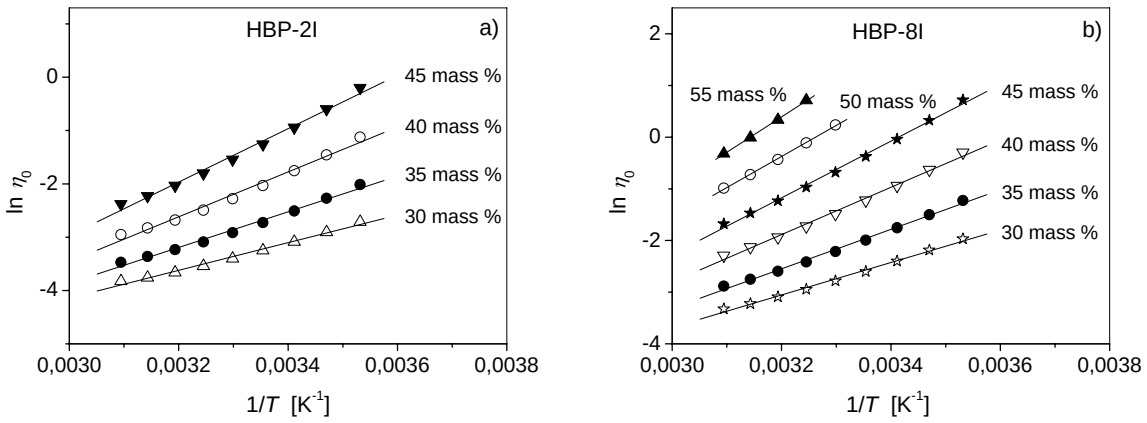

Figure 4.58. Dependence of ln η_o versus $1/T$ for the samples HBP-2I and HBP-8I

Table 4.33. Values of the flow activation energies (E_a^s) for different concentration of the solutions of the investigated HB polyesters

Sample	E_a^s [kJ/mol]					
	30 mass %	35 mass %	40 mass %	45 mass %	50 mass %	55 mass %
HBP-2I	21.6	27.8	35.0	41.6	/	/
HBP-3I	23.4	29.5	35.4	43.4	45.5	/
HBP-4I	27.8	32.0	37.5	45.3	45.7	51.1
HBP-4II	27.5	32.9	39.1	46.2	47.8	/
HBP-5I	27.4	32.7	40.1	46.8	50.6	54.6
HBP-6I	25.5	32.1	37.1	45.2	47.7	56.4
HBP-6II	28.5	34.3	40.6	45.7	46.3	/
HBP-8I	26.1	31.7	38.0	45.6	50.0	56.9
HBP-8II	28.4	33.6	38.8	46.0	49.1	/
HBP-10I	26.4	31.0	37.5	45.7	47.6	55.7
Sample	10 mass %	20 mass %	30 mass %	40 mass %	50 mass %	55 mass %
BH-2	7.42	11.1	21.7	32.5	/	/
BH-3	14.65	14.74	24.3	36.6	43.8	/
BH-4	9.8	16.0	24.6	37.4	46.1	53.9

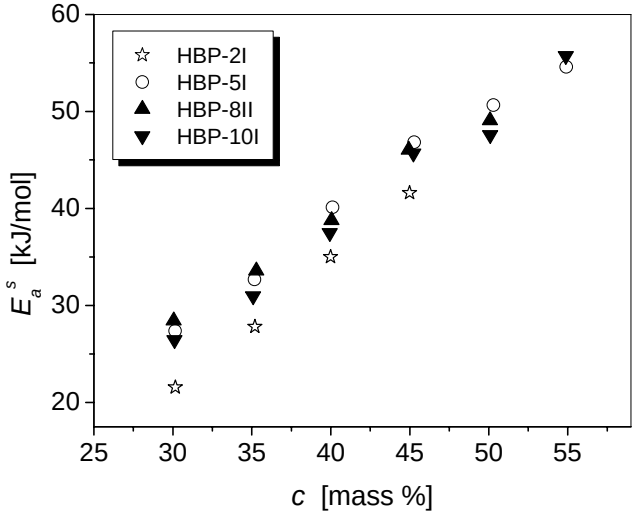

Figure 4.59. Dependence of the flow activation energy (E_a^s) versus concentration for the various HB polyesters

A linear dependence of the flow activation energy on the solution concentration (Figure 4.59 is observed for all samples. This behaviour is similar to the one found for dendrimers[116], indicating also the similarity in the architecture between investigated HB polyesters and dendrimers. From the dependences given in Figure 4.60 it can be observed that

flow activation energy increases up to the approximately fourth generation after what the value of the E_a^s does not change significantly. Such behaviour is connected to the reduction of the intermolecular hydrogen bonding at higher generations and it was also observed for dendrimers and Boltorn® HB polyesters in the solution[116,105] and in melt[118].

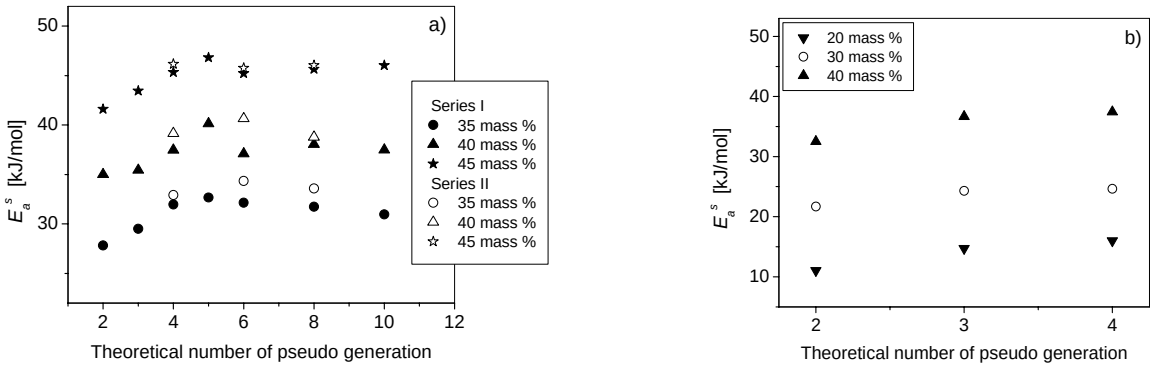

Figure 4.60. Dependence of the flow activation energy (E_a^s) versus theoretical number of pseudo generation at different concentrations for a) HB polyesters of I and II series and b) for the commercial samples

For all 50 and 55 mass % samples solutions the flow behaviour of the investigated HB polyesters is observed to be non-*Newtonian* at lower temperatures. As can be seen from the Figure 4.61, in this case the viscosity is a decreasing function of the shear rate, i.e. polymers exhibit shear thinning behaviour. This type of non-*Newtonian* flow behaviour is for the linear polymers usually explained as an intermolecular effect occurring because of the extension and orientation of the polymer chains in the solution. However, there is a low possibility that this is the reason of the shear thinning behaviour of polyesters used in this dissertation due to their highly branched structure. The most likely cause of this specific rheological behaviour of the highly concentrated solutions is relatively high extent of polar interactions between different molecules, because of the presence of the large number of end –OH groups. In such high concentrated solutions interactions between different macromolecules become very intense. As a consequence of that, macromolecules associate to form aggregated structures. The formation of the aggregates is further promoted by the very low thermal kinetic energy, due to the low temperatures applied during the measurements.

Since viscosity is decreasing continuously with increasing shear rate for the highly concentrated solutions of the HB polyesters (Figure 4.61), it can be concluded that the cleavage of the bonds present in the aggregates occurs in the same manner (i.e. continuously with increasing shear rate). This is especially noticeable for the lower generation samples, where a strong decrease of the viscosity at relatively low values of the shear rate is observed, after which viscosity continues to decrease with a somewhat lower intensity as the chain mobility increases and contributes to the breaking of the hydrogen bonds. That indicate that extent of the aggregation is bigger for the lower generation samples, as a consequence of the higher percentage of end –OH groups per molecule. This is also the reason why 50 and 55 mass % solutions of the lower generation samples show shear thinning up to the 50 ^{0}C (Table 4.30).

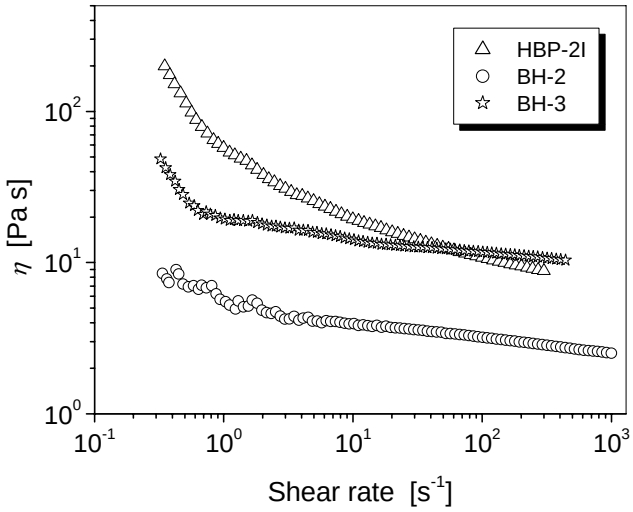

Figure 4.61. Dependence of the viscosity versus shear rate of the investigated HB polyesters, determined at 10 ^{0}C for the 55 mass % solutions

4.5.2. Melt rheology

The rheological properties of the self-synthesized and commercial HB polyesters in the molten state are investigated in the manner described in chapter 3.3.14. From the results presented in Figure 4.62 for the fourth and sixth generation samples it can be observed that the complex viscosity (η^*) and the storage modulus (G') of these polymers constantly decrease even above glass transition (Table 4.34). Since in the investigated temperature region no rubbery plateau is detected it can be concluded that these polymers are non-entangled. Similar behaviour is observed for HB polyesters of other generations (Appendix 7.5.2). Furthermore, it can be seen that η^* of the sample HBP-4II is higher than for the other two samples (Figure 4.62a) as a consequence of the lower degree of branching for the samples synthesized by one-step procedure. Beginning of the sharp η^* decrease of the sample HBP-4II starts at higher temperature than for the samples synthesized by the pseudo-one-step procedure, indicating somewhat higher values of the glass transition temperature (T_g). This can be confirmed from the results presented in Figure 4.62b where it can be seen that for the sample HBP-6II the maximum of the loss modulus curve (which is used for the determination of the T_g) appears at higher temperatures than for the sample HBP-6I. Figure 4.62 also shows that for the second series of the HB polyesters at temperatures higher than T_g, the difference between storage and loss modulus becomes higher ($G' < G''$) than for the samples of the series I. From this it can be concluded that the beginning of flow of the samples synthesized by one-step procedure starts at somewhat lower temperatures than for the adequate polyesters synthesized using the pseudo-one-step procedure.

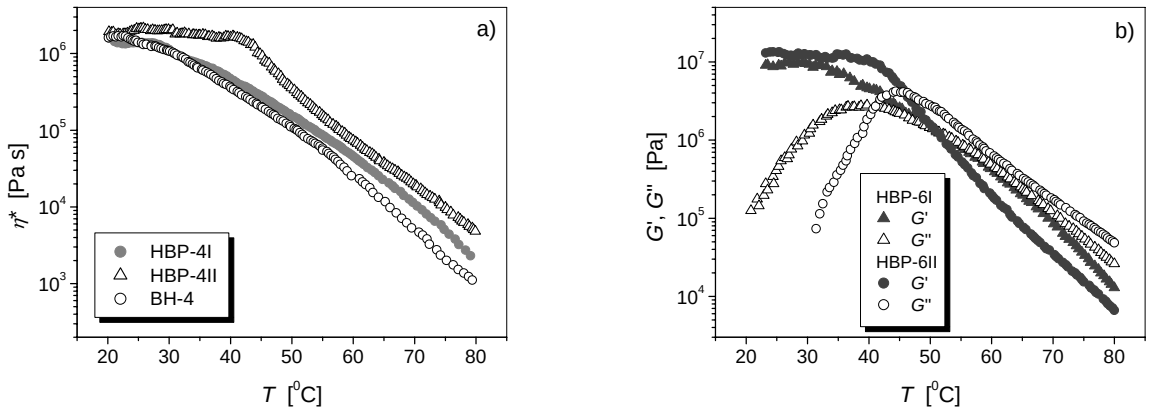

Figure 4.62. Temperature dependence at frequency of 1 Hz of the a) complex viscosity for HB polyesters of fourth generation and b) storage and loss modulus of the samples of sixth generation

The same conclusion can be made from the results presented in Figure 4.63, where the temperature dependence of the tan δ for the different HB polyesters is presented. Values of the tan δ for the sample HBP-4II start to increase at much lower temperature than tan δ of the samples HBP-4I and BH-4 (Figure 4.63a). A similar behaviour is observed for the other two samples of the second series. On the other side, the temperature dependence of the tan δ for the samples synthesized by pseudo-one-step procedure and commercial samples are similar to the HBP-4I (Figure 4.63b). The reason for this specific behaviour of the samples HBP-4II, HBP-6II and HBP-8II is probably slightly higher values of the polydispersity compared to the one determined for the samples of the series I (Table 4.16). The higher amount of the smaller molecules can have influence on the earlier softening of the polymer.

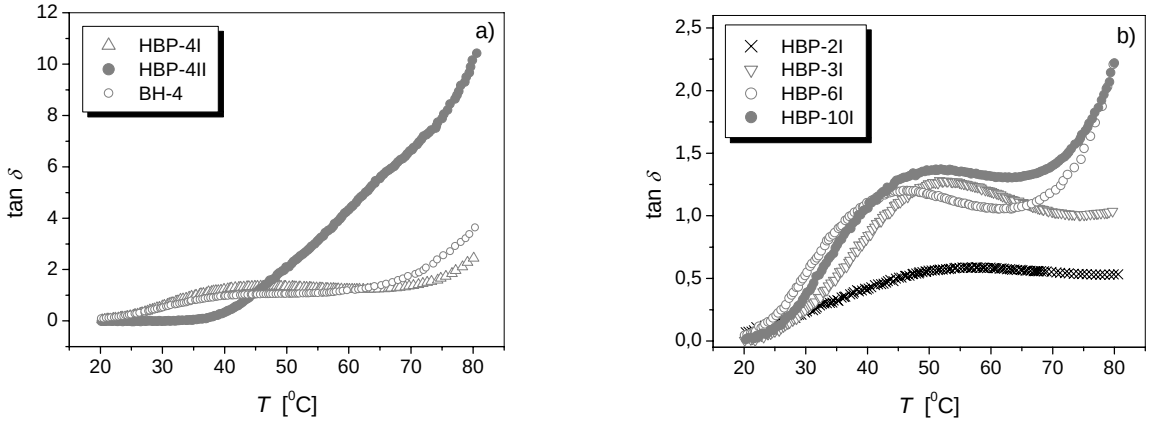

Figure 4.63. Temperature dependence of the tan δ for the selected HB polyesters

Values of the T_g for the investigated HB polymers are determined from the maximum of the loss modulus (G'') and tan δ temperature dependences. The glass transition temperature can also be determined from the inflection point in the temperature dependence of the storage modulus, but since T_g values obtained in this manner are relatively close to the values obtained from the maximum of the G'', they are not listed in Table 4.34. Determined values of

the glass transition temperatures for the investigated HB polyesters are in the temperature range between 20 and 45 ^{0}C, according to the position of the $(G'')_{max}$. On the other side, T_g values determined from the $(\tan \delta)_{max}$ are approximately 10 ^{0}C higher. For the samples HBP-2I value of the T_g is not determined from the $(\tan \delta)_{max}$ since, the tan δ peak have very low intensity and it is quite broad (Figure 4.63b).

Table 4.34. Values of the glass transition temperature (T_g) determined from the rheological measurements

Sample	T_g [^{0}C]		Sample	T_g [^{0}C]	
	$(G'')_{max}$	$(\tan \delta)_{max}$		$(G'')_{max}$	$(\tan \delta)_{max}$
HBP-2I	33	/	HBP-8I	40	51
HBP-3I	38	52	HBP-8II	44	/
HBP-4I	36	46	HBP-10I	35	52
HBP-4II	42	/	BH-2	21	37
HBP-5I	37	47	BH-3	31	45
HBP-6I	41	46	BH-4	31	38
HBP-6II	44	/	/		

In the investigated temperature and frequency region, samples HBP-2I, BH-2 and BH-3 show high dependence of η^* on frequency, i.e. non-*Newtonian* behaviour as a consequence of the relatively strong H-bonding of numerous peripheral –OH groups. As an example in Figure 4.64a the frequency dependence of the η^* for the sample HBP-2I at different temperatures is presented. Interestingly, a similar behaviour is observed also for the samples HBP-10I (Figure 4.64b). Results presented in the chapter 4.2.4. (Figure 4.30) show that the sample HBP-10I has the broader tail on the low molar mass side of the distribution than the other investigated HB polyesters. This indicate that in the structure of the HBP-10I a relatively high amount of the small molar mass components with more –OH groups per molecule are present, which further means higher possibility for the intermolecular H-bonding. Therefore, the complex viscosity of this sample decreases through the several decades in the investigated temperature and frequency region as a consequence of the H-bonds cleavage through the influence of the increasing deformation and temperature. Non-*Newtonian* behaviour is also observed for the samples HBP-3I, HBP-6II, HBP-8I and HBP-8II, but with much weaker frequency dependence. Beside that, for these four samples at temperatures higher than 65 ^{0}C the complex viscosity levels out at low frequencies to a plateau values. Other investigated HB polyesters show *Newtonian* behaviour at higher temperatures, indicating much lower degree of the polar interactions between the molecules (Figure 4.64c).

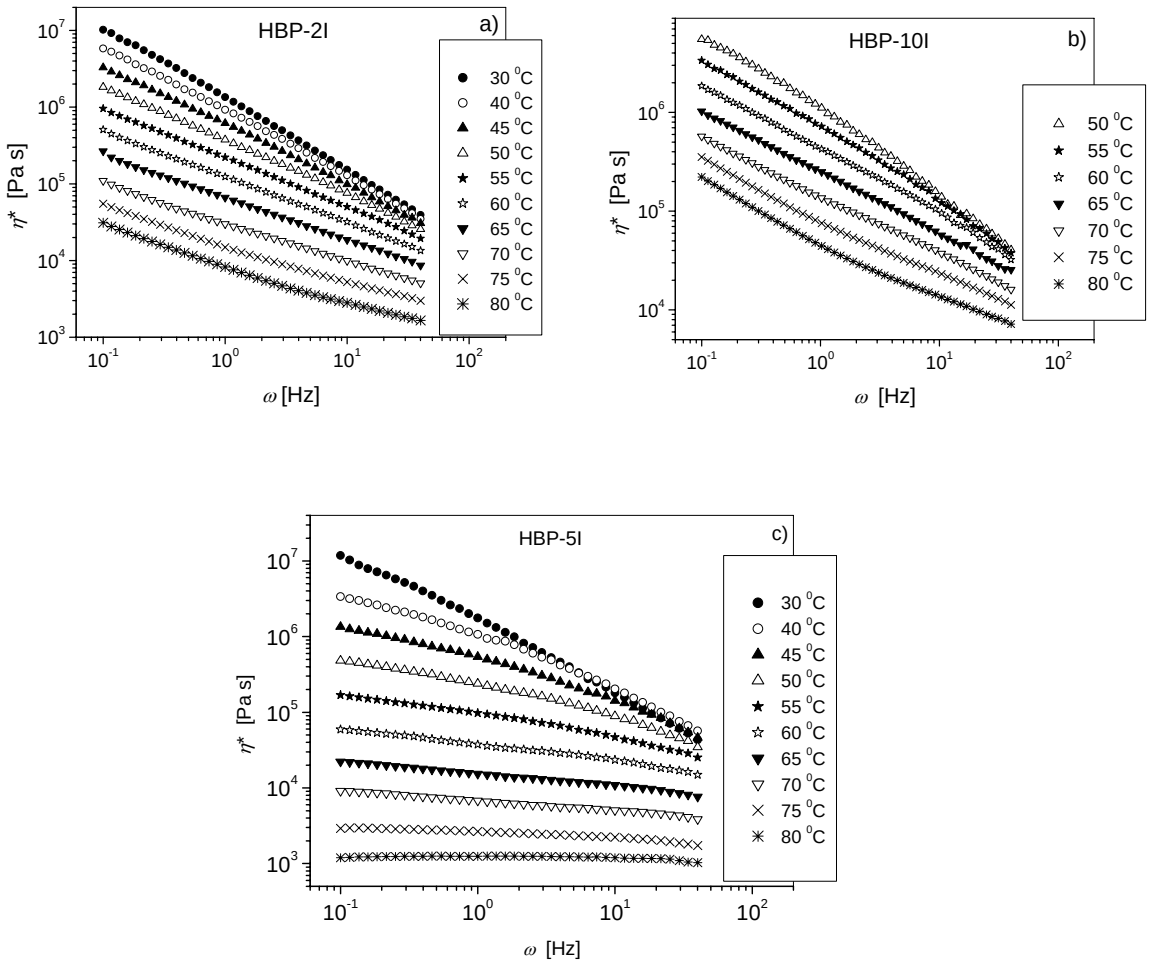

Figure 4.64. Frequency dependence of the complex viscosity at different temperatures for the samples a) HBP-2I, b) HBP-10I and c) HBP-5I

The frequency dependence of the storage and loss modulus of the samples HBP-2I and BH-3 at 45 ^{0}C (Figure 4.65a) show that for these two samples the curve of the storage modulus is in the entire frequency region located above that of the loss modulus. This implies that these samples have mainly elastic behaviour at 45 ^{0}C, since G' represents the elastic part of the complex viscosity. The same behaviour is also obtained for the sample HBP-10I. However, all other investigated samples show viscous behaviour ($G'' > G'$) at 45 ^{0}C up to the certain frequency after which the transition from more viscous to more elastic behaviour occurs ($G'' < G'$). As an example at Figure 4.65b the frequency dependences of the storage and loss modulus of the fourth generation samples are presented, while for the other selected samples these dependences can be found in Appendix 7.5.2. The intersection where this transition occurs ($G'' = G'$) appears for the sample HBP-4II at around 1.0 Hz, while for the other two fourth generation samples at around 1.3 Hz. All other samples show more elastic behaviour, since the crossover in G' and G'' appears at lower frequencies than for the fourth generation samples, i.e. for the samples HBP-3I and HBP-8I at 0.3 Hz and 0.4 Hz, respectively, while for the other samples at around 0.5 Hz.

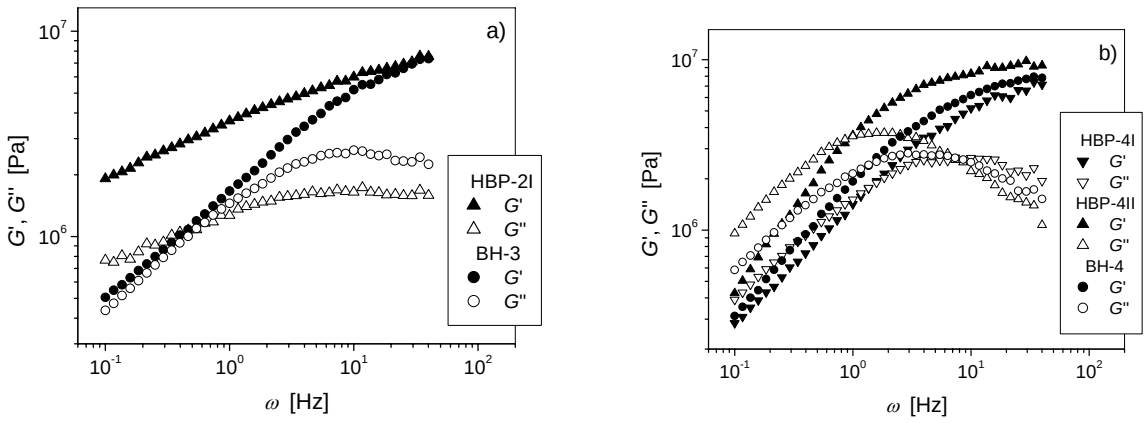

Figure 4.65. Frequency dependence of the storage and loss modulus of the selected HB samples at 45 ^{0}C

At 80 ^{0}C the trend of the frequency dependence of the storage and loss modulus of the sample HBP-10I did not change considerably (Figure 4.66b). Up to the ~ 10 Hz, G'' is lower than G', after what the transition from the elastic to viscous behaviour still does not occur completely since up to the 40 Hz, $G'' = G'$. On the other side, for the sample HBP-2I, G'' becomes higher than G' at ~ 0.4 Hz. For the other samples at 80 ^{0}C, G'' is higher than G' through the entire frequency region (Figure 4.66b), indicating viscous behaviour at higher temperatures. The same can also be observed from the results presented in Figure 4.67, where the values of the G' and G'' at 10 Hz (T = 80 ^{0}C) for the different samples are presented.

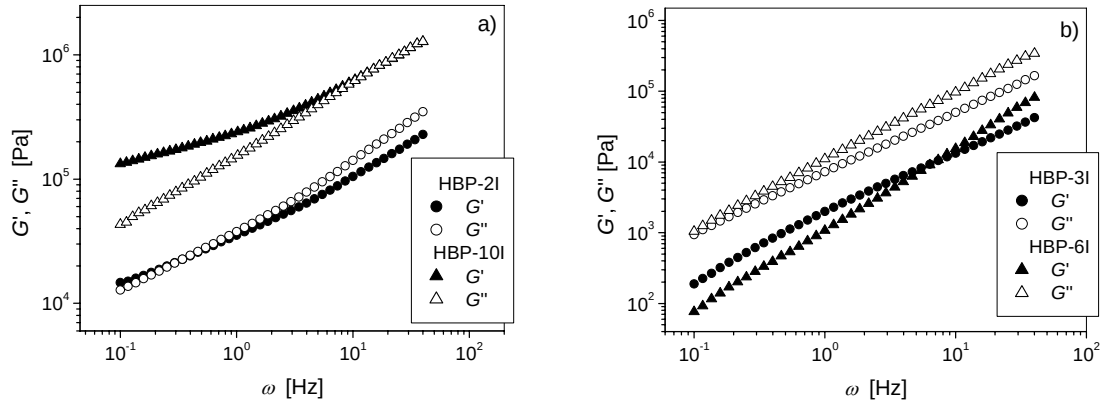

Figure 4.66. Frequency dependence of the storage and loss modulus of the selected HB samples at 80 ^{0}C

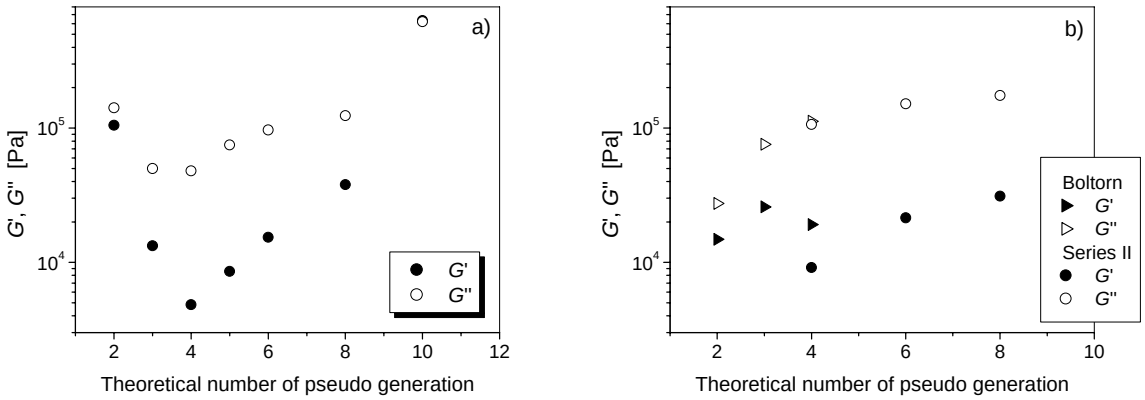

Figure 4.67. Dependence of the storage and loss modulus versus theoretical number of pseudo generation determined at 10 Hz ($T = 80^0$) for the a) samples of the series I and b) samples of the series II and commercial samples

When the rheological measurements of the investigated HB polyesters are performed at higher temperatures (T > 75 ^{0}C) it is observed that most samples show the classical terminal scaling of the loss modulus $G'' \sim \omega$ at low frequency region, except for the samples HBP-2I, BH-2, BH-3and HBP-10I, for which the exponent is lower than one. For the samples HBP-3I and HBP-8I it was observed that $G'' \sim \omega^{0.84}$. On the other side, at the entire examined frequency and temperature region, investigated HB polyesters show deviation from the terminal scaling of the G', i.e. in the dependence $G' \sim \omega^b$, the exponent b is always lower than 2. Non-terminal G' scaling is also observed for the other dendritic polymers presented in the literature[148].

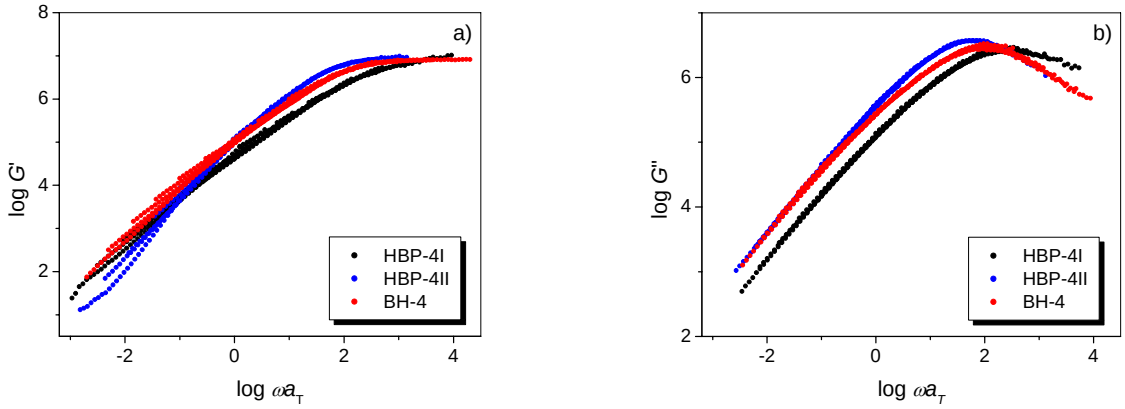

Figure 4.68. Master curves of the storage and loss modulus for the fourth generation samples ($T_0 = 60$ ^{0}C)

Using the time-temperature superposition principles, master curves of the determined rheological parameters are constructed. Shift factors (a_T) are determined for the temperatures higher than T_g (Table 4.34) by shifting the frequency dependences of the G' and G'' along the horizontal axes to obtain superposition on the corresponding reference curve ($T_0 = 60$ ^{0}C). In this manner, frequency dependences of the G' and G'' are enhanced on the several decades of frequencies (Figure 4.68). From the obtained values of the shift factors and the linear form of the equation (2.62), WLF parameters (C_1 and C_2) are determined and listed in Table 4.35. Beside them, in Table 4.35 are also listed values of the melt flow activation energy, E_a^m,

calculated at 80 ^{0}C (equation 2.63), values of the constants C_1^g and C_2^g ($T_0 = T_g$), fractional free volume, f_g, and values of the thermal expansion coefficient, α_f. For the determination of the constants C_1^g and C_2^g, values of the glass transition temperature obtained from the maximum of the loss modulus temperature dependences are used (Table 4.34). Equations which are used for the calculation of the parameters listed in Table 4.35 are given in chapter 2.4.4.

Table 4.35. Values of the WLF parameters, melt flow activation energy calculated at 80 ^{0}C, E_a^m, fractional free volume, f_g, and thermal expansion coefficient, α_f

Sample	C_1	C_2 [K]	E_a^m [kJ mol^{-1}]	C_1^g	C_2^g [K]	f_g	α_f [10^{-4} K^{-1}]
HBP-2I	62.5	459.4	298.5	66.5	432.0	0.006	0.15
HBP-3I	21.4	194.0	216.1	24.1	171.7	0.018	1.05
HBP-4I	25.5	240.3	215.9	28.3	216.5	0.015	0.71
HBP-4II	30.7	322.9	201.1	32.5	304.7	0.013	0.44
HBP-5I	22.6	212.6	212.5	25.4	189.2	0.017	0.90
HBP-6I	21.3	218.1	195.6	23.3	198.9	0.019	0.93
HBP-6II	27.7	276.3	208.0	29.4	260.3	0.015	0.57
HBP-8I	19.7	192.5	201.0	22.7	167.6	0.019	1.14
HBP-8II	9.55	103.4	154.9	11.3	87.4	0.038	4.40
HBP-10I	36.4	285.3	266.3	39.9	260.4	0.011	0.42
BH-3	28.4	275.3	214.0	31.4	249.1	0.014	0.56
BH-4	18.3	199.7	180.4	21.4	170.3	0.020	1.19

The obtained values of the melt flow activation energy at 80 ^{0}C indicate higher degree of the intermolecular H-bonding for the samples HBP-2I and HBP-10I, which is in agreement with results presented in Figures 4.64a and 4.64b. The decrease of the activation energy up to the sixth theoretical generation further indicates reduction of the intermolecular H-bonding, after which values of the E_a^m increase again for the samples HBP-8I and HBP-10I. For the samples HBP-4II, HBP-8II and BH-4 the melt flow activation energies have somewhat lower values than corresponding values obtained for the HB polyesters of the series I, which is consistent with results presented in Figure 4.63. The change of the fractional free volume at T_g for different samples is in accordance with the change of the melt flow activation energy. The increase of the f_g for the samples of the series I up to the sixth theoretical pseudo generation occurs as a consequence of the greater mobility of the branches. Calculated values of the f_g are for most investigated HB polyesters smaller than values usually reported for the linear polymers (0.025) but at the same time relatively close to the values obtained for other dendritic polymers[106].

The rheological behaviour of the self-synthesized HB polyesters strongly depends not only on the number but also on the type of the end groups. Therefore, the melt rheology of the third generation sample whose end –OH groups are modified with stearic acid (HBP-3$_{SA}$; M_{theor} = 29482 g/mol) is also performed. The strong influence of this type of modification on the rheological properties can be clearly seen from the results presented in Figure 4.69. Values of the complex viscosity for the sample HBP-3$_{SA}$ are lower in comparison with the

ones obtained for the HBP-3I, especially at temperatures higher than 30 ^{0}C (Figure 4.69a). This indicates that the presence of the long alkyl chain ends, instead of the polar –OH groups, reduces to a certain amount the possibility for the H-bonding. Similar conclusions can be made from the temperature dependences of the storage and loss modulus (Figure 4.69b). As a consequence of the reduction of the H-bonding, glass transition temperature also decreases by modification of the HB polyesters with alkyl chains. From the $(G'')_{max}$ and inflection point in the temperature dependence of the G' it is obtained that T_g for the HBP-3$_{SA}$ is 29 ^{0}C, while glass transition temperature of the sample HBP-3I is 38 ^{0}C (Table 4.34).

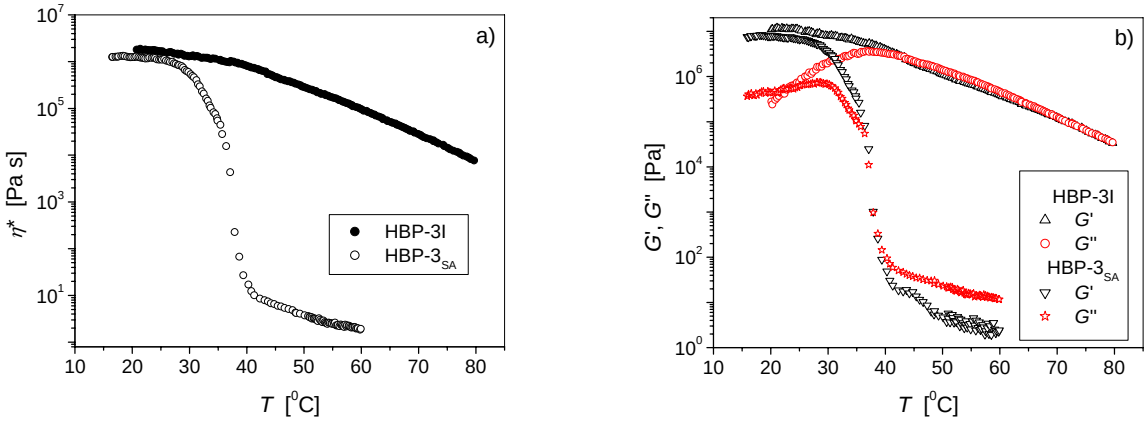

Figure 4.69. Temperature dependence of the complex viscosity and dynamic modulus of the samples HBP-3I and HBP-3$_{SA}$ at frequency of 1 Hz

However, the presence of such long terminal alkyl chains (C18) can induce crystallinity in the HB polyesters and in this manner limit the stronger reduction of the glass transition temperature[125]. Therefore, the sudden decrease of the η^*, G' and G'' values at around 37 ^{0}C for the HBP-3$_{SA}$ is ascribed to the melting of this sample. The same behaviour can be seen from the frequency dependences of the HBP-3$_{SA}$ complex viscosity at different temperatures, where a strong decrease of the η^* can be observed between 35 and 40 ^{0}C (Figure 4.70a). The non-*Newtonian* behaviour of the samples HBP-3$_{SA}$ up to the 40 ^{0}C s probably due to the intermolecular crystallization, i.e. interpenetration of end alkyl groups from the surrounding molecules[125]. Up to the 35 ^{0}C it is observed that HBP-3$_{SA}$ has elastic behaviour ($G' > G''$), while the opposite occurs at higher temperatures (Figure 4.70b).

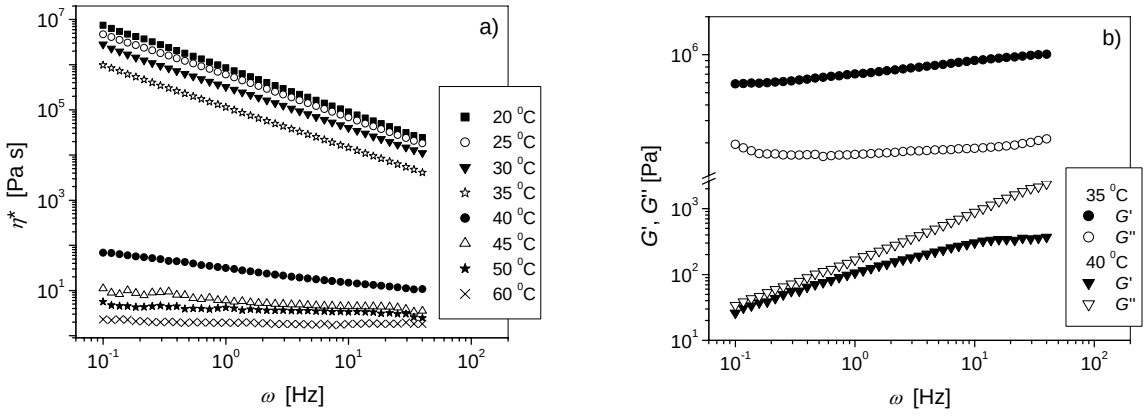

Figure 4.70. Frequency dependence of the complex viscosity and dynamic modulus of the sample HBP-3$_{SA}$ at different temperatures

4.6. Thermal stability of the hyperbranched polyesters

The thermal stability of the investigated HB samples was determined with non-isothermal thermogravimetric analysis in inert atmosphere (N_2). As an examples in Figures 4.71a and 4.71b are presented TG curves for the selected HB polyesters, determined at a heating rate of 10 ^{0}C/min. From these results it can be observed that the TG curves for all samples have approximately the same shape. Under the given experimental conditions a measurable mass loss of the self-synthesized polymers starting between 250 ^{0}C and 275 ^{0}C is detected. Therefore, it can be concluded that in these samples below 250 ^{0}C no measurable amount of evaporable compounds (moisture, un-reacted monomers) is present. The same can be observed for the commercial samples, except for the BH-2, where a considerable mass loss starts at somewhat lower temperatures (Table 4.36). Furthermore, from the results presented in Figure 4.71b it can be observed that the first series of the HB polyesters have better thermal stability than the samples of the second series. This can also be seen from the results listed in Table 4.36, where temperatures obtained for the mass losses of 5, 20, 50 and 80 mass % (T_5, T_{20}, T_{50} and T_{80}, respectively) are listed. For all three groups of the investigated samples, characteristic temperatures of degradation increase with the theoretical number of pseudo generation. For the samples of the series I this increase of the thermal stability is observed up to the fifth pseudo generation. During the synthesis of the higher generation samples, side reaction occurred in relatively high degree, which has been already proved by NMR, VPO and MALDI TOF measurements. One consequence of the side reactions is the formation of the cyclic macromolecules. Evaporable segments can not be made by breaking one bond in formed cyclic macromolecules, which is possibly the reason for the slight increase of the thermal stability from fifth to tenth pseudo generation.

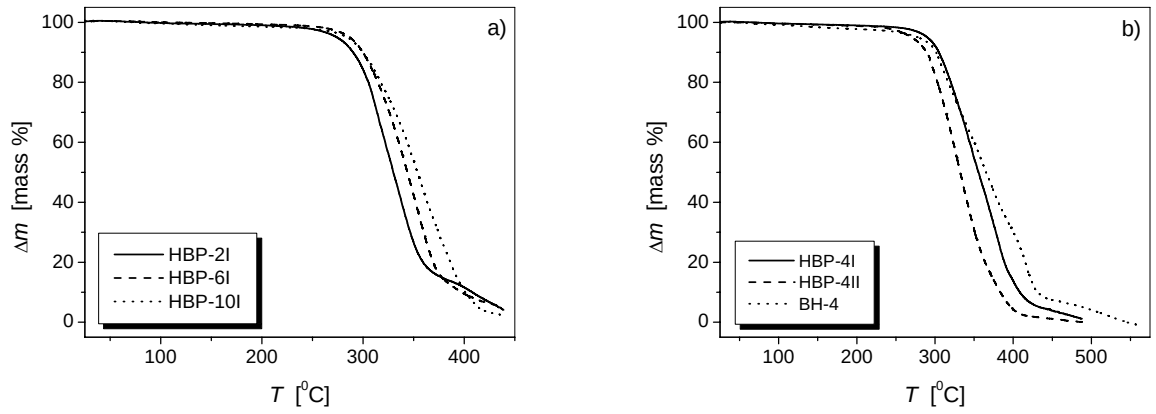

Figure 4.71. TG curves measured at heating rate of 10 ^{0}C/min for a) selected HB polyesters of series I and b) fourth generation HB polyesters

Table 4.36. Characteristic temperatures of the degradation for the investigated HB polyesters determined at heating rate of 10 ^{0}C/min

Sample	T_5 [^{0}C]	T_{20} [^{0}C]	T_{50} [^{0}C]	T_{80} [^{0}C]
HBP-2I	274	305	329	359
HBP-3I	281	309	335	364
HBP-4I	282	310	338	371
HBP-4II	269	303	332	364
HBP-5I	288	316	346	372
HBP-6I	287	315	344	370
HBP-6II	262	305	336	366
HBP-8I	286	313	341	362
HBP-8II	264	307	340	369
HBP-10I	284	318	354	386
BH-2	245	300	339	379
BH-3	265	318	353	409
BH-4	279	317	365	416

The thermal stability of the HB polyesters depends to a great amount on the chemical structure of the end groups. Therefore, thermogravimetric measurements are also performed on the samples HBP-3$_{SA}$. As can be seen from the results presented in Figure 4.73 the thermal stability of the HB polyesters increases significantly by modification of the end –OH groups with stearic acid. The influence of the other types of the end groups on the thermal stability of these HB polyesters is already discussed elsewhere[128].

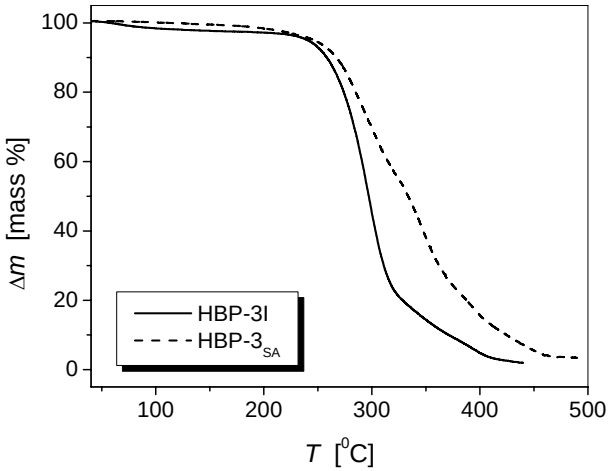

Figure 4.72. TG curves for samples HBP-3I and HBP-3$_{SA}$ determined at heating rate of 5 ^{0}C/min

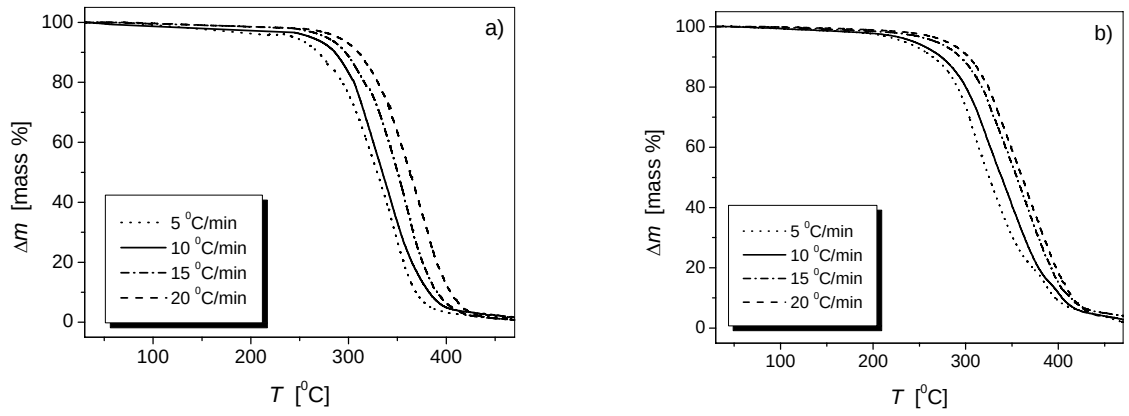

Figure 4.73. TG curves determined at different heating rates for samples a) HBP-6II and b) BH-2

In order to calculate the activation energy of thermal degradation (E_a^d) for the investigated HB polyesters, TG curves are measured at different heating rates. As an illustration in Figure 4.73 are presented TG curves for the samples HBP-6II and BH-2 determined at four different heating rates. Using *Ozawa-Flynn-Wall* method[127], the activation energies of thermal degradation for different HB polyesters are determined and presented in Figures 4.74a, 4.74b and 4.74c as curves of changing E_a^d with mass loss, i.e. degree of reaction (α). The various tendencies of E_a^d for different investigated HB polyesters imply that the thermal degradation of these polymers is a complex process. For the samples HBP-2I, HBP-3I and HBP-4I the activation energy of the thermal degradation increases with the generation number, but they are approximately constant in the region $0.10 < \alpha < 0.75$. Furthermore, for the samples HBP-3I and HBP-4I in the last phase of degradation ($\alpha > 0.75$) a slight increase of the values of E_a^d can be observed. Similar is detected for the samples HBP-4II, BH-2 and BH-3, however with much shorter region of constant E_a^d values. Up to the $\alpha < 0.30$ values of the E_a^d for the sample HBP-8I are nearly the same as for the HBP-4I, while for $\alpha > 0.30$ activation energy of degradation significantly increase as a consequence of the more complicated thermal degradation process. Boltorn® samples also show this significant increase of the activation energy, however only for higher values of α. Generally it can be observed that samples of the second series have lower values of the E_a^d compared with the ones obtained for the commercial samples and polyesters of the series I. This is consistent with previously detected lower thermal stability of these HB polyesters. On the other side, commercial samples show slightly higher thermal stability than polymers of the I series, which can also be observed from the results listed in Table 4.36.

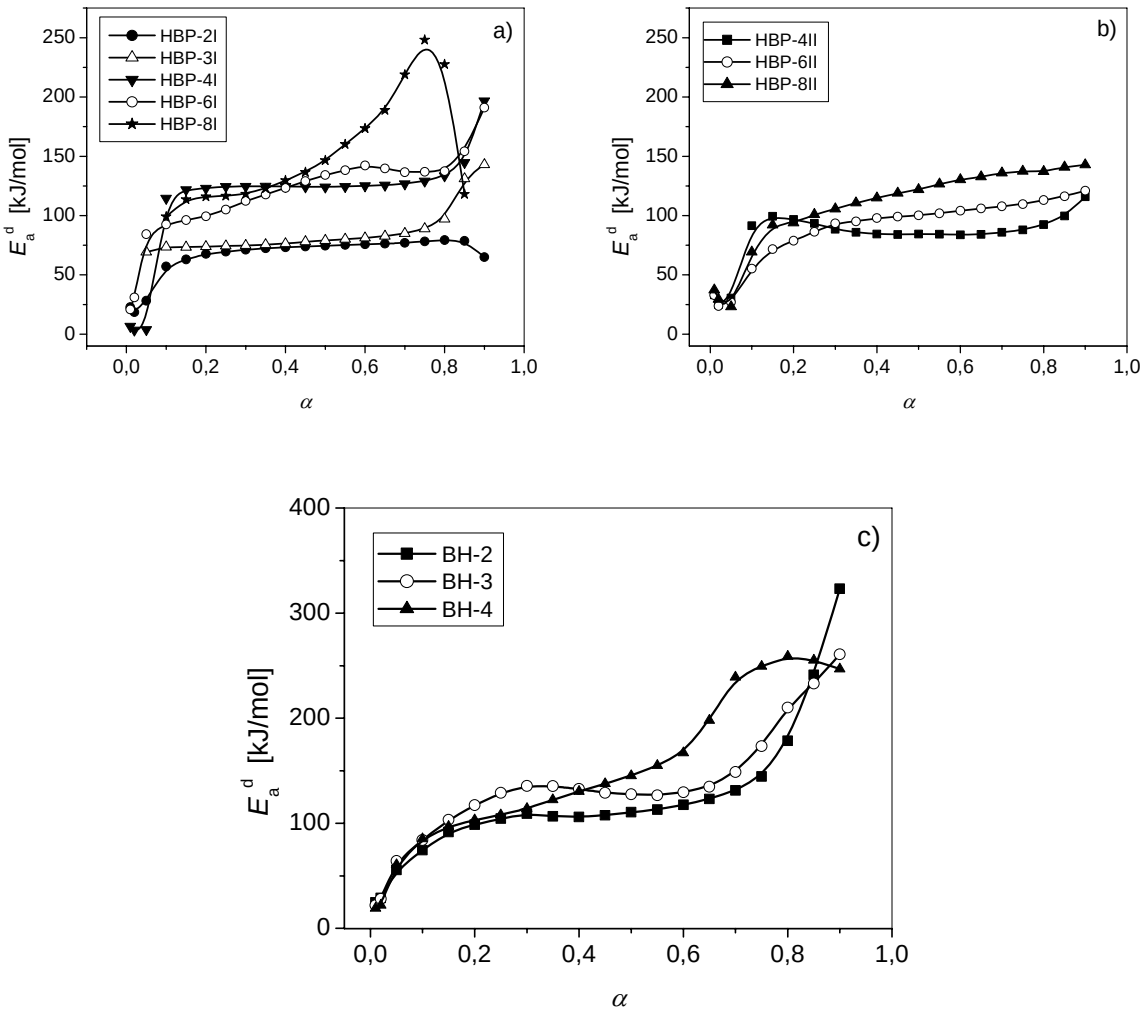

Figure 4.74. Change of the activation energies of thermal degradation (E_a^d) with degree of reaction (α) for a) selected samples of the I series, b) samples of the II series and c) commercial samples

5. Conclusions

In order to investigate properties of aliphatic hyperbranched polyesters hydroxy-functional hyperbranched polymers based on aliphatic polyesters were synthesized in this work via an acid-catalyzed esterification procedure in melt from the 2,2-bis(hydroxymethyl)propionic acid (AB_2 monomer) and the di-trimethylolpropane (B_4 functional core). Samples of different pseudo generations were obtained by changing the molar core/monomer ratio. Two different ways of synthesis were used: pseudo-one-step procedure for the samples of the series I (HBP-2I, HBP-3I, HBP-4I, HBP-5I, HBP-6I, HBP-8I and HBP-10I) and one-step procedure for the samples of the series II (HBP-4II, HBP-6II and HBP-8II). Beside the self-synthesized, three commercial Boltorn® hyperbranched polyesters (BH-2, BH-3 and BH-4) were also investigated. Five self-synthesized and two commercial HB polyesters were fractionated using the precipitation fractionation method in order to obtain three fractions of each sample. Beside that, end –OH groups of two self-synthesized and two commercial HB polyesters were modified with β-alanine, to obtain the following samples: HBP-3I_{AL}, HBP-4I_{AL}, BH-2$_{AL}$ and BH-3$_{AL}$, while the sample of the third pseudo generation was modified with stearic acid (HBP-3I_{SA}). To investigate molecular structure and properties of these HB polyesters the following experimental methods were used: IR, ^{13}C NMR and ^{1}H NMR spectroscopy, determination of the acid and hydroxyl number, VPO, MALDI-TOF MS, ESI MS, GPC, SLS, DLS, UC, viscosimetry of the diluted solutions, rheology of the concentrated solutions and melt and thermogravimetry. According to the obtained results the following conclusions were made:

- The results obtained from the ^{13}C NMR spectroscopy have shown that the structure of the HB polymers synthesized in this dissertation is consisted of higher amount of the linear units than what should be expected according to the ideal model. It has been obtained that around 50 % of all –OH groups which are present in the molecule of HB polyesters are situated on the linear repeating units. This indicates that reactivity of different –OH groups is not the same. This has been also confirmed from the values of the degree of branching, which are for all samples lower than 0.50. The portion of dendritic units increases with increasing degree of conversion, while the opposite is valid for the portion of terminal units. Furthermore, results obtained from the NMR spectroscopy and hydroxyl number titration have shown that the percentage of end –OH groups per molecule decreases with increasing theoretical number of pseudo generation, i.e. low generation HB polymers have a higher concentration of end hydroxyl groups. Similar conclusions were also made for the commercial HB polyesters. Furthermore, obtained results show that HB samples synthesized by one-step procedure have lower values of the degree of branching and higher portion of the linear units than samples synthesized by pseudo-one-step procedure, which indicates that during the one-step polycondensation –COOH groups from bis-MPA have lower accessibility to the –OH groups from the linear repeating units.

- Results obtained from the characterization methods such as NMR spectroscopy, determination of the acid number, MALDI-TOF and ESI mass spectrometry have shown that no matter which synthetic procedure is used for these HB polyesters (pseudo-one-step or one-step) it is not possible to completely prevent the occurrence of the side reactions during the synthesis. However, it has been shown that the extent of the side reactions is higher for the samples synthesized by one-step procedure. The most important side reaction is the formation of the poly(bis-MPA) and the deactivation of its focal –COOH group. In this manner HB structures without the B_4 (DiTMP) and with B_2 (bis-MPA itself) core molecule are formed. The absence of this side product is confirmed only for the samples HBP-2I and HBP-4II (results from ^{13}C NMR and MALDI-TOF MS). For all other investigated samples it has been shown that degree of conversion of –COOH groups decreases with increasing theoretical

number of pseudo generation. This further means that with decreasing the core/monomer ratio the fraction of the HB species with B_4 core decreases while at the same time the amount of the HB structures formed by self-condensation of bis-MPA increases. The main consequences of this side reaction are a significant lowering of the number average molar mass ($(M_n)_{NMR}$, $(M_n)_{VPO}$) of the final HB polyester compared with theoretical values and that the molar mass increases only up to the sixth pseudo generation.

- Formation of the cycles by intramolecular etherification and esterification is another side reaction which has a great influence on the properties of the HB polymers. Results obtained from the mass spectrometry and from the comparison of $(M_n)_{NMR}$ and $(M_n)_{VPO}$ show that the extent of cyclization increases up to the fifth, i.e. up to the sixth pseudo generation, respectively. On the other side, results obtained from ^{1}H NMR indicate that the amount of the formed ether groups decreases with increasing number of the pseudo generation. This further indicates that up to the fifth theoretical pseudo generation (or sixth for the series II) cyclization occurred through ester and ether bonds, while for the higher generation samples cycles are formed as a consequence of the intramolecular esterification. During the synthesis of the commercial samples the extent of the mentioned side reactions occurred in higher degree than for the samples synthesized in this dissertation.

- According to the results obtained by GPC measurements it has been concluded that all investigated HB polyesters have a relatively broad molar mass distribution (M_w/M_n = 1.39-2.33), which represents a consequence of the previously mentioned side reactions. Molar mass distribution increases with increasing degree of polymerization and beside that it was obtained that it increases up to the sixth pseudo generation. Commercial samples have a broader molar mass distribution than samples synthesized in this work. As a consequence of the higher extent of the side reactions, the polydispersity of the second series is higher than for the samples of the series I.

- From the results obtained by DLS and viscosimetry of the diluted solutions it was concluded that the thermodynamically best solvents for all investigated HB polyesters are a 0.7 mass % solution of LiCl in DMAc and NMP. The value of the limiting viscosity number and the hydrodynamic radius (R_η) determined in these two solvents at constant temperature increase up to the sixth pseudo generation. Values of the exponents α = 0.23-0.40 (from the KMHS equation) and ν = 0.34-0.46 (from the relationship $R_\eta \sim M$) indicate that these polymers (self-synthesized and commercial) have a less densely packed structure than the dendrimers but are more compact than linear polymers. The values of the limiting viscosity number are slightly higher for the second series than for the series I, due to the presence of the higher amount of linear units in the structure of the samples synthesized by a one-step procedure.

- Concentrated solutions ($c \leq 45$ mass %) of all investigated HB polymers show *Newtonian* behaviour in NMP at all measured temperatures, probably due to their globular shape and absence of the entanglements. However, 50 and 55 mass % solutions of all HB polyesters at temperatures $T \leq 50\ ^0$C show non-*Newtonian* behaviour. For the self-synthesized and commercial HB samples the η_o–M–c relationship has been established. Viscosity of the investigated concentrated solutions of HB polyesters increases more slowly with increasing molar mass than for the corresponding solutions of linear macromolecules.

- Melt rheology of the investigated HB polyesters from fourth till sixth pseudo generation shows that these samples behave as *Newtonian* liquids at temperatures $T > 70\ ^0$C. All other samples in the used temperature (30-80 ^{0}C) and frequency (0.1-40 Hz) region, as well as previously mentioned samples at lower temperatures show non-*Newtonian* behaviour. For this kind of rheological behaviour of the samples of fourth, fifth and sixth pseudo generation at different temperatures it is not possible to find a simply explanation. Results obtained from the rheological investigation of the HB polyesters melts clearly shows the difference in properties between samples synthesized using different procedures. Samples

synthesized by one-step procedure have higher values of the complex viscosity and the beginning of flow which starts at somewhat lower temperatures than for the samples obtained by pseudo-one-step procedure. By modification of the end –OH groups with stearic acid the rheological properties of the HB polyesters are changed. The presence of the long alkyl chain ends, instead of the polar –OH groups, reduces the possibility for the H-bonding, which is observed from the lower values of the complex viscosity and glass transition temperature for the sample HBP-3_{SA} in comparison to the values obtained for the HBP-3I.

- The thermal stability of the investigated HB samples was determined with non-isothermal thermogravimetric analysis. It has been obtained that thermal stability of all investigated samples increases with the increasing theoretical number of pseudo generation. For the polyesters of the series I this increase is observed up to the fifth pseudo generation, while for the samples of the series II an increase of the thermal stability occurs up to the eighth pseudo generation. Furthermore, the first series of the HB polyesters have better thermal stability than the samples of the second series. The activation energy of the thermal degradation shows various tendencies for different investigated HB polyesters, which imply that thermal degradation of these polymers is a complex process. The thermal stability of the modified sample HBP-$3I_{SA}$ is higher than for the HBP-3I.

Generally it can be concluded that the properties of the HB polymers based on aliphatic polyesters can be changed by choosing the adequate method for the synthesis and/or by changing the type of the end groups.

6. References

1) F. Vogtle, W. Wehner, E. Buhleier, Synthesis, **55** (1978) 155-158
2) D. A. Tomalia, H. Baker, J. Dewald, M. Hall, G. Kallos, S. Martin, J. Roeck, J. Ryder, J. Smith, Polymer J., **17** (1985) 117-132
3) G. R. Newkome, Z. Q. Yao, G. R. Baker, V. K. Gupta, J. Org. Chem., **50** (1985) 2003-2004
4) J. M. J. Fréchet, J. Macromol. Sci., Pure Appl. Chem., **A33 (10)** (1996) 1399-1425
5) Y. H. Kim, O. W. Webster, J. Am. Chem. Soc., **112** (1990) 4592-4593
6) M. Johansson, A. Hult, J. Coat. Technol., **67** (1995) 35-39
7) D. J. Massa, K. A. Shriner, S. R. Turner, B. I. Voit, Macromolecules, **28** (1995) 3214-3220
8) Y. Zhang, L. Wang, T. Wada, H. Sasabe, Macromol. Chem. Phys., **197** (1996) 667-676
9) T. Griebel , G. Maier, Polym. Prepr. (ACS, Polymer Division), **41(1)** (2000) 89-90
10) P. Persigehl, N. West, B. Zimmermann, O. Nuyken, Presented at the Freiburger Makromolekularem Kolloquium, Freiburg, (2000)
11) W. Burchard, Adv. Polym. Sci., **143** (1999) 113-194
12) P. J. Flory, *Principles of Polymer Chemistry*, Cornell University Press, Ithaca, NY (1953)
13) W. H. Stockmayer, J. Chem. Phys., **11** (1943) 45-55
14) P. J. Flory, J. Am. Chem. Soc. (1952), **74**, 2718-2723
15) C. J. Hawker, J. M. J. Fréchet, J. Am. Chem. Soc., **112** (1990) 7638-7647
16) S. J. E. Mulders, A. J. Brouwer, P. G. J. van der Meer, R. M. J. Liskamp, Tetrahedron Lett., **38** (1997) 631-634
17) P. M. Bayliff, W. J. Feast, D. Parker, Polym. Bull. (Berlin), **29** (1992) 265-270
18) A. B. Padias, H. K. Hall, D. A. Tomalia, J. R. Mc Connel, J. Org. Chem., **52** (1987) 5305-5312
19) I. Ihre, A. Hult, E. Söderlind, J. Am. Chem. Soc., **27** (1996) 6388-6395
20) C. J. Hawker, J. M. J. Fréchet, J. Chem. Soc., Chem. Commun., (1990) 1010-1013
21) K. L. Wooley, C. J. Hawker, J. M. J. Fréchet, J. Am. Chem. Soc., **113** (1991) 4252-4261
22) F. Zeng, S. C. Zimmerman, J. Am. Chem. Soc., **118** (1996) 5326-5327
23) C. J. Hawker, R. Lee, J. M. J. Fréchet, J. Am. Chem. Soc., **113** (1991) 4583-4588
24) H. R. Kricheldorf, O. Stöber, Macromol. Rapid Commun., **15** (1994) 87-93
25) M. Johansson, E. Malmström, A. Hult, J. Pol. Sci.: Part A: Polym. Chem., **31** (1993) 619-624
26) K. E. Uhrich, S. Boegeman, J. M. J. Fréchet, S. R. Turner, Polym. Bull., **25** (1991) 551-558
27) T. M. Miller, T. X. Neenan, E. W. Kwock, S. M. Stein, J. Am. Chem. Soc., **115** (1993) 356-357
28) K. Matyjaszewski, S. G. Gaynor, A. Kulfan, M. Podwika, Macromolecules, **30** (1997) 5192-5194
29) D. H. Bolton, K. L. Wooley, Macromolecules, **30** (1997) 1890-1896
30) A. Kumar, S. Ramakrishnan, J. Chem. Soc., Chem. Commun., (1993) 1453-1454
31) A. H. E. Müller, D. Yan, M. Wulkow, Macromolecules, **30** (1997) 7015-7023
32) D. Yan, Z. Zhou, Macromolecules (1999), **32**, 819-824
33) P. Bharathi, J.S. Moore, Macromolecules, **33** (2000) 3212-3218
34) E. Malmström, M. Johansson, A. Hult, Macromolecules, **28** (1995) 1698-1703

35) H. Magnusson, E. Malmström, A. Hult, Macromolecules, **33** (2000) 3099-3104
36) L. J. Hobson, W. J. Feast, Polymer, **40** (1999) 1279-1297
37) K. Dušek, J. Šomvársky, M Smrčková, W. J. Simonsick Jr., L. Wilczek, Polymer Bulletin, **42** (1999) 489-496
38) D. Parker, W. J. Feast, Macromolecules, **34** (2001) 2048-2059
39) H. R. Kricheldorf, L. Vakhtangishvill, G. Schwarz, R. P. Krüger, Macromolecules, **36** (2003) 5551-5558
40) A. Burgath, A. Sunder, H. Frey, Macromol. Chem. Phys., **201** (2000) 782-791
41) T. Emrick, H. T. Chang, J. M. J. Fréchet, Macromolecules, **32** (1999) 6380-6382
42) M. Suzuki, A. Ii, T. Saegusa, Macromolecules, **25** (1992) 7071-7072
43) J. M. J. Fréchet, M. Henmi, I. Gitsov, S. Aoshima, M. R. Leduc, R. B. Grubbs, Science, **269** (1995) 1080-1083
44) P. G. de Gennes, H. Hervet, J. Phys. Lett., **44** (1983) L351-L360
45) M. L. Mansfield, L. I. Klushin, Macromolecules, **26** (1993) 4262-4268
46) T. J. Prosa, B. J. Bauer, E. J. Amis, D. A. Tomalia, R. Scherrenberg, J. Polym. Sci. Part B: Polym. Phys., **35** (1997) 2913-2924
47) R. L. Lescanec, M. Muthukumar, Macromolecules, **23** (1990) 2280-2288
48) V. Petkov, V. Parvanov, D. Tomalia, D. Swanson, D. Bergstrom, T. Vogt, Solid State Communications, **134** (2005) 671-675
49) D. Hölter, A. Burgath, H. Frey, Acta Polym., **48** (1997) 30-35
50) P. Kambouris, C. J. Hawker, J. Chem. Soc. Perkin Trans., **1** (1993) 2717-2721
51) D. Hölter, H. Frey, Acta Polym., **48** (1997) 298-309
52) W. Radke, G. Litvinenko, A. H. E. Müller, Macromolecules, **31** (1998) 239-248
53) B. H. Zimm, W. H. Stockmayer, J. Chem. Phys., **17** (1949) 1301-1314
54) K. L. Wooley, J. M. J. Fréchet, C. J. Hawker, Polymer, **35** (1994) 4489-4495
55) A. Hult, M. Johansson, E. Malmström, Macromol. Symp., **98** (1995) 1159-1161
56) Y. H. Kim, O. W. Webster, Macromolecules, **25** (1992) 5561-5572
57) J. M. J. Fréchet, Science, **263** (1994) 1710-1715
58) D. A. Tomalia, A. M. Naylor, W. A. Goddard, Angew. Chem. Int. Ed. Engl., **29** (1990) 138-175
59) E. Malmström, A. Hult, U. W. Gedde, F. Liu, R. H. Boyd, Polymer, **38** (1997) 4873-4879
60) C. J. Hawker, F. Chu, Macromolecules, **29** (1996) 4370
61) M. P Stevens, *Polymer Chemistry*, 2nd ed., Oxford University Press (1990)
62) W. J. Feast, N. M. Stainton, J. Mater. Chem., **5** (1995) 405-411
63) D. Parker, W. J. Feast, Macromolecules, **34** (2001) 5792-5798
64) E. Schröder, G. Müller, K.-F. Arndt, *Polymer characterization*, Hanser Publishers, Munich, Vienna, New York (1988)
65) I. B. Rietveld, J. A. M. Smit, Macromolecules, **32** (1999) 4608-4614
66) A. Sunder, R. Hanselmann, H. Frey, R. Mülhaupt, Macromolecules, **32** (1999) 4240-4246
67) D. Yu, N. Vladimirov, J. M. J. Fréchet, Macromolecules, **32** (1999) 5186-5192
68) K. Martin, J. Spickermann, H. J. Räder, K. Müllen, Rapid Commun. Mass Spectrom,. **10** (1996) 1471-1474
69) H. R. Kricheldorf, D. Fritsch, L. Vakhtangishvill, G. Schwarz, Macromolecules, **36** (2003) 4337-4344
70) M. Yamashita, J. B. Fenn, J. Phys. Chem., **88** (1984) 4451-4459
71) E. Žagar, M. Žigon, Macromolecules, **35** (2002) 9913-9925
72) G. R. Newkome, J. K. Young, G. R. Baker, R. L. Potter, L. Audoly, D. Cooper, C. L. Weis, K. Morris, C. S. Johnson, Macromolecules, **26** (1993) 2394-2396

73) C. J. G. Plummer, A. Luciani, T. Q. Nguyen, L. Garamszegi, M. Rodlert, J. A. E. Månson,. Polymer Bulletin, **49** (2002) 77-84
74) M. D. Lechner, K. Gehrke, E. H. Nordmeier, *Makromolekulare Chemie*, 3. Auflage, Birkhäuser Verlag, Basel (2002)
75) P. Kratochvil, *Classical light scattering from polymer solution*, Elsevier (1987)
76) S. M. Aharoni, N. S. Murthy, Polym. Commun., **24** (1983) 132-136
77) W.-M. Kulicke, C. Clasen, *Viscosimetry of Polymers and Polyelectrolytes*, Springer-Verlag Berlin Heidelberg New York (2004)
78) M. L. Huggins, J. Am. Chem. Soc., **64** (1942) 2716-2718
79) T. H. Mourey, S. R. Turner, M. Rubinstein, J. M. J. Fréchet, C. J. Hawker, K. L. Wooley, Macromolecules, (1992), **25**, 2401-2406
80) M. Jeong, M. E. Mackay, R. Vestberg, C. J. Hawker, Macromolecules, **34** (2001) 4927-4936
81) J. M. J. Fréchet, C. J. Hawker, I. Gitsov, J. W. Leon, J. Macromol. Sci. Pure Appl. Chem., **A33** (1996) 1399-1425
82) L. J. Hobson, W. J. Feast, Chem. Commun., **21** (1997) 2067-2068
83) A. H. Widmann, G. R. Davies, J. Comput. Theor. Polym. Sci., **8** (1998) 191-199
84) J. Aerts, J. Comput. Theor. Polym. Sci., **8** (1998) 49-54
85) S. R. Turner, B. I. Voit, T. H. Mourey, Macromolecules, **26** (1993) 4617-4623
86) S. R. Turner, F. Walter, B. I. Voit, T. H. Mourey, Macromolecules, **27** (1994) 1611-1616
87) J. Hao, M. Jikei, M. Kakimoto, Macromolecules, **36** (2003) 3519-3528
88) B. J. Berne, R. Pecora, *Dynamic light scattering*, John Wiley & Sons, New York (1976)
89) M. Schmidt, W. H. Stockmayer, Macromolecules, **17** (1984) 509-514
90) W. Burchard, M. Schmidt, W. Stockmayer, Macromolecules, **13** (1980) 1265-1272
91) S. F. Sun, *Physical chemistry of macromolecules*, John Wiley & Sons, New York (1994)
92) M. D. Lechner, W. Mächtle, Progr. Colloid. Polym. Sci., **113** (1999) 37-43
93) W. Mächtle, Makromol. Chem., **185** (1984) 1025-1039
94) L. J. Gosting, J. Am. Chem. Soc., **74** (1952) 1548-1552
95) A. Einstein, Ann. Phys., **19** (1906) 289-306
96) P. J. Flory, T. G. Fox Jr., J. Am. Chem. Soc., **73** (1951) 1904-1908
97) W. R. Krigbaum, D. K. Carpenter, J. Phys. Chem., **59** (1955) 1166-1172
98) W. Burchard, Macromolecules, **10** (1977) 919-927
99) K. Ishizu, D. Takahashi, H. Takeda, Polymer, **41** (2000) 6081-6086
100) R.Scherrenberg, B. Coussens, P. Van Vliet, G. Edouard, J. Brackman, E. De Brabander, Macromolecules, **31** (1998) 456-461
101) M. L. Mansfield, L. I. Klushin, J. Phys. Chem., **96** (1992) 3994-3998
102) W. Burchard, K. Kajiwara, D. Nerger, J. Polym. Sci., Polym. Phys. Ed., **20** (1982) 157-171
103) S. Stechemesser, W. Eimer, Macromolecules, **30** (1997) 2204-2206
104) A. V. Lyulin, D. B. Adolf, G. R. Davies, Macromolecules, **34** (2001) 3783-3789
105) C. M. Nunez, B.-S. Chiou, A. L. Andrady, S. A. Khan, Macromolecules, **33** (2000) 1720-1726
106) A. Luciani, C. J. G. Plummer, T. Nguyen, L. Garamszegi, J.-A. E. Månson, J. Polym. Sci. Part B: Polym. Phys., **42** (2004) 1218-1225
107) M. Murat, G. S. Grest, Macromolecules, **29** (1996) 1278-1285
108) P. Welch, M. Muthukumar, Macromolecules, **31** (1998) 5892-5897
109) M. S. Matos, J. Hofkens, W. Verheijen, F. C. de Schryver, S. Hecht, K. W. Pollack, J. M. J. Fréchet, B. Forier, W. Dehaen, Macromolecules, **33** (2000) 2967-2973

110) M. Xu, X. Yan, R. Cheng, X. Yu, Polym. Int., (2001) 1338-1345
111) M. E. Mackay, G. Carmezini, Chem. Mater., **14** (2002) 819-825
112) R. W. Cahn, P. Haasen, E. J. Kramer, Materials Science and Technology, A Comprehensive Treatment, Vol. 12: *Structure and Properties of Polymers* Volume Editor E. L. Thomas, Weinheim, New York, Basel, Cambridge, Tokyo, VCH (1993)
113) F. Bueche, J. Chem. Phys., **20** (1952) 1959-1964
114) W.-M. Kulicke, *Fließverhalten von Stoffen und Stoffgemischen*, Hüthig und Wepf Verlag Basel, Heidelberg, New York (1986)
115) J. D. Ferry, *Viscoelastic Properties of Polymers*, 3rd ed, John Wiley & Sons inc., New York, Chichester, Brisbane, Toronto (1980)
116) S. Uppuluri, S. E. Keinath, D. A. Tomalia, P. R. Dvornić, Macromolecules, **31** (1998) 4498-4510
117) C. J. Hawker, P. J. Farrington, M. E. Mackay, K. L. Wooley, J. M. J. Fréchet, J. Am. Chem. Soc., **117** (1995) 4409-4410
118) I. Sendijarevic, A. J. McHugh, Macromolecules, **33** (2000) 590-596
119) T.-T. Hsieh, C. Tiu, G. P. Simon, Polymer, **42** (2001) 1931-1939
120) I. Bodnár, A. S. Silva, R. W. Deitcher, N. E. Weisman, Y. H. Kim, N. J. Wagner, J. Polym. Sci. Part B: Polym. Phys., **38** (2000) **38** 857-873
121) S. B. Kharchenko, R. M. Kannan, Macromolecules, **36** (2003) 407-415
122) H. Stutz, J. Polym. Sci. Part B: Polym. Phys., **33** (1995) 333-340
123) K. L. Wooley, C. J. Hawker, J. M. Pochan, J. M. J. Fréchet, Macromolecules, **26** (1993) 1514-1519
124) F. Chu, C. J. Hawker, Polym. Bull., **30** (1993) 265-272
125) E. Malmström, M. Johansson, A. Hult, Macromol. Chem. Phys., **197** (1996) 3199-2307
126) M. Rogunova, T.-Y. S. Lynch, W. Pretzer, M. Kulzick, A. Hiltner, E. Baer, J. Appl. Polym. Sci., **77** (2000) 1207-1217
127) C. A. Turi, *Thermal Characterization of Polymeric Materials*, Vol. 1 and 2, Academic Press, San Diego, London, Boston, New York, Sydney, Tokyo, Toronto (1997)
128) J. Vuković, D. Steinmeier, M. D. Lechner, S. Jovanović, B. Božić, Polymer Degradation and Stability, **91** (2006) 1903-1908
129) Y. Hong, J. J. Cooper-White, M. E. Mackay, C. J. Hawker, E. Malmström, N. Rehnberg, J. Rheol., **43** (1999) 781-793
130) D. Schmaljohann, P. Pötschke, R. Hässler, B. I. Voit, P. E. Froehling, B. Mostert, J. A. Loontjens, Macromolecules, **32** (1999) 6333-6339
131) C.-Y. Hong, Y.-Z. You, D. Wu, Y. Liu, C.-Y. Pan, Macromolecules, **38** (2005) 2606-2611
132) L. L. Miller, Y. Kunugi, A. Canavesi, S. Rigaut, C. N. Moorefield, G. R. Newkome, Chem. Mat., **10** (1998) 1751-1754
133) R. Esfand, D. A. Tomalia, Drug Discovery Today, **6** (2001) 427-436
134) R. Duncan, N. Malik, Proc. Int. Symp. Control. Release Bioact. Mater., **23** (1996) 105-106
135) S. A. Vinogradov, D. F. Wilson, Chem. Eur. J., **6** (2000) 2456-2461
136) Y. Gong, B. Matthews, D. Cheung, T. Tam, I. Gadawski, D. Leung, G. Holan, J. Raff, S. Sacks, Antivirial Res., **55** (2002) 319-329
137) M. Zhao, Y. Zhou, M. L. Bruening, D. E. Bergbreiter, R. M. Crooks, Langmuir, **13** (1997) 1388-1391
138) T. Emrick, H.-T. Chang, J. M. J. Fréchet, J. Woods, L. Baccei, Polym. Bull., **45** (2000) 1-7

139) G. Jannerfeldt, L. Boogh, J.-A. E. Månson, J. Polym. Sci. Part A: Polym. Chem., **37** (1999) 2069-2077
140) A. Star, J. F. Stoddart, Macromolecules, **35** (2002) 7516-7520
141) J. Fang, H. Kita, K.-I. Okamoto, J. Membr. Sci., **182** (2001) 245-256
142) K. Uhrich, Trends in Polym. Sci., **5(12)** (1997) 388-393
143) E. Arce, P. M. Nieto, V. Diaz, R. G. Castro, A. Bernad, J. Rojo, Bioconjugate Chem., **14** (2003) 817-823
144) Ch. Wohlfarth, B. Wohlfarth, *Optical Constants in Landolt-Börnskin*, New Series, Group III, Volume 38, Springer, Berlin (1996)
145) G. Bodor, *Structural Investigation of Polymers*, Ellis Horwood Limited, England (1991)
146) E. Žagar, M. Žigon, S. Podzimek, Polymer, **47** (2006) 166-175
147) J. Vuković, *A study of the dilute solution behaviour and thermal stability of hyperbranched polymers based on aliphatic polyesters*, Master thesis, Faculty of technology and metallurgy, Belgrade (2003)
148) S. Uppuluri, F. A. Morrison, P. R. Dvornić, Macromolecules, **33** (2001) 2551-2560

7. Appendix

7.1. IR spectra of selected hyperbranched polyesters

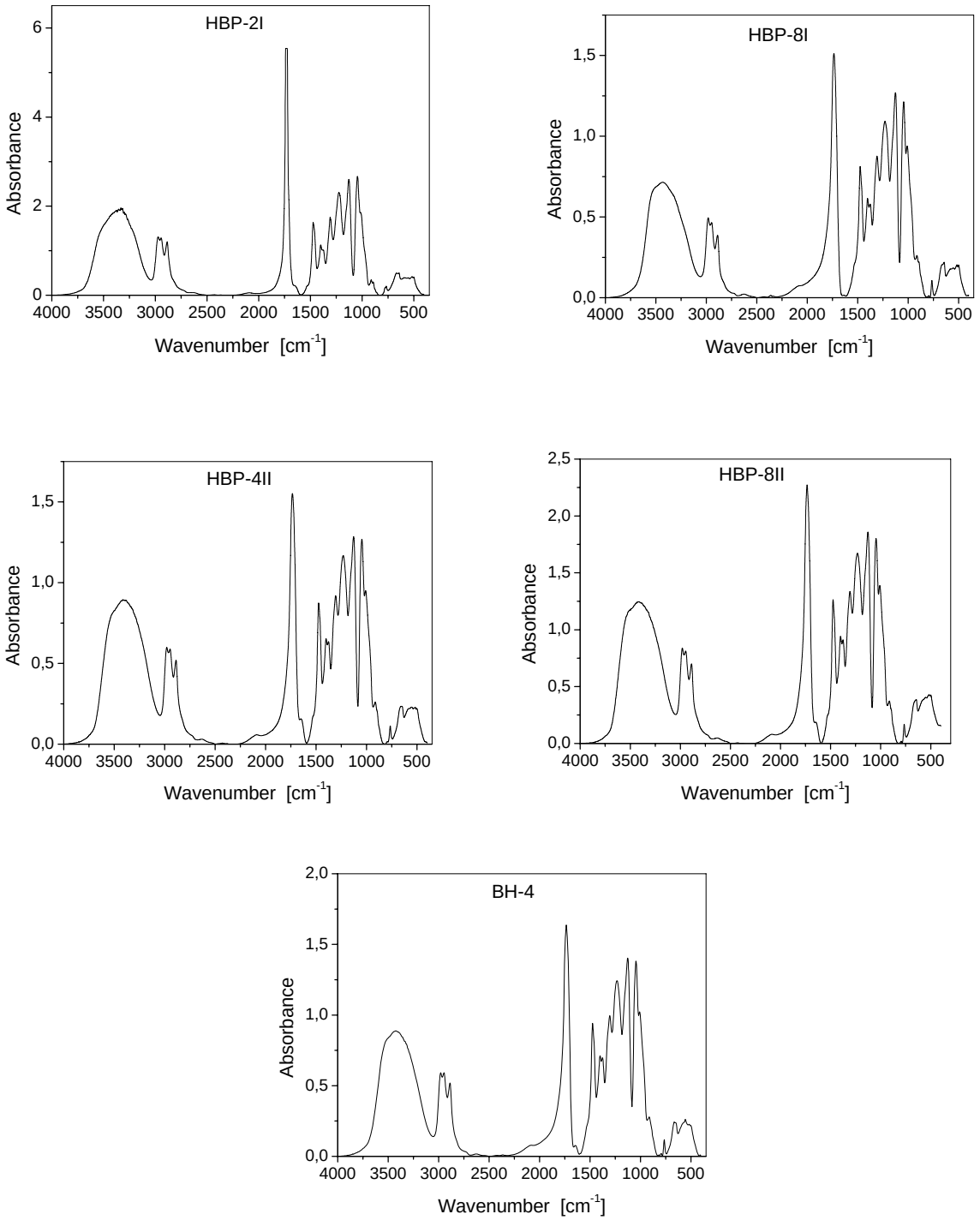

Figure 7.1. IR spectra of the samples HBP-2I, HBP-8I, HBP-4II, HBP-8II and BH-4

7.2. NMR spectra of selected hyperbranched polyesters

7.2.1. ^{13}C NMR spectra

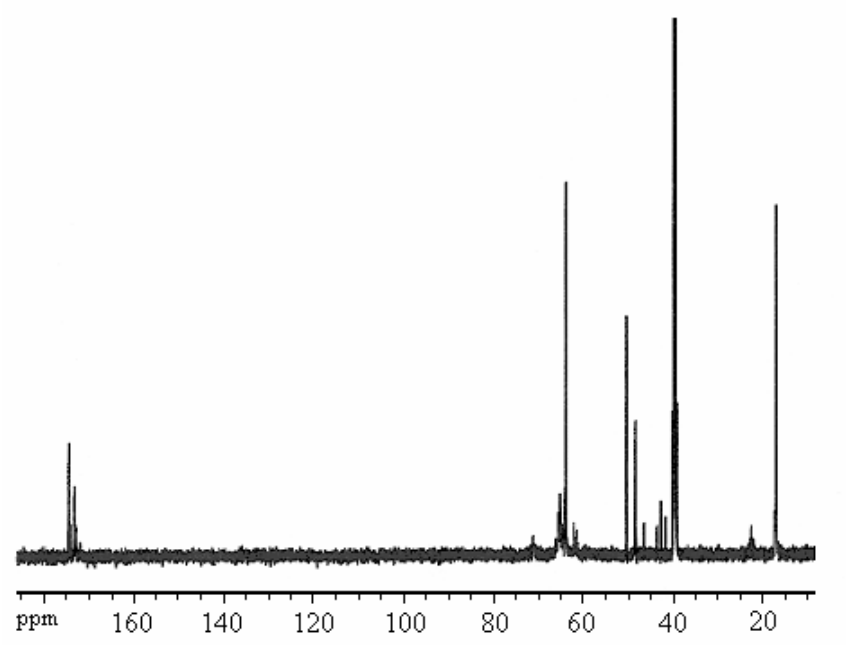

Figure 7.2. ^{13}C NMR spectrum of HBP-2I in DMSO-d_6

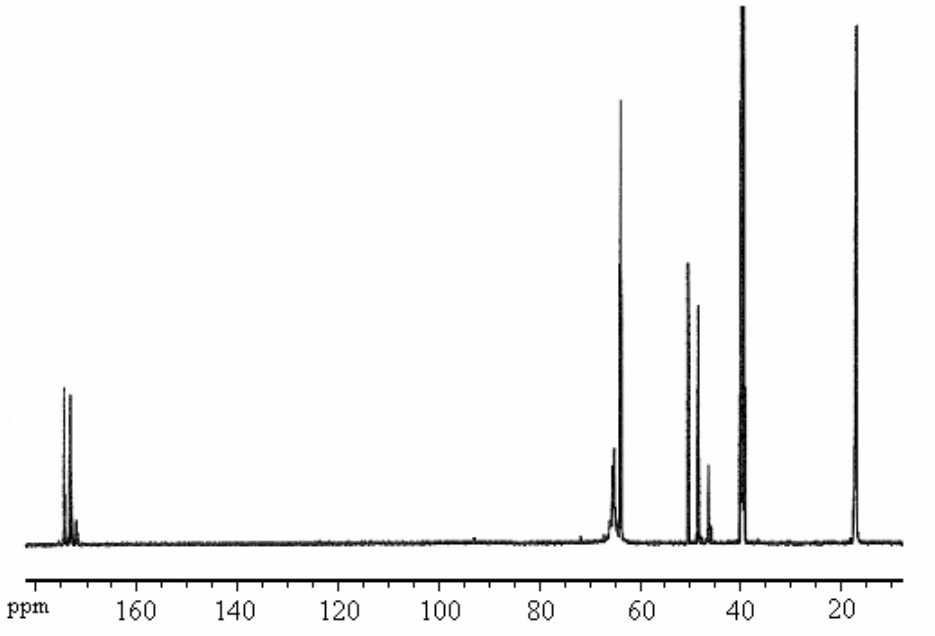

Figure 7.3. ^{13}C NMR spectrum of HBP-8I in DMSO-d_6

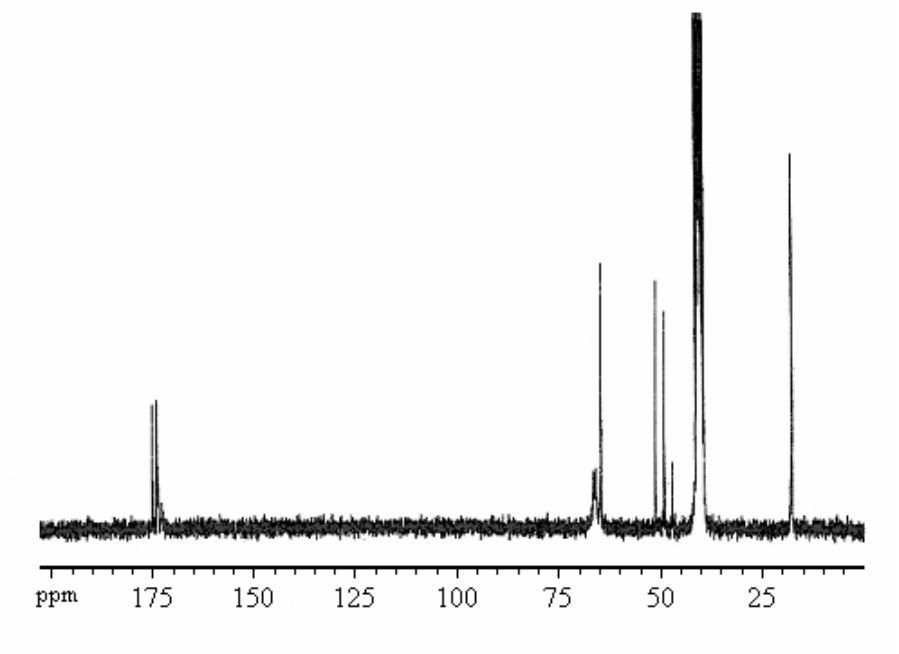

Figure 7.4. ^{13}C NMR spectrum of HBP-6II in DMSO-d_6

7.2.2. ^{1}H NMR spectra

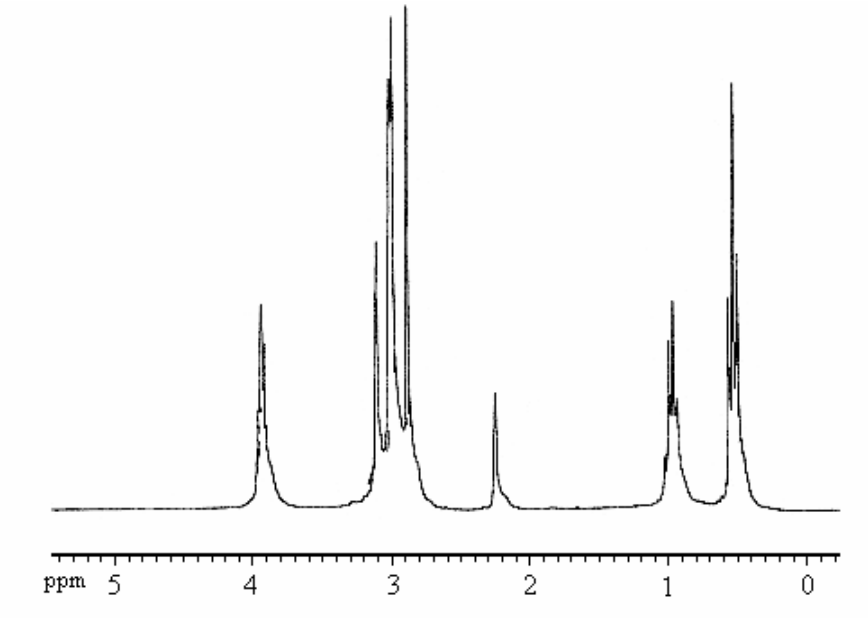

Figure 7.5. ^{1}H NMR spectrum of DiTMP in DMSO-d_6 (3 mass %)

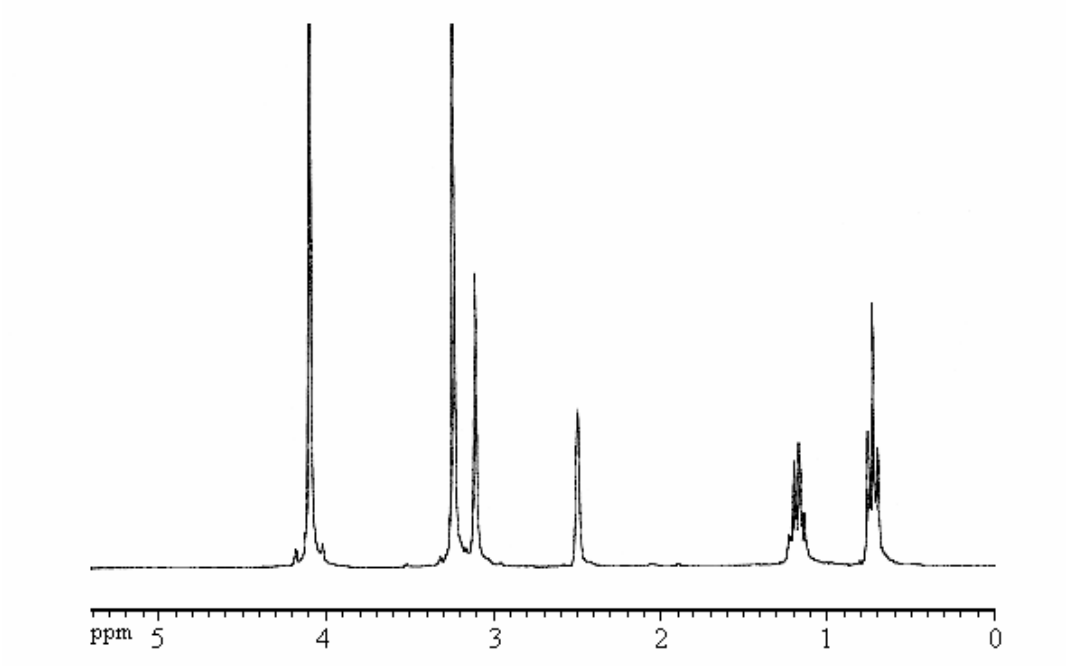

Figure 7.6. ^{1}H NMR spectrum of DiTMP in D_2O/DMSO-d_6 (3 mass %)

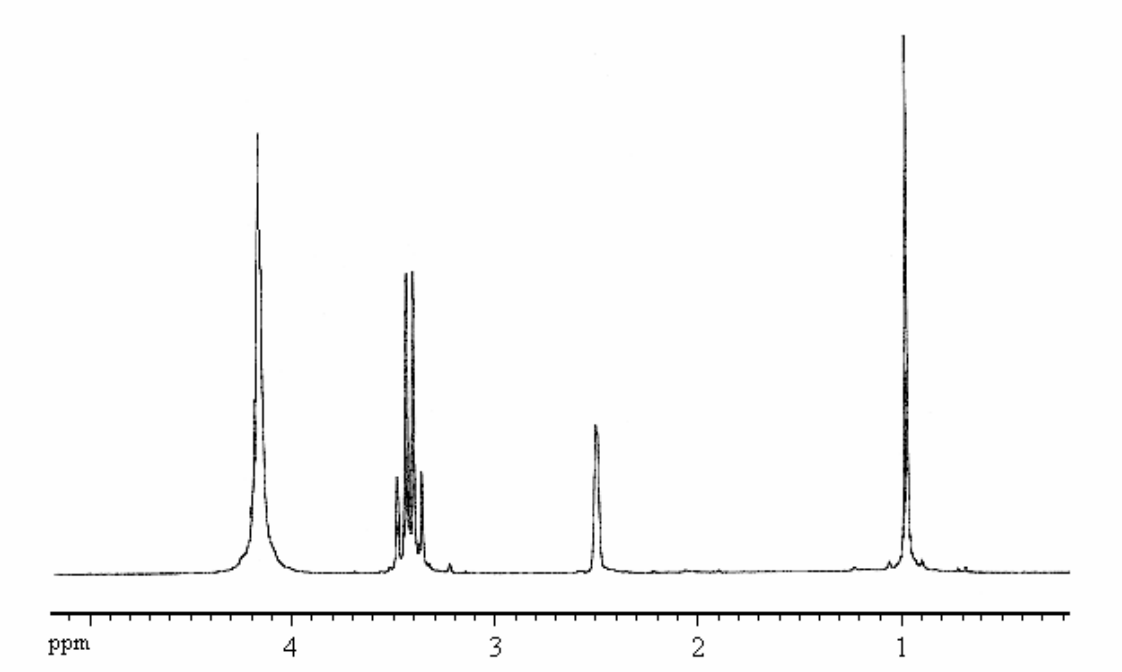

Figure 7.7. ^{1}H NMR spectrum of bis-MPA in D_2O/DMSO-d_6 (3 mass %)

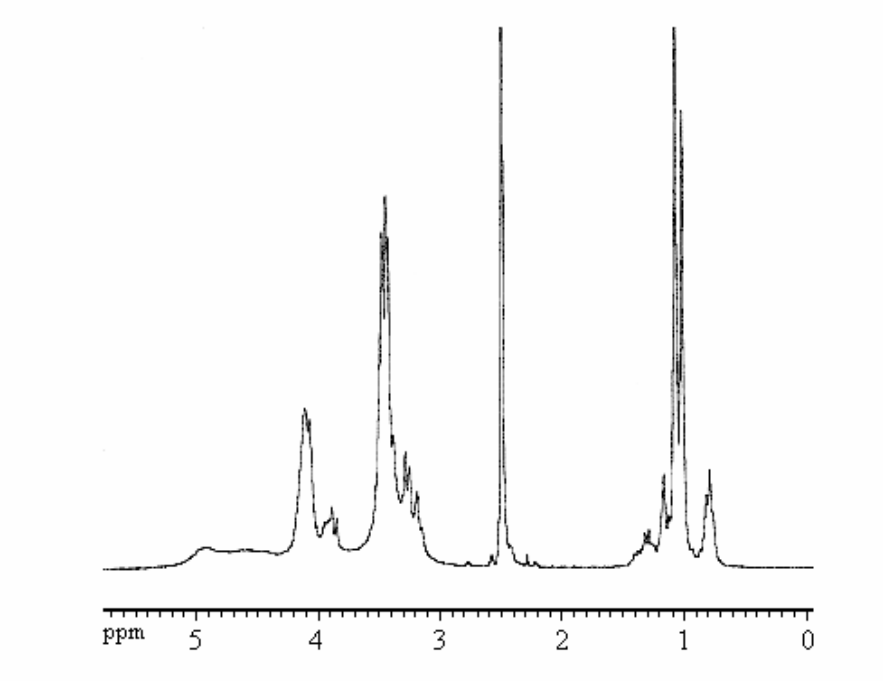

Figure 7.8. ^{1}H NMR spectrum of HBP-2I in DMSO-d_6 (3 mass %)

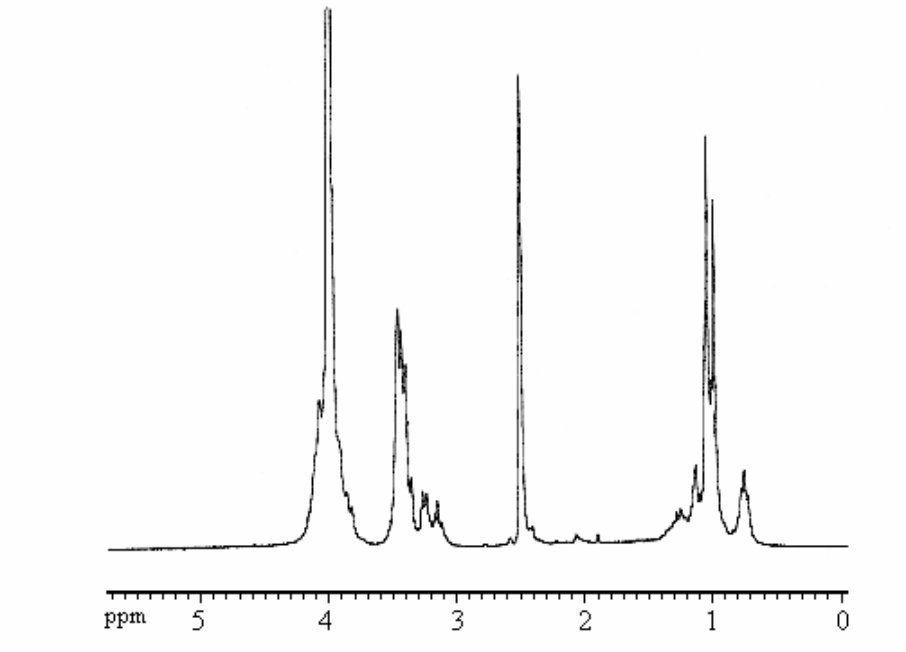

Figure 7.9. ^{1}H NMR spectrum of HBP-2I in D_2O/DMSO-d_6 (3 mass %)

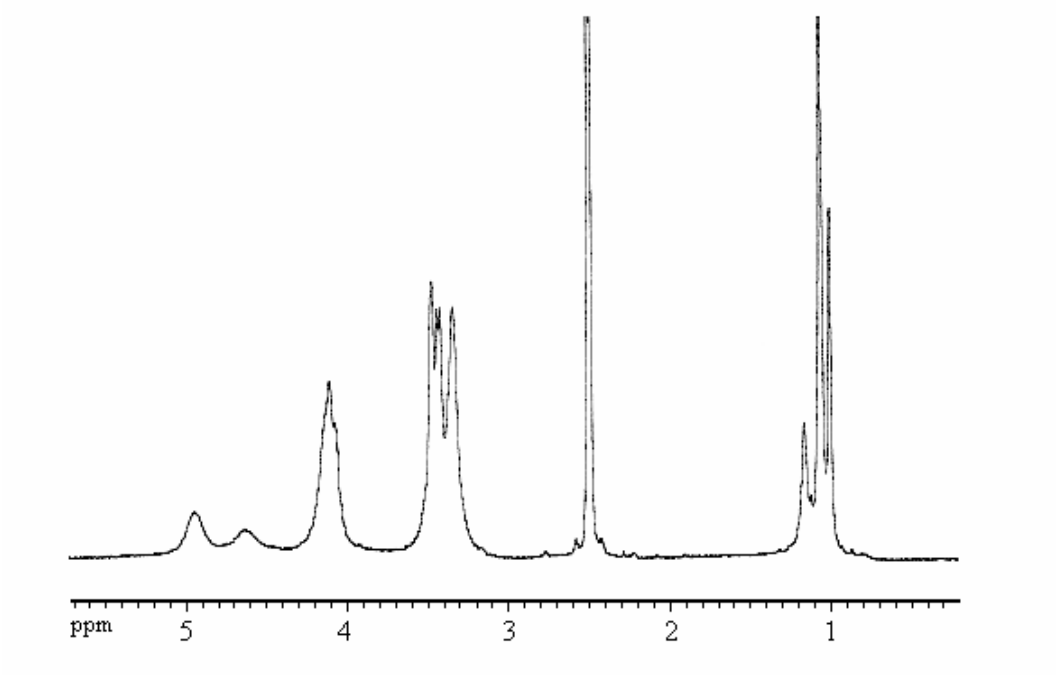

Figure 7.10. ^{1}H NMR spectrum of HBP-8I in DMSO-d_6 (3 mass %)

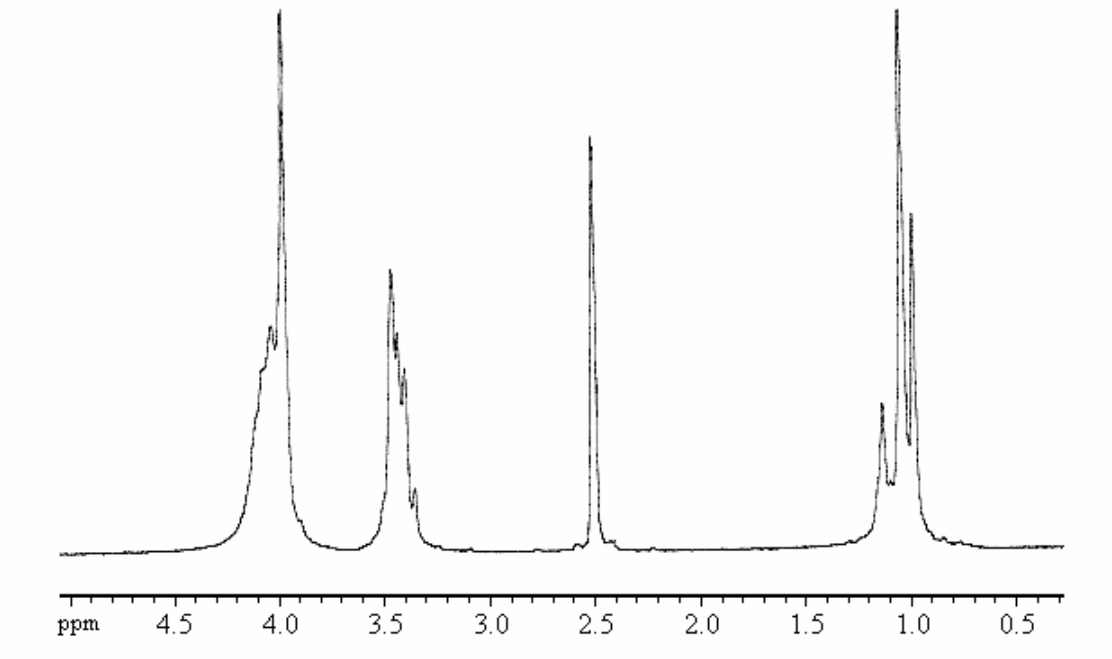

Figure 7.11. ^{1}H NMR spectrum of HBP-8I in D_2O/DMSO-d_6 (3 mass %)

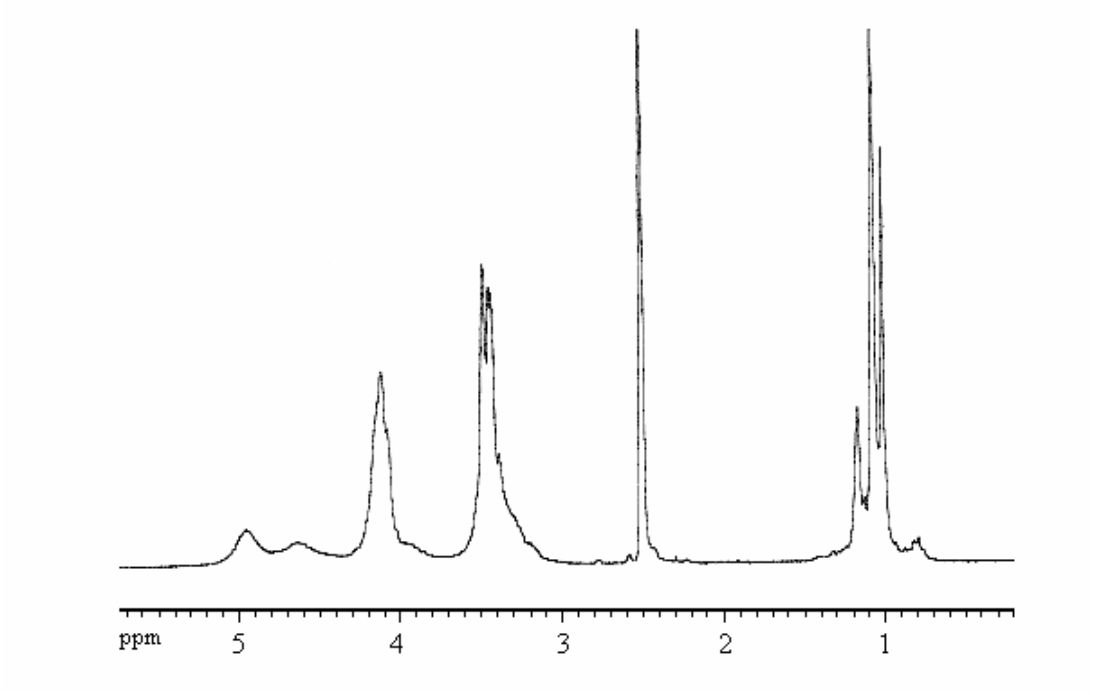

Figure 7.12. ^{1}H NMR spectrum of HBP-4II in DMSO-d_6 (3 mass %)

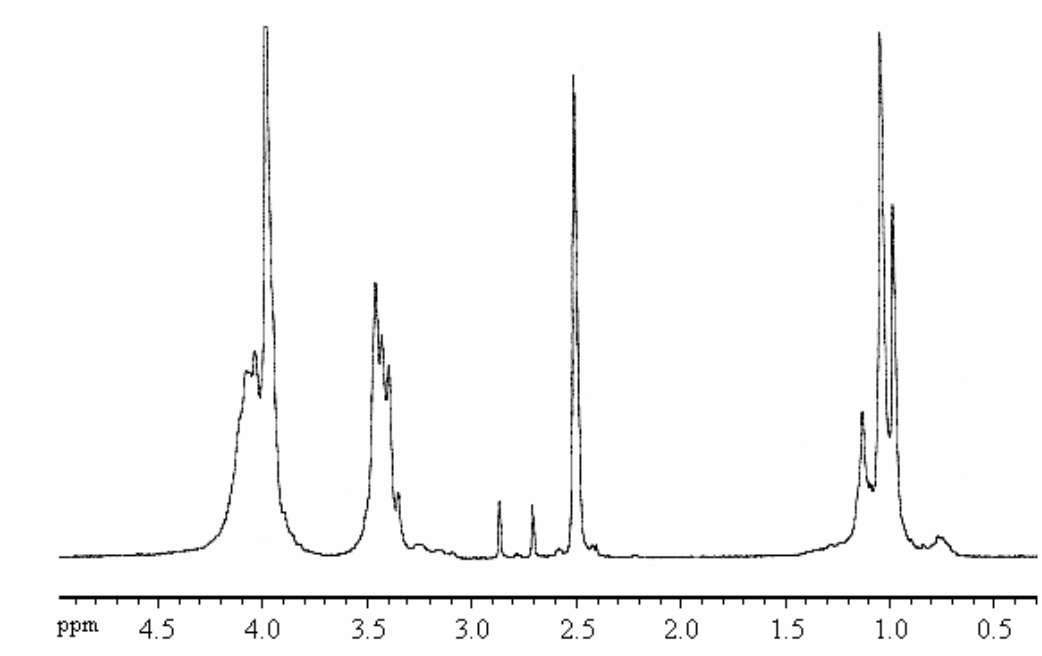

Figure 7.13. ^{1}H NMR spectrum of HBP-4II in D_2O/DMSO-d_6 (3 mass %)

7.3. Mass spectra of selected hyperbranched polyesters

7.3.1. MALDI-TOF mass spectra

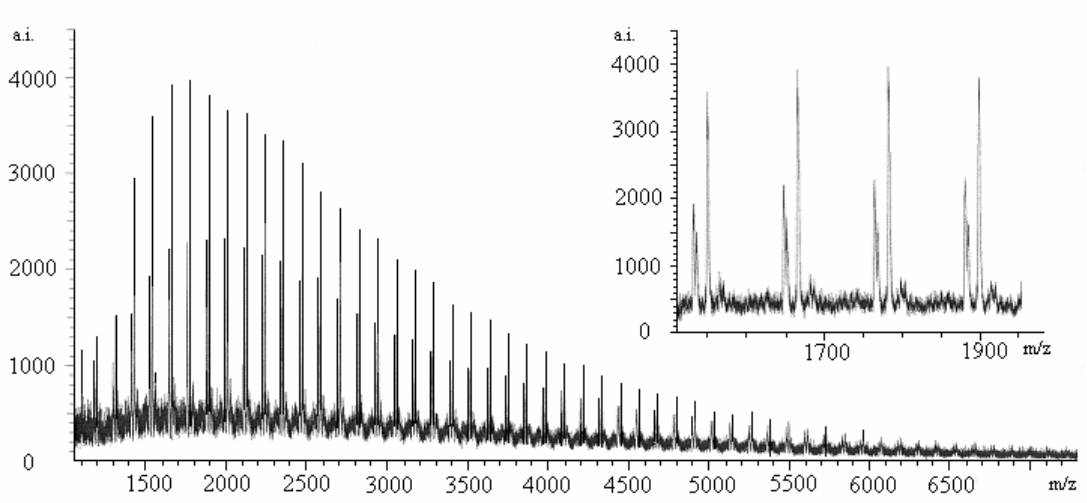

Figure 7.14. Full and enhanced MALDI-TOF mass spectra of HBP-6I

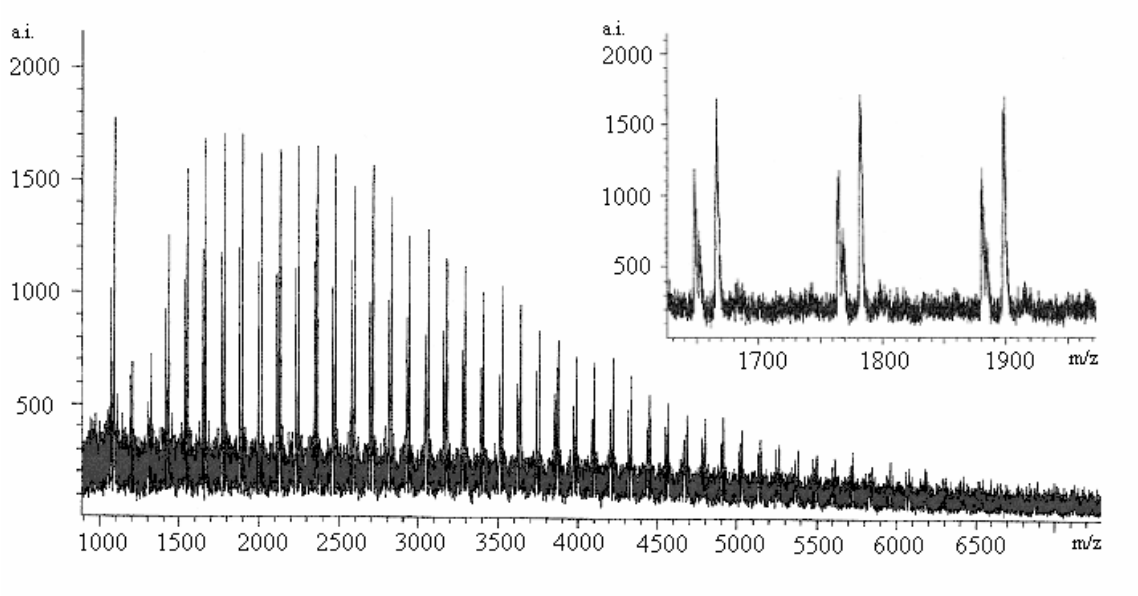

Figure 7.15. Full and enhanced MALDI-TOF mass spectra of HBP-6II

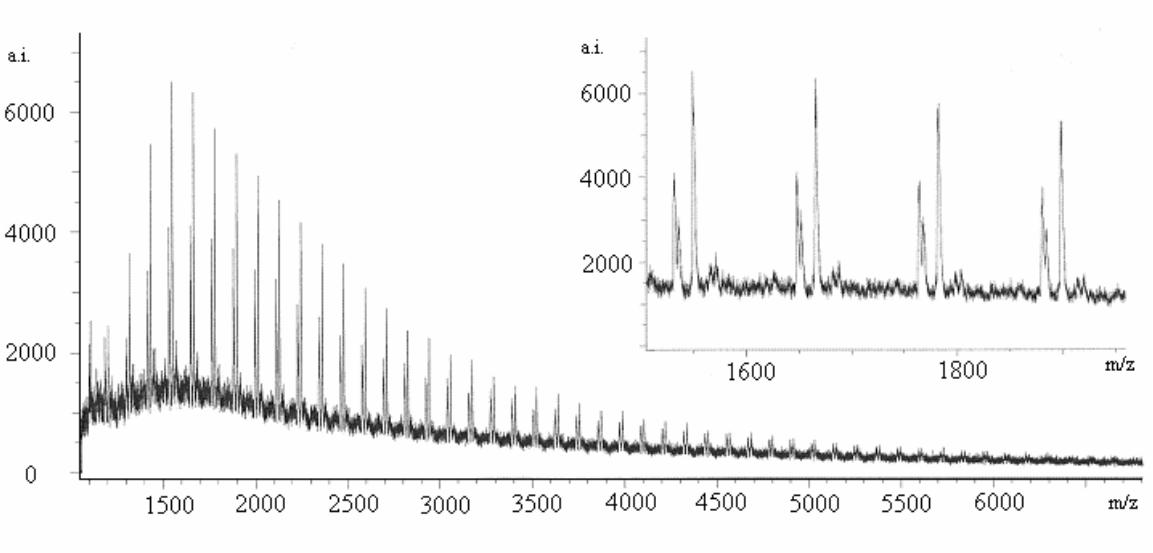

Figure 7.16. Full and enhanced MALDI-TOF mass spectra of HBP-10I

7.3.2. ESI mass spectra

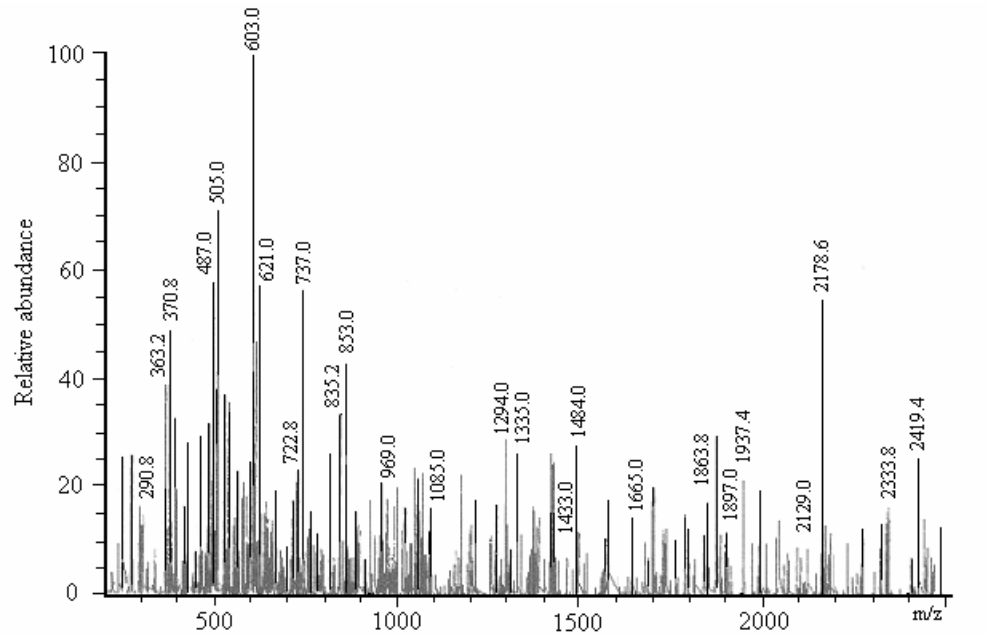

Figure 7.17. ESI mass spectrum of HBP-5I

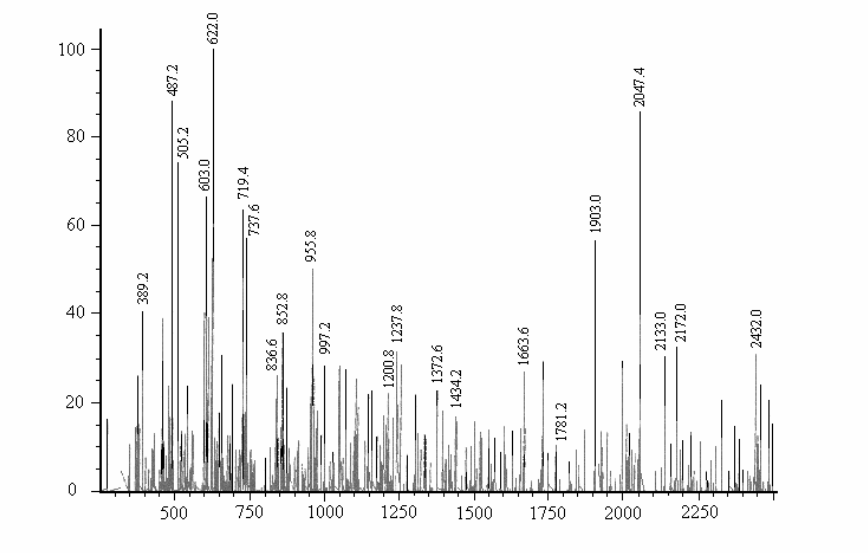

Figure 7.18. ESI mass spectrum of HBP-10I

7.4. GPC chromatograms of selected hyperbranched polyesters

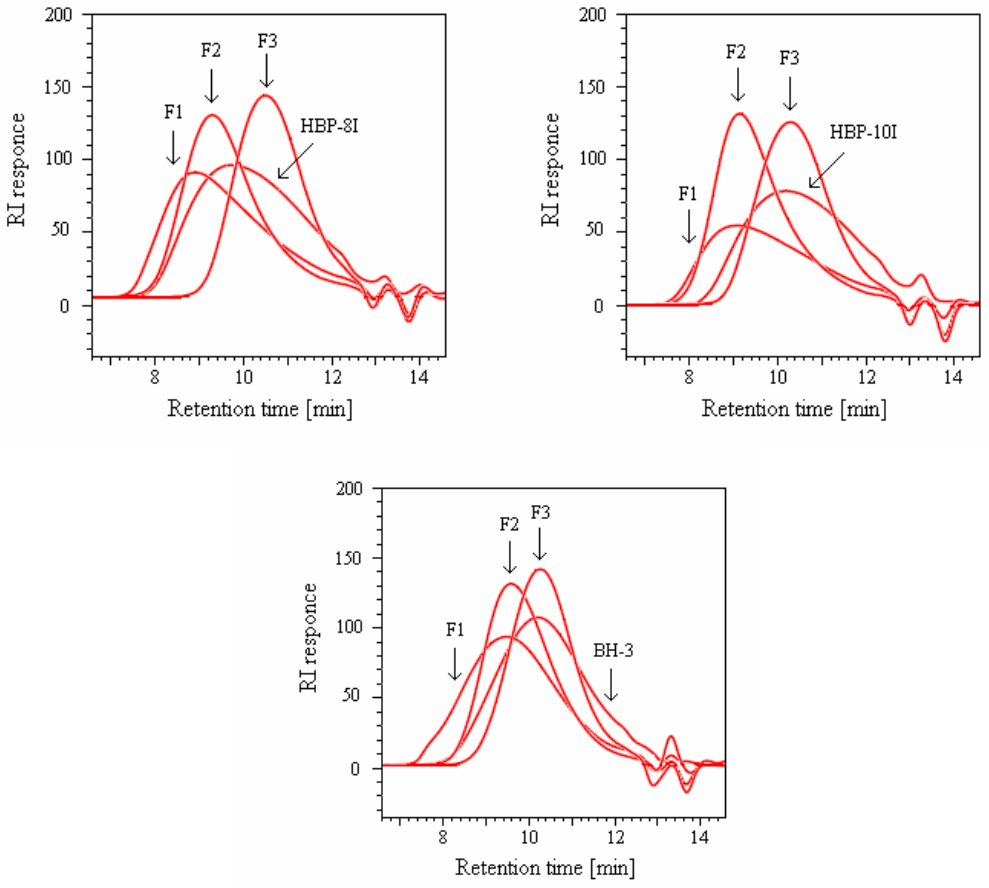

Figure 7.19. GPC profiles of different HB polyesters and their fractions

7.5. Rheological measurements of selected hyperbranched polyesters

7.5.1. Concentrated solutions

Table 7.1. Values of the zero shear viscosity (η_0) for the samples HBP-2I, HBP-3I, HBP-4I, HBP-4II and HBP-5I determined at different concentrations and temperatures

c [mass %]	η_0 [mPa s]								
	10 ^{0}C	15 ^{0}C	20 ^{0}C	25 ^{0}C	30 ^{0}C	35 ^{0}C	40 ^{0}C	45 ^{0}C	50 ^{0}C
HBP-2I									
30	66.3	54.7	45.6	38.8	33.3	29.0	25.6	23.3	21.8
35	133.7	103.2	81.4	65.4	54.2	45.6	39.4	34.7	31.1
40	325.1	232.6	173.3	131.2	102.3	82.7	68.7	59.2	52.2
45	819.7	550.1	389.3	284.0	213.6	164.9	131.2	107.7	92.7
50	/	/	/	/	/	/	/	210.1	164.6
55	/	/	/	/	/	/	/	/	399.4
HBP-3I									
30	89.9	73.5	60.6	50.1	42.7	37.0	32.5	29.2	26.7
35	202.9	156.5	122.7	97.0	77.9	63.8	55.1	49.1	44.3
40	431.3	312.8	231.6	174.9	135.9	109.7	91.3	77.5	67.9
45	1227.0	829.0	582.0	420.5	312.0	237.5	187.4	151.0	125.5
50	/	/	/	/	/	/	381.8	286.9	222.3
HBP-4I									
30	128.2	104.0	82.4	63.7	51.5	43.6	38.2	34.0	31.2
35	245.1	189.0	145.8	113.3	89.5	72.6	61.3	53.0	47.5
40	573.5	411.6	301.8	226.5	173.9	137.1	111.9	94.2	81.5
45	1679.0	1194.0	822.5	583.9	424.9	319.2	247.2	195.6	160.8
50	/	/	/	/	872.8	619.4	462.1	355.1	284.1
55	/	/	/	/	/	1329.0	930.7	699.9	522.2
HBP-4II									
30	122.2	98.8	80.7	66.2	53.8	44.9	38.3	33.1	29.8
35	259.5	198.8	154.7	121.7	95.6	77.0	63.8	54.2	47.3
40	660.0	479.3	353.7	265.5	202.7	157.7	124.9	102.3	85.9
45	1583.0	1075.0	751.2	535.1	388.7	289.4	221.7	174.2	142.5
50	/	/	/	/	/	722.4	533.8	395.8	305.2
55	/	/	/	/	/	/	/	725.1	539.5
HBP-5I									
30	127.7	105.2	83.6	66.4	53.6	44.9	39.5	35.1	31.8
35	263.2	203.3	157.4	121.8	95.4	77.3	64.5	55.5	49.3
40	613.4	442.5	320.3	235.9	176.3	135.3	108.5	90.1	77.6
45	1820.0	1221.0	841.2	594.8	426.0	313.8	242.1	191.9	160.6
50	/	/	/	/	960.7	684.9	489.5	361.0	279.9
55	/	/	/	/	/	/	822.2	583.5	429.8

Table 7.2. Values of the zero shear viscosity (η_0) for the samples HBP-6I, HBP-6II, HBP-8I, HBP-8II and HBP-10I determined at different concentrations and temperatures

c [mass %]	η_0 [mPa s]								
	10 ^{0}C	15 ^{0}C	20 ^{0}C	25 ^{0}C	30 ^{0}C	35 ^{0}C	40 ^{0}C	45 ^{0}C	50 ^{0}C
HBP-6I									
30	129.4	105.9	85.9	70.0	58.1	49.7	43.5	38.3	34.9
35	288.4	220.1	169.6	131.6	104.8	85.6	71.8	61.7	54.6
40	647.8	471.0	348.6	261.6	201.3	158.6	130.1	109.5	94.0
45	1773.0	1210.0	848.9	610.1	447.5	337.0	259.9	204.2	166.0
50	/	/	/	/	1042.0	744.3	548.2	414.7	323.1
55	/	/	/	/	/	1815.0	1255.0	892.1	653.2
HBP-6II									
30	133.3	112.4	90.1	71.2	56.4	46.3	39.6	35.4	32.4
35	258.7	225.3	170.7	128.6	98.0	78.1	64.7	56.3	50.5
40	596.5	503.3	367.9	271.2	203.5	154.6	122.3	98.4	82.6
45	/	1253.0	878.2	627.1	456.0	338.8	257.9	200.2	159.9
50	/	/	/	/	/	643.9	476.6	358.5	279.0
55	/	/	/	/	/	/	/	920.1	666.1
HBP-8I									
30	139.5	112.3	90.6	74.1	61.8	52.6	45.4	39.7	35.9
35	292.6	222.9	172.8	136.2	109.0	89.2	74.6	63.8	56.0
40	741.7	531.1	390.1	294.0	226.1	178.1	144.1	119.2	101.1
45	2049.0	1382.0	959.4	687.2	506.0	379.3	291.3	229.9	186.6
50	/	/	/	/	1266.0	895.8	647.9	483.2	371.8
55	/	/	/	/	/	2036.0	1396.0	990.1	726.4
HBP-8II									
30	132.3	107.4	85.4	67.2	53.8	44.8	38.7	34.4	31.3
35	286.7	221.8	172.7	134.4	104.9	83.2	68.4	58.6	51.4
40	667.5	489.9	360.2	269.9	205.4	159.4	127.4	105.4	896.9
45	1718.0	1210.0	843.0	600.2	434.9	324.2	248.6	194.4	157.5
50	/	/	/	/	/	803.2	585.8	436.5	329.9
55	/	/	/	/	/	/	/	883.1	643.6
HBP-10I									
30	135.1	109.4	88.9	71.8	59.0	49.3	42.9	38.1	35.2
35	275.0	212.2	166.7	132.2	105.2	86.1	71.8	61.9	56.2
40	648.9	469.8	374.4	262.8	202.4	160.2	130.7	109.0	93.5
45	1883.0	1272.0	885.7	635.1	466.7	349.2	268.4	210.6	171.8
50	/	/	/	/	1210.0	859.9	626.6	471.0	380.3
55	/	/	/	/	/	/	1485.0	1054.0	765.7

Table 7.3. Values of the zero shear viscosity (η_0) for the commercial samples BH-2, BH-3 and BH-4 determined at different concentrations and temperatures

c [mass %]	η_0 [mPa s]								
	10 ^{0}C	15 ^{0}C	20 ^{0}C	25 ^{0}C	30 ^{0}C	35 ^{0}C	40 ^{0}C	45 ^{0}C	50 ^{0}C
BH-2									
10	12.5	12.4	12.0	11.4	11.0	10.1	9.6	9.0	8.8
20	21.6	20.6	19.3	17.6	15.6	14.9	13.9	13.2	12.4
30	57.4	49.2	41.1	34.4	29.0	25.3	22.6	20.5	19.2
40	190.5	143.4	107.5	80.6	63.1	51.5	44.6	39.5	36.0
50	/	/	/	/	/	/	/	116.5	97.0
BH-3									
10	18.3	16.6	15.0	13.3	11.9	10.7	9.8	9.3	8.7
20	29.4	27.2	24.6	22.1	19.8	17.9	16.2	14.9	14.1
30	94.5	78.6	63.9	52.3	43.5	37.5	32.8	29.6	27.4
40	461.2	333.5	244.1	181.3	137.9	108.9	89.4	77.5	71.2
50	/	/	/	/	/	494.7	369.2	283.4	223.8
55	/	/	/	/	/	/	/	/	437.2
BH-4									
10	14.7	14.5	14.2	13.1	12.0	11.0	10.2	9.7	9.3
20	35.3	32.6	29.2	25.6	22.5	20.2	18.0	17.1	16.1
30	115.6	95.5	77.5	62.8	52.9	45.1	39.5	35.7	32.8
40	674.8	493.8	365.4	274.4	209.4	163.8	133.7	112.5	97.3
50	/	/	/	/	922.0	671.3	496.0	377.0	299.0
55	/	/	/	/	/	1669.0	1176.0	845.1	629.8

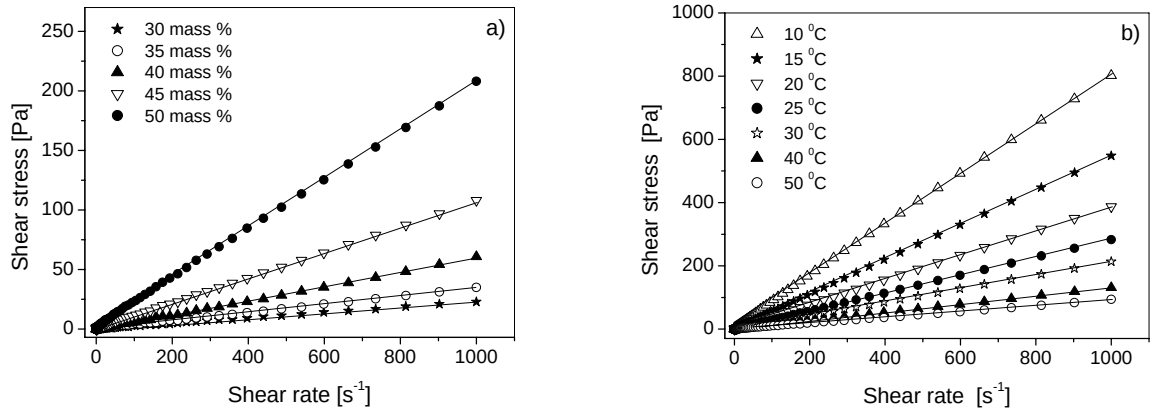

Figure 7.20. Dependence of the shear stress versus shear rate of the sample HBP-2I for a) different solution concentration at 45 ^{0}C and for b) 45 mass % solutions at different temperatures

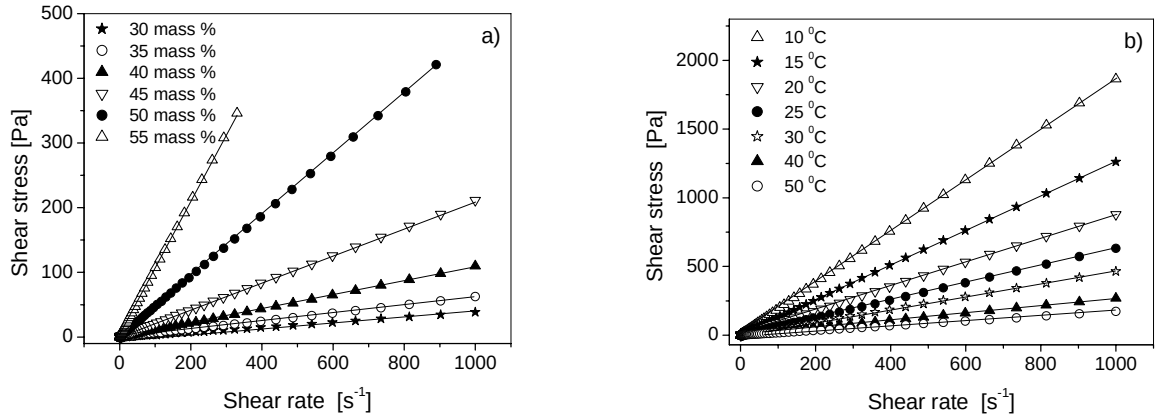

Figure 7.21. Dependence of the shear stress versus shear rate of the sample HBP-10I for a) different solution concentration at 45 ^{0}C and for b) 45 mass % solutions at different temperatures

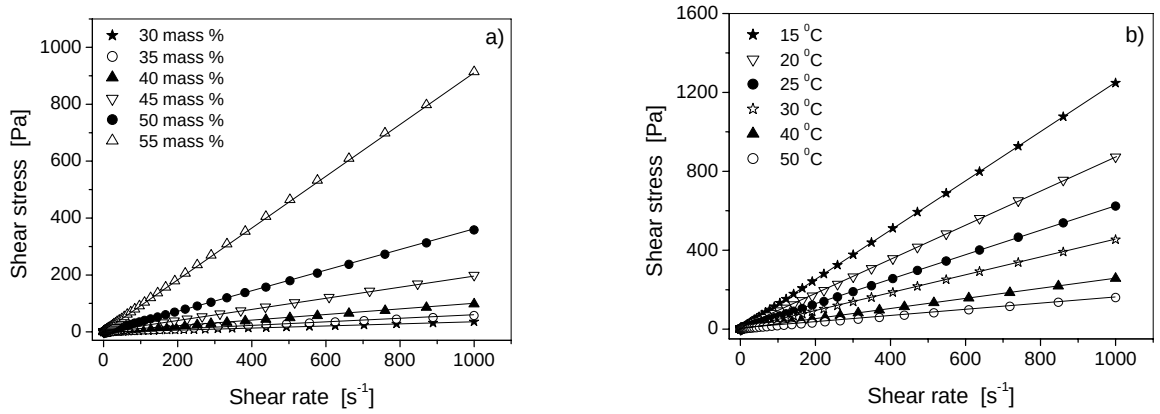

Figure 7.22. Dependence of the shear stress versus shear rate of the sample HBP-6II for a) different solution concentration at 45 ^{0}C and for b) 45 mass % solutions at different temperatures

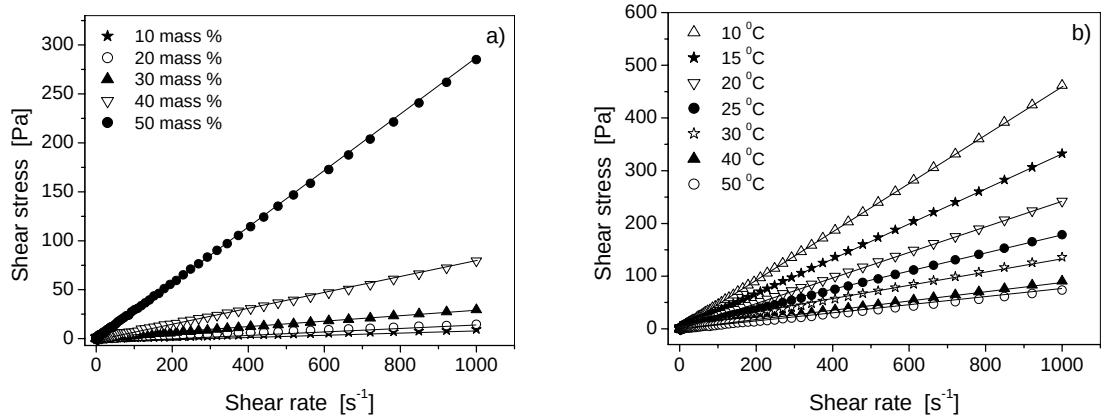

Figure 7.23. Dependence of the shear stress versus shear rate of the sample BH-3 for a) different solution concentration at 45 ^{0}C and for b) 40 mass % solutions at different temperatures

7.5.2. Melt rheology

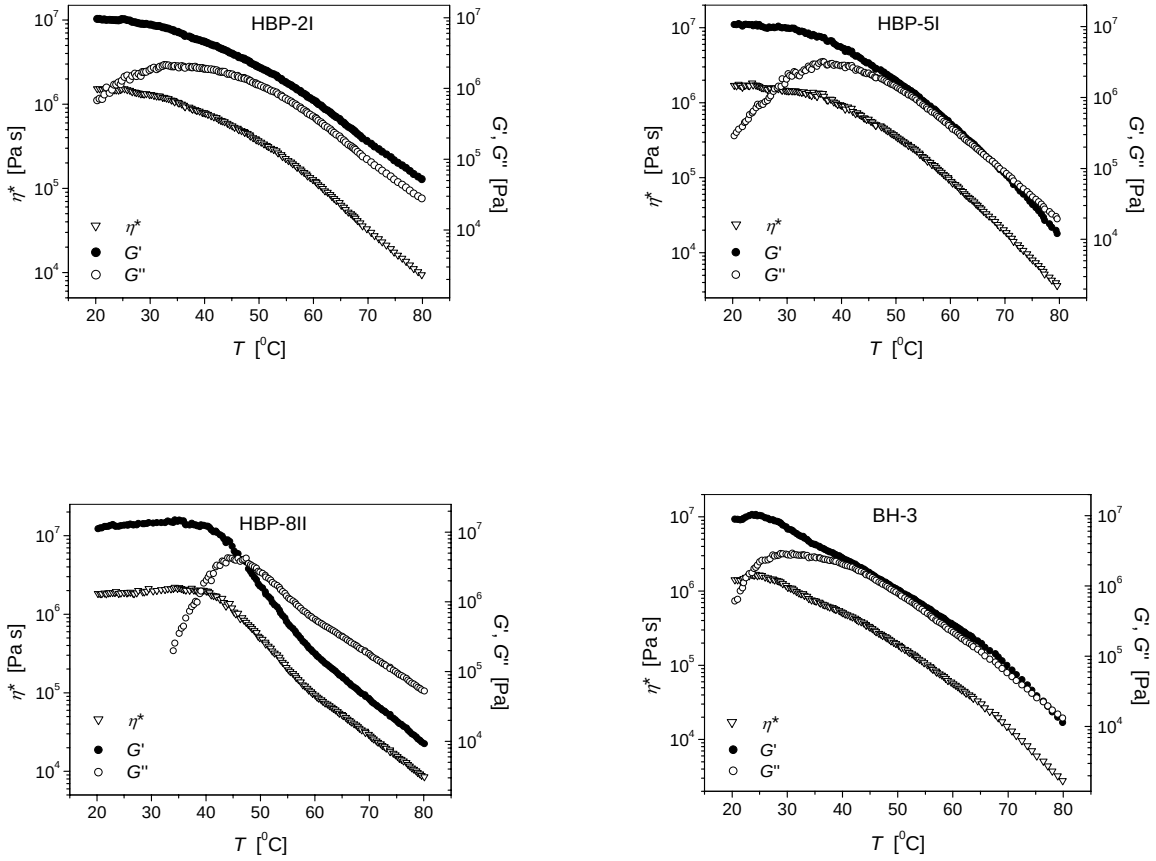

Figure 7.24. Temperature dependence at frequency of 1 Hz of the complex viscosity, storage and loss modulus for different HB polyesters

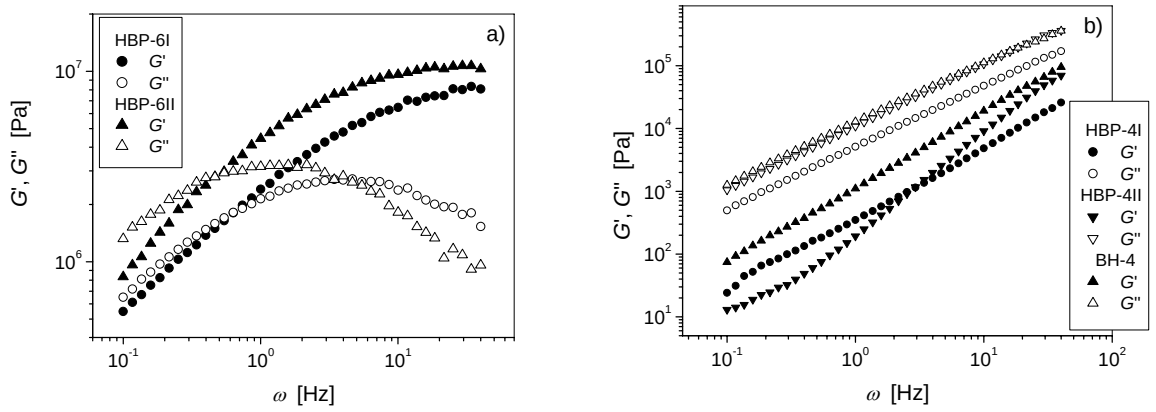

Figure 7.25. Frequency dependence of the storage and loss modulus for a) samples HBP-6I and HBP-6II at 45 ^{0}C and for b) samples HBP-4I, HBP-4II and BH-4 at 80 ^{0}C

8. List of Abbreviations

ATRP	Atom transfer radical polymerization
bis-MPA	2,2-bis(hydroxymethyl)propionic acid
DiTMP	Di-trimethylolpropane
DLS	Dynamic light scattering
DMAc	N,N-dimethylacetamide
DMF	N,N-dimethylformamide
DMSO	Dimethylsulfoxide
ESI MS	Electrospray ionization mass spectrometry
GPC	Gel permeation chromatography
HB	Hyperbranched
KMHS	*Kuhn-Mark-Houwink-Sakurada* equation
LVE	Linear viscoelasticity
MALDI-TOF MS	Matrix assisted laser desorption/ionization time of flight mass spectrometry
MSA	Methanesulphonic acid
NMP	N-methyl-2-pyrrolidinon
PAMAM	Poly(amidoamine) - commercially available dendrimers
PP50	Ethoxylated pentaerythritol
PPI	Poly(propyleneimine) - commercially available dendrimers
SANS	Small-angle neutron scattering
SAXS	Small-angle X-ray scattering
SCVP	Self - condensing vinyl polymerization
SLS	Static light scattering
TG	Thermogravimetric
THF	Tetrahydrofuran
TMP	2-ethyl-2-(hydroxymethyl)-1,3-propanediol
UC	Ultracentrifugation
VPO	Vapour pressure osmometry
WLF	*Williams-Landel-Ferry* equation

Declaration

I declare that I wrote this thesis myself. I did not use other auxiliary material than indicated. Other work is always cited.

I have not tried to get a Ph. D. before.

Osnabrück, September 2006

Jasna Vuković

Vita

Name:	Jasna Vuković
Born:	28th August 1976 in Jagodina, Serbia

Education and Academic Qualification:

9. 1983 - 6. 1991:	Elementary school in Jagodina, Serbia
9. 1991 - 6. 1995:	Gymnasium in Jagodina, Serbia → Matriculation examination, College entrance examination
10. 1995 - 9. 2000:	Studies at Faculty of Technology and Metallurgy, University Belgrad, Serbia, degree: Dipl.-Engineer of Technology
10. 2000 - 9. 2003:	Master studies at Faculty of Technology and Metallurgy, University Belgrad, Serbia, degree: Master of Technical Science
11. 2003 - till present:	Pursuing Ph. D. thesis at the Dept. Physical Chemistry, University Osnabrück, Germany

Employment History

12. 2003 - 08. 2005	Scientific auxiliary assistance at the Dept. Physical Chemistry, University Osnabrück, Germany
12. 2005 - 10. 2006	Scientific Assistant at the Dept. Physical Chemistry, University Osnabrück, Germany